Vrije Universiteit Brussel

Faculteit Ingenieurswetenschappen
Vakgroep Toegepaste Mechanica
Pleinlaan 2, B-1050 Brussel

Compliant Actuation for Biologically Inspired Bipedal Walking Robots

Ronald Van Ham

Jury:
Prof. dr. ir. D. Lefeber (VUB-MECH), promotor
Prof. dr. ir. J. Tiberghien (VUB-ETRO), chairman
Prof. dr. ir. J. Vereecken (VUB-META), vice-chairman
dr. ir. J. Naudet (VUB-MECH), secretary of the chairman
Prof. dr. ir. P.Kool (VUB-MECH)
Prof. dr. ir. Ph. Lataire (VUB-ETEC)
Prof. dr. ir.B. Van Gheluwe (HILOK-BIOM)
dr. ir. M. Wisse (Delft University of Technology)
Prof dr. ir. K. Berns (University of Kaiserlautern)

Contact information:

Vrije Universiteit Brussel
Faculty of Engineering
Department of Mechanical Engineering
Pleinlaan 2
1050 Brussels
Belgium
http://mech.vub.ac.be/
http://lucy.vub.ac.be/
http://mech.vub.ac.be/maccepa
ronald.van.ham@vub.ac.be
dirk.lefeber@vub.ac.be

Acknowledgements

First of all I want to thank my parents, who gave me a solid base in engineering, machining, logical thinking and practical skills. These skills proved to be of much more importance, both in research and in everyday live, than whatever professor ever taught me.

Special thanks goes to my promotor Dirk Lefeber, who has given me the opportunity to start this PhD research in this very challenging and promising field, while leaving me the freedom to perform my research in my own and sometimes unconventional way.

For many years, I was lucky to work amongst the most enthusiastic and passionate researchers one could imagine. Therefore, many thanks go to my colleagues of the department of Mechanical Engineering, especially to Björn Verrelst, Bram Vanderborght, Michaël Van Damme and Joris Naudet. The support they gave me, both mentally and scientifically, is greatly appreciated. Björn and I developed the second generation Pleated Pneumatic Artificial Muscles together and started the design of the biped Lucy. Bram boosted the development of Lucy and made her famous all over the world. His ideas were greatly appreciated during the design and the control of the biped Veronica. The software skills of Michaël were much appreciated for the development of the control software of Lucy, as was his strong belief from the first day on, in the novel actuator MACCEPA. The discussions with Joris about passive walking robots resulted in novel insights in the control strategy. I'm also grateful to Frank Daerden and Pieter Beyl, especially for their moral support concerning the non-model based control approach.

Although most of the mechanical parts and electronic circuits were designed and made by my colleagues and myself, the people of the technical staff deserve my gratitude, especially Jean-Paul Schepens and Andre Plasschaert. Besides doing the machining in the workshop, they created a pleasant working environment, shared their practical solutions, came up with fresh ideas and shared their incredible stock of useful parts. I also would like to thank Ludo Van Reet for the machining of some of the more difficult parts of Veronica.

Special thanks goes to all the persons, who took the time to read, correct and give comments on this text.

I thank also my friends, family and new neighbors in Lennik, for their interest, support and enthusiasm, especially Ellen, Joeri B, Joeri C, Grietje, Filip, Katrien, Nele, Nico, Renee.

And last but not least, I want to thank Heidi, for supporting me and believing in me, day and night and not only what this PhD is concerned, but also when it comes to other projects.

Brussels **Ronald Van Ham**
July 2006

Abstract

This thesis deals with compliant actuators and their use in energy efficient walking bipeds. Two types of actuators with adaptable compliance are discussed: *PPAM* (Pleated Pneumatic Artificial Muscles) and *MACCEPA* (Mechanically Adjustable Compliance and Controllable Equilibrium Position Actuator).

The PPAM is new type of pneumatic muscle, made to overcome shortcomings associated with the existing types of pneumatic muscles, like the presence of hysteresis and the threshold of pressure. The compressibility of air makes them inherently compliant, which can be employed to reduce shocks. Their main advantages are the high power to weight ratio, the adaptable compliance when used in an antagonistic setup and the fact that they can be directly coupled to the joint without a gearing mechanism. Drawbacks are that a joint actuated by two PPAM has a strong non-linear angle-torque characteristic and that the control signals for a certain compliance or equilibrium position are dependent of the current position. A second design of the PPAM concept, which resulted in an extended life time, is used in the biped *Lucy*. This planar biped is actuated with 12 PPAM's, giving the ability to control the six pin joints, both in equilibrium position and in compliance. The control strategy is based on the generation of trajectories for each joint out of the objective locomotion parameters. Ways to adapt the compliance in order to lower energy consumption are studied.

The second type of compliant actuator, the MACCEPA, is entirely developed during this thesis, and patented. It is an electrical actuator of which the compliance and equilibrium position are fully independent and both are set by a dedicated servo motor. The angle-torque characteristic is quasi linear up to 60 degrees, which makes the MACCEPA comparable to a torsion spring, which allows to modify equilibrium position and spring constant online. Moreover, the concept can be implemented using standard off-the-shelf components. This actuator was used to build the biped *Veronica*. This is a planar biped, with 6 MACCEPA actuators, each powering one pin joint. The strategy of using the compliance for energy efficient walking, as elaborated in this PhD, is based on the concept of passive walkers. The compliant actuators are used to modify the natural frequencies of the limbs online, in order to achieve a smooth and stable walking motion. In this way the settings of the MACCEPA are only changes a few times each step, defining the passive motions. Since the developed passive walking robot is not limited to one walking speed, but can be controlled while still using natural motions, this concept is entitled *Controlled Passive Walking*.

Contents

Appendices

A1. R. Van Ham, B. Verrelst, F. Daerden & D. Lefeber. Pressure control with on-off valves of Pleated Pneumatic Artificial Muscles in a modular one-dimensional rotational joint. International Conference on Humanoid Robots, Karlsruhe and Munich, October 2003, abstract pp. 35 + CDROM.

A2. R. Van Ham. B. Verrelst, F. Daerden, B. Vanderborght & D. Lefeber. Fast and Accurate Pressure Control Using On-Off Valves. International Journal of Fluid Power 6 (2005) No. 1 pp. 53-58

A3. R. Van Ham, B. Verrelst, B. Vanderborght, F. Daerden & D. Lefeber. Experimental results on the first movements of the pneumatic biped "Lucy". 6th International conference on Climbing and Walking Robots and the Support Technologies for Mobile Machines, Catania, September 2003, pp. 485-492.

Preface

Anyone who has ever been involved in the design and construction of a robot is aware of the efforts that are required in various fields of engineering: mechanics, electronics, software engineering, hardware engineering, control theory, etc. Those specifically involved in the design of walking robots will be fully aware of the loads of both theoretical and practical challenges. Such a task requires teamwork of people with various backgrounds and interests. Teamwork generally introduces problems not encountered by an individually working researcher, but also triggers the outcome of new ideas, applications and goals. The *Robotics & Multibody Mechanics* research group of the *Vrije Universiteit Brussel* makes no exception of this generality. The knowledge gained within the scope of this PhD work is not only restricted to bipedal robots (which is the main application discussed in this PhD), but also for orthoses, prostheses and rehabilitation robots. Recently, these applications are under study within the *Robotics & Multibody Mechanics* research group. However, the new insights and methodologies, elaborated on in this PhD, will be discussed within the scope of making efficient bipedal walking robots.

This work can be divided into two threads. Both are related to the development of actuators with adaptable compliance, and to the implementation in a prototype of an energy efficient bipedal walking robot, each with a specific control strategy. The first thread focuses on the optimisation of PPAM actuators, a kind of pneumatic artificial muscle, and is closely related to previous and ongoing research within the *Robotics & Multibody Mechanics* research group. Based on these actuators the bipedal walking robot *Lucy* was built with a specially designed pressure regulating valve system, and controlled by an inverted pendulum based trajectory generator and a joint trajectory tracking controller. The second thread starts with the development of an innovative actuator with adaptable compliance: MACCEPA. This electrical actuator opens new perspectives for the easy control of bipeds, as will be shown, since it embraces some interesting properties that have not been clustered together in previous designs. With this new actuator the biped *Veronica* was built and a novel strategy, *Controlled Passive Walking*, based on the online adaptation of the natural frequencies of the limbs, is implemented.

Chapter 1

Introduction

All truly great thoughts are conceived by walking
Friedrich Nietzsche

The research done in this work on bipedal walking robots has three main purposes. The first is the development of walking robots that can operate in a human environment, e.g. moving between and over obstacles and climb on stairs. These robots can be used as geriatric assistants, automated workers in dirty and dangerous environments, and even to help people in their house.

A second reason is to study human walking, both normal walking and gait disorders, by gait synthesis instead of gait analysis, as is usually done. Gait analysis is done by registering the motion of the joints of a human, while gait synthesis means building bipedal walking robots, based on human walking. This is actually restricted to actuated passive walkers, since they use similar natural mechanisms as humans to create the walking motion.

The third reason is to develop the technology, concepts and control strategies that is necessary for the design of orthoses, prostheses and exoskeletons. Also step rehabilitation robots can be built using the same concepts and technologies used in bipedal walking robots.

The current humanoid robots Asimo, HRP2 and Qrio are active controlled robots, meaning the joints are continuously controlled by a high bandwidth controller. This results in versatile robots, but their high energy consumption is their major drawback. To address this issue, bipedal walking robots can also be built based on the concept of passive walking. These robots use the natural dynamics to generate the walking pattern. Here the energy consumption is comparable to humans, but they are not as versatile as the active controlled robots, since the natural motions cannot be adapted online. A way to adapt the natural dynamics is to use actuators with adaptable compliance.

The *Robotics & Multibody Mechanics Research Group* of the *Vrije Universiteit Brussel* has performed extended research, both in the fields of bipedal walking and compliant actuators. In section 1.1 and 1.2, the research done on these topics in the research group is briefly described. Section 1.3 describes the authors' contributions:

- improvements to the PPAM
- design of a valve island with on/off valves and speed up circuitry
- bipedal walking robot Lucy with PPAM actuation
- development of MACCEPA actuator
- bipedal walking robot Veronica with MACCEPA actuation and a novel control strategy.

1.1 R&MM Research Group - Actuators with adaptable compliance

About ten years ago, the Pleated Pneumatic Artificial Muscle (PPAM), which is a type of pneumatic muscle, was developed at the *Vrije Universiteit Brussel* [1.01]. Pneumatic muscles are high power, lightweight actuators that are used to drive a joint directly, without gearing mechanism. The compressibility of air makes them inherently compliant, which can be exploited to absorb shocks. Moreover, when two muscles are used in an antagonistic setup to actuate a joint, the compliance of the joint can be adjusted. E.g. when the pressure in both muscles is increased, the joint becomes stiffer. When the pressure in one muscle is increased, and lowered in the other, the equilibrium position can be varied. The most widely known type of pneumatic muscle is the McKibben muscle [1.02], although it has some drawbacks such as the presence of considerable hysteresis, making precise position control difficult and imposing the necessity to have a threshold of pressure thereby preventing low working pressures. To overcome these drawbacks a new type of muscle, the PPAM, shown in figure 1.1, is developed. The muscle membrane layout is arranged into radially laid folds that can unfurl free of radial stress [1.01] when inflated. In this new design, the hysteresis is noticeably lowered and no threshold of pressure is required.

Fig.1.1: Asymmetric inflation of 1st generation PPAM

The limited life span of the muscles, due to the crumple of the fibres near the fittings, was the reason to start the development of a second generation PPAM's within the scope of this PhD, in cooperation with Björn Verrelst [1.03]. Figure 1.2 shows a picture of the second generation PPAM.

Fig.1.2: 2nd generation PPAM

In the first generation, the tension is transferred by the stiff longitudinal fibres, spread all over the surface of the membrane. This results in the pile-up and crumple of the fibres near the end fittings, since the deformation is different for a fibre at the top and at the bottom of a fold. When only a strand of stiff fibres is placed at the bottom of each fold, while the rest of the folded membrane is made out of a more flexible airtight material, each strand has the same deformation. Doing so ensures a more equal unfolding of the membrane, which is clear when comparing fig 1.1 and fig 1.2. As a result, the lifetime of the muscle increases drastically: from 20.000 for the 1st generation to more than 400.000 cycles for the 2nd during a durability test, moving a payload of 130 kg up and down, have been achieved. Because the height of the fold is the same along the longitudinal axis, a problem occurs: as the height of the folds is designed to unfurl completely in the centre, this results in a surplus of fold height close to the fittings.

To overcome this behavior, ways to obtain a variable height of the folds along the length of the muscle are investigated. The research of this third generation of muscles, shown in figure 1.3, is still in a conceptual phase. Besides the variable fold height, the new concept is oriented towards an automated production process.

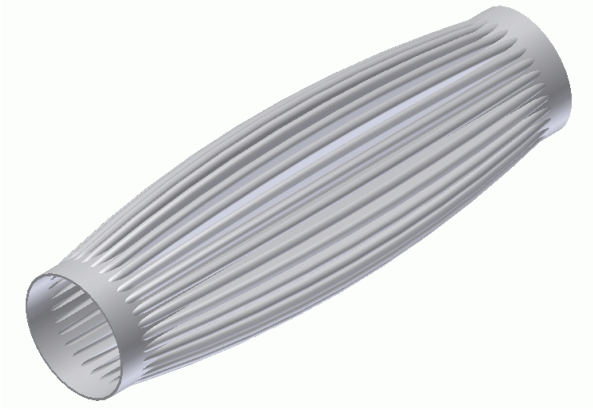

Fig.1.3: CAD Drawing of 3rd generation PPAM

Parallel to the improvements of the PPAM, other concepts to achieve adaptable compliance were studied. Muscles are very easy to use from a mechanical point of view, but the control is quite difficult because of the strong non-linear force-displacement relation. In a joint actuated by 2 PPAM, also the fact that the pressures, which should be set to achieve a certain equilibrium position, are dependent of the current position complicates the control. This results in the fact that to keep a certain equilibrium position in a moving joint, the required pressures in the muscles are varying. This will be further discussed in section 6.1.9. In case of autonomous robots, the local production or storage of pressurised air remains a problem. Also the fact that the pressure control valves are relatively heavy, contradicts with the use of lightweight actuators, depending on the application.

For these reasons, research was done to design a simple electrical actuator with adaptable compliance and energy storage. Existing electrically powered actuators with adaptable compliance are based on the antagonistic setup of 2 non-linear series elastic actuators [1.04], resulting in complex mechanisms or mechanisms with strong non-linear characteristics, as will be shown in chapter 3. Therefore, a new approach based on only one compliant element was chosen. By variation of the point to which the compliant element, e.g. a spring, is attached to, adaptable compliance can be achieved. The MACCEPA is a promising compliant actuator of this type, with a quasi linear angle-torque characteristic. A picture of a demo setup is given in figure 1.4.

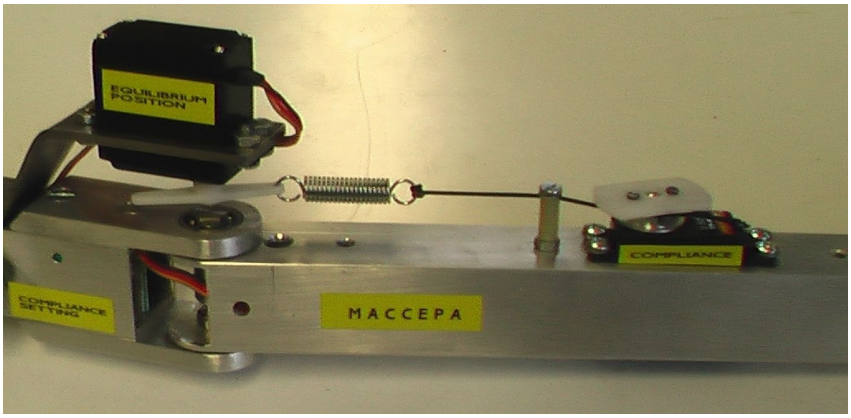

Fig.1.4: Demo MACCEPA setup

1. 2 R&MM Research Group - Bipedal walking robots

Some 15 years ago, Hans De Man started research at the *Robotics & Multibody Mechanics Research Group* of the *Vrije Universiteit Brussel* in the domain of legged robots, focussing on footless hopping monopods. He developed control strategies based on joint trajectories, generated according to objective locomotion parameters [1.05]. After evaluation of the developed theories in simulation, a real robot model, actuated by electrical drives, was built [1.06]. A picture of OLIE (One Leg Is Enough) is given in figure 1.5. The reflected inertia of the electrical motors makes the joints of the robot stiff, resulting in substantial load of the drive mechanism caused by impact at touch down.

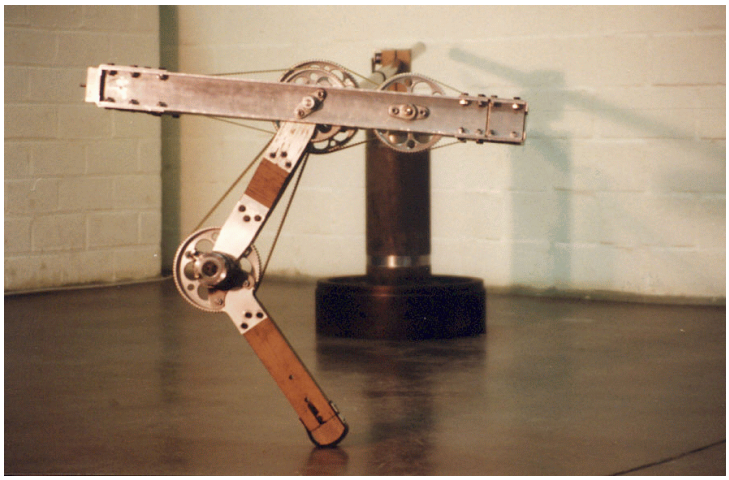

Fig.1.5: Hopping robot Olie (One Leg Is Enough)

Jimmy Vermeulen implemented these theories for a hopping robot with an actuated foot, in order to be able to provide small correcting ankle torques [1.07]. He extended the theory to a planar biped with quasi zero ankle torques, in order to position the zero moment point (ZMP) in the vicinity of the ankle joint [1.08]. The developed trajectory generator is

based on fast converging iteration loops, which makes the method suitable for real-time applications.

The development of the PPAM has led to a number of setups where the actuation is done by an antagonistic setup of 2 PPAM's. This allows to power a joint bidirectionally, while having inherent and adaptable compliance. To study the ability to store energy in dynamically walking robots actuated by PPAMs, a one-dimensional hopping setup [1.09] was studied, named Adam (figure 1.6). It was found that the energy losses could be compensated by exerting pressure pulses at specific moments in time.

Fig.1.6: ADAM, 1DOF hopping robot with PPAM

Approximately 5 years ago, the development of the walking robot *Lucy* [1.10] was started, in cooperation with Björn Verrelst and Bram Vanderborght. Lucy, shown in figure 1.7, is a planar biped with 6 joints, each actuated by 2 PPAMs of the 2nd generation [1.03]. Each leg has three 1 DOF joints: a hip, a knee and an ankle. The robot is connected to a frame with a horizontal, a vertical slider and a rotational joint to ensure lateral stability. The current control architecture consists of a trajectory generator and a joint trajectory tracking controller [1.11]. The trajectory generator calculates the required trajectories for the different joints based on objective locomotion parameters. The joint trajectory tracking controller [1.12] comprises three units: a computed torque unit, a delta-P unit and a

multilevel bang-bang controller. Until now the compliance of the muscles has not yet been exploited to decrease the energy consumption and to reduce the control efforts during walking. A compliance controller able to reduce control effort and energy consumption was developed for a single DOF pendulum [1.13]. Currently, research is done on a double pendulum of which the compliance is adapted as a function of the frequencies in the desired trajectory. If successful, this concept will be introduced in the control of the biped Lucy.

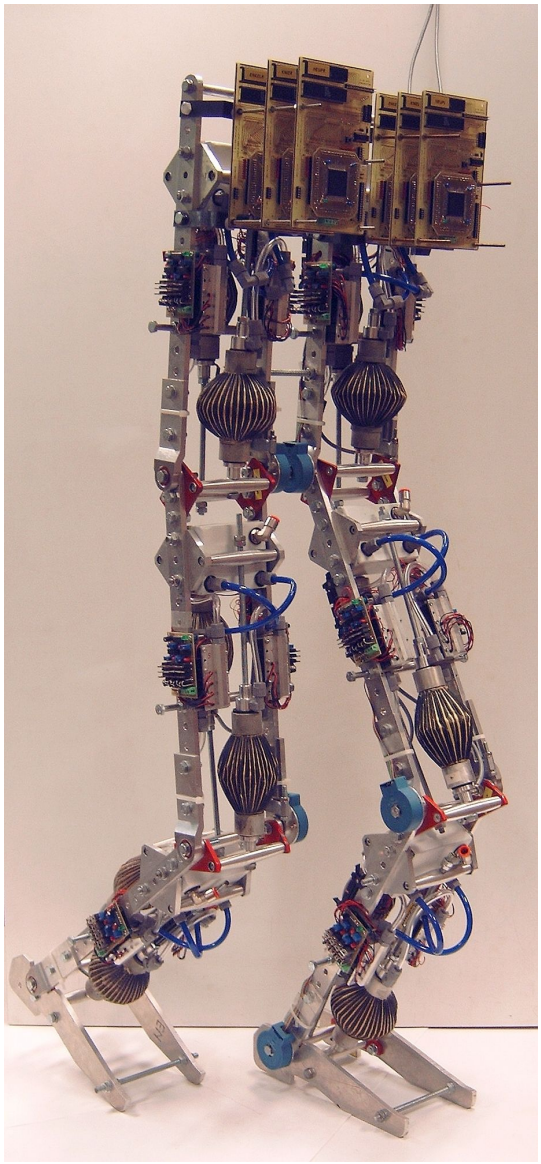

Fig.1.7: Lucy, biped with PPAM actuation

After the MACCEPA was developed, a new biped with these actuators was built: *Veronica*. The overall design is similar to Lucy: a planar biped with 6 DOF. Both for mechanical and electronic design, a modular approach has been chosen. In practice, this means that 3 MACCEPA

actuators are connected serially, to form one leg. The control strategy is based on passive walkers, but with the ability to control the compliance of each joint during walking. Therefore, this approach is called *Controlled Passive Walking*.

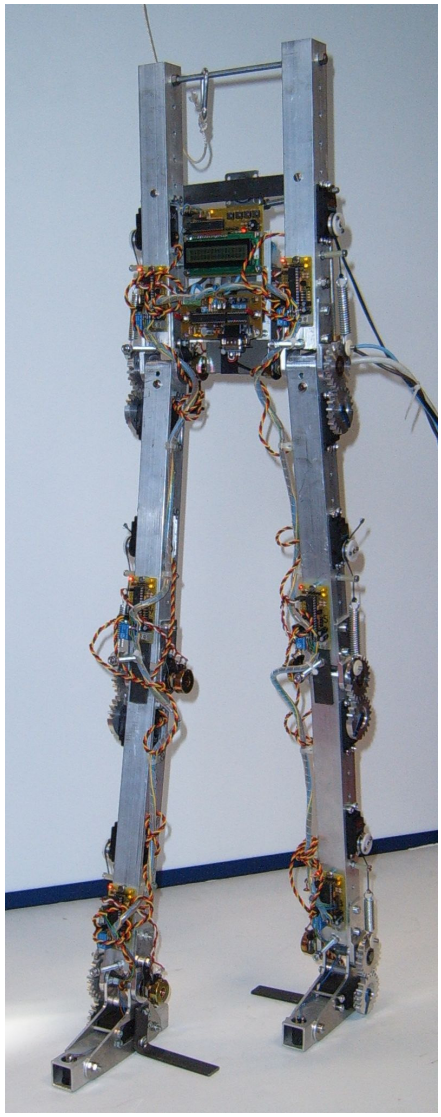

Fig.1.8: Veronica, MACCEPA powered biped

1.3 Own contributions

As mentioned before, the own work done during the PhD is based on two different actuation technologies, the *PPAM* and the *MACCEPA*. The topics addressed during this PhD are:

- PPAM design 2nd generation
- 1 DOF hopping robot
- Valve island with on/off valves and speed up circuitry

- Bipedal walking robot Lucy with PPAM actuation
- 1 DOF Pendulum with compliance adaptation
- PPAM design 3rd generation

- Development of MACCEPA and design of 1 DOF setup
- Bipedal walking robot Veronica with MACCEPA actuation
- Concept of Controlled Passive Walking

The research done on the PPAM and the design of the bipedal walking robot Lucy was done in cooperation with Björn Verrelst and Bram Vanderborght. This research is described thoroughly in a number of publications. The development of the valve island with on/off valves and speed up circuit [1.15], the MACCEPA actuator and design and control of the Controlled Passive Walking biped Veronica is mainly own work. The research on the latter two started more recently and the number of publications on this topic is lower. Therefore this text focuses specifically on the research on the MACCEPA and on the Controlled Passive Walking biped Veronica.

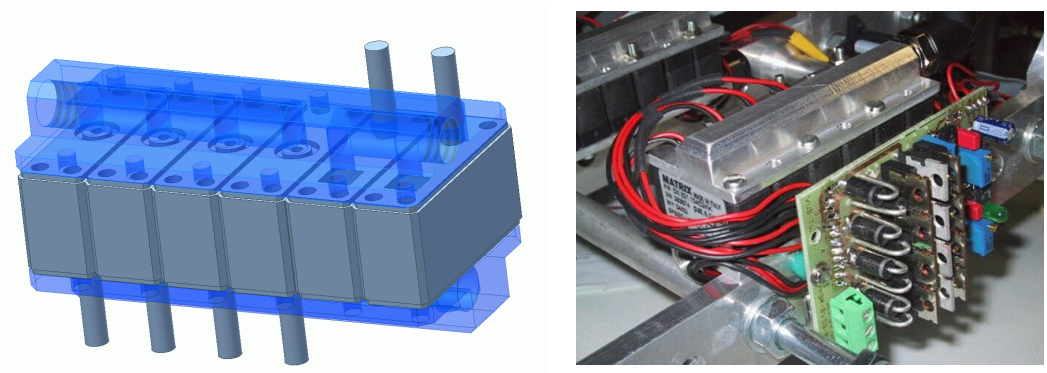

Fig.1.9: CAD drawing of valve island and picture of complete pressure regulating valve

To give an overview of the preceding work on the PPAM and its applications, three papers are included in the appendix. The first paper describes the design and control of a joint, actuated by an antagonistic setup of two PPAM's [1.14]. It is shown how both the equilibrium position and the compliance of the joint can be controlled. A second paper [1.15] describes the development of an enhanced speed-up circuitry for on/off valves used in the pressure regulating valve island. The reason for this research was the lack of commercial available low-weight and fast acting pressure regulating valves. The third paper discusses the mechanical and electronic design of the biped Lucy [1.16]. In this paper, results of the first movements of the biped are given as well.

Since this text reports on new concepts in two fields—walking robots and compliant actuators—the state of the art of each of them is given in

chapters 2 and 3 respectively. Chapter 2 describes the two main approaches in bipedal walking: active controlled bipeds and passive walkers. The first type is based on the precise control of each joint angle, while the latter is based on the tuning of the natural frequencies of the limbs. A short introduction to the idea of Controlled Passive Walking, which could be seen as an intermediate approach, is given at the end of chapter 2. In the same chapter the need for actuators with adaptable compliance for Controlled Passive Walking is shown.

In chapter 3, an overview of existing actuators with adaptable compliance is given. The different designs are divided into three categories. The working principle of the first category is based on the antagonistic setup of two non-linear springs. This group also includes a joint actuated by two PPAM's, as used in the biped Lucy. A second group, named Structural Controlled Stiffness, is based on the variation of elastic properties of the compliant element. Making e.g. the length of the compliant element very short results in a very stiff state, which is not possible with e.g. two pneumatic muscles since their pressure is limited. A third category is called Mechanically Controlled Stiffness. Here the compliance can be adjusted by a variation of the fixation points where the elastic element is attached. One of the designs presented in this category is the MACCEPA actuator.

In chapter 4 the working principle of the MACCEPA concept, which is patented, is explained in more detail. An equation for the torque as a function of the angle between actual position and equilibrium position is derived. The influence of the design parameters is described and a linearised equation, valid between approximately -60° and 60° is given. The placement of the different components is discussed and some special embodiments are given. The extension to 2 and 3 DOF joints of the MACCEPA concept is shown with examples. The section concludes with a summary of the advantages and disadvantages of the concept.

In chapter 5, both the mechanical and electronical design of the biped Veronica is discussed. It is a planar biped with six 1 DOF pin joints. The overall design is done in a modular way. Each joint consists of a MACCEPA actuator. On each joint a PIC microcontroller is placed, which controls the motors, reads the angle and angular velocity of the joint and handles the communication. The overall control software runs on a standard PC. Both hip joints are linked, using a bisecting mechanism, to keep the upper body upwards. The angle of the knee joints is limited, so they cannot be overstretched.

Chapter 6 describes the concept of Controlled Passive Walking. The concept is introduced by means of a 1 DOF joint with a MACCEPA

actuator. The main idea is that the natural frequencies can be adapted in such a way that the resulting natural motion can be used for bipedal walking. This is actually what is done in passive walkers. However for most passive walkers the frequency of the limbs is fixed during design, since the tuning is done by variation of the mass distribution in the limbs. With Controlled Passive Walking the natural frequencies can be adapted by the compliance settings of the actuators, and thus can be varied during normal operation. To conclude the chapter, walking experiments with Veronica are discussed.

Finally chapter 7 gives a summary and some general conclusions of this work.

References:

[1.01] F. Daerden. Conception and realization of pleated pneumatic artificial muscles and their use as compliant actuation elements. PhD Thesis, Vrije Universiteit Brussel, July 1999.

[1.02] H. F. Schulte. The characteristics of the McKibben artificial muscle. The Application of External Power in Prosthetics and Orthotics. Publication number 874, pp. 94–115. National Academy of Sciences–National Research Council, Lake Arrowhead, 1961.

[1.03] B. Verrelst , R. Van Ham, B. Vanderborght, D. Lefeber, F. Daerden & M. Van Damme. Second Generation Pleated Pneumatic Artificial Muscle and Its Robotic Applications, Advanced Robotics, accepted for publication in 2006

[1.04] G. Pratt and M. Williamson, Series elastic actuators. Proceedings of the IEEE/RSJ International Conference on Intelligent Robots and Systems (IROS-95), Vol. 1, Pittsburg, PA, July 1995, pp. 399–406.

[1.05] H. De Man, D. Lefeber, F. Daerden and E. Faignet. Simulation of a new control algorithm for a one-legged hopping robot (using the multibody code mechanica motion), Proceedings of the International Workshop on Advanced Robotics and Intelligent Machines 1996, Manchester, UK.

[1.06] H. De Man, D. Lefeber and J. Vermeulen. Design and control of a robot with one articulated leg for locomotion on irregular terrain. Proceedings of the 12th Symposium on Theory and Practice of Robots and Manipulators, 1998, Paris, France, pp. 417–424.

[1.07] J. Vermeulen, D. Lefeber and B. Verrelst. Control of foot placement, forward velocity and body orientation of a one-legged robot. Robotica, Vol. 21, 2003, pp. 45–57.

[1.08] J. Vermeulen, B. Verrelst, D. Lefeber, P. Kool and B. Vanderborght. A real-time joint trajectory planner for dynamic walking bipeds in the sagittal plane. Robotica, Vol. 23, Issue 06, november 2005, pp. 669-680

[1.09] B. Verrelst, F. Daerden, D. Lefeber, R. Van Ham, T. Fabri. Introducing Pleated Pneumatic Artificial Muscles for the actuation of legged robots: a one-dimensional setup. CLAWAR 2000: 3rd International Conference, Madrid, October 2000, pp. 583–590.

[1.10] B. Verrelst, R. Van Ham, B. Vanderborght, F. Daerden & D. Lefeber. The Pneumatic Biped "LUCY" Actuated with Pleated Pneumatic Artificial Muscles. Autonomous Robots 18, pp.201-213, 2005

[1.11] B. Vanderborght, B. Verrelst, R. Van Ham & D. Lefeber. Controlling a Bipedal Walking Robot Actuated by Pleated Pneumatic Artificial Muscles. Robotica, accepted for publication in 2006

[1.12] B. Verrelst, J. Vermeulen, B. Vanderborght, R. Van Ham, J. Naudet, D. Lefeber, F. Daerden & M. Van Damme. Motion Generation and Control for the Pneumatic Biped "Lucy". International Journal of Humanoid Robotics (IJHR), Vol. 3, No. 1 (2006) pp. 1-35

[1.13] B. Vanderborght, B. Verrelst, R. Van Ham, M. Van Damme, D. Lefeber , B. Meira Y Duran & P. Beyl. Exploiting natural dynamics to reduce energy consumption by controlling the compliance of soft actuators. The International Journal of Robotics Research (IJRR), Vol. 25 Issue 4, april 2006, pp. 343-358

[1.14] R. Van Ham, B. Verrelst, F. Daerden & D. Lefeber. Pressure control with on-off valves of Pleated Pneumatic Artificial Muscles in a modular one-dimensional rotational joint. International Conference on Humanoid Robots, Karlsruhe and Munich, October 2003, abstract p. 35 + CDROM.

[1.15] R. Van Ham, B. Verrelst, F. Daerden, B. Vanderborght & D. Lefeber. Fast and Accurate Pressure Control Using On-Off Valves. International Journal of Fluid Power Vol. 6 (2005) No. 1 pp. 53-58

[1.16] R. Van Ham, B. Verrelst, B. Vanderborght, F. Daerden & D. Lefeber. Experimental results on the first movements of the pneumatic biped "Lucy". 6th International conference on Climbing and Walking Robots and the Support Technologies for Mobile Machines, Catania, September 2003, pp. 485-492.

Chapter 2

Active and passive walking robots

Some leaders have strived to have full control over people, but history taught us that probably it is better to wonder what people want to do themselves. Maybe history will teach us also that for some mechanical applications it is better to use the natural behaviour than forcing unnatural motions. Bipedal walking might be the pioneering application.
(Ronald Van Ham)

In the field of walking robots two main approaches can be distinguished. On one side are the—by far most popular—actively controlled bipeds. These robots, which have demonstrated smooth and versatile motions, are based on the mainstream control paradigm: precise joint-angle control. This means that all joints are controlled continuously to track a specific trajectory. In general this requires actuators with higher precision and faster response than human muscles have [2.01]. A high bandwidth controller and sufficient data communication bandwidth between controller and actuators is necessary as well. The employability of this type of robots is restricted due to the relatively high power consumption of these robots. To address this issue, passive-dynamic walkers were proposed as a new design and control paradigm [2.02]. In contrast to mainstream robots, which actively control every joint at all times, passive-dynamic walkers do not control any joint at any time. Although these walkers have no actuation or control, they can walk downhill with remarkably humanlike gaits [2.03]. The walking motion is achieved by tuning the mass distribution in the limbs. These down-hill passive walkers are however of little practical use. Replacing gravitational power by actuator power results in a class of level-ground walking passive-dynamic machines [2.04]. To actuate a passive-dynamic machine, compliant actuation is used, e.g. series elastic actuator or pneumatic muscle. The major consequence of the current design concept of passive-dynamic bipeds is that they can only walk at a predefined walking speed and that they encounter difficulties to start and stop. This is so, because they are tuned to walk in a specific limit cycle, which means that the conditions at the end of each step exactly match the start condition. If the starting conditions are within the basin of attraction a stable walking motion is obtained, as explained in section 2.2. When adaptable compliance is introduced, the capabilities of passive-dynamic walking robots can be extended, while the low energy consumption and the relative simple control are preserved. Since the concept, which we will introduce, is based on passive-dynamics, while requiring minimal control, we propose to name this concept *Controlled Passive Walking* (CPW).

In section 2.2, a short overview of the actively controlled walking bipeds is given. The real passive walkers, which can only walk down a slope, are discussed in section 2.3, while the level-ground passive walkers are discussed in section 2.4. Section 2.5 explains why the elaborated system in this work is based on passive walkers. The basic principles of controlled passive walking are addressed shortly in section 2.6, and more details on CPW are found in chapter 6.

2.1 Active walking bipeds

Active walking bipeds is a group name for all bipedal walking robots using the control paradigm of precise joint-angle control. A central processing unit generates trajectories, fulfilling certain locomotion behaviour, such as desired walking speed and boundary conditions such as Zero Moment Point (ZMP) stability criteria [2.05]. The generated joint data are sent to the local controllers of the actuators at each sample time. The position—and if required the velocity—of each joint is measured, and compared with the required values. The actuators are controlled continuously to follow the imposed trajectory, usually in closed loop. This control structure is the same as used in most industrial robots. This is not a coincidence: the control strategies and technology of active walking bipeds are based on—or even copied from—the existing industrial robots. Also the existing actuators e.g. electrical servo motors, hydraulic and pneumatic drives are used in walking bipeds. For industrial robots, the weight of the actuators is not such an important design constraint as it is for walking machines. Industrial robots are placed on a solid base, fixed on the ground, in contrast with walking bipeds.

One of the main issues of a walking biped is the overall stability, since it is a dynamically unstable machine. The control of active walking bipeds requires new high level control strategies, although the control strategy is still based on generating trajectories. Trajectories for each joint should be designed in such a way that a stable step pattern is generated, which achieves the desired step length and walking speed. Some ways to generate the step patterns are the zero moment point approach [2.05], [2.06], the hybrid zero dynamics approach [2.07], [2.08], the inverted pendulum approach [2.09] and the virtual model control [2.10]. In general, these approaches require significant computing power since they are model-based. Joint trajectories can also be generated with a non model-based approach, e.g. hand-designed trajectories [2.11]. The latter example requires less computing power, but is still based on the principle of precise joint-angle control.

The major advantage of the ability of controlling the angle of each joint is that the robot can perform almost every motion, within the angle, velocity and torque limits of the actuators and within the stability limits of the robot. Some examples of actively controlled humanoid robots are the ASIMO (Honda) [2.12], QRIO (Sony) [2.13], Partner Robot (Toyota) [2.14] and HRP2 (Kawada Industries) [2.15], which are able to perform a variety of tasks. It is worth mentioning that all of these examples are Japanese. Both the Japanese government and the Japanese industry invest heavily in the development of humanoid robots. In Japan strong belief exists that

such robots will become the geriatric assistants of the future. On the other hand, the robots contain the latest hi-tech realizations of the companies building them, and so they are built to stand up to the competition.

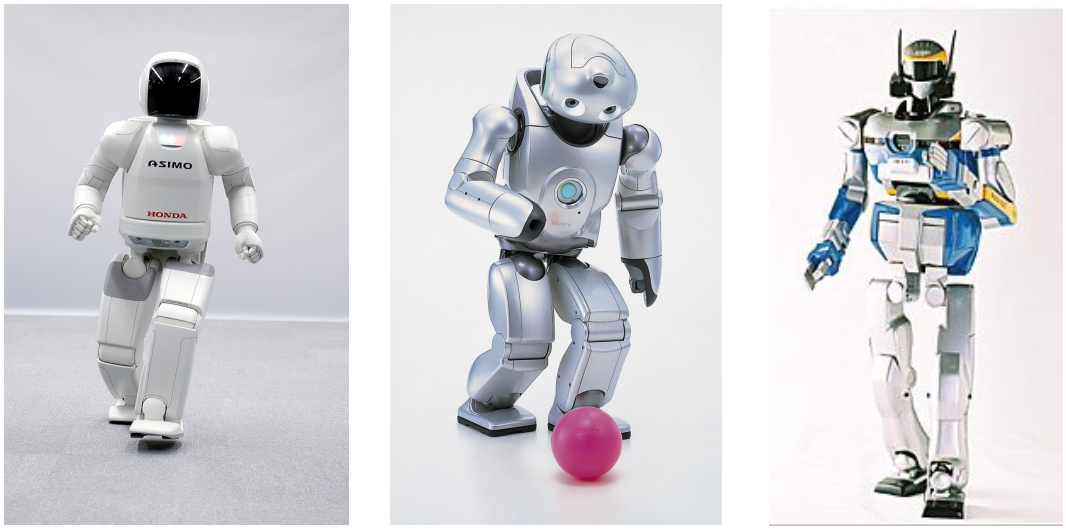

Fig.2.1: ASIMO (Honda), QRIO (Sony) and HRP-2 (Kawada Industries)

South Korea has built a number of humanoids as well, e.g. the Korea Advanced Institute of Science and Technology has built a series of humanoids, with the latest model KHR-3 (HUBO) [2.16]. A joint venture of the Kist Korean Institute and Samsung Electronics developed the Humanoid robot RX. The newest Chinese robot named "Huitong" has a sword-fighting ability.

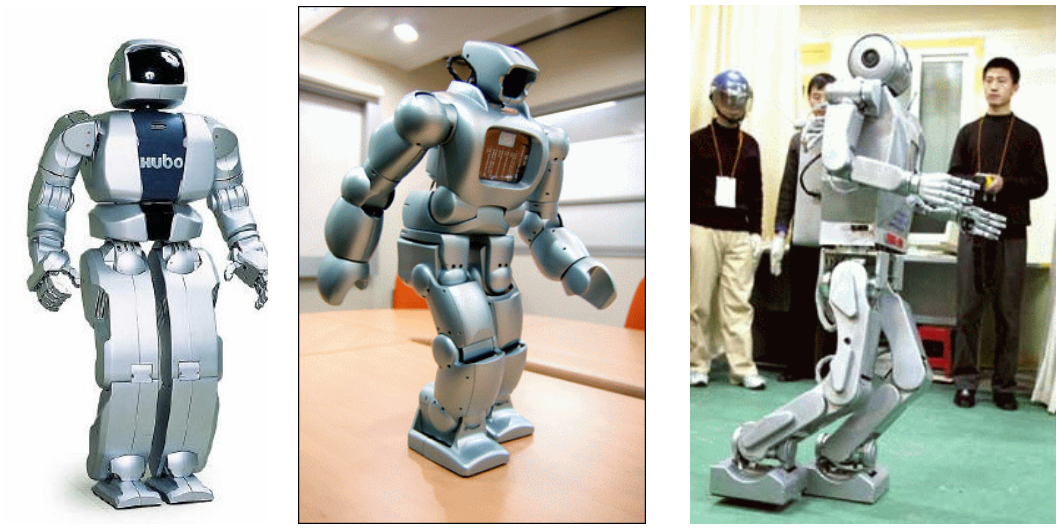

Fig.2.2: Hubo KHR-3 (Korea), Humanoid robot RX(Korea) and Huitong (China)

In the rest of the world, humanoid robots are also built, but due to the more restricted budgets they are less attractive and more research oriented machines. Although missing the fancy appearance, the control strategies used are not less innovative. In Germany, the Technische Universität München built the biped Johnnie [2.17], and the Universität Hannover developed the Bipedal Autonomous Robot BARt-UH [2.18]. At the Vrije Universiteit Brussel, Lucy, a biped actuated with pneumatic muscles, was built [2.19]. At Inria, France the Bipop team works on the BIP robot [2.20]. The Research Institute of Nantes in France and the University of Michigan have developed control software that allows the two-legged under-actuated robot Rabbit to walk naturally and even to run [2.21]. In France the Rabbit robot [2.22] is a test platform, designed to advance the fundamental understanding of bipedal walking. In a joint project, researchers form the University of Göttingen, the University of Glasgow and the University of Stirling recently developed Runbot [2.23]. This 2D robot is currently the fastest walking robot, in terms of leg length per second, in the world. Some of these realisations are shown in figure 2.3.

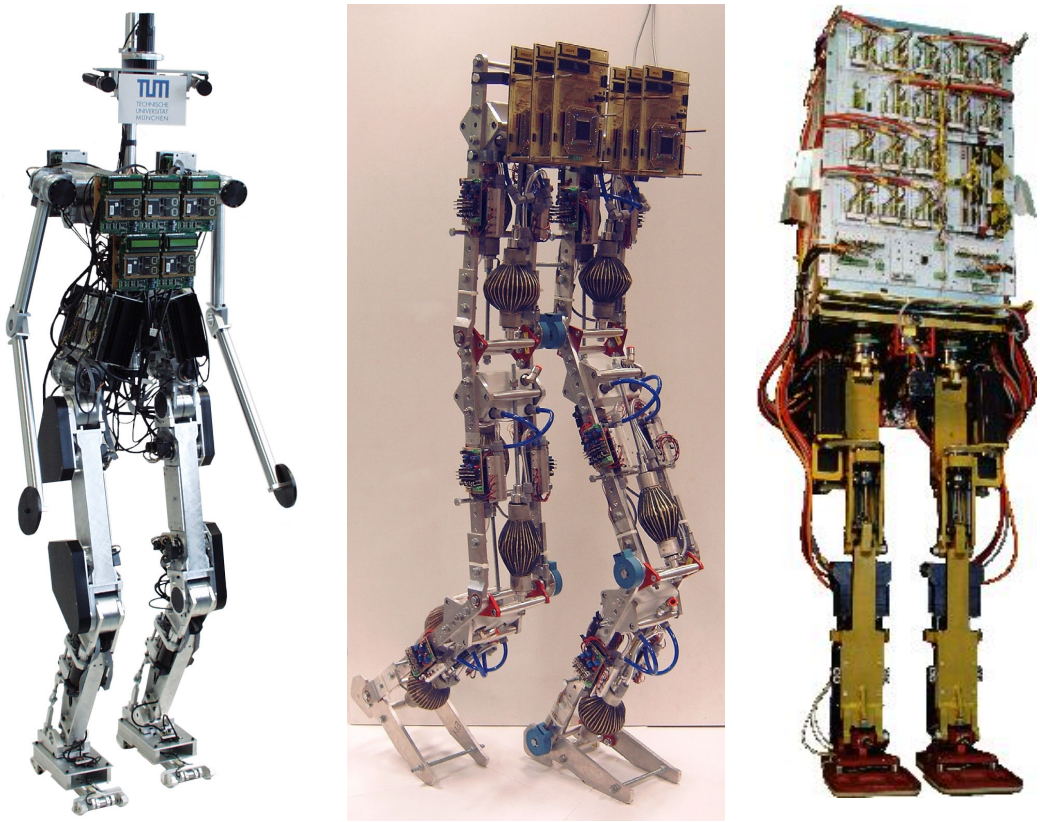

Fig.2.3: Pictures of Johnnie (Germany), Lucy (Belgium), Bip (France)

While having the ability to perform a variety of motions, the major drawback of actively controlled bipeds is the high energy consumption.

Since the generated trajectories do usually not correspond to natural motions of the legs and since stiff actuators are used, continuous control of the actuators is required, and energy is thus consumed continuously.

2.2 Passive walking robots – walking down a slope

In the previous paragraph, the actively controlled bipeds were discussed. Their major drawback is the high energy consumption, when compared to humans [2.24]. A solution for this is the exploitation of the *natural dynamics* of the locomotive system. In 1989, McGeer [2.02] introduced the idea of *passive dynamic walking*, inspired by research of Mochon and McMahon [2.25]. They showed that the motion of the swing leg in human locomotion is merely the result of gravity acting on an unactuated double pendulum. McGeer extended the idea and showed that a completely unactuated and therefore uncontrolled robot can perform a stable walk [2.26]. The intelligence needed for walking is comprised in the design of the robot and not in the control. A passive dynamic walker has to be launched with such initial values of the leg angles and velocities, that they are nearly identical to the starting conditions of each subsequent step. This will result in a periodic or cyclic walking motion, requiring a minimal energy input to compensate friction losses and impact losses at heel strike. These losses can be compensated by making the robot walk down a slight slope.

The simplest system that can perform a passive dynamic walking motion consists of two rigid legs interconnected by a passive hinge. The legs are not articulated and thus act as single pendulums. Since the feet cannot be lifted, space must be provided to allow the leg to swing from the back to the front. In passive walking toys, dating back to the 1800s [2.27], specially designed feet make the body toddle. This causes the feet to be lifted out of the sagittal plane. Another solution is to equip the slope with blocks placed at the footholds of the robot. This way, the leg can swing freely between the blocks and end up on top of the next block, while preserving the two-dimensional motion.

In figure 2.4, a prototype of a two-dimensional passive dynamic walking robot with non-articulated legs is shown. Actually, four legs are used for lateral stability, but the two inner and the two outer are interconnected. For this *simplest walker*, the stance leg acts as an inverted pendulum, while the swing leg is a normal pendulum whose hinge point moves. By changing the moments of inertia of the legs and the slope angle, the natural frequencies of the pendulums can be tuned to obtain a certain step length and step speed.

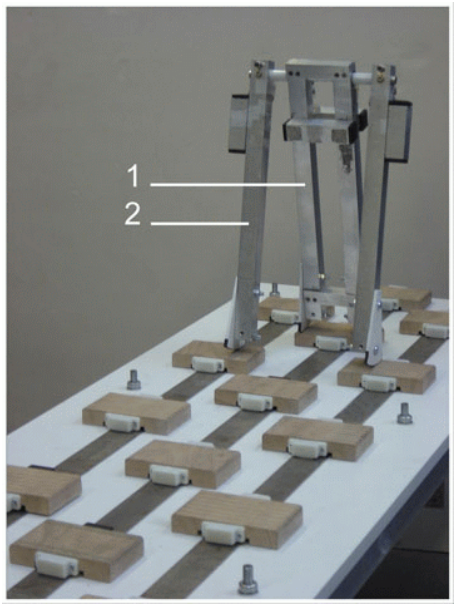

Fig.2.4: Prototype of a passive dynamic walking robot with four legs (two-dimensional walking behaviour), walking on slope equipped with blocks.

The motion patterns have to be cyclic for periodic walking, meaning that the end condition of a step should be equal to the start condition. Depending on the stability of the system, a certain error is allowed. To visualize the concept, a phase graph of a walking motion can be used [2.28]. In figure 2.5, a phase graph with three parameters is shown. Note that the simplest walker has four parameters in phase space: two joint angles and two angular velocities.

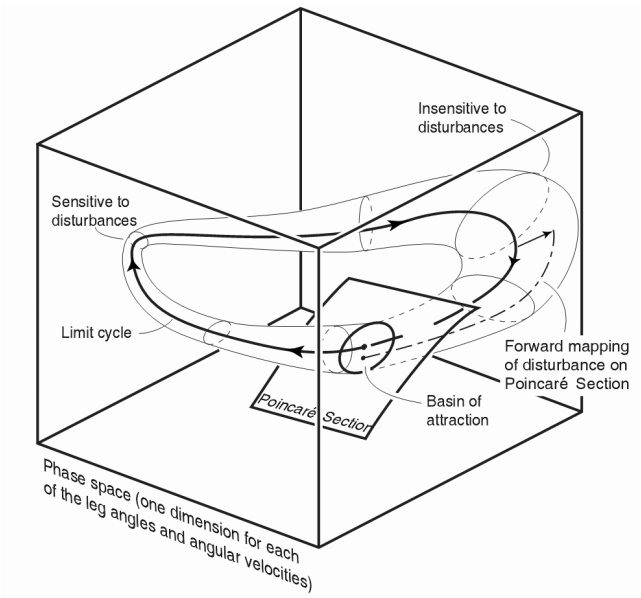

Fig. 2.5: 3D phase graph for stability analysis of cyclic (walking) motions. [2.28]

In the ideal case, when there are no disturbances, the limit cycle describes the evolution of the state variables. At every moment of the limit cycle, a basin of attraction can be defined. When a disturbance within this basin occurs, the system will be attracted to its limit cycle. A disturbance outside this region will result in an undesired behaviour, and will probably make the robot fall. When the basins of attraction of all points of the limit cycle are connected, a tube around this limit cycle is formed. A variation of the *diameter* of the tube means that the sensitivity with respect to disturbances of the robot varies within the time of a single step.

Passive dynamic walkers can also be built with articulated legs, thus having two legs with knee joints, resulting in two double pendulums. The knee can bend to achieve the necessary space to be able to swing the leg to the front. A slope without blocks thus can be used. Simulations of passive walkers with articulated legs were performed by McGeer [2.26], Garcia [2.29] and Dankowicz [2.30]. In figure 2.6 a design of a passive walker by McGeer with articulated legs is shown, which is built by Garcia et al. [2.29]. It is worth mentioning that a system to lock the knee is required when using articulated legs. As shown in figure 2.6, a mechanism is placed in the knee to prevent the lower leg to overstretch, resulting in stretched legs during the stance phase. The stretched leg can support the weight of the robot without consuming energy, unlike most active controlled bipeds, which generally walk with bend knees avoiding as such the singular position of the knee joint.

Fig.2.6: Close copy of McGeer's walker by Garcia [2.29]

The practical use of passive dynamic walkers is actually restricted to toys and to research in order to understand the fundamentals of walking. Nevertheless, they are the groundwork to build actuated passive dynamic walkers, which are able to walk on level ground. In the next paragraph, some of these robots will be discussed.

2.3 Passive walking robots on level ground

To make passive walkers walk on level ground, a minimal actuation is required. Of course these robots are not purely passive anymore since actuation is used, but they are based on the same concepts. Hurmuzlu [2.30], Spong [2.32], Van der Linde [2.33] and Asano [2.34] studied 2D models where some form of actuation was added. Wisse [2.35], Piiroinen [2.36], Adolfsson [2.37], Kuo [2.38] and Mombauer [2.39] simulated 3D models.

At this moment, an increasing number of research groups are building state-of-the-art actuated passive walkers [2.24]: the Biorobotics and Locomotion Lab at Cornell University [2.40], the Delft Biorobotics Laboratory [2.41], the Computer Science and Artificial Intelligence Laboratory at MIT [2.42] and the department of Adaptive Machine Systems of the Osaka University [2.43]. All of them are building walking robots, based on the concept of passive dynamic walking.

Figure 2.7a shows the Cornell biped, which is actuated with electrical motors that are used to tension a spring connected to the joints. Denise, a biped from Delft (figure 2.7b) and Que-Kaku, form Osaka (figure 2.7c) are actuated by pneumatic artificial muscles. Both the electrical motors with springs and the pneumatic muscles are compliant actuators, meant to compensate the energy lost due to friction and impact. All three bipeds demonstrate that walking can be accomplished with extremely simple control. These robots do not rely on sophisticated real-time calculations or on substantial sensory feedback from continuous sensing of angles, velocities, forces and/or torques. The control is based on sensing the touch down of the feet, and then taking the appropriate control action, e.g. increase the pressure in a muscle, or increase the pre-tension of the spring. This means that there is no continuous control; only some control actions are taken during the course of a step. E.g. in Que-Kaku, the duration of the increased pressure in the muscles is modified to achieve stable walking on different terrains.
The control of the MIT biped Toddler (figure 2.7d) is based on reinforcement learning. The robot is able to adapt itself to different terrains like e.g., bricks, wooden tiles and carpet as it walks. Though actuated by electrical motors, the control of the robot is based on passive walking. Recently, the Delft Biorobotics Laboratory built a new passive walker, actuated with electric motor, in series with a spring [2.44].

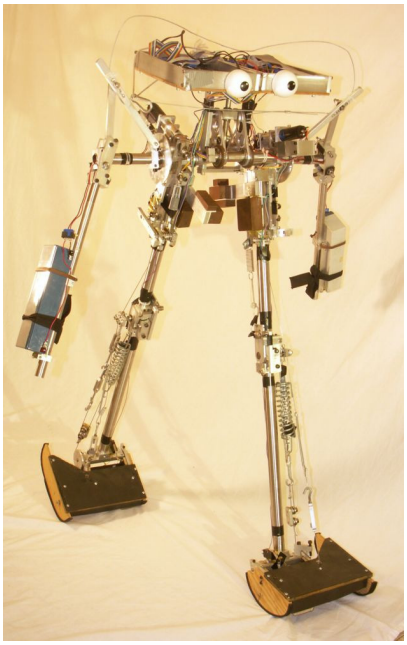

a) The Cornell biped

b) The Delft biped Denise

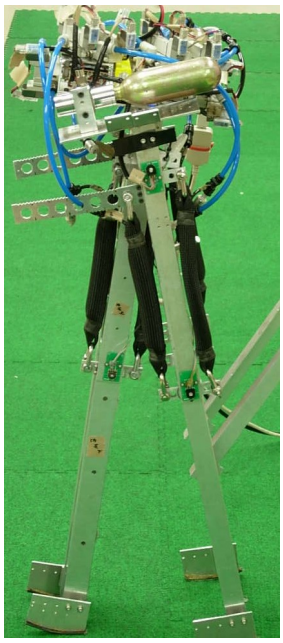

c) Que-Kaku V20 From Osaka

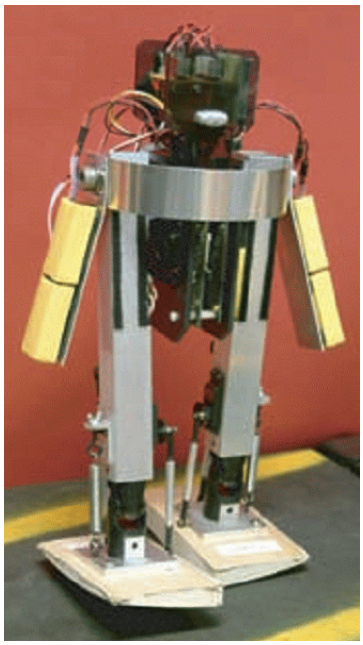

d) The MIT learning biped

Fig.2.7: Pictures of state-of-the-art passive walkers

The presented state-of-the-art prototypes of 3D actuated passive walking robots are very humanlike and walking efficiently. The applicability is however restricted due to the limited number of combinations of possible natural motions.

2.4 Starting point to develop a multi purpose energy efficient walker

In figure 2.8, an overview of the evolution of bipedal robots is given. On the left side the active controlled bipeds, based on the ideas and control strategies used in industrial robots are represented. The control paradigm based on precise joint-angle control results in the ability to perform an almost unlimited number of motions within the limits of overall stability. The major drawback is the high energy consumption, reducing the autonomous working time. The actuators and joint tracking control strategies are mainly based on technology used for industrial robots. On the right side of figure 2.8, passive-dynamic walking bipeds are shown. The major drawback of these bipeds is that they have one walking speed which is defined during design. Since the number of possible motions is very restricted, they have difficulties to start and stop. However they have the advantage of high energy efficiency, comparable to the efficiency of humans [2.04].

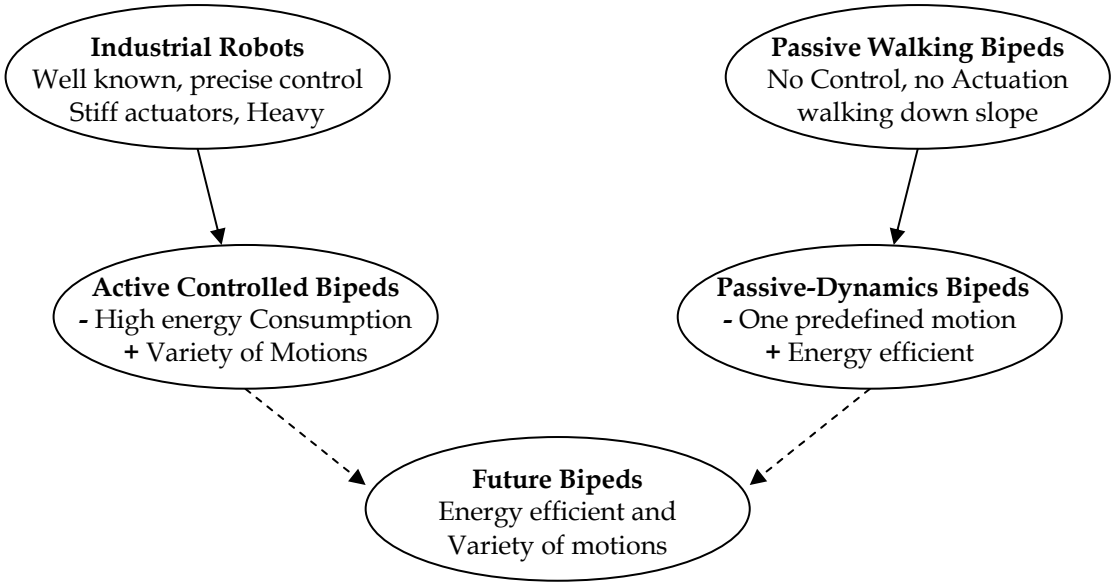

Fig.2.8: Evolution of walking robots

Currently, research is done on both types of bipeds to develop a bipedal robot that is both energy efficient and able to perform a variety of motions. In [2.45] the concept of Active Variable Passive Stiffness (AVPS) is introduced. The idea is to adapt the compliance of the actuators in a passive walker to obtain the desired natural motion. In the *Robotics and Multibody Mechanics Research Group* of the *Vrije Universiteit Brussel* the active controlled robots are used as a starting approach for the biped Lucy

[2.46]. The joint tracking controllers follow the calculated trajectories, while a compliance controller should adapt the compliance in order to lower the energy consumption. Actually the goal to lower energy consumption is the same for both, only the starting point differs. Adherents of both approaches are convinced that their starting point is the best to come to the ultimate energy efficient multi-purpose bipedal walking robot.

Therefore, I will express some thoughts based on my personal point of view, to stress why I think passive walkers are the best starting point to build a walking robot. Some of these thoughts may not be scientifically rigorous.

-When looking at myographical data of human cyclic walking [2.47], it can be seen that there is only muscle activation in the beginning of a swing motion. In the intermediate time no data is sent. This contradicts with active controlled walking, which requires a continuous stream of data between controller and actuators.

- Human muscles have lower frequency response than actuators required for active controlled walking. Why would one use actuators and controllers with a higher bandwidth than is required for normal walking?

-When trying to imitate human walking, it is important to understand the basic principles. Starting form the passive walkers, researchers have to understand the principles of efficient human walking [2.48], which is not the case with active controlled robots. Thus the way to learn the most about human walking, which is a marvellous example, is starting from passive walkers.

- The passive dynamic walkers have a very humanlike motion, without any control. Wouldn't it be easier to add a minimal control to adapt these energy efficient motions, than to generate completely new, artificial and energy consuming motions?

- Control and mathematics have become an addiction for some researchers, which prevents them to see the simple and straightforward solutions, 'invented' and thoroughly tested by nature, that do not require complex calculations.

Although realizing that these thoughts can be subject to discussion, they are my reasons to start from the passive dynamics approach.

In the next paragraph a novel approach—actually an extension of the passive-dynamic walking on level ground—is introduced.

2.5 Principle of Controlled Passive Walking (CPW)

Passive dynamic walking is based on the natural motion of a pendulum. To explain the concept of controlled passive walking, some basic theory about a pendulum is required. To simplify the explanation, the effects of gravity will be neglected by using a torsion pendulum. In figure 2.9, a didactic setup is shown with a solid disc with mass M and radius r. The disc hangs on a massless torsion wire at a fixed point. The angular displacement from its equilibrium position is called α. The torque T applied by the wire on the disc is linearly proportional to the displacement α. This can be written as:

$$T = -\kappa.\alpha \tag{2.1}$$

where κ is the torsion spring constant of the wire. The natural rotation frequency f of the torsion pendulum is given by:

$$f = \frac{1}{2\pi}\sqrt{\frac{\kappa}{I_p}} \tag{2.2}$$

where I_p is the polar moment of inertia of the disc.

Fig.2.9: Didactic torsion pendulum setup.

Most physics textbooks in which this example is given, explain how the natural frequency can be influenced by the moment of inertia of the object. Often this is illustrated with a dancer who changes his rotational velocity by stretching the arms when making a pirouette. Note that this is also the

way passive walkers are designed: by tuning the masses and their position, the moment of inertia of the limbs is defined, and thus also the natural frequency.

Looking at formula 2.2 reveals that the parameter κ can also be used to change the frequency. When using another torsion wire, with a different torsion constant, the natural frequency will also change. Both adjustments, varying the moment of inertia or changing torsional stiffness of the cable can easily be performed before the motion is activated, but are not easily adapted during the motion itself. A possible way to vary κ online is to increase or decrease the length of the torsion wire. The longer the length of the cable, the lower the torque will be for a certain angle, and thus the lower the natural frequency will be:

$$T = \left(\frac{G.I}{L} \right).\alpha \tag{2.3}$$

Another parameter that can be adjusted and that does not influence the natural frequency, is the equilibrium position. This is the position where the torsion wire does not apply a torque on the disc. This is also the symmetric position for all the natural motions of the torsion pendulum. By rotating the cable at the fixation point at the top, the equilibrium position can be set.

A fourth parameter that influences the motion of the pendulum is damping, resulting in energy dissipation. In case of the didactic setup, there is air friction causing damping. Since the basic idea of passive-dynamics is energy efficiency, methods to increase energy dissipation will not be discussed here.

The possible ways to adapt the natural motion of the torsion pendulum can be transferred to passive bipeds walking down a slope. The natural frequency of the legs is tuned during the design to match the required step length. This is comparable with changing the moment of inertia of the disc in the torsion pendulum example. When a torsion spring is used, of which both equilibrium position and compliance can be adjusted online, a variety of natural motions and thus walking speeds are possible. The moment of inertia of the limbs can be used as a prescaler of the natural frequency. This defines the range of natural frequencies that can be obtained by adapting the compliance.

Besides the actuation by push off of the feet [2.03], level ground passive walkers can also be actuated by adapting the equilibrium position of a spring. In this way, energy can be put in a passive-dynamic system. Wisse [2.49] uses an antagonistic setup of a spring and a pneumatic muscle as

actuator in the knee joint, as shown in figure 2.10. The relative pressure in the muscle is set either to 0.15 or to 0.35MPa. This way, two equilibrium positions are defined. When the pressure in the muscle is set to 0.35MPa, the equilibrium position will be closer to the side of the muscle. On the other hand, when the pressure is set to 0.15MPa, the equilibrium position will shift towards the side of the spring. By switching the pressure in the muscle at the correct time instant, called *phasic activation* [2.45], energy can be put into the system.

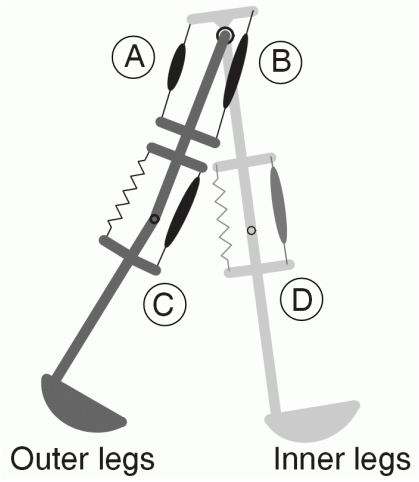

Fig.2.10: Schematic structure and muscle attachments of Mike [2.28].

Instead of using 2 settings for the equilibrium position and compliance, more settings can be used to obtain a variable step length. When using an actuator with adaptable compliance, the natural frequency can be adjusted, giving the possibility to adjust the step frequency. Also other step patterns can be obtained, e.g. walking down or up a slope, walking on stairs. This is the main idea behind Controlled Passive Walking: instead of adjusting the moments of inertia of the limbs, which are fixed, the compliance and equilibrium position of the actuators are adjusted to select a specific natural motion. Therefore, an actuator with adaptable compliance and controllable equilibrium position is required. In chapter 6, Controlled Passive Walking will be discussed in more detail.

2.6 Conclusion

In this chapter the two starting points to build walking bipeds were described: *Active Walking Bipeds* and *Passive Dynamics Bipeds*. To combine the advantages of both approaches—variety of motions and energy efficiency—the concept of *Controlled Passive Walking* is introduced. On this basis the necessity for actuators with adaptable compliance is explained.
In chapter 3 the state-of-the-art of actuators with adaptable compliance will be discussed and a novel design will be introduced.

References

[2.01] F.E. Zajac. Muscle and tendon: properties, models, scaling, and application to biomechanics and motor control. Crit. Rev. Biomed. Eng. Vol. 17, 1989, pp. 359-411.

[2.02] McGeer, "Passive Dynamic Walking", Int. J. Rob. Res., Vol. 9, no.2 April 1990. pp. 62-82.

[2.03] S.H. Collins, M. Wisse, A. Ruina. A 3-D Passive Dynamic Walking Robot with Two Legs and Knees, International Journal of Robotics Research (2001), Vol. 20 (7) pp. 607-615.

[2.04] S. Collins, A. Ruina, R. Tedrake, M. Wisse. Efficient Bipedal Robots Based on Passive-Dynamic Walkers, Science, Vol. 306, 18 February 2005, www.sciencemag.org

[2.05] M. Vukobratovic and B. Borovac. Zero-moment point - thirty five years of its life. Int. J. of Humanoid Robotics, Vol. 1, no. 1, pp. 157–173, March 2004.

[2.06] M. Vukobratovic. How to control the artificial anthropomorphic systems. IEEE Trans. System, Man and Cybernetics SMC-3, pp. 497–507, 1973.

[2.07] C. Chevallereau, G. Abba, Y. Aoustin, F. Plestan, E. R. Westervelt, C. Canudas-De-Wit, and J. W. Grizzle, “Rabbit: a testbed for advanced control theory,” IEEE Control Systems Magazine, Vol. 23, no. 5, pp. 57–79, October 2003.

[2.08] J. Vermeulen, B. Verrelst, D. Lefeber, P. Kool & B. Vanderborght. A real-time joint trajectory planner for dynamic walking bipeds in the sagittal plane. Robotica, Vol. 23, Issue 06, november 2005, pp. 669-680

[2.09] S. Kajita, F. Kanehiro, K. Kaneko, K. Fujiwara, K. Yokoi, H. Hirukawa. Biped walking pattern generation by a simple three-dimensional inverted pendulum model, Advanced Robotics, Vol. 17, Number 2, 2003, pp. 131-147

[2.10] J. E. Pratt, C.-M. Chew, A. Torres, P. Dilworth, and G. Pratt. Virtual model control: An intuitive approach for bipedal locomotion. Int. J. of Robotics Research, Vol. 20, no. 2, pp. 129–143, 2001.

[2.11] J. Hodgins, Biped gait transitions. Proc., IEEE Int. Conf. on Robotics and Automation. IEEE, 1991, pp. 2091–2097.

[2.12] http://world.honda.com/ASIMO/

[2.13] http://www.sony.net/SonyInfo/QRIO/

[2.14] http://www.toyota.co.jp/en/special/robot/

[2.15] http://www.kawada.co.jp/global/ams/hrp_2.html

[2.16] http://ohzlab.kaist.ac.kr/

[2.17] F. Pfeiffer, K. Loffler, and M. Gienger. The concept of jogging johnnie. In Proc., IEEE Int. Conf. on Robotics and Automation, pp. 3129 – 3135, Washington DC, May 2002.

[2.18] A. Albert, M. Gerecke, W. Gerth, J. Hofschulte, T. Lilge, R. Strasser. Investigation of Bipedal Walking for Autonomous Service Robots. SPIE - Robotics and Machine Perception Newsletter, Vol. 12, Nr. 1, 2003, SPIE -- The International Society for Optical Engineering, S. pp. 11-12.

[2.19] B. Vanderborght, B. Verrelst, R. Van Ham & D. Lefeber. Controlling a Bipedal Walking Robot Actuated by Pleated Pneumatic Artificial Muscles, Robotica, accepted for publication in 2006

[2.20] http://www.inrialpes.fr/bipop/

[2.21] Y. Aoustin, A. Formal'sky. On Stabilization of Biped Vertical Posture in Single Support Using Internal Torques. Robotica, Vol. 23, pp. 65-74, 2005.

[2.22] C. Chevallereau, G. Abba, Y. Aoustin, F. Plestan, E.R. Westervelt, C. Canudas-De-Wit, J.W. Grizzle, RABBIT: a testbed for advanced control theory, Control Systems Magazine, IEEE, Vol. 23, pp. 57-79, Issue 5, Oct. 2003

[2.23] T. Geng, B. Porr, and F. Wörgötter, Fast Biped Walking with A Sensor-driven Neuronal Controller and Real-time Online Learning. International Journal of Robotics Research, Vol. 25, No.3, pp. 243-259, March 2006, Sage press.

[2.24] S. Collins, A. Ruina, R. Tedrake, M. Wisse, Efficient Bipedal Robots Based on Passive-Dynamic Walkers, Sience magazine, Vol. 307, 18 Februari 2005.

[2.25] S. Mochon and T.A. McMahon. Ballistic walking. J. Biomechanics, 13, pp. 49–57, 1980.

[2.26] T. McGeer. Powered flight, child's play, silly wheels, and walking machines. In Proc., IEEE Int. Conf. on Robotics and Automation, pages 1592–1597, Piscataway, NJ, 1989.

[2.27] G. T. Fallis. Walking toy ('improvement in walking toys'). U. S. Patent, No. 376,588, January 17 1888.

[2.28] M. Wisse. Essentials of dynamic walking-Analysis and design of two-legged robots. PhD Thesis, September 2004

[2.29] M. Garcia, A. Chatterjee, A. Ruina, and M. J. Coleman. The simplest walking model: Stability, complexity, and scaling. ASME J. Biomech. Eng., 120(2), pp. 281–288, April 1998.

[2.30] J. Adolfsson, H. Dankowicz, and A. Nordmark. 3d passive walkers: Finding periodic gaits in the presence of discontinuities. Nonlinear Dynamics, Vol. 24(2): pp. 205–229, 2001.

[2.31] Y. Hurmuzlu, Dynamics of bipedal gait. Part 2: Stability analysis of a planar five-link biped. ASME J. of Applied Mechanics, 60(2): pp. 337–343, 1993.

[2.32] M. W. Spong and F. Bullo. Controlled symmetries and passive walking. In IFAC Triennial World Congress,Barcelona, Spain, 2002.

[2.33] R. Q. van der Linde. Passive bipedal walking with phasic muscle contraction. Biological Cybernetics, Vol. 81(3): pp. 227–237, September 1999.

[2.34] F. Asano and M. Yamakita. Virtual gravity and coupling control for robotic gait synthesis. IEEE Trans. on Systems, Man and Cybernetics, Part A, Vol. 31(6): pp. 737–745, 2001.

[2.35] M. Wisse and A. L. Schwab. A 3d passive dynamic biped with roll and yaw compensation. Robotica, 19: pp. 275–284, 2001.

[2.36] P. T. Piiroinen. Recurrent Dynamics of Nonsmooth Systems with Application to Human Gait. PhD thesis, Royal Institute of Technology, Stockholm, Sweden, 2002.

[2.37] J. Adolfsson. Passive control of mechanical systems; Bipedal walking and auto-balancing. PhD thesis, Royal Institute of Technology, Stockholm, Sweden, 2001. ISSN 0348-467X.

[2.38] A. D. Kuo. Stabilization of lateral motion in passive dynamic walking. Int. J. Robot. Res., Vol. 18(9): pp. 917–930, September 1999.

[2.39] K. Mombauer, M. Coleman, M. Garcia, A. Ruina. Prediction of Stable Walking for a Toy That Cannot Stand Still, Physical Review E, Vol. 64, Issue 2, Aug 2001

[2.40] http://ruina.tam.cornell.edu/research/

[2.41] http://dbl.tudelft.nl/

[2.42] http://www.ai.mit.edu/projects/leglab/

[2.43] T. Takuma, K. Hosoda, M. Ogino, M. Asada. Stabilization of quasi-passive pneumatic muscle walker. 4th IEEE/RAS International Conference on Humanoid Robots, 2004

[2.44] E. Schuitema, D. G. E. Hobbelen, P. P. Jonker, M. Wisse, J. G. D. Karssen. Using a controller based on reinforcement learning for a passive dynamic walking robot, Proceedings of 2005 5th IEEE-RAS International Conference of Humanoids Robots

[2.45] R.Q. van der Linde, Actively controlled ballistic walking, Proceedings of the IASTED International Conference Robotics and Applications 2000,August 14-16, 2000 – Honolulu, Hawaii, USA

[2.46] B. Vanderborght, B. Verrelst, R. Van Ham, M. Van Damme, D. Lefeber, B. Meira Y Duran & P. Beyl. Exploiting natural dynamics to reduce energy consumption by controlling the compliance of soft actuators, The International Journal of Robotics Research (IJRR), Vol. 25 Issue 4, April 2006, pp. 343-358

[2.47] S. Mochon, T. McMahon. Ballistic walking. J. Biomechanics 1980 Vol. 13: pp. 49–57.

[2.48] J. E. Pratt and G. A. Pratt. Exploiting Natural Dynamics in the Control of a Planar Bipedal Walking Robot. Proceedings of the Thirty-Sixth Annual Allerton Conference on Communication, Control and Computing, Monticello, Illinois, September 1998

[2.49] M. Wisse and J. van Frankenhuyzen. Design and Construction of 'Mike'; A 2D autonomous biped based on passive dynamic walking International Conference on Adaptive Motion of Animals and Machines(AMAM) 2003; Kyoto, Japan

Chapter 3

Compliant actuators

If you can't explain it simply, you don't understand it well enough
Albert Einstein

Stiffness Isn't Everything
G. A. Pratt, M. M. Williamson, P. Dillworth, J. Pratt, K. Ulland & A. Wright

To explain what a compliant actuator is, a definition of a non-compliant actuator —better known as a stiff actuator—is useful. An actuator is a device that is able to move to a certain position or to track a predefined trajectory. A stiff actuator will, once a position is reached, remain in this position, whatever the external forces working on the actuator (of course within the force limits of the device). Stiff actuators can be found in almost all traditional, position controlled applications. Most electrical drive systems are stiff, although an electrical motor is not stiff due to the magnetic field. However the gearbox, which is required to lower the speed and increase the torque, results in a higher reflected inertia. A worm gear with a high gear ratio is even self locking due to friction. This means that whatever torque is applied on the outgoing axis, within the limits of the system, no rotation can be achieved.

A compliant actuator on the other hand will allow a certain deviation from the equilibrium position, depending on the resultant external force. The equilibrium position of a compliant actuator is defined as the position of the actuator where the actuator generates no force or torque. This position can be controlled directly, while the actual position depends also on the stiffness and on the external torque. Since for a stiff actuator these two positions are the same, the equilibrium position is specifically introduced for compliant actuators.

The stiffness of an actuator is comparable to the stiffness of a linear spring. The variation of the length of a linear spring depends on the force working on the spring, according to Hooke's Law:

$$F = -k.(x - x_0) \tag{3.1}$$

This means that a spring with rest length x_0 and actual length x generates a force F. If the length equals the rest length, no force is generated comparable to a compliant actuator being in its equilibrium position. When a spring with linear force-displacement characteristic is used, the stiffness—inverse of the compliance—can be defined as:

$$k = -\frac{F}{x} \tag{3.2}$$

When the relation is not linear, and thus the stiffness varies with the position, the local stiffness is defined as the variation of the force as a function of the position:

$$k = -\frac{dF}{dx} \tag{3.3}$$

In case of a spring, the equilibrium position, being the position where no force is generated, is fixed. A compliant actuator can change this position, e.g. by changing the attachment point of the spring.

Some remarks have to be made concerning terminology. Since *compliance* is the opposite of *stiffness*, both terms can be used to describe the compliant or non-stiff behaviour of an actuator. To describe an actuator with a *variable stiffness*, also the term *adjustable compliance* is used, but also *variable compliance*, *adjustable stiffness*, and *controllable stiffness* are used. These examples are given to show there is no standard terminology (yet) to describe this type of actuators, also each of them has certain advantages. In this chapter a number of existing designs are described, with the terminology used by the inventors.

An example of a compliant actuator is the Series Elastic Actuator (SEA) [3.01], which is basically a linear spring in series with a stiff actuator. The compliance of this actuator is fixed by the selection of the spring, and can therefore not be changed during operation. More detailed information about the SEA can be found in section 3.1.

It is worth mentioning that the discussion in this work about compliant actuators is restricted to conventional actuators, used in the majority of robotic and automated mechanical systems, e.g. hydraulic, pneumatic, and electric actuators. Recently, advances in material technology have introduced new substances, making it possible to build structurally strong articulated mechanisms that are compact and lightweight. Examples of such materials which can be used to develop novel actuators are shape memory alloys (SMAs), electrorheological fluids (ERFs), electrostrictive and magnetostrictive materials (including piezoelectric substances) and electroactive polymers [3.03]. The use of these new materials as compliant actuators is not obvious, since their operation speed is very low, with response times in the scale of tens of seconds, or their displacement is too small for robotic applications.

Actuators with a fixed compliance can be used for force control [3.01] or safe human-robot interaction [3.03], but e.g. not to control the natural frequency of a mechanical system. As explained in section 2.7, this can be done by introducing adaptable compliance, comparable to a spring with a variable spring constant. A number of mechanisms with adaptable compliance have already been designed by several research groups.

One way to vary the compliance of an actuator is by software control of a stiff actuator. Based on the measurement of the external force or torque, a certain deviation is calculated by the controller and set by the stiff actuator. This type of compliant actuator requires an actuator, sensor and controller that are all fast enough for the application. But it allows changing the compliance during operation. Thus the characteristic of an imitated spring is programmed and as such adjusted online, this is often referred to as *active compliance*. A disadvantage of this active compliance is

the continuous energy dissipation; whereas energy could be stored and subsequently released again when a passive element (e.g. a spring) would be used. Another disadvantage is that the bandwidth of the controller is too slow to deal with impacts. Also the contact with a stiff environment will lead to chatter. In section 3.2 the active compliance will be discussed in more detail.

To combine energy storage and adaptable compliance, an elastic element to store the energy is needed, together with a way to adapt the compliance. A substantial number of designs have been developed. However 3 main ideas can be distinguished.

The first group of adaptable compliant actuators with energy storage can be described as an *antagonistic setup of 2 non-linear springs*. The idea is that 2 actuators with a non-adaptable compliance, with a non-linear force-displacement characteristic, are coupled antagonistically, which means that they work against each other. By controlling both actuators the compliance and equilibrium position of this antagonistic setup can be set. In section 3.3 this principle is described more in detail and some examples can be found there as well.

A second group uses the *Structural Stiffness Control*. By varying the dimensional properties of a (leaf) spring, like length or moment of inertia, the stiffness constant of a spring can be adapted. For example, when an elastic beam is clamped at one side, the other end will behave compliant. This means that when exerting a force orthogonal to the beam, a certain deformation will occur. The deformation for a certain force, thus also the compliance, depends on the material properties of the beam, the length and the moment of inertia of the beam. Examples on changing the latter two parameters can be found in section 3.4.

A third group is named Mechanically Controlled Stiffness. By varying the points where a compliant element is attached to the structure of a joint, the compliance of this joint can be changed. An innovative type of actuator within this group, presented in this PhD, is the MACCEPA (Mechanically Adjustable Compliance and Controllable Equilibrium Position Actuator). This actuator has only one compliant element, a linear spring, of which the physical properties are not changed. The actuator behaves as a torsion spring of which the spring characteristics and the equilibrium position can be controlled independently during operation. With properly chosen design parameters a quasi linear torque-angle characteristic can be obtained, which facilitates control. The principles and detailed design of this new type of actuator is elaborated in section 3.5 and chapter 5.

Section 3.6 discusses some applications of compliant actuators. Such actuators can for example be used to make human-robot interaction safe. Another application is the adaptation of the natural frequency of mechanical systems. By using the natural dynamics of a system—motions based on oscillations on the eigen-frequency—drastically reduces energy consumption. An example is *Controlled Passive Walking* in robots and prostheses.

In section 3.7, the range of the compliance of the different types is discussed. Each actuator with variable compliance has a specific range over which the compliance can be set. Some types can change from very stiff to medium stiff and others from very compliant to medium stiff. Obviously, this will have a certain impact on the applicability of the different compliant actuator types.

3.1 Series Elastic Actuator

The Series Elastic Actuator [3.01], developed at the Massachusetts Institute of Technology, is essentially a spring in series with a (stiff) actuator. The compliance is determined by the spring constant and is therefore not adjustable during operation. The SEA is a compliant actuator allowing force control in an easy way. In figure 3.1 a typical setup of a SEA for force control purpose is shown. The elongation of the spring is used as force measurement and returned in the feedback loop.

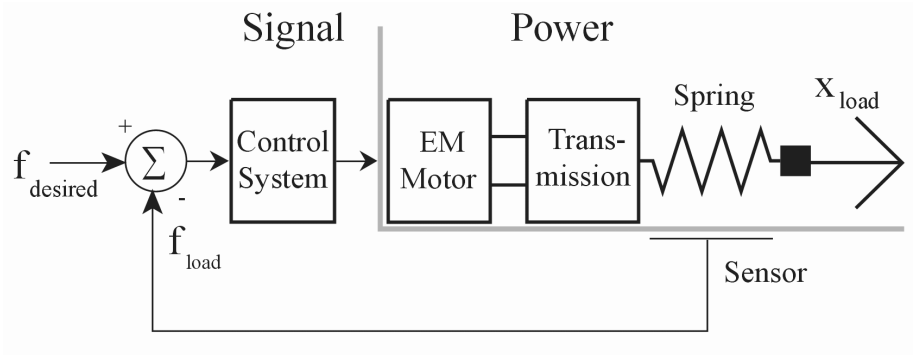

Fig. 3.1: Force control with Series Elastic Actuator, taken from [3.04]

In figure 3.2, two CAD drawings are shown. The left picture represents a hydraulic SEA, while the right one depicts a SEA with an electrical motor, as they are now commercially available from Yobotics [3.05], a MIT spin-off. This company used the SEA to build the RoboWalker: a powered orthotic brace that augments muscular functions of the lower extremities of the human leg. The inherent compliance of the SEA makes the orthosis safe and comfortable.

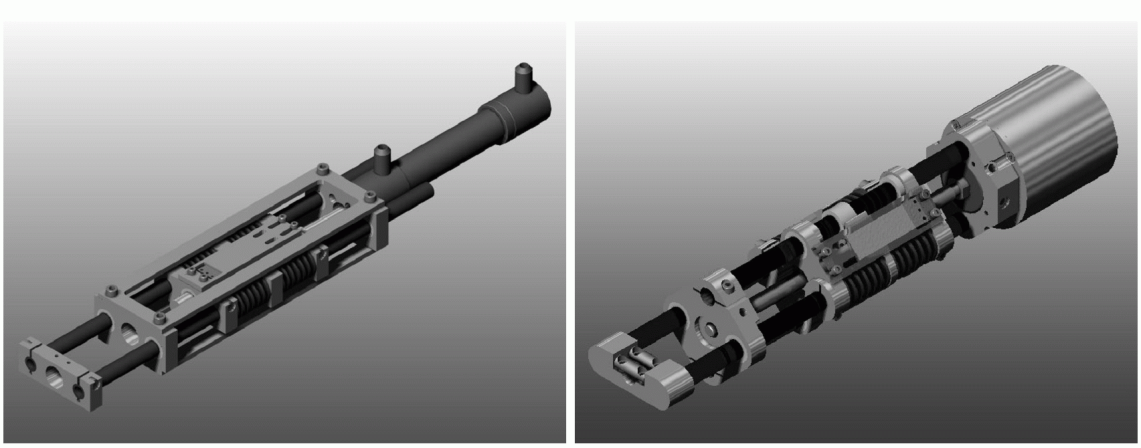

Fig. 3.2: CAD drawing of a hydraulic and an electric series elastic actuator

Also at MIT, the *Spring Flamingo* (figure 3.3) was built. It is a planar biped powered by six Series Elastic Actuators, placed in the upper body. The motion is transferred to the joints by cables. To prevent the robot from falling sideways, it is connected with a beam to a ball joint in a fixed point, restricting the motion of the robot to a circular path. Although this robot has compliant actuators, it is not a passive walker, but a force-controlled robot based on the idea of passive walking.

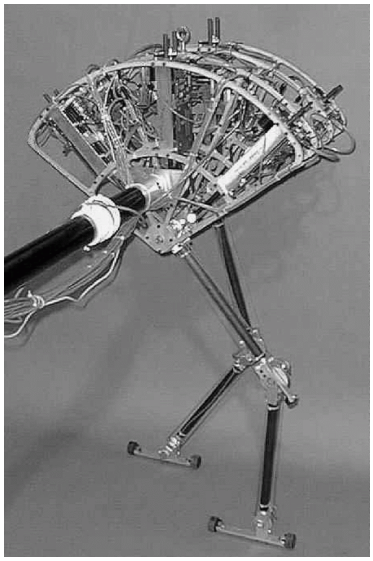

Fig. 3.3: Photograph of the MIT Spring Flamingo

3.2 Active Compliance actuators

Compliance can also be generated by software. Two control paradigms can be distinguished: Impedance control and Admittance Control. Both are based on the idea that the relation between force and displacement must be controlled. Admittance control means that the force is measured, and a displacement from the current position is calculated depending on the required compliance. The motor is then controlled to set this

displacement. In case of impedance control, the position is measured. The position and required compliance are used to calculate the force. Thus, both paradigms are based on the implementation of Hooke's Law, equation 3.1, in the software of the controller [3.06]. Since these types of actuators require continuous control, they are not inherently passive. No energy can be stored and thus power is required both to accelerate and decelerate a mass. Therefore this method to obtain compliance is called Active Compliance control.

The acceleration of the actuator is limited. Therefore, the system will not be able to react fast enough when an impact occurs. Passive systems have an *unlimited* bandwidth to absorb shocks, while for active compliant systems the bandwidth is restricted due to the controller and the acceleration limits of the actuator and also due to the signal delay and the sensor resolution.

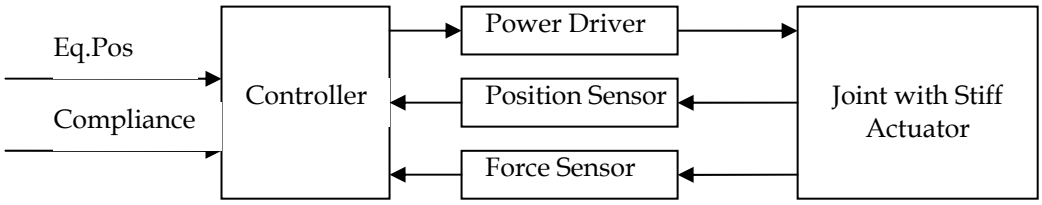

Fig.3.4: Control scheme active compliance

Nevertheless, since the compliance is actively controlled, the compliance is not limited to a linear relation between force and deviation [3.07]. By using active compliance, any force-deviation relation can be generated, e.g. quadratic, exponential, even hysteresis and non-symmetrical relations can be obtained. Moreover, during normal operation this relation can be adjusted.

Another advantage is that only one standard actuator is required. All systems with passive adaptable compliance discussed in the next section, require at least two actuators. Obviously, the use of less actuators results in compacter design with less weight.

Notice that for impedance and admittance control, compliance and equilibrium position are both controlled by one motor. However, Sulzer et al. developed the MARIONET [3.08], which is an active controlled system where the compliance and equilibrium position are controlled by two separate motors. In figure 3.5 a schematic drawing of the MARIONET is given. On the left side, only the rotator subsystem is drawn. It consists of a disc rotating around point x_C, which is driven by a belt, the drive motor is placed in x_D. This motor controls the position where no torque will be generated by the actuator, defined as the equilibrium position. On the

right the complete system is drawn, including the arm. From a point x_L on the arm, a cable runs around a pulley x_P on the disc towards the tensioner motor, which is force controlled. The drive motor is position controlled and will set the equilibrium position, which is where the arm collides with the pully x_p.

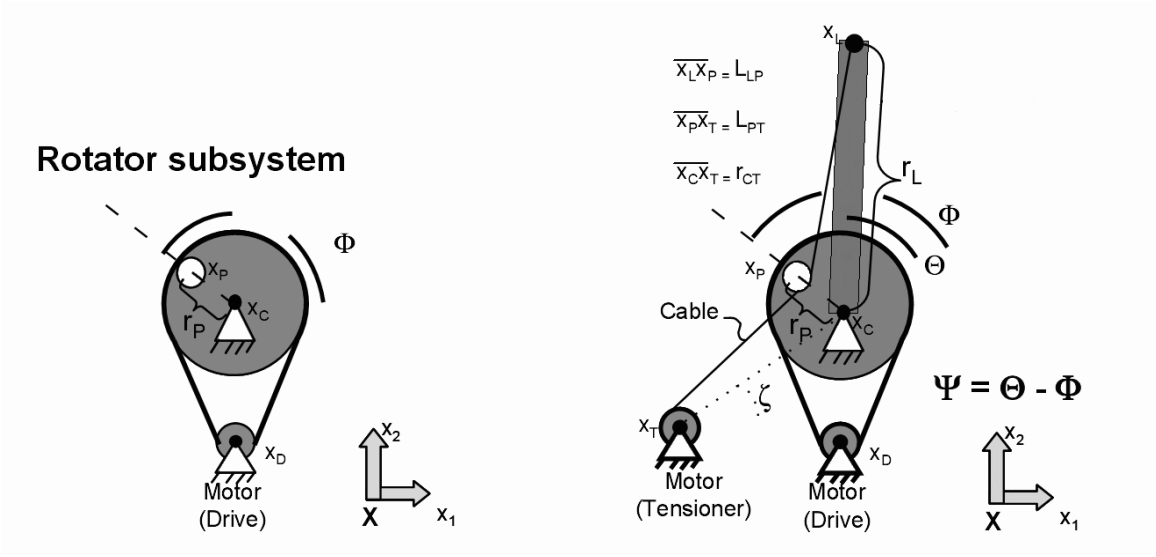

Fig.3.5: MARIONET Schematics, taken from [3.08]

The MARIONET is capable of delivering torque to a joint with advantages that include remote actuation, independent control of compliance and equilibrium, and the ability to span multiple joints. The drawback of this type of active compliance is the use of two motors, and the friction introduced by the cables and pulleys.

For some applications, active compliance has major advantages, e.g. when compactness and weight are important issues, or when online adaptation of the force-displacement relation is required. However, for walking robots, where the energy efficiency is very important, the continuous control of the motor is not justifiable. For this purpose, actuators with adaptable passive compliance are more suitable. In the next sections some designs are discussed.

3.3 Antagonistic setup of 2 non-linear springs

Fig. 3.6: Antagonistic setup of biceps and triceps in human arm. [3.09]

The best-known example of an antagonistic setup is the combination of biceps and triceps in the human arm. When the biceps contracts and the triceps relaxes, the arm is flexed. When the triceps contracts and the biceps relaxes, the arm extends. One of the reasons why an antagonistic setup is required, is the fact that muscles can only pull and not push. However, more can be achieved with this setup: when both biceps and triceps contract, the elbow becomes stiff, when they both relax, the elbow becomes very compliant and the arm hangs freely. In the abovementioned explanation, only the extreme cases were described. In reality, the muscles in the human arm are controlled in a continuous way and thus can cover a whole range of positions and compliances. The elucidated biologically inspired concept of an antagonistic setup is used in a number of mechanical actuators to obtain adaptable compliance.

3.3.1 The necessity of non-linear springs

It is not without a reason that section 3.4 is named *antagonistic setup of 2 non-linear springs*. The non-linearity of the spring is essential to obtain the adaptable compliance. To explain this, a simple linear antagonistic setup—as given in figure 3.7—is used. The two springs are linear and have the same spring constant. In the figure, x_{0A} and x_{0B} are the controllable positions when no force is applied by the springs (the rest length of the springs is assumed zero). These positions can be controlled by two position controlled stiff actuators. The force on the block in the centre, applied by both springs, is the sum of the forces of both springs:

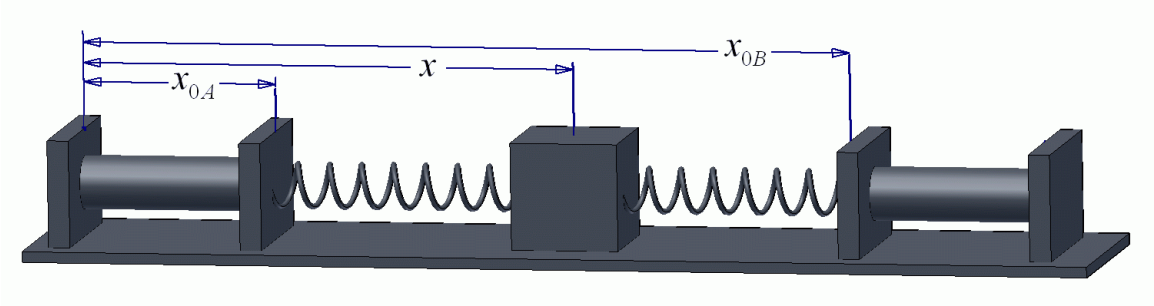

Fig. 3.7: Demonstration of necessity of non-linear springs.

$$F = -\kappa(x - x_{0A}) + \kappa(x_{0B} - x) = -2\kappa x + \kappa(x_{0A} - x_{0B}) \qquad 3.4$$

To calculate the stiffness, equation 3.3 can be used:

$$k = -\frac{dF}{dx} = 2\kappa \qquad 3.5$$

This result is independent of the controllable parameters x_{0A} and x_{0B}. In case of an antagonistic setup with two linear springs, the compliance is thus fixed and cannot be changed during operation.

When two springs with a quadratic characteristic are used, the force is:

$$F = -\kappa(x - x_{0A})^2 + \kappa(x_{0B} - x)^2 = 2\kappa x(x_{0A} - x_{0B}) + \kappa\left({x_{0B}}^2 - {x_{0A}}^2\right) \quad 3.6$$

The local stiffness is then:

$$k = -\frac{dF}{dx} = 2\kappa(x_{0B} - x_{0A}) \quad 3.7$$

As can be seen the stiffness is a linear function of the difference between the controllable parameters. The equilibrium position is the position where no forces are generated:

$$2\kappa x(x_{0A} - x_{0B}) + \kappa\left({x_{0B}}^2 - {x_{0A}}^2\right) = 0 \quad 3.8$$

$$\Rightarrow \quad x = \frac{{x_{0A}}^2 - {x_{0B}}^2}{2(x_{0A} - x_{0B})} = \frac{x_{0A} + x_{0B}}{2} \quad 3.9$$

This is the average of x_{0A} and x_{0B}. Thus, by controlling the two positions x_{0A} and x_{0B}, both compliance and equilibrium position can be set. This principle is used in a number of different designs, which are described in the following sections.

3.3.2 Biologically inspired joint stiffness Control

Migliore et al. [3.10] describe a device based on the antagonistic setup of two non-linear springs. This *biological inspired joint stiffness control* is a rotational joint, actuated by two series elastic actuators. In figure 3.8, a picture of the experimental setup and a schematic drawing of the working principle are given. At the top of the figure, the two position controlled servomotors (agonist and antagonist servo) are shown. They control the attachment points of the springs.

As explained before, the springs have to be non-linear to obtain a system with adaptable compliance. To obtain a linear angle-torque characteristic, quadratic springs are required, as shown in the example in section 3.4.1. The linear characteristic of the spring is transferred into a quadratic characteristic, by using special shaped pieces, over which two wheels roll, as shown in figure 3.9. The centres of the wheels are interconnected by a linear spring.

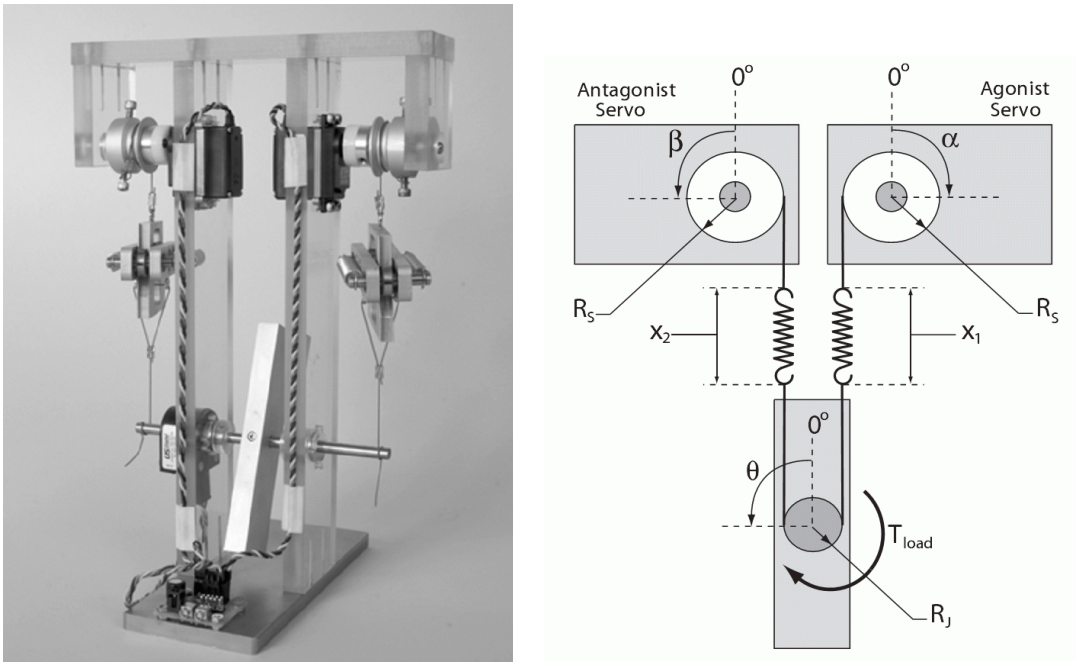

Fig. 3.8: Picture and schematic drawing of antagonistic setup of two SEA

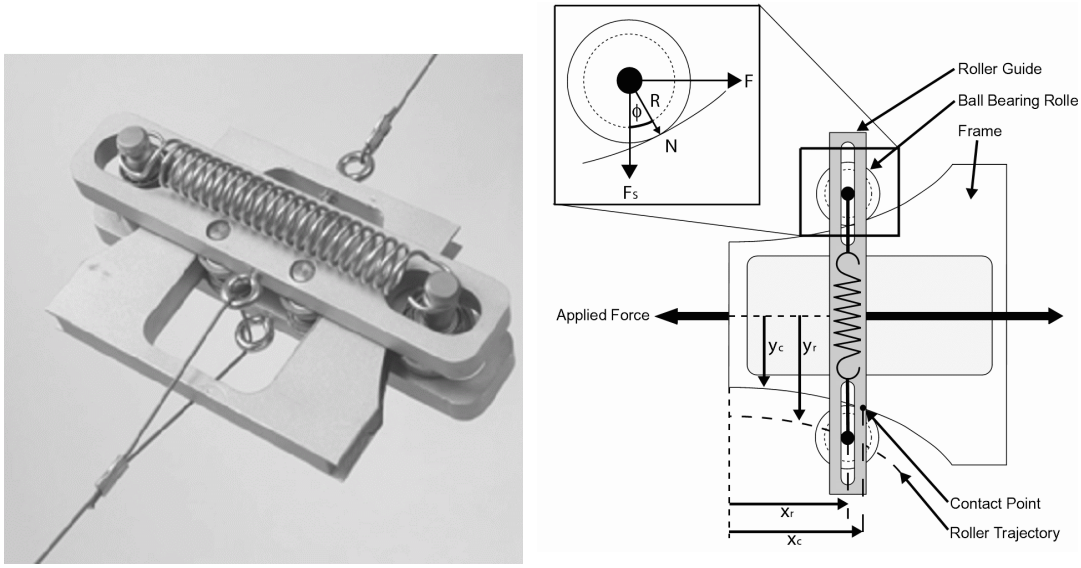

Fig. 3.9: Picture and schematic of quadratic spring device

The advantage of this design is that the force-elongation characteristic of the springs can be chosen during design and thus also the resulting compliance characteristic of the overall system. The drawback is the size and the extra complexity and friction of the mechanisms to make the quadratic springs.

3.3.3 Variable Stiffness Actuator

Tonietti et al. [3.11] describe the *Variable Stiffness Actuator* (VSA). This design is based on the same antagonistic setup. However it is not as obvious as the previous design. In figure 3.10 two CAD views of the VSA are shown. The VSA consists of three pulleys (*1*, *2*, *3*) over which a timing (thoothed) belt (*10*) is placed. Two of the pulleys (*2*, *3*) are controlled, each by a servo motor (*5*, *6*). The other pulley (*1*) is connected to the arm (*4*). On the belt between the pulleys, three tensioning mechanisms (*7*, *8*, *9*) are placed. Although all three tensioning mechanisms are equal, their function is different. The two tensioning mechanisms (*8*, *9*), neighbouring the pulley connected to the arm, form the non linear springs. The other mechanism (*7*) is just a tension mechanism to keep the timing belt (*10*) to the pulleys.

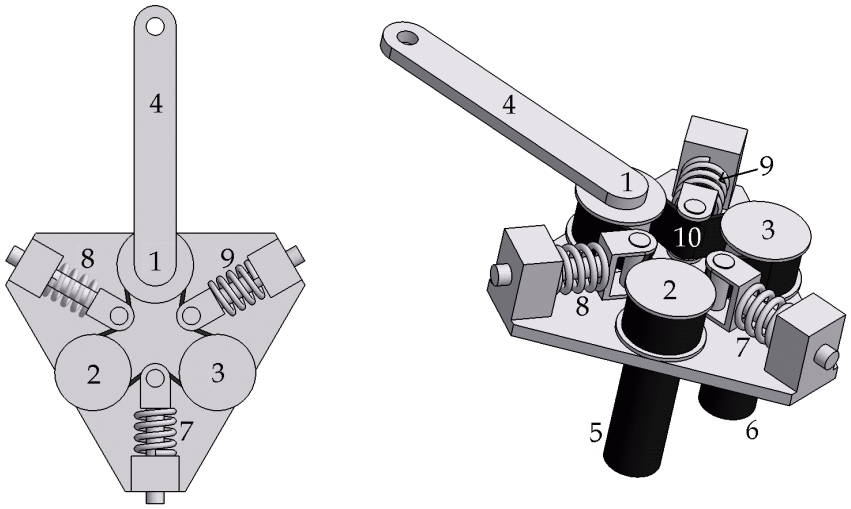

Fig. 3.10: Two CAD views of the VSA

The attentive reader could see that the VSA is actually made with two SEA: (2, 5, 8) and (3, 6, 9). The two springs (8, 9) of each SEA are linear, but due to the tension mechanisms, they are made non-linear. The mechanism that makes the springs non-linear is shown in figure 3.11. The big circle on the left represents the pulley with the arm (1), and the big circle on the right is either pulley 2 or 3, depending on the considered SEA. As can be seen from figure 3.11, the length of the spring is a non-linear function of the length of the belt between the two pulleys. The complete formula for the torque can be found in [3.11].

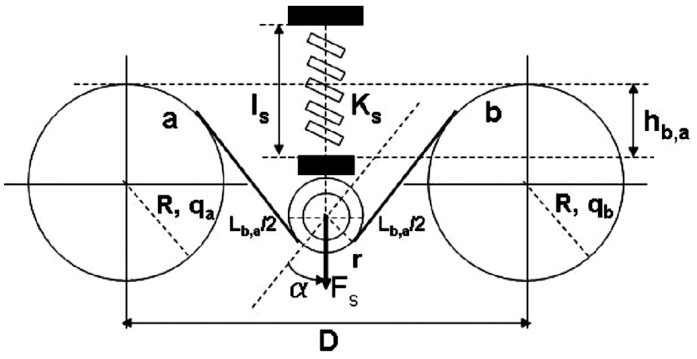

Fig. 3.11: Mechanism to make the springs non-linear in the VSA [3.11]

To make the VSA stiffer, the pulley (2) with motor (5) has to rotate counter clockwise and the pulley (3) with motor (6) has to rotate clockwise. As a result, the two springs in the mechanism (8, 9) are compressed, and spring (7) elongates, to keep the belt tight to the pulleys. When rotating both pulleys (2, 3) in the same direction, the spring's length does not change and as such the compliance will stay the same, but the equilibrium position will change. As is the case for each antagonistic setup, both actuators have to be used to influence only one variable: compliance or equilibrium position.

The control of the VSA is more complicated than the previous design, since the springs are not purely quadratic, as shown in section 3.3.1. The VSA described in this section is the first generation. The researchers are working currently on a more compact implementation, VSA-II, for which they are currently filing in a patent.

3.3.4 Actuator with Mechanically Adjustable Series Compliance

Another design based on the same principle, is the Actuator with Mechanically Adjustable Series Compliance (AMASC), developed by Hurst et al. [3.12] at the Robotics Institute of Carnegie Mellon University. As can be seen in figure 3.12, the AMASC is a rather complex mechanism, with a great number of pulleys and cables. Nevertheless, the advantage is that only one actuator is used to control respectively compliance or equilibrium position. Thus, each of the actuators has its specific function, allowing different motor types in order to optimize the weight of the complete actuator. The working principle is still based on the antagonistic setup of two non-linear springs.

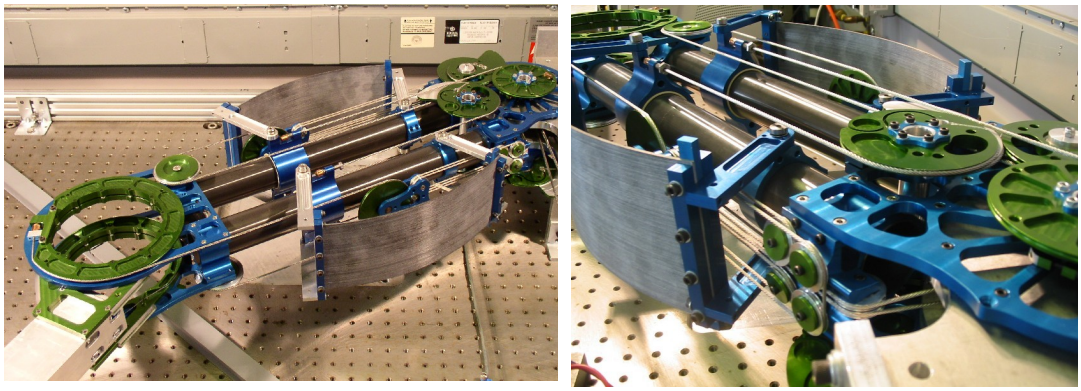

Fig. 3.12: AMASC: Actuator with Mechanically Adjustable Series Compliance [3.12]

In figure 3.13, a schematic overview of the AMASC is given. The springs F_Y are two fiberglass leaf springs, which are placed on both sides of the prototype, as can be seen on the photographs in figure 3.12. In the case of the AMASC, the non-linear spring is formed by a set of spiral pulleys, shown right in figure 3.13, in series with the fiberglass plate. Since the reduction ratio of the pulleys varies proportionally with the fiberglass spring deflection, one can create an output spring function:

$$F_z(z) = K.z^2 \qquad 3.10$$

Instead of using these quadratic springs in a straightforward antagonistic setup, as was done in the previous devices, a number of pulleys are used to uncouple the control of compliance and equilibrium position.

The *leg* of the actuator is placed on pulley J_2. One motor controls the angle θ_1 of pulley J_1, which is the setting for the equilibrium position. When, for example, this motor turns counter clockwise, the set of floating pulleys Z_A will move to the left, and the set of floating pulleys Z_B to the right. This will result in a counter clockwise rotation of the leg, which is connected to pulley J_2. All this can be done without changing the lengths of the springs, thus keeping the compliance constant.

On the other hand, when the displacement X_3—controlled by the second motor—moves to the left, both sets of pulleys Z_A and Z_B will also move to the left. This will elongate both springs, and thus make the joint stiffer, while the equilibrium position is kept constant.

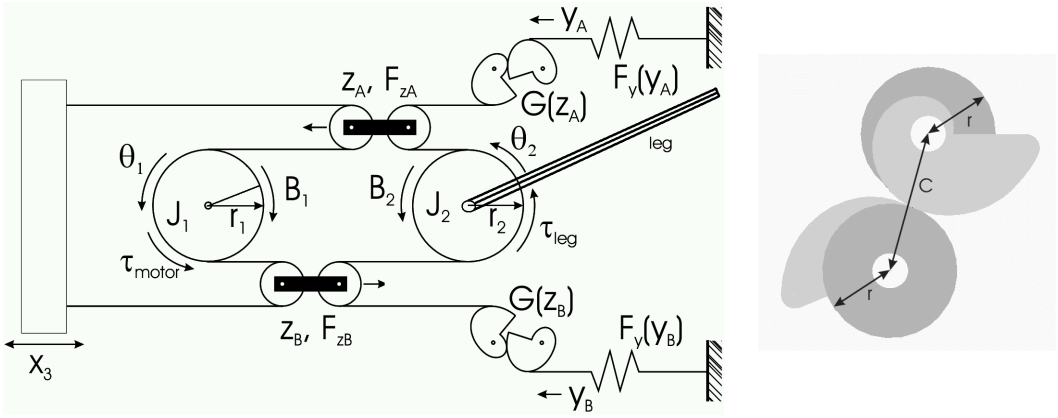

Fig. 3.13: Schematic overview of the AMASC and the logarithmic spiral pulleys [3.12]

The AMASC is an actuator of which the compliance and the equilibrium position can be controlled independently, each by a dedicated motor. This makes the control easier and allows one to design the two motors separately in order to meet the demands of a specific application, e.g. compliance varies slowly while the equilibrium position has to be set faster. The main disadvantage of the AMASC is its complexity.

3.3.5 Pneumatic Artificial Muscles

A Pneumatic Artificial Muscle (PAM) is a device which, when pressurized, contracts axially while expanding radially. The compressibility of air makes them inherently compliant, which means it acts like a spring. The force-contraction characteristic of pneumatic muscles is strongly nonlinear. Thus they can be used to achieve adaptable compliance by means of an antagonistic setup.

In figure 3.14, two antagonistic setups with artificial muscles are shown: the left setup is linear, the right one rotational.

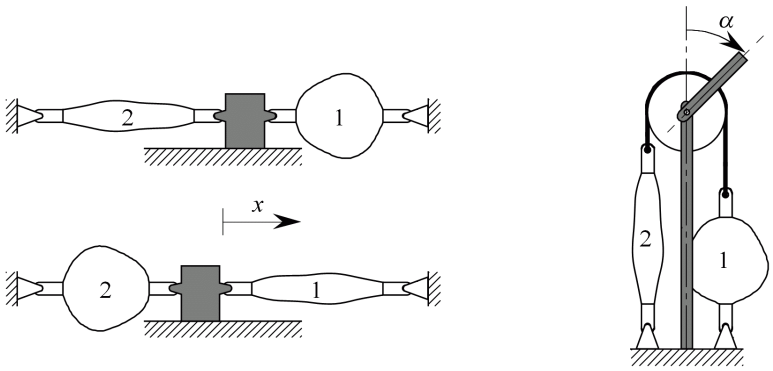

Fig. 3.14: Antagonistic (linear and rotational) setup of artificial muscles

A substantial number of different pneumatic artificial muscles types exists, but all are based on the same principle. When a specifically designed

volume is pressurized, it will expand in one and contract in another direction. An overview of the different designs can be found in [3.13]. The most widely known design is the McKibben Muscle [3.14]. It has the advantage that its overall shape resembles a thin cylinder, which is easy to use in robotic devices. A number of commercially available pneumatic muscles are based on this design, e.g. Festo Muscle [315], Merlin Air Muscle Actuator [3.16], and Shadow Muscle [3.17]. One of the drawbacks is the hystereris introduced by friction, which makes them difficult to control. In addition, the McKibben type of muscles has a substantial threshold of pressure, before any force is generated. The *Pleated Pneumatic Artificial Muscle* (PPAM), designed at the Vrije Universiteit Brussel, drastically reduces hysteresis and overcomes the threshold of pressure. Artificial muscles are discussed in detail in papers in the appendix.

Pneumatic muscles are actuators with a high power to weight ratio and can be directly coupled to the joint, without heavy and complex gearing mechanism. The drawbacks of a joint actuated by two pneumatic muscles are the non-linear torque-angle characteristic, the presence of hysteresis, and the need for pressurized air.

3.4 Structure Controlled Stiffness

As an alternative to the antagonistic setup of two non-linear springs, variations in stiffness can also be achieved through manipulation of the *effective* structure of a spring, also called *Structure Controlled Stiffness* (SCS) [3.18]. As an example, bending a leaf spring is a form of storing energy. However, apart from simple loading (energy storage) and unloading (energy return) of the leaf spring, an extra step of altering the leaf spring's *effective* stiffness is introduced. To understand the basic concepts of a SCS actuator, consider the small deflection beam equation:

$$M = \left(\frac{E.I}{L} \right).\theta \qquad 3.11$$

M is the bending moment, E the material modulus, I the moment of inertia, L the effective beam length, and θ is the angle of bending or slope. In this representation of bending, the term EI/L represents the bending stiffness. In order to control the stiffness of the structure, any of the three parameters in this bending stiffness can be manipulated.

The parameter E is a material property, which cannot be controlled by a structural change, but for some materials it can be changed e.g. by changing the temperature. The temperature can however not be changed fast enough to be useful to create adaptable compliant actuators for bipedal walking. Examples of mechanisms where the moment of inertia I

and the length of the elastic element L are changed, are discussed in the following sections.

3.4.1 Variation of moment of inertia by axial rotation

A series elastic actuator can be built with a passive element with variable mechanical impedance, resulting in an actuator with adaptable compliance. As spring, an elastic beam with a rectangular cross section can be used. When the two dimensions of the cross-section differ, the compliance can be changed by rotating the beam. A prototype of a spring with variable stiffness used in wearable robotic orthoses [3.18] is shown in figure 3.15. The function of the helicoidal spring is to reduce the effects of buckling.

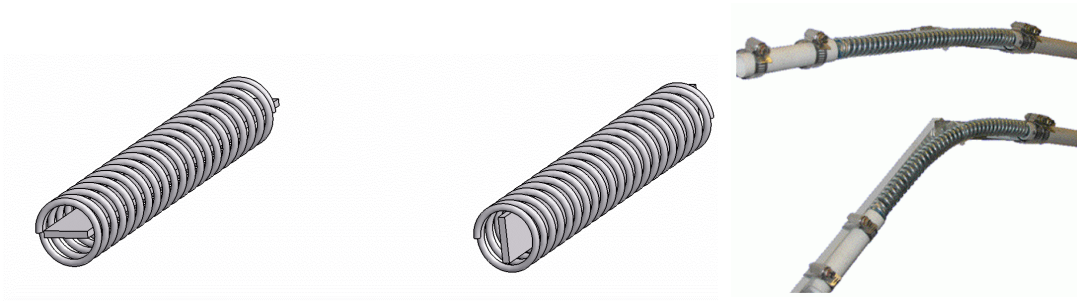

Fig. 3.15: Variation of moment of inertia by rotating the beam.

When the moment of inertia is calculated with the well-know formula, it can be seen that it varies, depending on the width to thickness ratio of the beam.

$$I_{stiff} = \frac{thickness.width^3}{12} \qquad 3.12$$

$$I_{compliant} = \frac{width.thickness^3}{12} \qquad 3.13$$

This is a very easy way to obtain a compliant element with two predefined settings of the compliance. To be able to use an intermediate setting of the compliance, solutions for the buckling should be studied.

3.4.2 Union is strength: increasing the moment of inertia

Another way to make a passive element with variable mechanical impedance, based on the variation of the moment of inertia, is proposed in [3.19]. The structure consists of many layered sheets as shown in figure 3.16. When external forces act on the element, the latter bends, as is depicted on the right of figure 3.16.

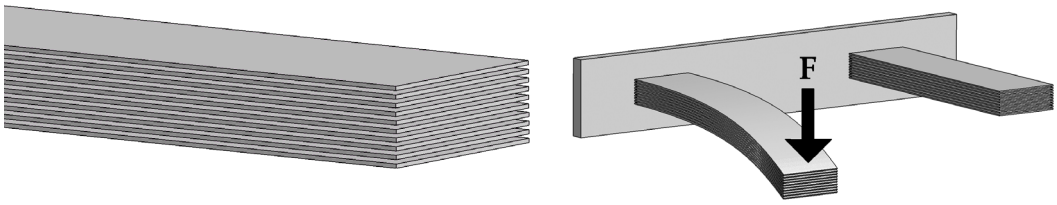

Fig. 3.16: Laminated structure and deformation

If the sheets are pressed together, they will not slip due to friction. As a result, the element stiffens and larger forces are needed to bend the element. Thus the idea is to increase the stiffness of this element by pressing the sheets together, for which several methods can be applied. In [3.20] electrostatic forces are used, while in [3.19] vacuum is used. To be able to create a vacuum, the sheets are covered with a rubber or vinyl sheet in order to make an airtight chamber. By decreasing the pressure in the chamber, the atmospheric pressure generates a normal force on the sheets.

To estimate the variation of compliance of the element, the moment of inertia in both normal and vacuumed state can be calculated. Consider that the number of sheets is *n* and that each sheet acts separately. The total moment of inertia of the element is then given by:

$$I_{Compliant} = \frac{n.width.thickness^3}{12} \qquad 3.14$$

On the other hand, the moment of inertia in the vacuumed state is expressed by:

$$I_{Stiff} = \frac{width.(n.thickness)^3}{12} \qquad 3.15$$

In this case the element becomes one block and the thickness of the element changes from *h* to *nh*. Consequently, the stiffness of the element can be increased by n square as n increases. For example, ten sheets result in a hundredfold stiffness increase. This is an effective method to get a large stiffness range since the number of sheets can be increased easily when using thin sheets, such as films. Based on the same idea, a two-dimensional variant can be made by using wires with a square cross section [3.19].

The advantages of this system are the simple construction and the wide stiffness range possible. However, the friction makes the precise control of the compliance difficult. Moreover, the compliance will depend on the deflection when the volume is vacuumed.

3.4.3 Mechanical Impedance Adjuster

Another way to adjust the compliance is to vary the effective length of a compliant element. In [3.21] the *Mechanical Impedance Adjuster* is introduced, which is depicted in figure 3.17. The compliant element is a leaf spring, connected to the joint by a wire and a pulley. The effective length of the spring can be changed by a slider. A roller is placed on the slider, to hold the leaf spring close to the structure. The motor rotates the feed screw, which moves the slider, and thus changes the compliance.

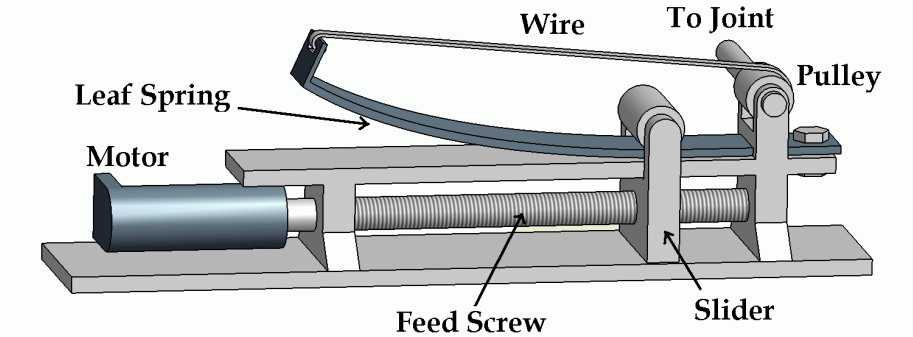

Fig. 3.17: Conceptual design of Mechanical Impedance Adjuster

A rotational version was developed [3.22] for implementation in a robotic joint. In figure 3.18, a conceptual drawing of the proposed design is shown. The left image shows the situation when the mechanism is compliant, the right when it is stiff. The two spindles, which are actuated by a motor, can move the slider up and down. The four wheels, placed on the slider, roll over the leaf spring. When the slider is moved upward, the effective length of the leaf spring is shortened.

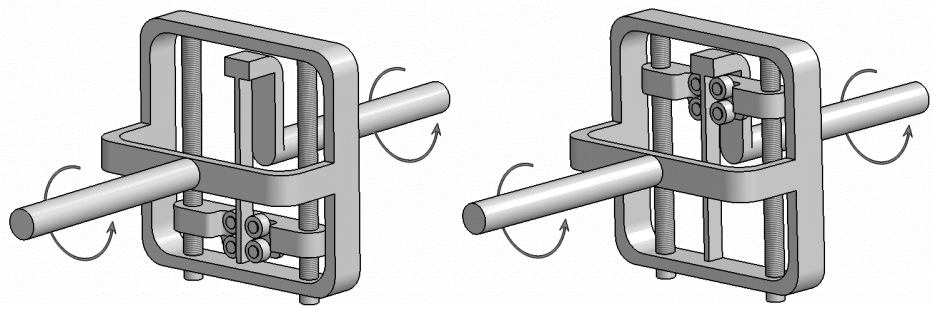

Fig. 3.18: Conceptual design of rotational Mechanical Compliance Adjuster

An advantage of this mechanism is that it is easy to construct. It is easy to control, since the setting of the compliance and the equilibrium position are completely independent. This mechanism allows all possible intermediate states between compliant and very stiff. This implies one actuator for the compliance and one actuator for the equilibrium position, allowing to dimension them separately.

3.4.4 Jack Spring Actuator

Recently, a new type of actuator, based on the structure controlled stiffness concept, was presented in [3.23], named *Jack Spring Actuator*. A helical spring is used as compliant element. The active coil length can be changed by inserting an axis into the spring, with a surface that can slide between the rings of the spring. The length between the endpoint, where the force is applied, and this ring is the active coil region, as shown in figure 3.19. The remaining part of the spring is the inactive region, since no forces are working on it. The actual rest length of the spring is the active region. The spring constant can be calculated with equation 3.16 [3.24], where D is the coil diameter of a helical spring, d the wire diameter, n_a the number of active coils and G the shear modulus. Thus by rotating the inner axis, the number of active coils, n_a, can be changed, and thus also the spring constant.

$$K = \frac{G.d^4}{8.D^3.n_a} \qquad 3.16$$

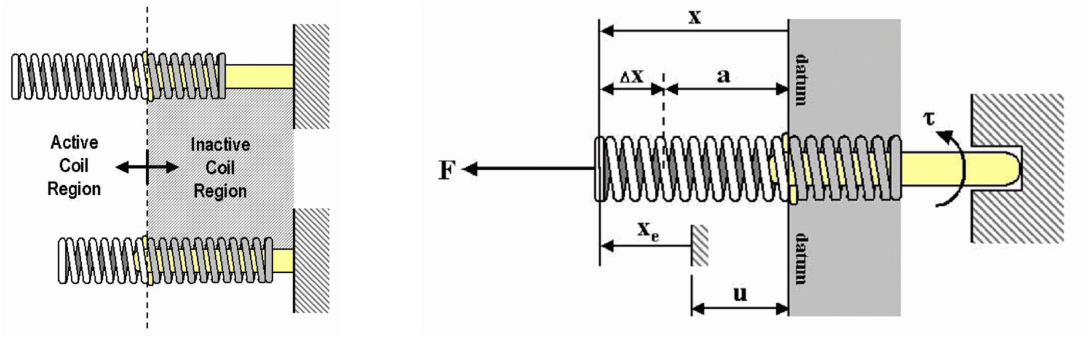

Fig. 3.19: Active and inactive coil region in the Jack Spring Actuator

The Jack Spring Actuator is a novel, compact and easy to implement design. The external force can act in both directions. In combination with a stiff actuator, both compliance and equilibrium position are adaptable. However, both are coupled. Moreover, setting the compliance, while forces are working on the spring, results in friction and deformation of the space where the surface has to slide.

3.5 Mechanically Controlled Stiffness

The previously discussed designs have a number of drawbacks, e.g. complexity, coupling between control of equilibrium position and compliance, non-linear angle-torque characteristic and the use of pressurized air. To overcome these drawbacks, a different approach was

chosen, not based on an antagonistic setup or on a structural change, but on the variation of the attachment points of an elastic element.

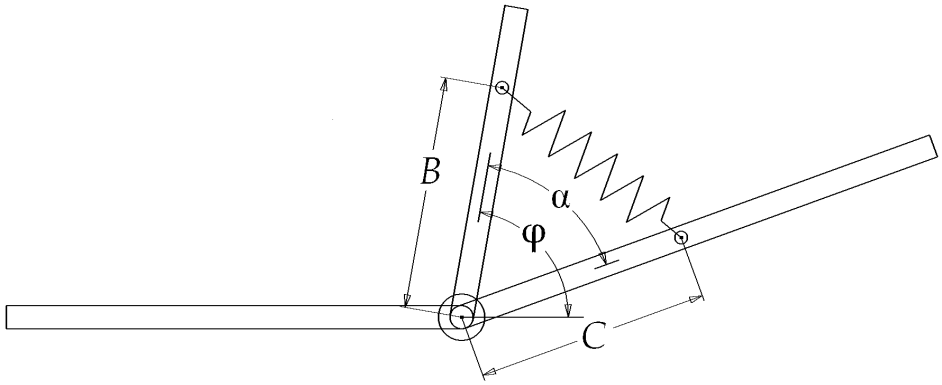

Fig. 3.20: Mechanically Controlled Stiffness Basics

In figure 3.20, a schematic drawing of the new concept is given. The body on the left is considered grounded. The right body is the actuated arm rotating around the joint. The third body, pointing upwards in the figure, is a lever arm, of which the position φ relative to the first body can be controlled by a motor. Between a point on the arm and a point on the lever arm, a spring with zero restlenght is placed. In case of zero restlenght, this spring tends to line up the arm and the lever arm. Since no torque is applied to the arm when the arm is in line with the lever arm, the lever arm determines the equilibrium position of the joint. By varying the points where the spring is attached, e.g. by varying the length *B* and *C*, the torsion stiffness of the joint can be adjusted. In this setup, the rest length of the spring should be zero, which is not possible in a real setup. Therefore, in the next sections, two examples based on this principle are discussed.

3.5.1 Lever arm length adjustment

A first type of actuator based on *Mechanical Controlled Stiffness* is developed at the Vrije Universiteit Brussel. As shown in figure 3.21, the proposed system is a rotative joint consisting of grounded arm *1* and arm *2*, connected by an axis *8*. The lever arm *3* is also placed on the same rotation axis. The position of lever arm *3*, relative to arm *1*, can be controlled by servomotor *4*. The spring *7* generates a torque that tends to line up body *2* and *3*. This is done by the cable *9* that runs from a point on body *3* to a point on body *2*. Servomotors *5* and *6* rotate the threaded spindles, which move these points to or away from the rotation axis, resulting in shorter or longer lever arms and thus a lower or higher torque. The spindle, powered by servomotor *5*, also moves the point where the spring *7* is attached. The left side of figure 3.21 shows the situation with short lever arms, resulting in a joint with low stiffness. On the right side, the situation is shown where the lever arms are longer, which makes the joint stiffer.

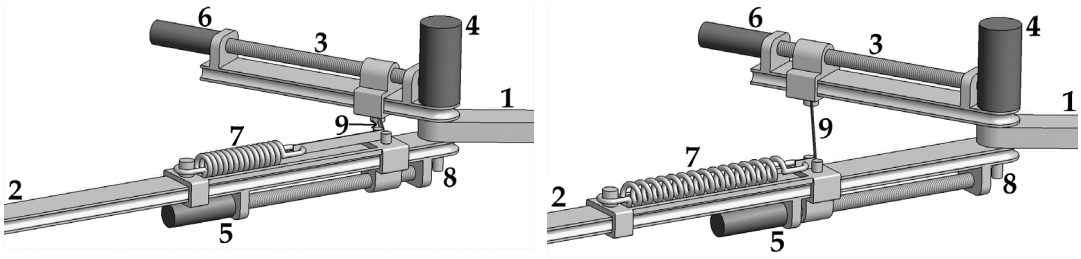

Fig. 3.21: Variation of the length of the lever arms

The variation of the compliance is based on the variation of the length of the lever arms and uses only one passive element, which is fundamentally different from the antagonistic setup or structural controlled stiffness. This design has a number of drawbacks. The use of three motors, of which two are controlled together, is expensive, but difficult to avoid. The number of motors could be reduced by connecting both sliders by means of a cable, running through the rotation axis. However, this will result in a complex mechanism with considerable friction. For practical reasons, the two points that ensure tensioning of the cable cannot be placed on the same distance from the rotation axis, resulting in non-linearity of the torque-angle characteristic for small angles. Also for larger angles, the torque-angle characteristic will become non-linear since the cable will follow a straight line (a chord) instead of an arc with the rotation axis as centre. This is because the length of an arc is a linear function of the angle, which is not the case for a chord.
Also the fact that friction occurs in the point where the cable is guided around arm 2, resulting in hysteresis, made this design unfavorable, especially with respect to passive walking.

3.5.2 MACCEPA

Starting from the previous design, a new design was developed, named *Mechanically Adjustable Compliance and Controllable Equilibrium Position Actuator* or *MACCEPA*. In figure 3.22 the essential parts of the MACCEPA are drawn. As can be seen there are also 3 bodies pivoting around one rotation axis. Around the rotation axis, a lever arm is pivoting, depicted as a smaller body in figure 3.22. A spring is placed between a fixed point *c* on the lever arm and a cable that runs around *b* (a fixed point on the right body) and is attached to a pre-tension mechanism.

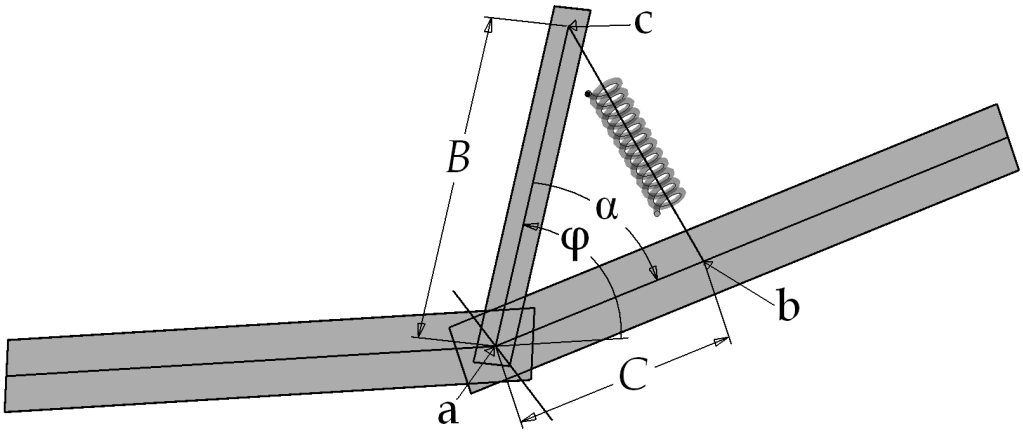

Fig. 3.22: Working principle of the MACCEPA

The angle φ between the lever arm and the left body is set by a classical actuator (e.g. a servomotor). When α—the angle between the lever arm and the right body—differs from zero, the force due to the elongation of the spring will generate a torque *T* that tends to line up the right body with the lever arm. When the angle α is zero—this is the equilibrium position—the spring will not generate any torque. The equilibrium position itself is determined by the value of *φ*. A second classical actuator, present in the pre-tension mechanism, determines the length of the piece of cable between points *c* and *b*, thus setting the pre-tension of the spring. This pre-tension will influence the torque for a certain angle α, thus controlling the spring constant of the equivalent torsion spring used to model the device. In figure 3.23 a CAD drawing of the MACCEPA prototype is shown.

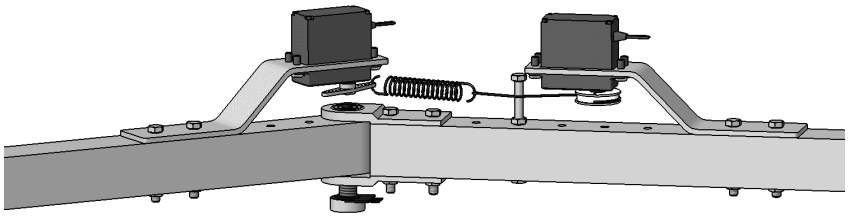

Fig. 3.23: CAD drawing of the MACCEPA prototype

The advantages are that the MACCEPA actuator can be built with standard off-the-shelf components and that it has a linear angle-torque characteristic. The control of compliance and equilibrium position are fully independent and these control signals are independent of the current position. However, the friction in the joint depends on the setting of the compliance and the servo motors require some place in the structure.

The development of this novel type of actuator with adaptable compliance, which is one of the main topics dealt within this PhD, is described in detail in chapter 4.

3.6 Applications of adaptable compliance in robotics

Compliant actuators offer certain advantages, but are probably less suited for classical position controlled applications, which are easier to control with stiff actuators. Examples of novel applications for compliant actuators are controlled passive walking, safe human-robot interaction and comfortable actuated prostheses and orthosis. For these applications actuators with adaptable compliance offer new possibilities, e.g. compliance control for natural frequency adaptation. Copying control strategies for stiff actuators to compliant actuators will generally not work, therefore new control strategies should be developed.
Applications requiring adaptable compliance can be divided into two groups, depending on the primary use of the compliance.

3.6.1 Adaptable compliance to adjust the natural dynamics

The natural dynamics of a mechanical system can be adjusted so the system will have a natural motion close to the desired motion as to reduce energy consumption. Some examples of applications are:

- Controlled Passive Walking. As described in section 2.5, an actuator with adaptable compliance is required to extend the possibilities of passive walkers. The setting of the compliance can also be used to maximize the amount of energy which can be stored during touchdown of the feet and be released during take-off.

- Many prostheses researchers focus on the enhancement of comfort for the user. Most prostheses nowadays are still passive, but the more advanced ones have an actuator and a compliant element. The compliance is fixed during the design phase and set to an average value, such that the natural frequency of the device is fixed. Thus only for a certain stiffness of the ground and walking speed will this give a more or less comfortable feeling to the user. In contrast, when the compliance is adaptable, the latter can be chosen to obtain an optimal behaviour for a wide range of circumstances and desired motions.

3.6.2 Adaptable compliance in robot-human interaction

Adaptable compliance can also be used to make the interaction between robots and humans safer and more natural. Some examples of applications are:

- Nowadays industrial robots are heavy machines, and actuated by stiff actuators, meaning that they do not comply when a collision

occurs thereby inducing severe damage. Thus for safety reasons they are placed in a human free environment. However, for some applications it is useful to have robots and humans fulfilling tasks together [3.03]. This requires safer robots, which can be achieved by making the joints of the robot compliant. However, with a compliant joint it is harder to place e.g. the tool centre point in an exact position or to track a certain trajectory accurately. In this case an actuator with adaptable compliance can act stiff for precise positioning at low speeds (grasping and placing an object) and compliant when positioning is not that important when moving at higher speeds (moving from one position to another).

- Most robotic toys are actuated by stiff electrical drives. This results in the typical "artificial way of moving and interaction". Especially for cuddly toys, like Aibo [3.25] or Anty [3.26], a compliant movement is preferred. When children play with these toys it happens that they impose other motions than the toy is doing, which can damage the driving mechanism. Compliance in the actuation can prevent this from happening and give the cuddly toys a more natural feeling. Adaptable compliance can also be used to emphasise emotions, e.g. angriness by making the joints stiffer, or tiredness by making the joint more compliant.

- Step rehabilitation is generally done by a substantial number of physiotherapists, resulting in expensive sessions—limited in time—which extends the overall rehabilitation process. Therefore, robots to assist in the rehabilitation process are being proposed, e.g. Lokomat [3.27], Autoambulator [3.28], which impose gait-like motion patterns to the legs of a patient. Paraplegic patients often suffer from severe spasms, which is not uncommon when not having full control over the muscles. When using stiff actuators this can hurt the patient or inversively, the spasms can destroy the actuators of the robotic orthosis. Adding compliance to the actuation system could prevent these specific problems. Additionally, in the beginning of the rehabilitation process a relatively high stiffness might be preferred, which could gradually be lowered when the patient has regained a certain level of control over the legs. The Altacro project [3.29] intends to build a step rehabilitation robot with adaptable compliance.

3.7 Range of Compliance

An important constraint when choosing the type of compliant actuator is the range of desired compliances. For example, an industrial robot, like described in section 3.7.2, should be compliant when moving fast. When

precision is required, the arm is typically moving slowly and a stiff actuator is preferred. For precise position control, the actuator should be as stiff as possible. Therefore, the compliance should be able to change from very stiff to medium compliant. The range in between is not that important, and the linearity within this range is of minor importance. For this application, the Structural Compliance Control is preferable, since this type can be made very stiff and the linearity between the two extremes is not an issue. The other types like the antagonistic setup of two non-linear springs and the Mechanically Controlled Stiffness theoretically also can be made very stiff, however in practice there are limitations. For example, when using two pneumatic muscles, the joint can be made stiffer by increasing the pressure in both muscles. This pressure however is limited to e.g. 4 bars for PPAMs, or 8 bars for Festo Muscles, limiting the stiffness. Also actuators based on Mechanically Controlled Stiffness cannot be made very stiff in practice. This would require very long lever arms and in the MACCEPA, a very large elongation of the spring, which would result in an inelastic deformation.

On the other hand, for applications where the natural frequency has to be adjusted, the joint does not require a complete stiff mode. It should be able to be very compliant and the angle-torque relation is preferably as linear as possible within the working range. Therefore, the antagonistic setup and especially the Mechanically Controlled Stiffness are more suitable. In figure 3.24 rough estimation of the range of compliance for the different types of compliant actuators is shown graphically. Note that the ranges in the figure are general values, since it strongly varies within a group and depends on the design parameters of the actuator.

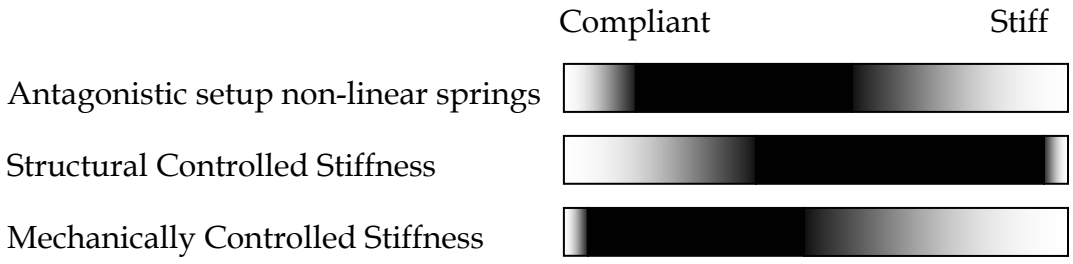

Fig. 3.24: Range of compliance

The range of compliance thus is an important criterion to decide whether a certain compliant actuator is suited for a certain application. Moreover, this is not the only design criterion. Controllability, linearity, power, size and cost also ought to be taken into account.

3.8 Conclusion

In this chapter, three concepts to create adaptable compliant actuators, which can store energy and thus can be used for passive motions, are presented and examples are given. The first concept covers the compliant actuators based on the *antagonistic setup of two non-linear springs*. The second one is the adaptable compliance achieved by *structural stiffness control*. The third concept is the *mechanically stiffness control*, in which the MACCEPA is a novel actuator with independently controllable compliance and equilibrium position. A number of applications—besides the use for passive walking—are given. The range of compliance for each type—in relation to the application—is discussed.

References:

[3.01] G. Pratt and M. Williamson. Series elastic actuators. in Proc. Of the IEEE/RSJ International Conference on Intelligent Robots and Systems (IROS-95), Vol. 1, Pittsburg, PA, July 1995, pp. 399–406.

[3.02] C. Mavroidis. Development of Advanced Actuators Using Shape Memory Alloys and Electrorheological Fluids, Online publication: 20 February 2002, http://www.coe.neu.edu/Research/robots/papers/NDE.pdf

[3.03] M. Van Damme, F. Daerden & D. Lefeber. A Pneumatic Manipulator used in Direct Contact with an Operator, ICRA 2005 IEEE International Conference on Robotics and Automation, Barcelona, Spain, April 2005, pp. 4505-4510.

[3.04] D.W. Robinson. Design and Analysis of Series Elasticity in Closed-loop Actuator Force Control. PhD. Thesis 2000, Massachusetts Institute of Technology.

[3.05] http://yobotics.com/

[3.06] B. R. Shetty and M. H. Ang Jr. Active Compliance Control of a PUMA 560 Robot. Proceedings of the 1996 lEEE, International Conference on Robotics and Automation Minneapolis, Minnesota - April 1996

[3.07] R. Colbaugh, K. Glass, K. Wedewardt. Adaptive Compliance Control of Electrically-Driven Manipulators. Proceedings of the 35th Conference on Decision and Control, Kobe, Japan December 1996

[3.08] J. S. Sulzer, M. A. Peshkin and J. L. Patton. MARIONET: An Exotendon-Driven Rotary Series Elastic Actuator for Exerting Joint Torque. Proceedings of the 2005 IEEE 9th International Conference on Rehabilitation Robotics, June 28 - July 1, 2005, Chicago, IL, USA

[3.09] http://www.arrowvale.worcs.sch.uk/sportscollege/muscles.htm

[3.10] S. A. Migliore, E. A. Brown and S. P. DeWeerth. Biologically Inspired Joint Stiffness Control. Proceedings of the 2005 IEEE, International Conference on Robotics and Automation, Barcelona, Spain, April 2005

[3.11] G. Tonietti, R. Schiavi and A. Bicchi. Design and Control of a Variable Stiffness Actuator for Safe and Fast Physical Human/Robot Interaction. Proceedings of the 2005 IEEE, International Conference on Robotics and Automation, Barcelona, Spain, April 2005

[3.12] J.W. Hurst, J. Chestnutt, and A. Rizzi. An Actuator with Physically Variable Stiffness for Highly Dynamic Legged Locomotion. Proceedings of the 2004 International Conference on Robotics and Automation, May, 2004

[3.13] Daerden F. Conception and realization of pleated pneumatic artificial muscles and their use as compliant actuation elements. PhD Thesis, Vrije Universiteit Brussel, July 1999

[3.14] H. F. Schulte. The characteristics of the McKibben artificial muscle. In The Application of External Power in Prosthetics and Orthotics. Publication 874, pages 94–115. National Academy of Sciences–National Research Council, Lake Arrowhead, 1961.

[3.15] http://www.festo.com

[3.16] http://www.merlinsystemscorp.co.uk/

[3.17] http://www.shadow.org.uk/index.shtml

[3.18] K.W. Hollander and T.G. Sugar. Concepts for Compliant Actuation in Wearable Robotic Systems. US-Korea Conference on Science, Technology and Entrepreneurship (UKC2004)

[3.19] S. Kawamur, T. Yamamoto, D. Ishida, T. Ogata, Y. Nakayama, Tabat and S. Sugiyama. Development of Passive Elements with Variable Mechanical Impedance for Wearable Robots. Proceedings of the 2002 IEEE International Conference on Robotics & Automation Washington, DC - May 2002

[3.20] O. Tabata, S. Konishi, P. Cusin, Y. Ito, F. Kawai, S. Hirai, and S. Kawamura. Microfabricated Tunable Bending Stiffness Device. Proc. of the 13th Annual Int. Conf. On Micro Electro Mechanical Systems, Miyazaki, 1999.

[3.21] T. Morita, S. Sugano. Design and Development of a new Robot Joint using a Mechanical Impedance Adjuster. IEEE International Conference on Robotics and Automation, 1995

[3.22] http://www.sugano.mech.waseda.ac.jp/wendy/arm/mia1-e.html

[3.23] K. W. Hollander, T. G. Sugar and D. E. Herring. A Robotic 'Jack Spring' For Ankle Gait Assistance. Proceedings of IDETC/CIE 2005,ASME 2005 International Design Engineering Technical Conferences 2005,Long Beach, California, USA, September 24-28

[3.24] J.E. Shigley, and C.R. Mischke. Mechanical Engineering Design. 1989 5ed. McGraw-Hill Publishing Co., New York.

[3.25] http://www.sony.net/Products/aibo/index.html

[3.26] http://anty.vub.ac.be/

[3.27] http://www.hocoma.ch/

[3.28] http://www.autoambulator.com

[3.29] http://mech.vub.ac.be/multibody/topics/altacro.htm

Chapter 4

MACCEPA, the Mechanically Adjustable Compliance and Controllable Equilibrium Position Actuator

An inventor is simply a fellow who doesn't take his education too seriously.
(Charles F. Kettering)

Simplicity is the ultimate sophistication.
(Leonardo DaVinci)

In chapter 3 different designs of actuators with adaptable compliance were described. Every design has its own advantages and disadvantages, depending on the application. For Controlled Passive Walking the most important are: the simplicity, weight, controllability of the compliance, the ability to store energy and the ability to vary from very compliant to medium stiff. Therefore, the aim of this work is to elaborate and test new ideas to make an actuator with adaptable compliance. This has led to the development of the MACCEPA (Mechanically Adjustable Compliance and Controllable Equilibrium Position Actuator). The working principle of the MACCEPA, already introduced in section 3.6.2, is discussed profoundly in this chapter.

4.1 Presentation and modelling

In this section, the functioning of the MACCEPA is discussed in detail. First, the requirements of the new actuator are given, and then the basic concept is explained. The basic concept is further elaborated and the generated torque calculation is derived. Subsequently, the influence of the design parameters is investigated. Finally, the relation between the setting of the compliance and the natural frequency is discussed.

4.1.1 Requirements

In a robotic arm or bipedal leg, a rotational actuator is usually the most suitable type. The ease of control, modelation and implementation are the criteria to define the requirements. A rotational actuator with adaptable compliance can be modelled as a torsion spring for which separate control of the equilibrium position and the compliance is an extra asset. The torque applied by the torsion spring should preferably be symmetrical around the equilibrium position, and should be preferably as linear as possible in the working range. To be able to recover energy, a passive, naturally compliant element, e.g. a spring, is required. This passive element will also prevent damage of the actuator due to impact.
From the engineering point of view, the mechanism should also be simple (simplicity results usually in robustness and low-cost), lightweight (especially in autonomous machines) and it should be easy to control the compliance (it is preferable that the control of the equilibrium position and of the compliance are completely independent).

4.1.2. Basic concept

The concept of this novel rotational actuator is explained by means of a basic setup given in Fig. 4.1. Consider a stick connected to the ground by means of a pin joint. The stick can thus rotate free around the joint axis. This setup can be seen as a robot link, steered by an actuator driving the

joint. Numerous possibilities exist to apply a torque to this link, e.g. by a motor via a gearing mechanism, a direct drive motor, an antagonistic setup of 2 artificial muscles, etc. Another fairly simple method consists in attaching a string to a fixed point on the arm and pull the string, as shown in figure 4.1. When the hand, pulling on the string, is on the right side, a torque is applied to the link, which will tend to rotate the arm in the clockwise direction. Pulling to the left will result in a counter clockwise torque. The angle between the rope and the arm will determine the relation between the pulling force and the torque. The smaller this angle, the smaller the torque will be for a given force. When the angle is zero, no torque can be applied by the hand, whatever the force is. Therefore the position of the hand and the force of the hand determine the applied torque.

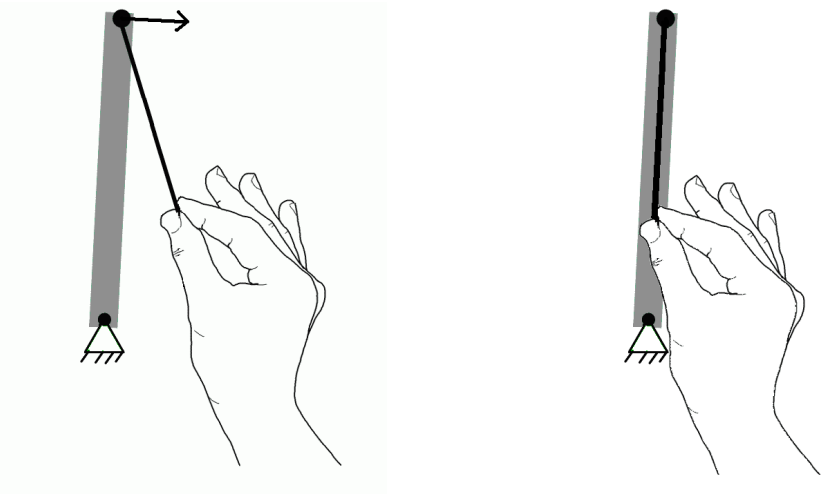

Fig.4.1. Basic concept of MACCEPA

The previous argumentation can be inverted. Instead of moving the hand, one can rotate the arm, while assuming that the direction of the string doesn't change and a constant force is applied on it (is the case for small angles). When the link is aligned with the string, no torque is applied. When one tries to rotate the arm clockwise, a counter clockwise torque appears, and vice-versa.

Thus in the example above, the position of the hand defines the equilibrium position for which no torque is generated. The bigger the deviation of this position, the bigger the angle between the link and the string and the bigger the reaction torque, in case of a constant applied force on the string.

The constant force can be generated by a force controlled motor [4.01], but in this case no energy can be stored. Instead, an elastic element, like a linear spring, can be placed to store energy. However, the pulling force in

this case is not constant, since the force depends on the elongation of the spring. The following sections show that through an apt choice of specific design parameters, this non-constant pulling force can be exploited to build an actuator with adaptable compliance, for which the generated torque varies linearly with the angular deviation out of the equilibrium position.

4.1.3 Working principle

In this section, the basic concept of the compliant actuator is discussed in more detail. Figure 4.2 shows a schematic drawing of the MACCEPA (Mechanically Adjustable Compliance and Controllable Equilibrium Position Actuator). As can be seen, there are 3 bodies pivoting around one rotation axis. The left body in figure 4.2 was not drawn in figure 4.1, but it is actually the reference body to which the generated actuator torque is applied and it can be considered as grounded. The smaller body is a lever arm rotating around the same rotation axis. Point *c* on this smaller body is comparable with the position of the hand in figure 4.1. A spring is placed between the point *c* on the lever arm and a cable that runs around point *b*, which is a fixed point on the right body. The cable is attached to a pre-tension mechanism.

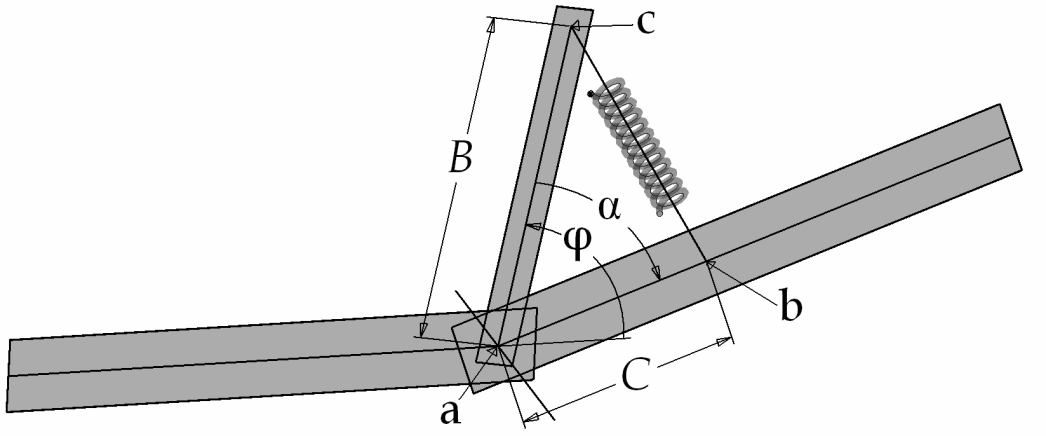

Fig.4.2. Working principle of the Maccepa

The angle φ between the smaller lever arm and the left body is set by a traditional position controlled actuator (e.g. a servomotor). Thus, this actuator defines the position of point *c*, where the spring is attached. When α, the angle between the lever arm and the right body, differs from zero, the force due to the elongation of the spring will generate a torque T that tends to line up the right body with the lever arm. When the angle α is zero—this is the equilibrium position—the spring will not generate any torque. This equilibrium position is determined by the value of φ, set by the servomotor.

This mechanism is thus a compliant actuator, since the equilibrium position can be controlled and a deviation from this equilibrium position is allowed. When pulling the actuator out of equilibrium, a returning torque is generated, which is function of the applied angular deviation.

To achieve adaptable compliance, the relation between the deviation and the reaction torque must be variable. This can be realized by a pre-tension mechanism, which determines the length of the cable between the spring and point *c*, and thus the pre-tension of the spring. The pre-tension mechanism, based on a second servomotor with a spool, is located on the right arm. This pre-tension influences the torque for a certain angle α, thus controlling the spring constant of the equivalent torsion spring used to model the device.

4.1.4 Calculation of the torque

In this section an equation will be formed for the torque, delivered by the MACCEPA.

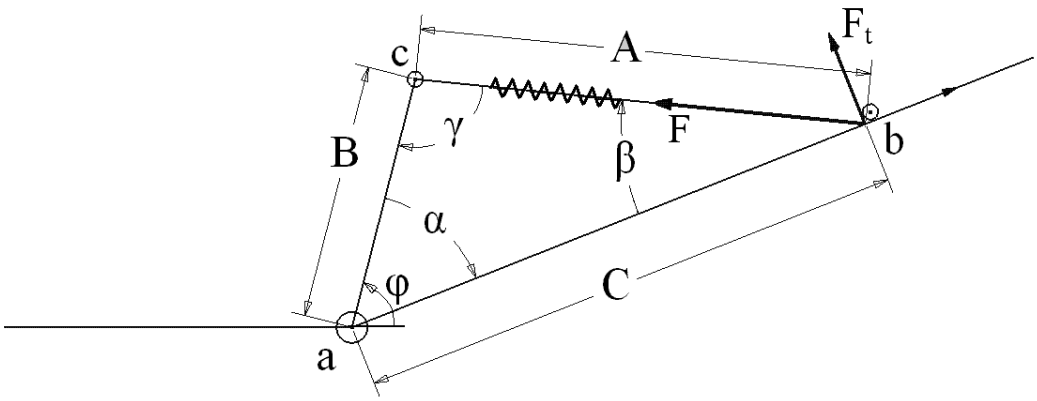

Fig.4.3. Scheme of the Maccepa

a = Rotation point
b = Fixed point on right body. The cable between the spring and the pre-tension mechanism is guided around this point.
c = Fixed point on lever arm, where the spring is attached
T = Torque applied by MACCEPA
F = Force due to extension of the spring
Ft = Component of F orthogonal to line *ab,* that generates torque
k = Spring constant, assuming linear spring
B = Length lever arm, which sets equilibrium position
C = Distance between point *a* (rotation point) and point *b* on the right body

P = Extension of the spring caused by pre-tensioning (equals the total extension of the spring when α = 0)
α = Angle between lever arm and right body
φ = Angle between extension of left body and lever arm, equilibrium position

Note that |C-B| is constant and equals the length *A* when α = 0
The extension of the spring, equal to $A-|C-B|+P$, has two independent causes: the variation of the length *A*, which is a function of α, and the setting of the pre-tensioning *P*.

The generated torque T equals:

$$T = C.F_t = C.F.\sin\beta \tag{4.1}$$

The force F, due to the elongation of the spring is:

$$F = k.\left(A-|C-B|+P\right) \tag{4.2}$$

Combining equation (4.1) and (4.2), results in:

$$T = C.\sin\beta.k.\left(A-|C-B|+P\right) \tag{4.3}$$

Using the sine rule

$$\frac{\sin\beta}{B} = \frac{\sin\alpha}{A} \tag{4.4}$$

and the cosine rule:

$$A = \sqrt{B^2 + C^2 - 2BC\cos\alpha} \tag{4.5}$$

The generated torque is then:

$$T = k.B.C.\sin\alpha.\left(1+\frac{P-|C-B|}{\sqrt{B^2+C^2-2.B.C.\cos\alpha}}\right) \tag{4.6}$$

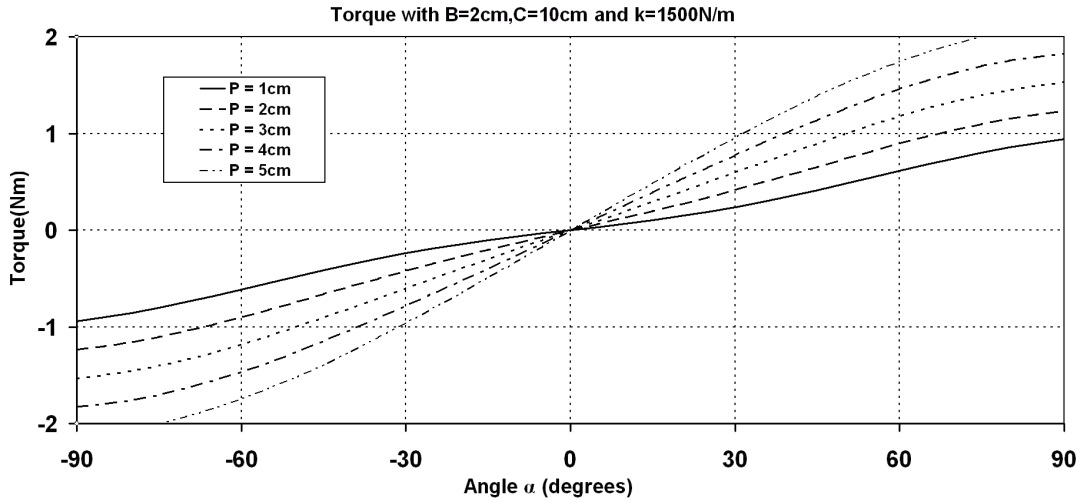

Fig.4.4. Torque as a function of angle α when pre-tension is altered

Figure 4.4 shows the torque generated by the MACCEPA as a function of α when the pre-tension P is altered.
Keeping in mind the requirements for compliant actuators that were listed in section 4.2.1, figure 4.4 for the torque shows that:

- The absolute value of the torque is symmetrical around the equilibrium position (T is an odd function of α)
- T is quasi linear for a substantial range of α
- The torque is independent of the equilibrium position φ, see equation 4.6. This implies that compliance (determined by the spring constant k and the amount of pre-tensioning P) and equilibrium position (φ) can be controlled independently.

In figure 4.5 the torque is split up into two parts. The lower curve represents the torque generated without pre-tension of the spring *(P=0)* and thus only the torque due to variation of the length A. Since the elongation of the spring for small angles of α is nearly zero, the generated torque is also nearly zero. This can be seen in the graph for angles between 0° and 15°. This explains why a MACCEPA without pre-tension is not usable as (linear) torsion spring. The upper curve is the torque generated by the MACCEPA with pre-tension, as calculated with equation 4.6. The curve in the middle is the result when the torque without pre-tension is subtracted from the total torque. This is thus the torque generated by the introduction of the pre-tension.

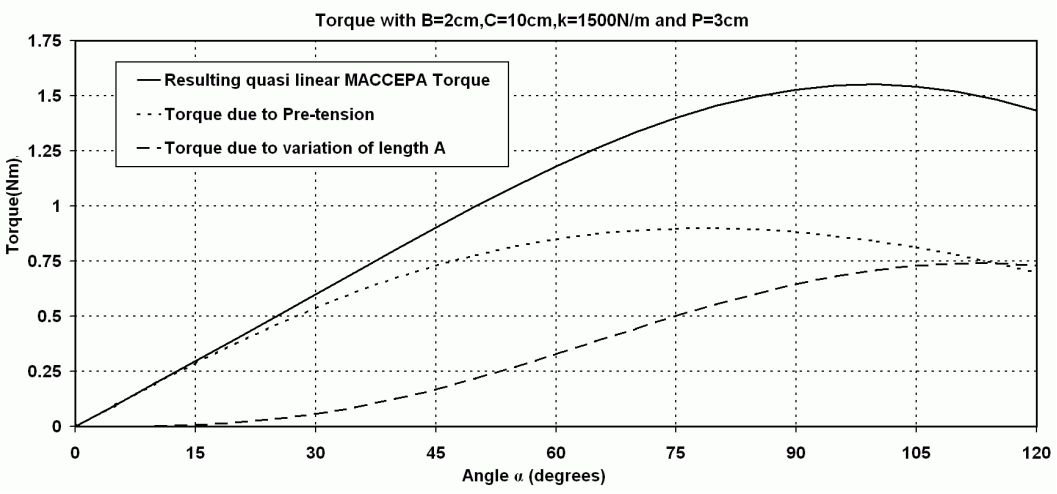

Fig.4.5. Torque generated by MACCEPA, split up in two parts

In the next section the influence of the design parameters B, C and k will be studied, to show that the non-linearity of the torque can be changed.

4.1.5 Influence of the design variables

The design variables *k*, *B* and *C* are chosen during design and are fixed during normal operation. In this chapter the influence of these variables will be investigated in detail.

Before talking about linearity, one should define the working range for α. As a useful working range, we assume -45° to 45°. It is worth mentioning that this range represents the functional range of the compliance of the actuator and that the rotation of the joint itself is not limited to 90°. Indeed, the equilibrium position φ can vary over a range of 360° and even more. Because of the symmetrical torque characteristics, the following discussion only regards the range between 0° and 45°.

In figure 4.6 one can see that the factor *C/B* influences the non-linearity of the torque *T* with respect to *α*. For increasing values of the ratio *C/B*, the torque curves become more linear. Note that formula 4.6 shows that *B* and *C* can be swapped without changing the result, so it is one of the two ratios *B/C* or *C/B* which should be high enough. In figure 4.7 the correlation coefficient of a linear regression—between 0 and 45°—is shown as a function of the ratio *B/C*. One can see that for a *B/C* or *C/B* ratio of a little above 5 the correlation coefficient is 0.99. This can be used as a guideline during design, when working with the above mentioned range of -45° to 45°. To extend the range, a larger value of *C/B* or *B/C* can be used to linearize the torque curve. Obviously, there are certain practical limits: the overall size of the actuator can become rather large for very high ratios. Anyway, even for high *B/C* ratios, there are limits on the linearity.

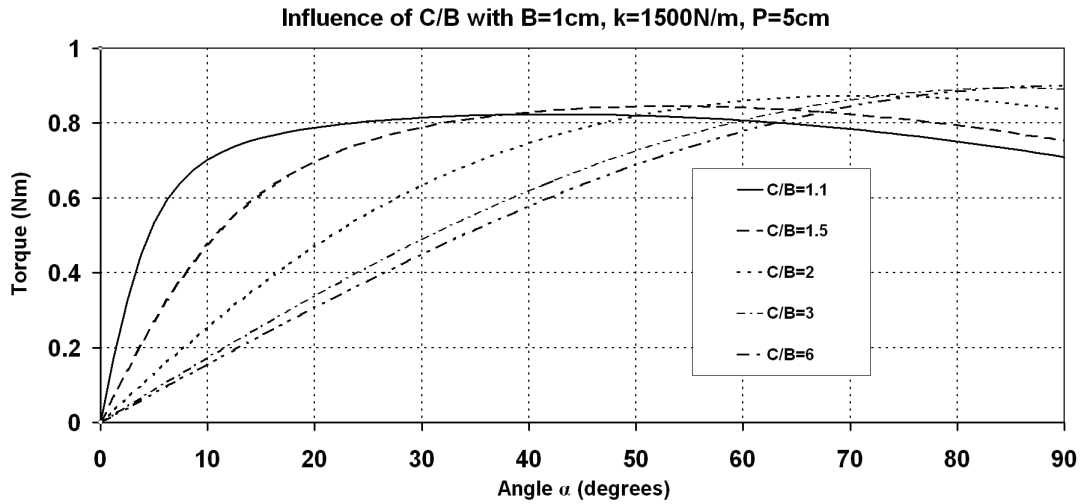

Fig.4.6. Influence of C/B

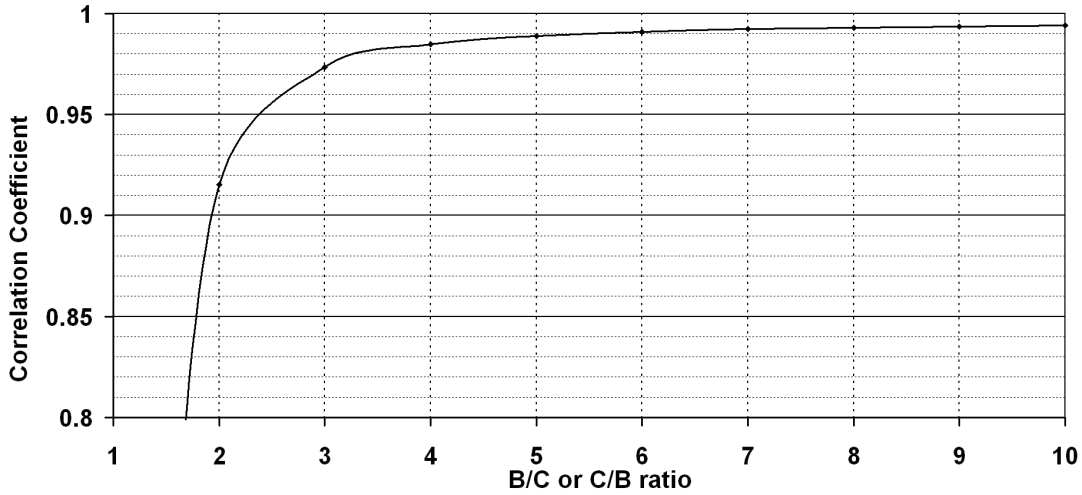

Fig.4.7. Correlation coefficient of linear regression as a function of B/C or C/B

In figure 4.8 the influence of the length of the lever arm *B*—while *C/B* is kept constant—is depicted. If the length of the lever arm is doubled, the torque is also approximately doubled. Since *B* and *C* can be swapped, the influence of *C* is analogous.

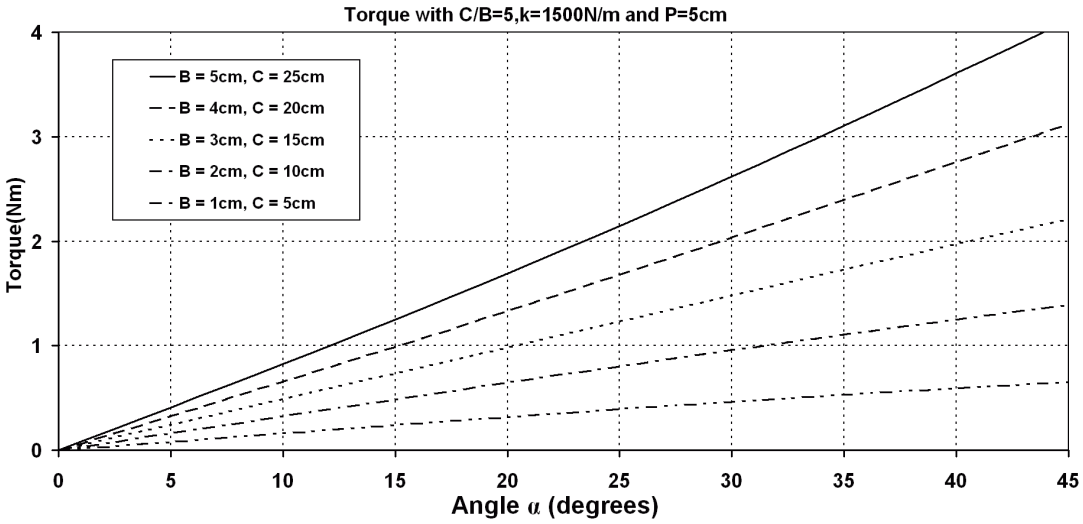

Fig.4.8. Influence of the lever arm B (or C) on the torque with C/B constant

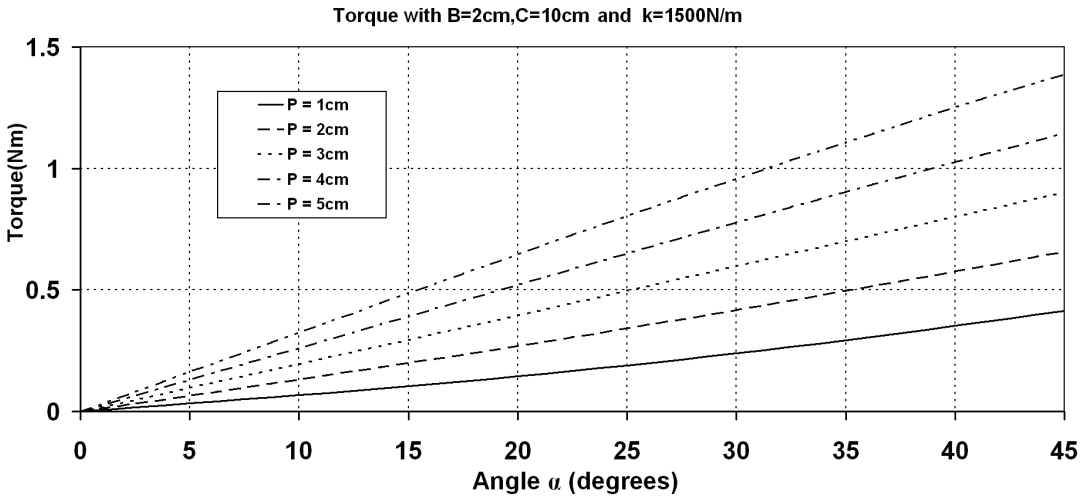

Fig.4.9. Influence of the Pre-tension P (detail of figure 4.4)

In figure 4.9, the quasi linear influence of the pre-tension *P* on the torque, for a range of α between 0° and 45°, is shown. Looking at formula 4.6, the spring constant *k* has a linear effect. Since changing the spring constant scales the curves shown in figure 4.4, parameter *k* can be used as prescaler of the torsional stiffness of the MACCEPA actuator.

We can conclude that, in order to obtain a correlation coefficient of .099 within the range of 0° and 45°, the ratio *B/C* or *C/B* should be at least 5 and that the parameters *B*, *C*, *k* and *P* have a more or less linear influence on the torque *T*.

4.1.6 Natural frequency adjustment

To calculate the natural frequency of a joint actuated by a MACCEPA, we can linearize formula 4.6 for small angles:

$$T = k.B.C.\alpha.\left(1 + \frac{P - |C - B|}{\sqrt{B^2 - 2BC + C^2}}\right) \quad 4.7$$

$$T = \alpha.k.B.C.\left(1 + \frac{P - |C - B|}{|C - B|}\right) \quad 4.8$$

$$T = \alpha.\frac{k.B.C}{|C - B|}.P \quad 4.9$$

The constants B, C and k, which are fixed during the design, can be combined into a single constant μ:

$$\mu = \frac{k.B.C}{|C - B|} \quad 4.10$$

The linearised torque (formula 4.9) now becomes:

$$T = \alpha \,.\, \mu \,.\, P \quad 4.11$$

which is the torque-angle relation of a torsion spring with spring constant $\mu.P$.

It is worth mentioning that this linearization, depending on the application, can be used for angles up to ±45°, due to the quasi linear torque characteristic. In figure 4.10, the torque calculated with equation 4.1 and with the linearised equation 4.4 (μ = 37.5N) can be compared.

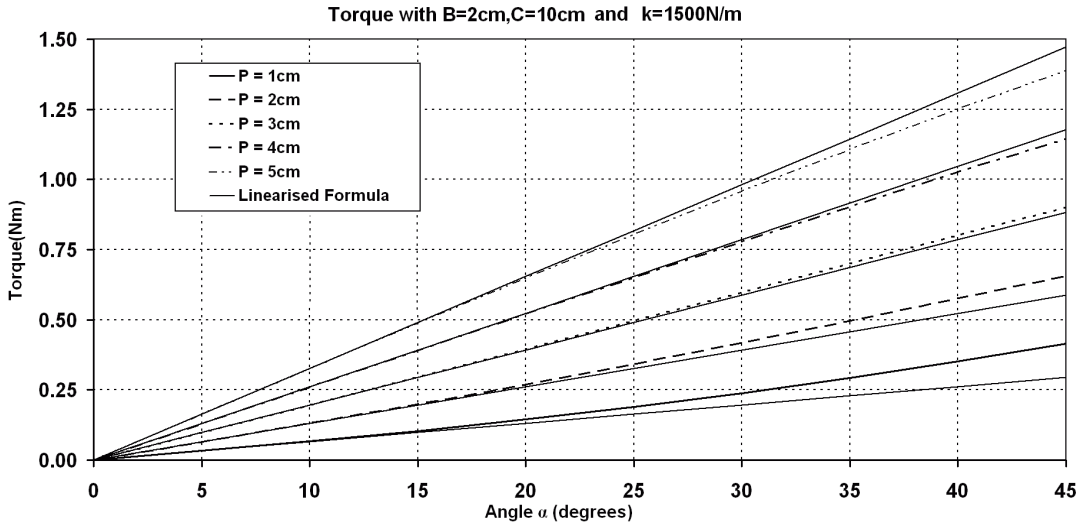

Fig.4.10. Comparison of formula 4.1 and the linearised formula 4.4

In figure 4.10 it can be seen that some of the linearised torques are above the exact values, some are below. A pre-tension of about 3.5cm will give the most linear torque curve. This curve is plotted in figure 4.11. It can be seen that for angles between -45 and 45°, the linearised formula is quasi perfect to predict the torque. This knowledge can be used to build a linear torsion spring with a normal linear spring.

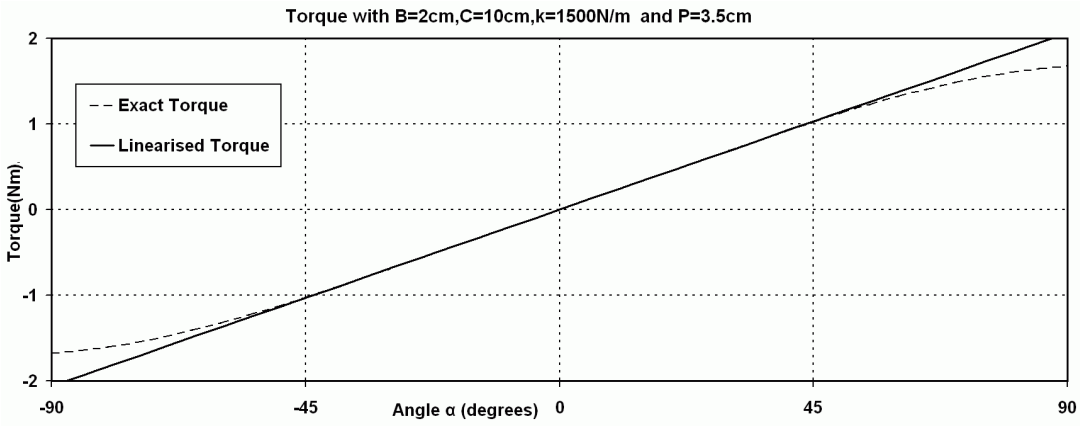

Fig.4.11. MACCEPA as linear torsion spring

The described setup is actually a torsion pendulum with adaptable compliance. The natural frequency f of a torsion pendulum, with moment of inertia I around the rotation axis and torsion constant κ, is given by:

$$f = \frac{1}{2\pi}\sqrt{\frac{\kappa}{I}} \qquad 4.12$$

and for a joint actuated by a MACCEPA this relation can be written as follows:

$$f = \frac{1}{2\pi}\sqrt{\frac{\mu.P}{I}} \qquad 4.13$$

This equation relates the compliance, determined by the pre-tension P, to the natural frequency for a joint actuated by a MACCEPA actuator. It can easily be inverted to calculate the pre-tension necessary to obtain a certain natural frequency.

Equations 4.11 and 4.13 show that the constant μ characterizes the behaviour of the MACCEPA actuator.

4.1.7 Negative spring constant

In some cases it could be useful to have a torsion spring with negative spring constant. Therefore the MACCEPA can also be used. When de lever arm is rotated 180°, the spring constant is negative, as shown in figure 4.12. This can be used to lower the natural frequency of system; however it is worth mentioning that the system can become unstable.

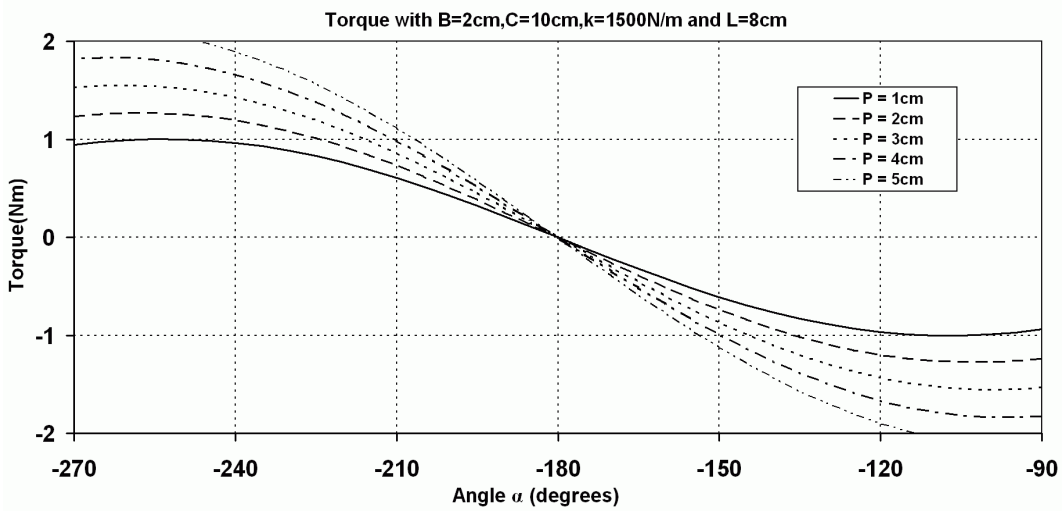

Fig.4.12 MACCEPA as torsion spring with negative spring constant

4.1.8 Motor requirements

In this section some remarks are made, which should be taken into consideration when designing a MACCEPA joint for a specific application. It is assumed that a *B/C* ratio is chosen such that a quasi linear torque-angle characteristic is achieved. If this is not required, a smaller ratio can be chosen. Obviously, this will have an influence on the other design parameters.

To define the angular range of the servomotors, a number of parameters should be known, like the required maximum absolute value of the angle α. Also the required angle range φ should be known. Note that finally the arm will be able to move over an angle φ + α. However, in order to be able to apply the maximum torque, the range will be limited to φ – α; and this both positive and negative. This choice is related to the type of application, e.g. torque control or Controlled Passive Walking. The desired angle φ directly defines the range of the servomotor for the equilibrium position. This range does not need to be limited to 180° or 360°.

To define the maximum range of motion for the servomotor that sets the compliance, several parameters should be taken into account. The spring has a rest length and a maximum elongation, before non-elastic deformation will occur. The maximum elongation of the spring is the sum of the maximum pre-tension and the maximum elongation of the length A, which is defined by B, C and the limit on the absolute value of α. The maximum pre-tension defines the range of the servomotor for the compliance. Note that several pre-tension mechanisms can be chosen, e.g. a spool directly placed on a servomotor, a linear drive or a spindle mechanism.

The servomotor for the compliance should be able to deliver the required torque to extend the spring to its maximum elongation. The pre-tension mechanism used will obviously have an influence.

The torque prerequisite of the servo for the equilibrium position is defiend by the maximum required torque. When all these parameters are known, the torque—that has to be delivered by the servomotor—can be calculated, using equation 4.6 and the geometrical setup in case of maximal generated torque.

4.1.9 Advantages and disadvantages of the MACCEPA concept

The MACCEPA actuator can deliver torque in both directions, which is not the case for e.g. the MARIONET actuator [4.01]. Moreover, the generated torque is symmetrical around the equilibrium position.

As explained before, the setting of the equilibrium position and the compliance are independent, and controlled by a specific servomotor. Therefore, the characteristics, e.g. size, torque and velocity of both servomotors can be optimised for their specific task. Consider a system where the equilibrium position is continuously changed, but the compliance only once in a while, e.g. in rehabilitation robotics. The compliance can then be set by a smaller motor with a higher gear ratio,

reducing the overall weight of the system. This is an advantage compared to most antagonistic setups.

Another advantage is that both settings—equilibrium position and compliance—are done by position controlled actuators. When considering passive motions, a certain setting is imposed, and then both actuators just have to maintain their position. This can be achieved by using a non-backdrivable gearing mechanism, which consumes no power during passive dynamic motions. This can also be achieved by a brake system, but this introduces an extra component and increases the complexity of the system.

The control signal sent to the motor defining the equilibrium position is independent of the actual position. This is a major advantage compared to pneumatic muscles, where the pressures that should be set for a certain equilibrium position, depend on the current position as well, due to their deformation. This is particularly awkward when taking into account that the pressures will vary when the actual position varies. This results in an equilibrium position that is difficult to control.

The MACCEPA is a simple and straightforward design, compared to other mechanisms with adaptable compliance. It can be built with a limited number of standard off-the-shelf components. It uses two position controlled motors and only one passive element to store energy, where all the designs based on an antagonistic setup of 2 non-linear springs use at least two.

Another advantage is that the actuation in not limited to electrical power: also hydraulic drives can be used. For the low-level position control of the 2 actuators, all existing control strategies—designed for the specific actuators—can be used.

A disadvantage is that the stiffness of the MACCEPA actuator is limited, due to the inelastic deformation of the spring. When the pre-tension is too high, the spring is elongated too much, and will endure a remaining deformation. This will change the spring constant and the rest length of the spring, and thus drastically change its characteristics. However, it can be prevented easily by setting a limit on the pre-tension.

Another disadvantage that comes forward when the MACCEPA actuator has to be put on the structure of the robot. The position and weight of the servomotors also have an influence on the dynamic behaviour of the mechanism.

Both motors have to deliver torque, even when none of them is moving. This is a drawback during passive motions, since lowering the energy consumption is one of the main reasons to use passive motion. This could be resolved when servomotors with a self locking mechanism are used, e.g. a worm gear.

Another disadvantage, which can also be found in antagonistic setups of 2 non-linear springs, is the fact that the friction in the joint is increased when the stiffness is increased. This influence can be decreased when using roller bearings in the joint.

4.2 Experimental setup

In this section, an experimental setup is used to perform two basic experiments to show the independent control of compliance and equilibrium position.

4.2.1 Design of experimental setup

In figure 4.13 a CAD drawing of the first prototype of the MACCEPA is depicted. On the right hand side, the body with the pre-tension mechanism is shown, on the left hand side, the body with the actuator controlling the equilibrium position is shown. The rotation axis between these bodies is supported by 2 roller bearings. A potentiometer is placed on this axis to measure the angle between the two bodies, which is the actual angle of the joint. Servomotors, electrical motors with integrated position controller, are used to set the equilibrium position and to pre-tension the spring.

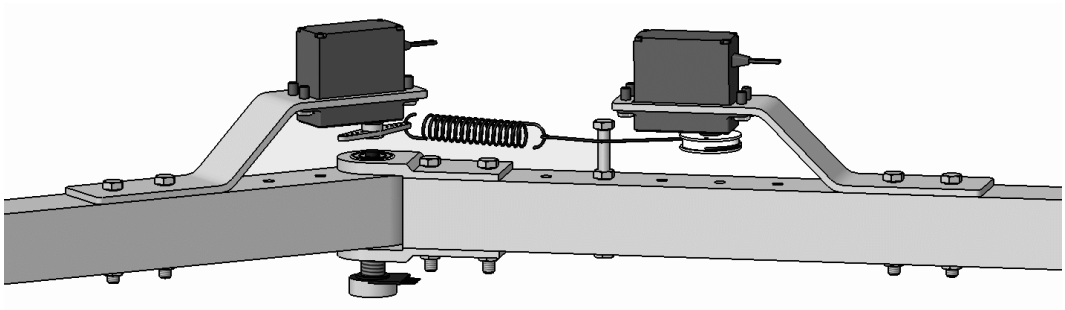

Fig.4.13. CAD drawing of the first MACCEPA prototype

The servomotor on the left, which is held in place by a bracket on the left body, has the same rotation axis as the joint and thus sets the angle between the left body and the lever arm, which is actually the equilibrium position of the joint. A number of different mechanisms can be used to pull on the cable in order to pre-tension the spring. On the right side of figure 4.13, a second servomotor with a spool is shown. By rotating this

motor, the cable winds up and the pre-tension of the spring is changed. As such the compliance of the equivalent torsion spring in the joint is altered as well. However, for the first prototype, a lever arm is used for the pre-tension, since this was a standard component, shipped together with the Protech B525 BB-MG servomotors [4.02] (see figure 4.14). This makes it more difficult to set a specific value for the compliance. However, for the first experiments the compliance is only set to *high* or *low* and these two situations are compared. In figure 4.14, a picture of the first prototype is shown. A Microchip [4.03] PIC16F877A microcontroller is used to control both servos and read the analog angle information. The data is exchanged with a PC through a RS232 serial interface. The parameters of the setup are: k = 1642 N/m, B = 2 cm and C= 10.4 cm, while P can vary from 0 till 4 cm.

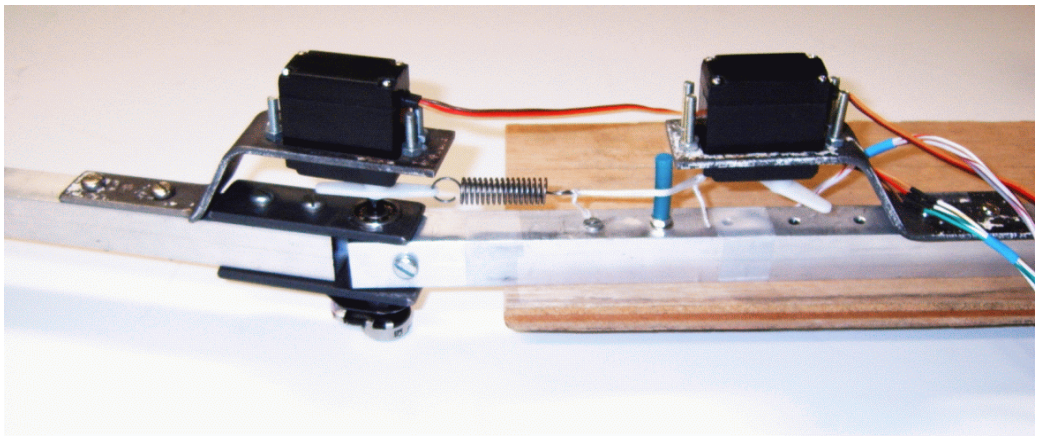

Fig.4.14. Picture of the first MACCEPA prototype

4.2.2 Experiment 1: changing compliance

In a first experiment the difference in natural movements with altered compliance was registered. The setup is placed in a horizontal plane (this means the rotation axis is vertical), so gravity does not influence the experiment. During the experiment the equilibrium position, defined in the experiments as the position where both arms are aligned, is set to 0°. As can be seen in figure 4.15, the joint is initially made relatively compliant by choosing a low value for P. The arm is manually pulled out of the equilibrium position and subsequently released, resulting in a passive oscillation around the equilibrium position with a certain frequency. After the joint stops oscillating, the joint is made stiffer by choosing a higher value for P, and it is once again pulled out of the equilibrium position. This is done for increasing values of the stiffness. Comparing the frequency for the first experiment 1.44Hz (stiffness setting 29%) and the last 2.6Hz (stiffness setting 98%), is according to the equation 4.13.

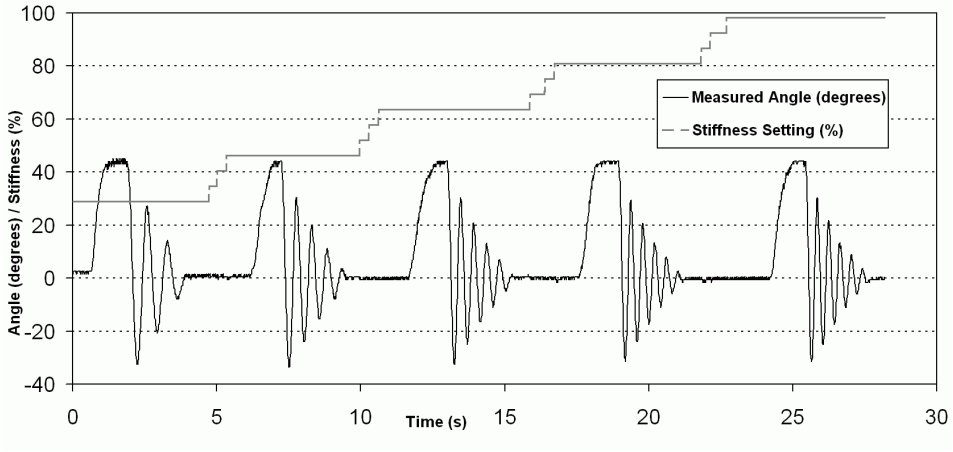

Fig.4.15. Variation of the natural frequency for different settings of the compliance.

4.2.3 Experiment 2: changing equilibrium position

The experiment in figure 4.16 shows the independence between the natural frequency and the equilibrium position. The dashed line is the set value of the equilibrium position. This time, the compliance is kept constant during the experiment. The full line is the measurement of the angular position. In the beginning of the experiment, the equilibrium position is set to 45° and the joint is pulled to 0° and released (at about 2 sec). The joint oscillates with a certain frequency, depending on the compliance setting. In a second experiment the equilibrium position was set to -30° and the joint is pulled to an angle of about 15°. Releasing the joint results in an oscillation with the same frequency. The two experiments show that the eigenfrequency is a function of the compliance, and that it is independent of the equilibrium position.

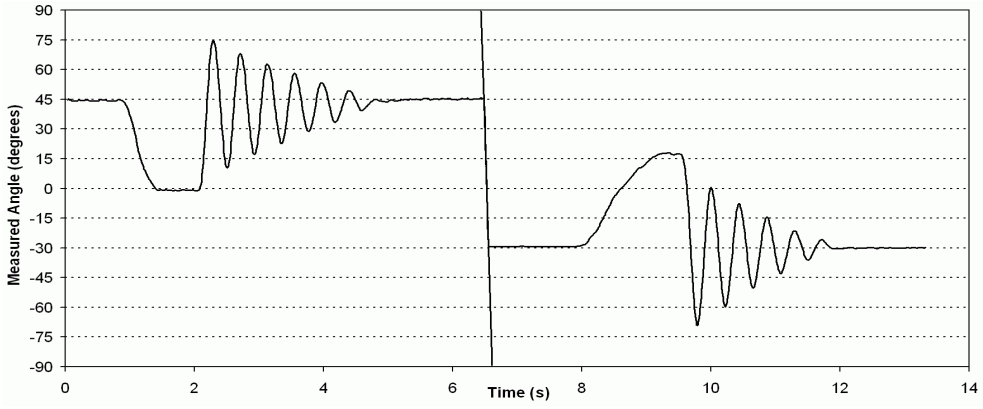

Fig.4.16. Natural frequency independent of equilibrium position

4.2.4 Experiment 3: influence of gravity

In this experiment the joint is placed vertical, so the gravity works in the same plane as the torque generated by the MACCEPA. In this experiment different values for the stiffness are chosen. The equilibrium position is changed so the arm is in rest horizontal. When the arm is pulled manually to -35° and released, this results in an oscillation with a frequency depending on the stiffness setting. However the influence of the variation in stiffness is smaller than in experiment 1, since the resulting torque is a weighted sum of the influence of the gravity, which is constant, and the torque generated by the MACCEPA, which is influenced by the stiffness setting.

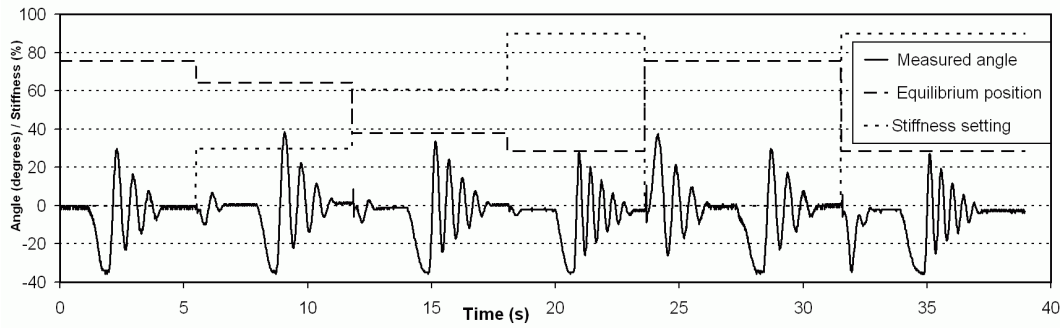

Fig.4.17 MACCEPA in gravitational field

4.3 Other embodiments

In the previous sections, the MACCEPA actuator was introduced, a formula for the torque was derived, the linearised formula was given and a prototype was presented. In this section, a number of other embodiments will be described, based on the same working principle as the first prototype. In section 4.4.1 the *slimline variant* will be presented, which is more convenient to be included as actuation in a robot leg. Section 4.4.2 will describe the *compact variant*, which is based on the fact that *B* and *C* are interchangeable in formula 4.1. In section 4.4.3 and 4.4.4, the position of the pre-tension motor and the position of the spring are discussed. Additionally, the advantages and disadvantages of each embodiment are given.

4.3.1 Slimline variant

The previously discussed setup is well suited for illustrative and conceptual purposes and experimental tests. However to incorporate this actuation mechanism into a robotic application, e.g. a leg of a walking robot, a smaller variant is needed. Therefore, different options for the placement of the actuator that controls the equilibrium position have been

studied. In the previous design the lever arm, determining the equilibrium position, was directly actuated by a servomotor in line with the rotation axis of the joint. One option is the use of a cable to connect the motion of the actuator to the lever arm, which can be useful when it is preferred that the actuator is positioned further away from the rotation axis. When for example it is preferred to keep the weight of the legs as low as possible, the actuator can be placed in the upper body. Using a belt or chain are similar possibilities. In the slimline variant prototype a gearing mechanism connects the actuator with the lever arm. The design, as shown in figure 4.18, with two equal gear wheels was chosen, resulting in a gear ratio of 1/1. The gear ratio can be used to optimize speed or torque characteristics. The advantage is that the actuator can be incorporated into the structure of the leg, close to the rotation axis, resulting in a smaller design. The first gear wheel is mounted on the servomotor. The axis of the second gearwheel coincides with the rotation axis of the joint and rotates independently of the motion of the left and right body. This second gearwheel acts as the lever arm to which the spring is connected, by means of a pin.

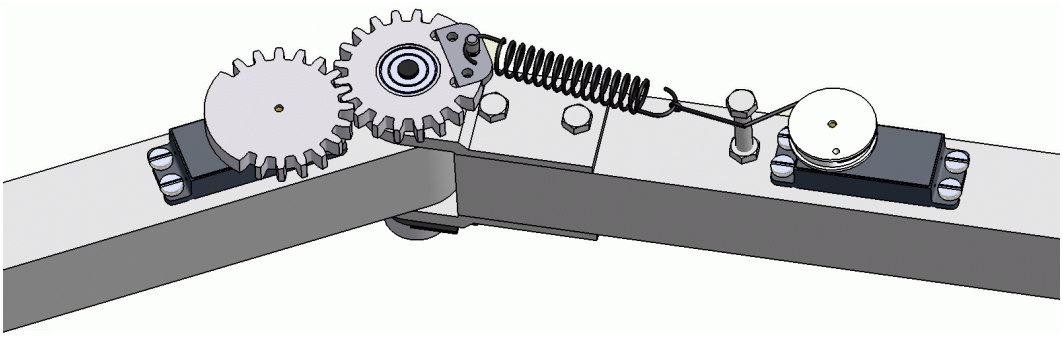

Fig.4.18. CAD Drawing of the MACCEPA Slimline Variant

In figure 4.19, a picture of this so-called Slimline MACCEPA prototype is given. The structure is made out of aluminum tubes with an external size of 30 by 30 mm. The servomotors are of the same type as the ones used in the conceptual design: B525 BB-MG of Protech. The generated maximum torque of 1.25 Nm is very high, compared to other servos of comparable size. The gears have a diameter of 40 mm, and the pin is placed at a distance of 20 mm from the rotation axis. A potentiometer is placed on the rotation axis, on the opposite side of the gear wheel including the lever arm. In figure 4.19 a relief spring can be seen which has been added on the right side of the pre-tension actuator. This does not change the working principle of the MACCEPA, but the relief spring reduces the power consumption of the pre-tension actuator when holding a certain position. The relief spring should be as long as possible, to keep the force in the working range as constant as possible. When the pre-tension actuator is in

its middle position, the force generated by the relief spring is preferably equal to the force of the spring of the MACCEPA.

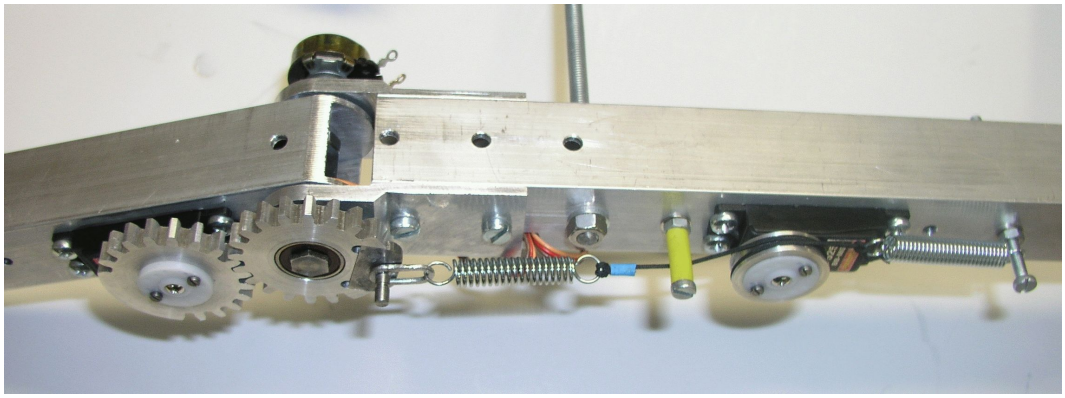

Fig.4.19. Picture of the Slimline MACCEPA

4.3.2 Compact variant

As mentioned before, the formula for the torque shows that *B* and *C* can be exchanged. To obtain a more or less linear torque characteristic the *C/B* or the *B/C* ratio should be at least 5, as can be seen in figure 4.7. The *C/B* ratio of 5 or more results in a variant as mentioned before. A *B/C* ratio of 5 or more results in a compact MACCEPA variant. The standard variant requires a certain length on one of the bodies for the length *C* plus the length of the pre-tension mechanism. The angle that the cable has to make around the point between the spring and the pre-tension mechanism is limited. In case of a *B/C* ratio of 5, the limit is 22.6° (See figure 4.3, when $\alpha = 90^o$ then $\beta = 11.3^o$), resulting in relatively low stress in the cable.

In the compact variant, figure 4.20, the spring is connected to the lever arm and as such positioned more closely to the rotation axis. To connect the cable to the pre-tension mechanism, the cable can be guided in a tube with low friction coefficient (e.g. Teflon), as shown in figure 4.20, or by using a mechanism with a standard pulley and a pulley that can rotate about 2 axes, which is more complex, but yields less friction. In the compact variant, the cable bends twice over a large angle, about 90° on 2 places. Also torsion occurs in the cable. This is a drawback for this design compared to the standard variant.

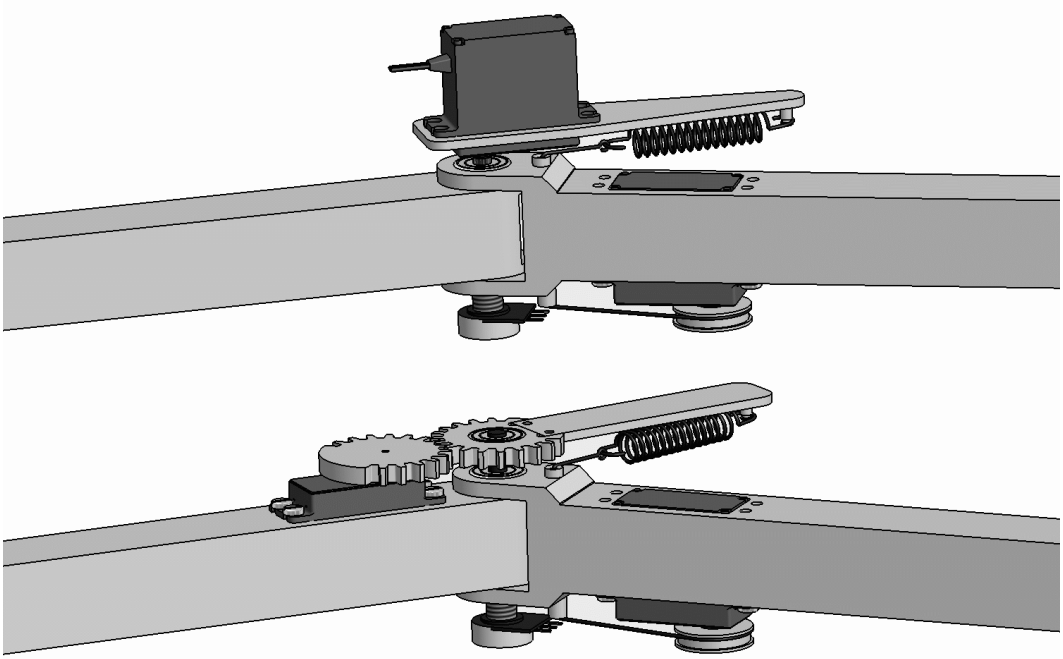

Fig.4.20. Two embodiments of the compact variant

In the upper CAD drawing in figure 4.20, the motor controlling the equilibrium position is placed in such a way that the motor shaft connects the motor to the left body. Around the motor shaft a bearing is placed allowing the right body to rotate around the same axis. The case of the motor is connected to the long lever arm. As such, a compact version of the Maccepa is obtained. The second CAD drawing is the compact slimline variant.

4.3.3 Placement of the pre-tension mechanism

In the previous paragraphs the pre-tension mechanism is placed on the right body, which is the body different from the one with the actuator used for setting the equilibrium position. The principle of this setup is shown in figure 4.21b. In figure 4.21a the pre-tension mechanism is placed between a point on the lever arm and a point on the right arm. This is the place where the spring was positioned before. In this case, the pre-tension is not fixed to a body, but tensioned in between the cable. Due to inertial forces, this can result in a rocking motion, eventually damaging the joint mechanism. The situation in figure 4.21c is analogous to the situation in figure 4.21b. The cable is guided over 1 point in both cases, but in the situation of figure 4.21b the angle by which the cable bends due to the guiding around the protrusion is smaller than in figure 4.21c, resulting in less friction losses. Obviously, the friction can be lowered using pulleys instead of guiding the cable by a protrusion, but this again requires a more complex design. Figure 4.21d and figure 4.21e are two embodiments with the pre-tension mechanism placed on the same body as the actuator which

controls the equilibrium position. Although the cable is in both cases guided around 2 protrusions, the first embodiment is preferable, since the angle that the cable makes around the protrusion is smaller. This results in less friction and less bending stress in the cable. It is worth mentioning that the protrusions or pulleys have to be designed in such a way that the cable is pulled against the protrusion or pulley for every possible angle of the joint. Other placements of the pre-tension mechanism are possible. As long as the length of the path of the cable does not change when the joint moves, the equilibrium position and compliance remain decoupled.

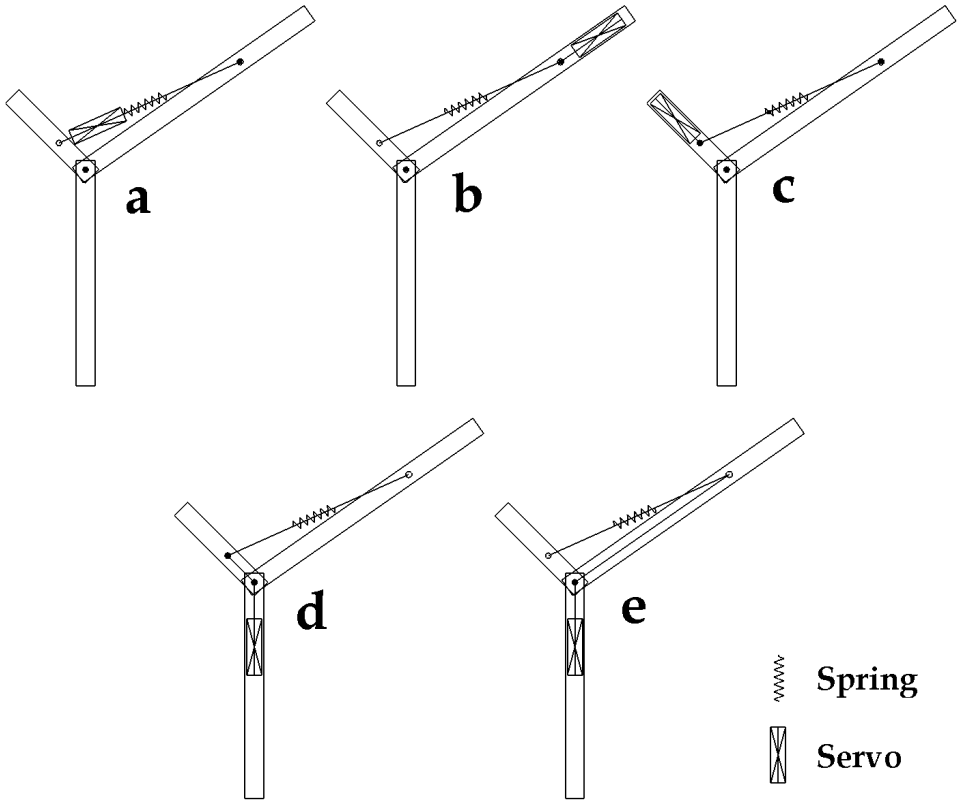

Fig.4.21. Different possible location of the pre-tension mechanism

Note that the placement of the servomotor will have implications on the moment of inertia of the joint, since the weight of the motors generally should be taken into account when designing a robot arm.

The pre-tension mechanism can be positioned at different locations, all with their specific advantages and disadvantages. The position of the spring is important as well. When the MACCEPA is used as an actuator for Controlled Passive Walking, the equilibrium position and compliance are set in the beginning of a motion. To save energy, it is recommended to keep these settings constant during the motion. Depending on the specific placement of the spring, the cable does or does not slide over the

protrusions, which of course strongly influences the friction losses. Preferably, the cable should not slide during passive motions, since then friction losses are avoided when the compliance is kept constant. Therefore, the setup shown in figure 4.21b is preferable for Controlled Passive Walking.

4.3.4 Location of the spring

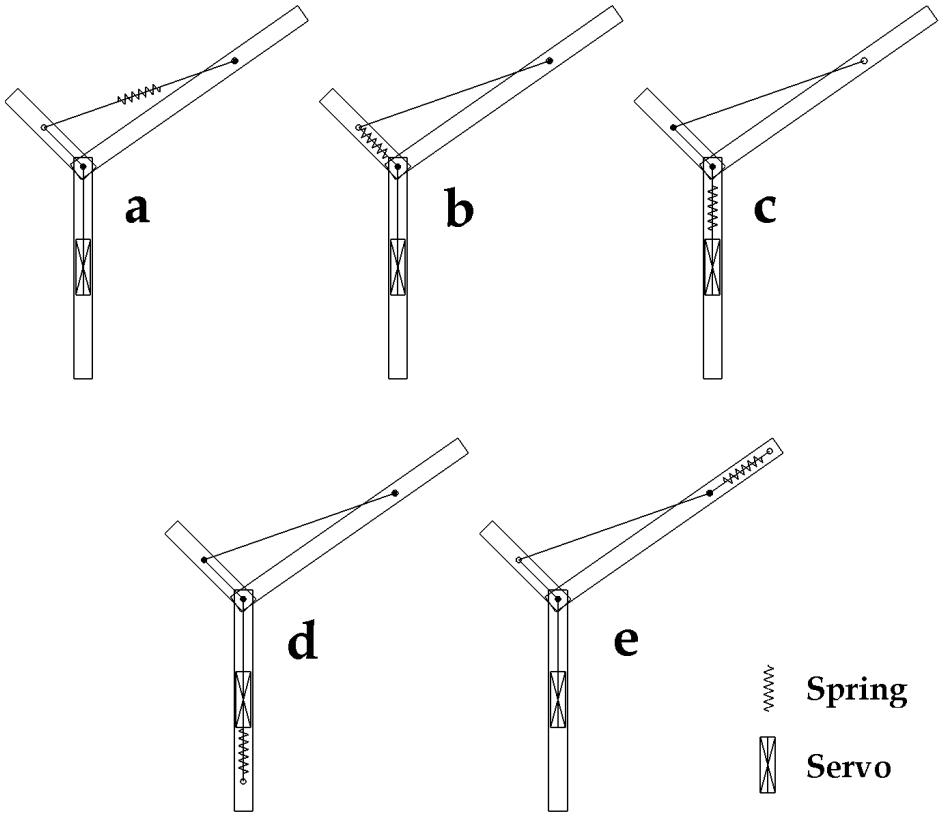

Fig.4.22. Different possible location of the spring

To study the different options of the spring placement, the configuration of figure 4.21d is chosen. Note that the other configurations in figure 4.21 result in similar options. In the previous paragraph, the spring is positioned between a point on the lever arm and a point on the right body. The other possible locations of the spring are depicted in figure 4.22. Figure 4.22a shows the placement described above. In figure 4.22b the spring is placed between 2 points on the lever arm. In this case, when using passive motion, the cable slides over the protrusion and energy is dissipated during the entire motion. The situation of figure 4.22c introduces friction at two locations: in a point on the lever arm and in a point on the rotation axis of the joint, resulting in a less optimal configuration. Figure 4.22d is comparable, but here the pre-tension mechanism is not fixed to the body but tensioned within the cable, which

has the same disadvantage as in the situation of figure 4.21a, concerning rocking. In figure 4.22e, the spring and the pre-tension mechanism are placed on different bodies, resulting is friction losses on the protrusion, but the bending angle of the cable is substantially smaller than in figure 4.22b.

As shown above, the spring and the pre-tension mechanism can be placed in different positions. Friction is an important parameter, but the overall size of the MACCEPA as well. When the overall size is important, e.g. in case of a walking robot, the number of places to put the spring and the pre-tension mechanism is restricted, which can result in a sub-optimal solution concerning friction losses. To reduce the inertia of a body, the actuators can be placed away from the rotation axis on another body by using e.g. cables. This choice however introduces friction losses at the place where the cables slide along the protrusions. Friction can be reduced using pulleys, but these will result in a more complex design of the MACCEPA.

4.4 Extension to more DOF MACCEPA joints

Until now, a joint with 1 rotational degree of freedom (1 DOF setup) has been described. In some situations, a rotational actuator with more degrees of freedom and adaptable compliance is useful, e.g. for a hip—3 DOF—or ankle—2 DOF—of a biped robot. First, a system with 2 degrees of freedom will be described, where the angle between the two intersecting axes is 90°. Thus, the left and right bodies are connected by a universal joint. Two options are considered: the compliance can be the same for both rotations, or the compliance can be controlled independently for both rotations. Subsequently, 3 DOF joints are presented.

4.4.1 MACCEPA 2 DOF rotational joint with 1 compliance.

This first option—same compliance for both rotations—requires three servomotors, since three variables need to be controlled: two equilibrium positions and one compliance. A system with 2 rotational degrees of freedom where the angle between the two intersecting axes is 90° is shown in figure 4.25. The left and right bodies are connected by a universal joint, as illustrated in Figure 4.23.

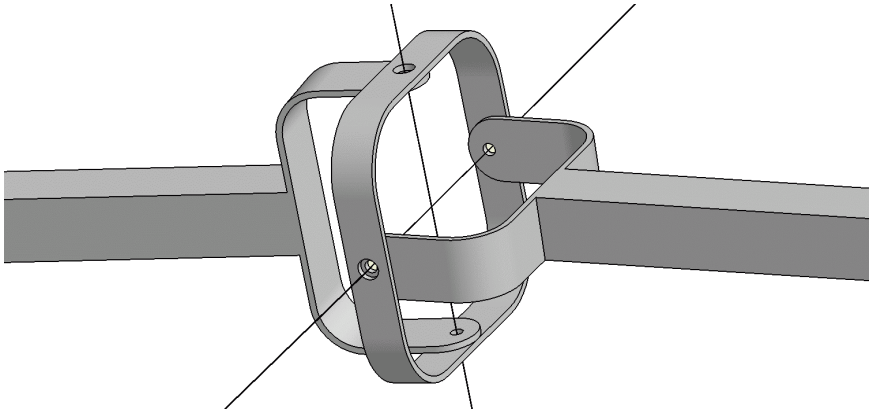

Fig.4.23. Universal joint with two orthogonal rotation axes

The small lever arm in the 1 DOF setup rotates around the same rotation axis of the joint which connects both bodies. In the 2 DOF case, that lever arm should be able to rotate around two orthogonal axes, which requires an additional universal joint. The axes have to coincide to make the control of the equilibrium position and compliance independent. If the two axes of each rotation need to coincide, the four axes have to go through the same point. This results in a configuration of two cardan joints inside one another, centered at the same point. The cardan joint of the lever arm has to be actuated by two servomotors, to make the control of both equilibrium positions independent. In Figure 4.24, a CAD drawing of the inner cardan joint is shown. This is actually the lever arm, which is positioned by two servomotors, one for the rotation about each axis. The two rotation axes of the lever arm are clearly depicted.

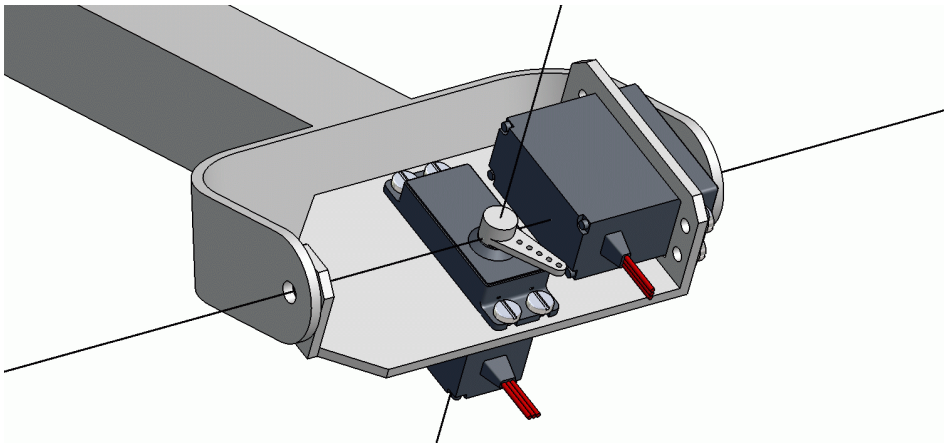

Fig.4.24. Lever arm actuated by two servomotors

The universal joint of figure 4.23 is placed around the lever arm construction of figure 4.24. When a spring with pre-tension mechanism, as used in the 1 DOF setup, is added, the 2 DOF setup is complete, as shown in figure 4.25. The outer universal joint is used to connect the left and right bodies. The lever arm, to which the spring is connected, can now be

rotated around two axes, relatively to the left body. The other end of the spring is connected to a pre-tension mechanism at the right body, similar to the pre-tension mechanism of the 1 DOF setup. With this setup, the equilibrium positions around both axes and the compliance can be controlled independently. Thus, each of the three actuators has its own function and does not interfere with the others, as was the case in the 1 DOF setup.

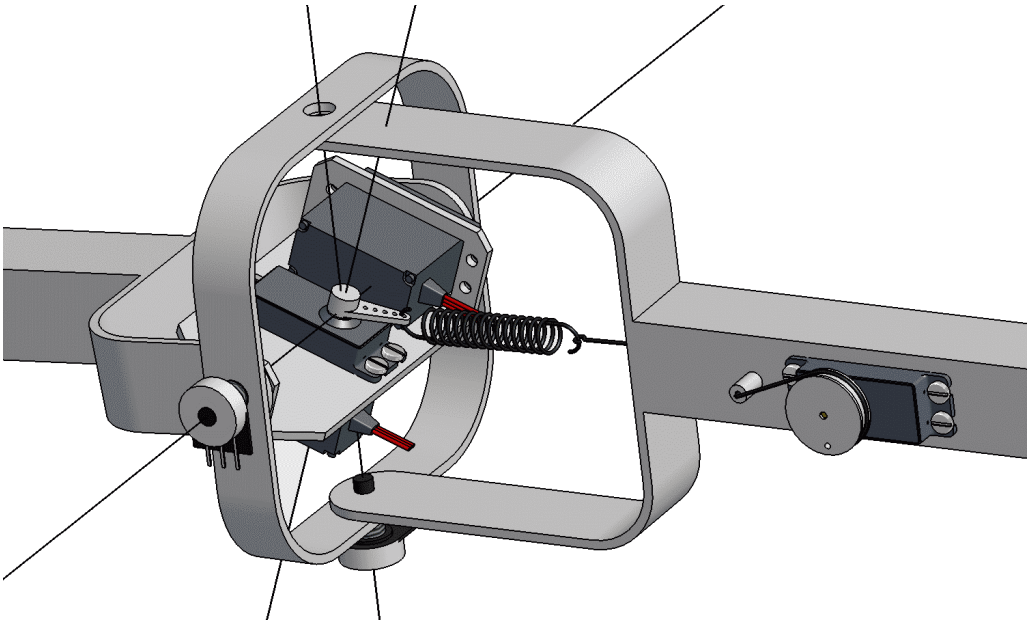

Fig.4.25. MACCEPA with two degrees of freedom and one compliance

It is worth mentioning that when the MACCEPA is not in the equilibrium position, the two axes of each rotation do not necessarily have to coincide. Actually, the point on the lever arm where the spring is connected, describes a sphere, centered around the point where the axes coincide. Also the point where the cable is guided to the pre-tension mechanism describes a sphere with the same centre. A plane can be defined by these two points (point on the lever arm and the guiding point of the pre-tension) and the centre point of the universal joint. The angle α, as defined for the standard 1 DOF MACCEPA in figure 4.3, can be measured in this plane and can thus be used to calculate the generated torque with equation 4.6 or equation 4.11.

4.4.2 MACCEPA 2 DOF rotational joint with 2 compliances

In some cases, the ability to control both compliances independently is worth the cost and complexity of a fourth motor. A setup with 2 rotational degrees of freedom for which the angle between the two intersecting axes is 90 degrees is proposed. The bodies are connected by a universal joint, as shown in figure 4.26.

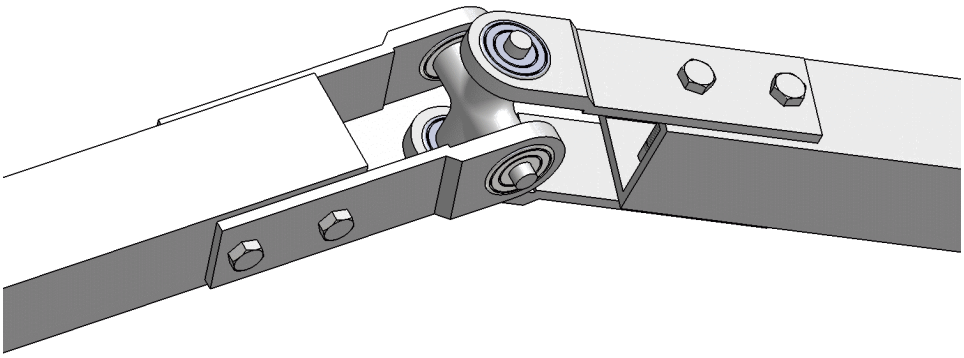

Fig.4.26. Universal joint

Concerning friction, it is preferable that the motors that sets the equilibrium position and the pre-tension mechanism are placed on different bodies. Since the pre-tension mechanism needs the most space, it is mounted on the larger body. Thus, the motors for the equilibrium positions should be placed on the smaller lever arm, as was also done in the setup shown in the upper part of figure 4.18. In this case the motor is placed on the cross-shaped piece of the universal joint, as shown in figure 4.27.

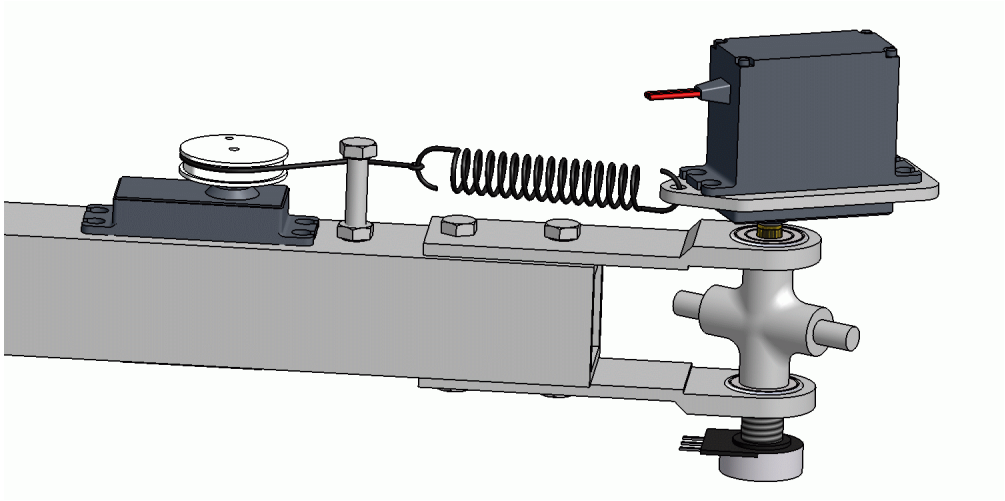

Fig.4.27. Equilibrium position actuator placed on cross piece of the universal joint.

The shaft of the motor is connected to the cross-shaped part. The servomotor rotates relatively to the cross piece and thus relatively to the right body as well. A plate, acting as lever arm, is placed on the servomotor. The spring is connected to a pre-tension mechanism, similar to the one used in the 1 DOF setup. This construction allows a second 1 DOF MACCEPA to be placed on the other connection of the cross piece of the cardan, resulting in a 2 DOF joint with 4 motors. A CAD drawing of a

complete 2 DOF MACCEPA with 2 independently controllable compliances is depicted in figure 4.28.

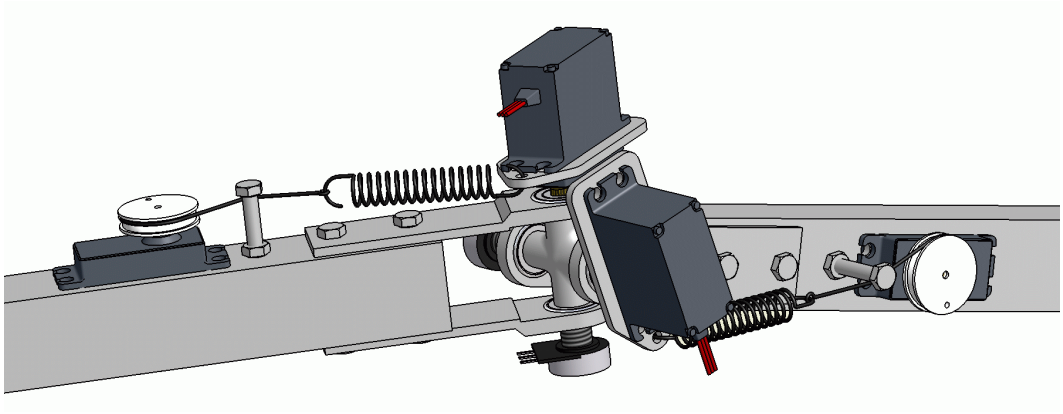

Fig.4.28. Complete MACCEPA with 2DOF and two independent compliances

Obviously, the actions of the four motors are completely independent. When one of the four parameters, one of the equilibrium positions or one of the compliances has to be changed, only the corresponding servomotor has to be controlled.

4.4.3 MACCEPA 3 DOF spherical joint

In the preceding sections, joints with 2 degrees of freedom with one or two compliances were presented. In some cases, like a hip joint of a 3D walking robot, a third degree of freedom can be useful. An extra degree of freedom that can be introduced is an axial rotation. In figure 4.29, a design, based on the compact variant presented in section 4.3.2, is shown.

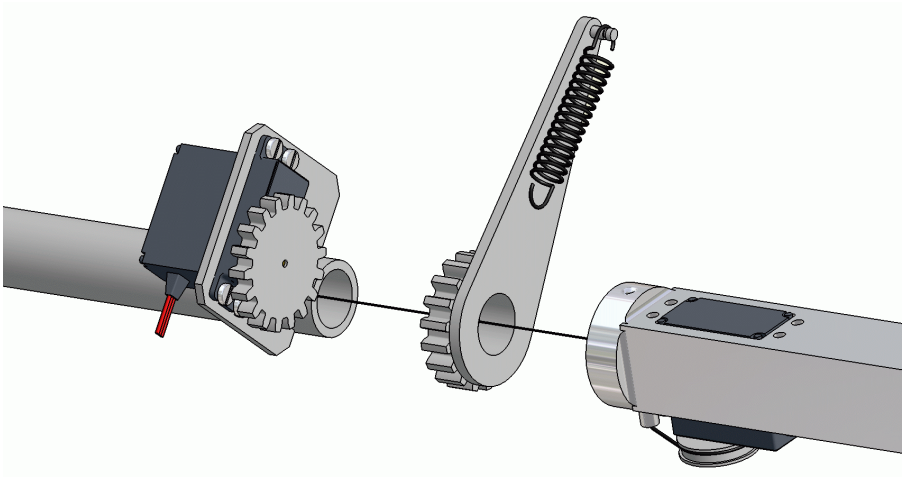

Fig.4.29.a Axial implementation of the MACCEPA

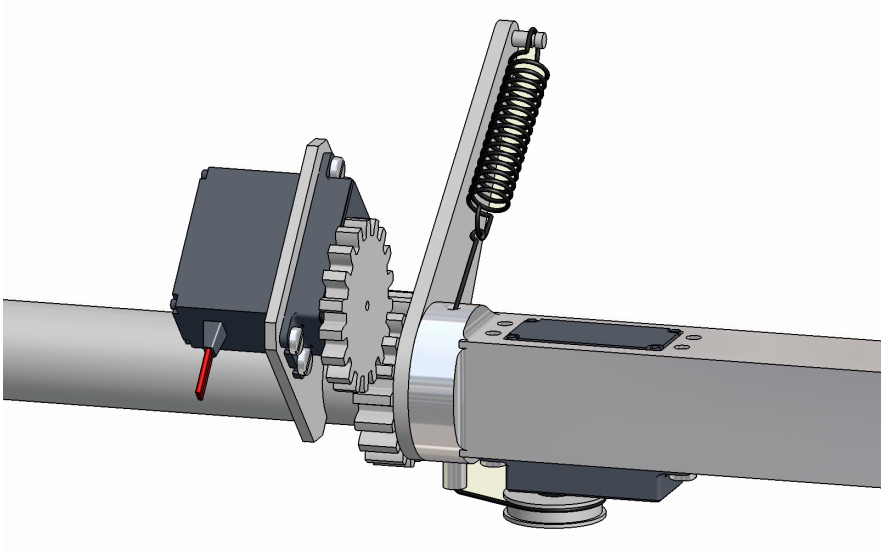

Fig.4.29.b Axial implementation of the MACCEPA

This axial implementation can be combined with the 2 DOF designs from sections 4.5.1 and 4.5.2. The resulting setup with 3 degrees of freedom and 2 independently controllable compliances—one for the axial rotation and one for the 2 remaining dimensions—is shown in figure 4.30. The setup with 3 degrees of freedom and 3 independently controllable compliances is shown in figure 4.31. It is worth mentioning that in the last case, each motor controls one specific parameter; either an equilibrium position or a compliance of one of the joints. In this way, the 6 parameters of the 3 DOF joint can be controlled independently.

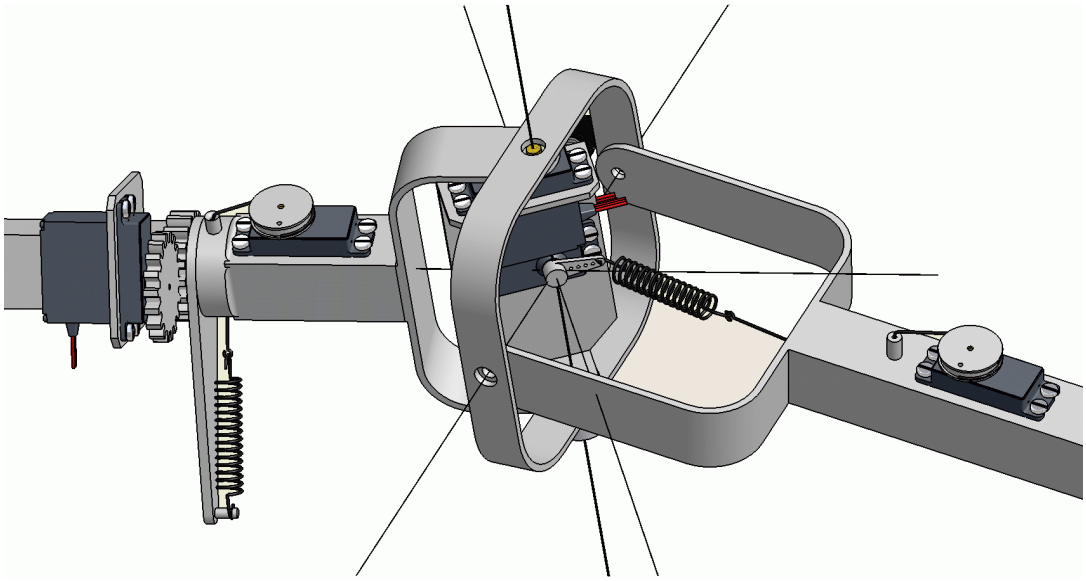

Fig.4.30. Spherical MACCEPA with 3 rotational DOF and 2 Compliances

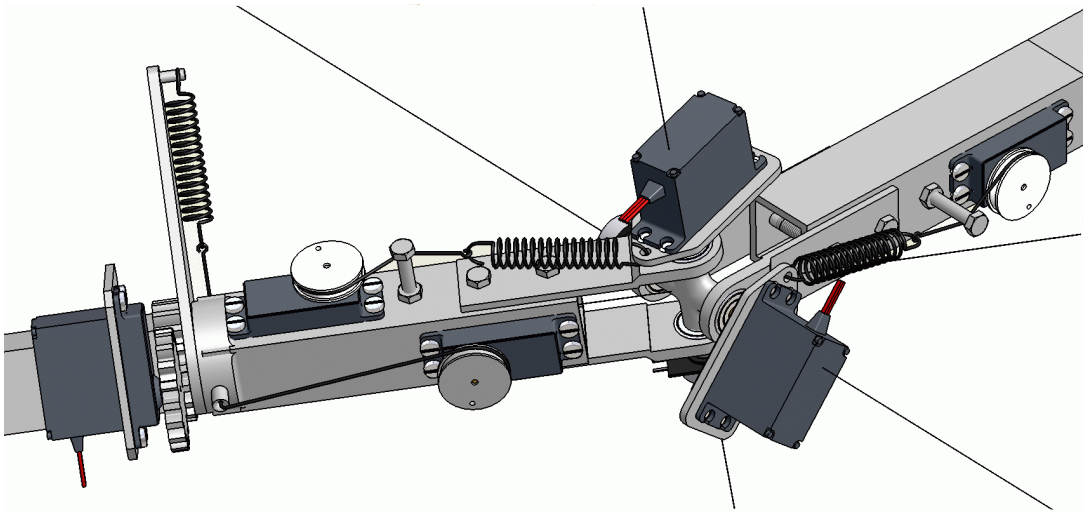

Fig.4.31. Spherical Maccepa with 3 rotational DOF and 3 Compliances

4.4.4 Overview

As shown in the examples above, it is possible to build 2 or 3 degrees of freedom joints with separate or common adjustable compliances for each rotation. In all the presented designs, the control of each variable (equilibrium position or compliance) is completely independent from the other. Thus, the control of one parameter requires the action of only one actuator, e.g. one servomotor. In table 4.1 the different embodiments are compared.

	Number of rotations	*Number of independent compliances*	*Number of control parameters = number of required servomotors*
1Dof, Stiff Actuator	*1*	*0*	*1*
1Dof, 1 compliance	*1*	*1*	*2*
2Dof, 1 compliance	*2*	*1*	*3*
2Dof, 2 compliances	*2*	*2*	*4*
3Dof, 2 compliances	*3*	*2*	*5*
3Dof, 3 compliances	*3*	*3*	*6*

Table 4.1 Comparison of the 1, 2 and 3DOF MACCEPA joints

4.5 Conclusions

The MACCEPA (Mechanically Adjustable Compliance and Controllable Equilibrium Position Actuator) was presented in detail. The most important properties are:

- The value of the torque is symmetrical around the equilibrium position (*T* is an odd function of α)

- The torque is a quasi linear function of the angle α (with proper dimensioning)

- The torque is a quasi linear function of the pre-tension P

- The compliance (determined by the spring constant k and the pre-tension *P*) and equilibrium position can be controlled independently.

- Since both settings—equilibrium position and compliance—are done by position controlled actuators, a non-backdrivable gearing mechanism can be used. This way no power is consumed during passive dynamic motions.

- Since each servomotor has its specific function, the dimension can be optimised for the specific task.

- Compared to other mechanisms with adaptable compliance, the MACCEPA is a simple and straightforward design, which can be built with a strictly limited number of standard off-the-shelf components.

- Joints with 2 and 3 rotational degrees of freedom can be built, according to the same principle.

- The actuation in not limited to electrical power, hydraulic drives can be used as well.

- Due to the series passive element, the motors will not be damaged when impacts occur on the joint.

- The MACCEPA introduces extra forces on the joint, which result in extra friction depending on the pre-tension

- The linearised formula for the torque corresponds to a linear torsion spring:

$$T = \alpha . \mu . P$$

References:

[4.01] J. S. Sulzer, M.A. Peshkin and J.L. Patton. MARIONET: An Exotendon-Driven Rotary Series Elastic Actuator for Exerting Joint Torque. Proceedings of the 2005 IEEE 9th International Conference on Rehabilitation Robotics, June 28 - July 1, 2005, Chicago, IL, USA

[4.02] http://www.protech.be/

[4.03] http://www.microchip.com/

Chapter 5

Veronica

Variable joint Elasticity RObot with
a Naturally Inspired Control Approach

A good simulation, be it a religious myth or scientific theory, gives us a sense of mastery over experience. To represent something symbolically, as we do when we speak or write, is somehow to capture it, thus making it one's own. But with this appropriation comes the realization that we have denied the immediacy of reality and that in creating a substitute we have but spun another thread in the web of our grand illusion.
Heinz R. Pagels

Theories are always very thin and insubstantial, experience only is tangible.
Hosea Ballou

Theory guides. Experiment decides.
(An old saying in science)

In this chapter, the mechanical and electronic designs of the bipedal walking robot Veronica are described. The main goal of this robot is to demonstrate the concept of Controlled Passive Walking. Therefore, it will not be a full 3D robot, but a planar walking biped with an upper body, legs and feet. The hip, the knee and the ankle will be actuated by MACCEPA's. For the design of this robot a modular approach is chosen. This means that both mechanics and electronics are based on the assembly of a number of modules. The modules should be as similar as possible in order to reduce the development efforts and the production costs. Some minor differences between the modules are however unavoidable.

This chapter is divided into two main parts: the overall mechanical design and the electronic design. Since the natural frequency of the limbs of Veronica can be adapted easily—in contrast with existing passive walkers—during operation, no simulations are needed in the design stage in order to obtain a fixed pre-required natural frequency. The spring can be used as a prescaler for the natural frequencies. Some preliminary tests are preformed to select the spring, which defines the range of compliance.

5.1 Mechanical design

Veronica is a planar walking biped with six DOF. Both legs have three joints: a hip, a knee and an ankle. For passive robots, the *intelligence of walking* is embedded in the structure of the robot, by tuning the masses and the moments of inertia of each limb. This contradicts with the idea of Controlled Passive Walking, where the natural frequencies should be adaptable on-line. Of course, the mass distribution still is important, as it defines the range of the available natural frequencies. The in-operation adaptability of the natural frequencies, by means of actuators with adaptable compliance, puts the intelligence of this type of passive walkers in the parameters set by the controller. These parameters are the compliance and equilibrium position in the different phases. Thus, actuators with adaptable compliance are a necessity for Controlled Passive Walking. MACCEPA actuators were chosen, for the following reasons:

- Independent control of compliance and equilibrium position
- Control signals independent of the current position (this will be explained in detail in chapter 6)
- Quasi linear angle-torque characteristic
- Ability to store and release energy
- Simple and low cost design

The overall height of the robot is about 1 meter, for reasons of ease of transportation and availability of small size high torque servomotors. To achieve an overall size of 1 meter, the length of the torso, upper leg and lower leg are chosen to be 30 cm and the height of the foot joint above the ground is 10 cm.

5.1.1 Placement of the actuators

As described in chapter 4, different designs of MACCEPA actuators can be used. In order to have slim legs, preferable for humanlike robots, the slimline MACCEPA is the obvious choice for the planar walking biped concept. In figure 5.1, the slimline Maccepa is shown. As can be seen on the CAD drawing, the limited number of components results in a simple and straightforward joint mechanism.

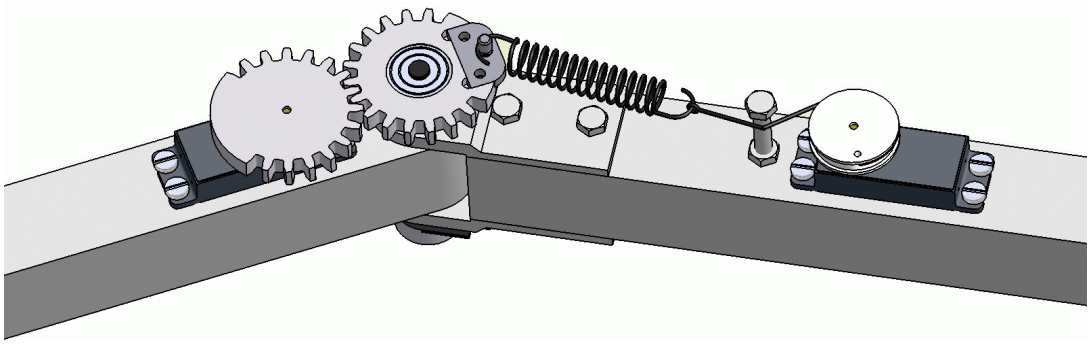

Fig.5.1. Slimline MACCEPA

Having figure 5.1 in mind representing e.g. a knee joint, it is worth mentioning that it can be used in two configurations. In one configuration the pre-tension motor is placed in the upper leg, in the other it is placed in the lower leg. One can notice that the global functioning and control are not affected by the choice between these two configurations, except for the different mass distributions in the leg. The space to integrate the MACCEPA in the ankle joint is limited. Since the pre-tension mechanism needs more space than the equilibrium position actuator, the orientation of all the MACCEPAs are chosen in such a way that the pre-tension mechanism is placed in the limb above the joint. In figure 5.2, a CAD drawing of the assembly of six equal MACCEPA modules is shown. The gearwheels, spools and springs are omitted for clarity.

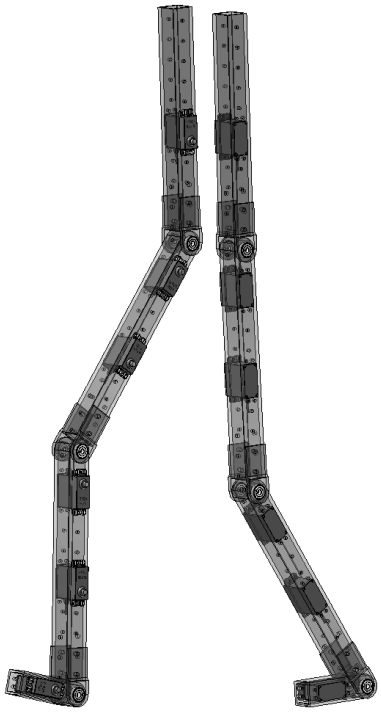

Fig.5.2 Assembly of 6 equal MACCEPA Modules

5.1.2 Structure of the feet

It is worth mentioning that passive walkers generally have unactuated ankle joints and round feet. However, it is not our intention to make a passive walker, but a robot with a passive motion that can be controlled. Therefore, the ankle joint is provided with a compliant actuator.

For practical reasons, there are some restrictions on the combination of the six equal modules, shown in figure 5.2. As an example, three possible placements of the servo motor are shown for the ankle in figure 5.3. The left configuration has already the shape of a foot. It allows the joint to rotate counterclockwise over a large angle, but the clockwise rotation is limited due to a collision with the rest of the structure. The working range of the angle, shown in the middle configuration, is symmetric, but the height of the foot joint is too high, compared with the other limbs. Therefore, the option on the right is developed. In this case, the servomotor is placed horizontally, under the joint. The only objection that could be formulated is the fact that the structure of the foot module is different from the other modules. This is however only the case for the mechanical design, and not for the electronics.

Fig.5.3 Placement of servomotor in foot

5.1.3 Lock up mechanism in the knee

Level ground passive walkers require actuators to compensate for energy losses, due to friction and impact. The required torques are however much less than for actuated walking robots. The properties of the actuators are selected such that the actuators only provide a minimal torque and energy supply, required to maintain the walking motion. Therefore, these types of robots are not able to stand on a leg, when it is not stretched. A lock up mechanism is used in order to keep the leg in a stretched singular position, so the leg is able to carry the load of the robot during the stance phase. Some passive walking robots do not even have an actuator in the knee, and just use a passive or active locking mechanism. An example of a passive walking robot with a passive locking mechanism in the knee [5.01] is given on the left side of figure 5.4. An active locking mechanism is a mechanism that completely locks the knee when it is stretched. The knee cannot be bent in either direction until the mechanism unlocks the knee. One of the three types of failure of two-dimensional passive walking models is a collapse through the stance knee [5.02]. This is prevented by using an active locking mechanism, since this keeps the stance leg stretched, whatever external torque is applied to it. This allows for a greater variety of motions and implicitly makes the robot more robust for external perturbations and deviations in natural frequency, meaning that tuning of the mass distribution of the legs is less critical. In the robot Denise [5.02], shown in the right of figure 5.4, the active locking is achieved by controllable knee latches.

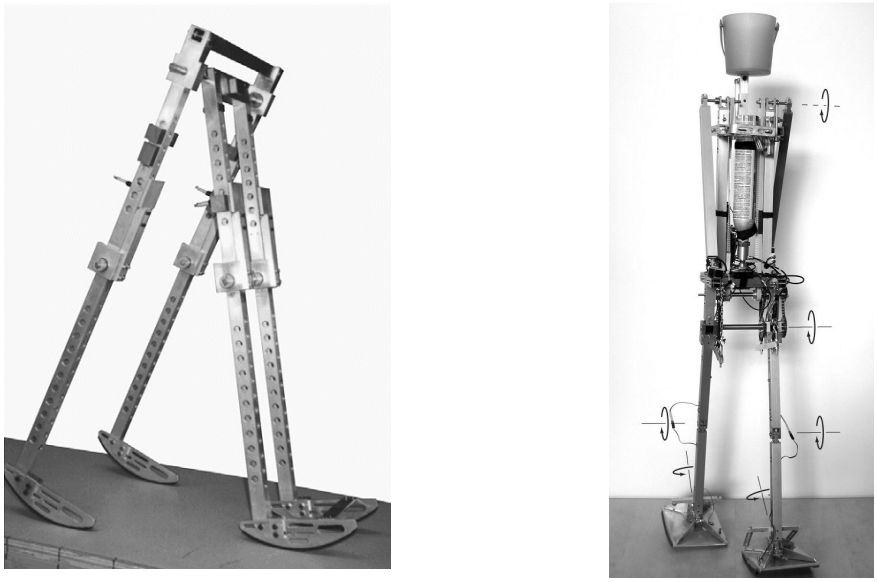

Fig.5.4 Examples of robots passive and active knee locking: Passive walker by Garcia, Cornell, and Denise from Delft University

Since Veronica has actuators with adaptable compliance, the knee locking mechanism can be a combination of both. A passive locking mechanism preventing overstretching of the leg is placed on the knee, as shown in figure 5.5. When the equilibrium position of the MACCEPA in the knee is set to the front and the compliance is not too high, a torque will be applied to keep the knee stretched. This combination of an active and passive locking mechanism allows the lower leg to swing passively to the stretched position due to the forward swing of the upper leg, or it can be pulled actively to the front by the compliant actuator at the knee. To reduce the required torque to keep the knee stretched, the passive knee locking mechanism allows overstretching of the knee (by a few degrees).

Fig.5.5 CAD drawing of the knee joint of Veronica

5.1.4 Bisecting hip mechanism

To ensure that the upper body is stabilized in the upright position, while the alternating swing leg swings passively to a forward position, is not simple. Previously proposed solutions, including McGeer's *levered isotonic tendons* [5.03] and variable springs [5.04], are fairly complex solutions. Therefore, in [5.02] a bisecting hip mechanism is proposed for the robot Max. Figure 5.6 shows the implementation with an auxiliary axle connected to the legs with one straight and one cross-over chain. The outer legs are connected to the gear in the middle. This gear is connected to the upper axle by a cross-over chain. This causes both axles to rotate in the opposite direction. The upper axle is connected with a straight chain to a gear, which is connected to the inner pair of legs. This way, the angle of both sets of legs are opposite, relative to the upper body.

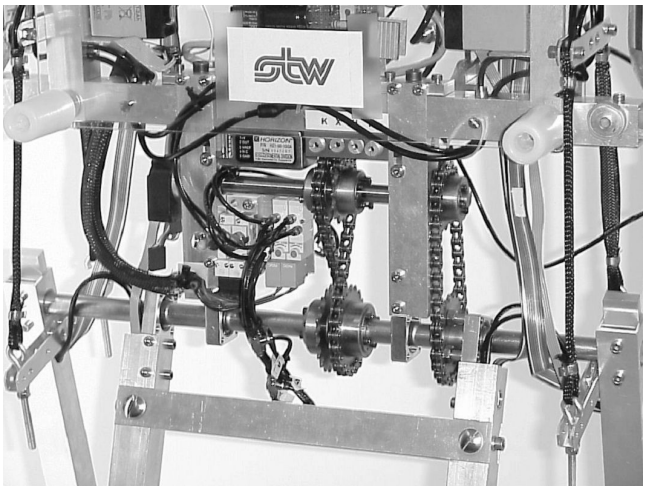

Fig.5.6 Bisecting mechanism of biped Max [5.02]

It is worth mentioning that rather large torques are transmitted through the chain wheels and axles. This can damage the mechanism when e.g. the robot falls. Other ways to implement the bisecting mechanism are the use of a four-bar linkage, a differential gearbox, or cables and pulleys [5.05]. In Veronica, a lever mechanism is used, as shown in figure 5.7. When the right leg moves to the front, the lever arm is pulled down on the left side, and lifted on the other. This forces the left leg backward with the same angle as the right leg is moved forward. When the lever mechanism is symmetrical, the values of the angle of the left and right leg relative to the torso, are the same, with an opposite direction. This means that the torso is always in the bisecting orientation of both legs.

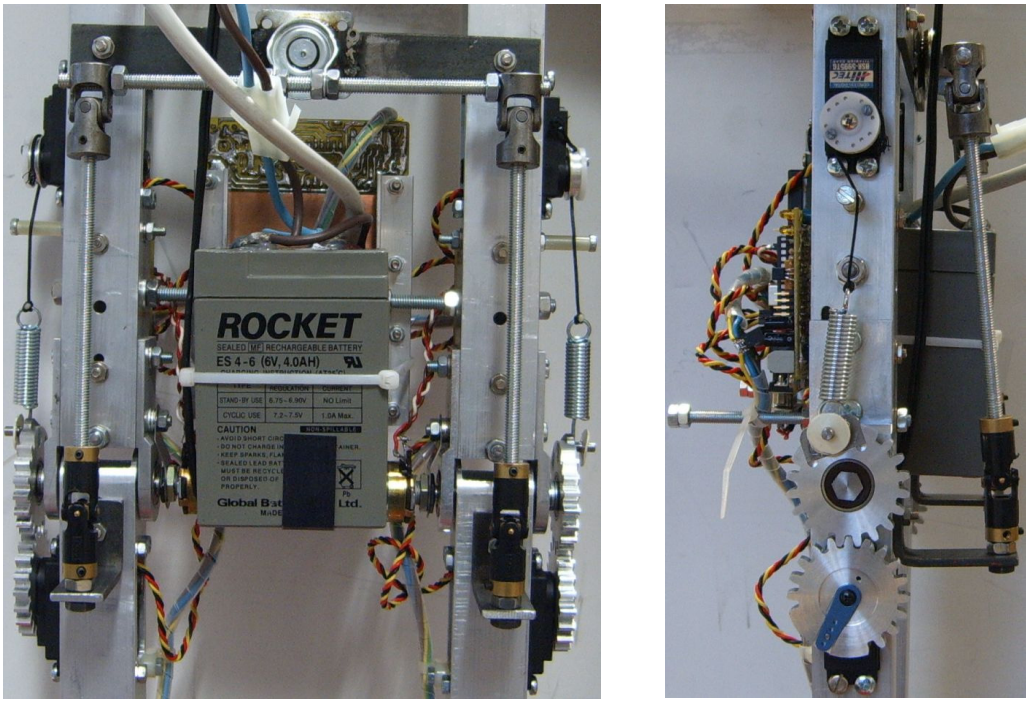

Fig.5.7 Two orthogonal views of the bisecting mechanism of Veronica

5.1.4 Lateral stability

A planar walking biped needs a system to ensure lateral stability. Several solutions have been developed for other robots. Each of them has certain advantages and disadvantages, depending on the purpose of the robot. The main goal of Veronica is to demonstrate the principle of Controlled Passive Walking. In the following sections a number of possibilities to achieve lateral balancing are explained, and the advantages and disadvantages are discussed.

Rotating beam

A solution for the lateral stability is to connect the robot to a ball joint by means of a beam, e.g. Spring Flamingo [5.06]. On the side of the robot, the beam is connected to the hip joint or to the upper body. The ball joint is placed on a stand, so that the robot has a circular path around this point.

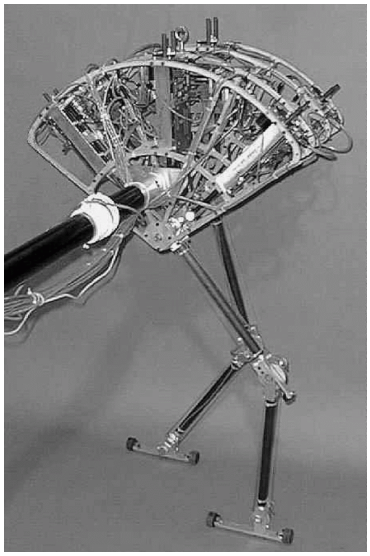

Example: Spring Flamingo - Massachusetts Institute of Technology [5.06]

Advantages:

- *endless* path
- cables can be guided by the beam to an external control and power unit
- beam can be lifted to reduce influence of gravity during tests
- absolute position can easily be measured

Disadvantages:

- requires large free space in the lab
- inner and outer foot have different path length; difference depending on the length of the beam and the lateral space between the feet, feet slip sideways
- inertia of the beam (can have a stabilizing effect)

Symmetric legs

When using four legs of which the two inner and two outer are coupled, the centre of gravity and zero moment point will always stay in the sagittal plane, because of the symmetry, assuming a level ground. The two inner legs can also be designed as a single leg, resulting in three legs, of which the outer two are coupled.

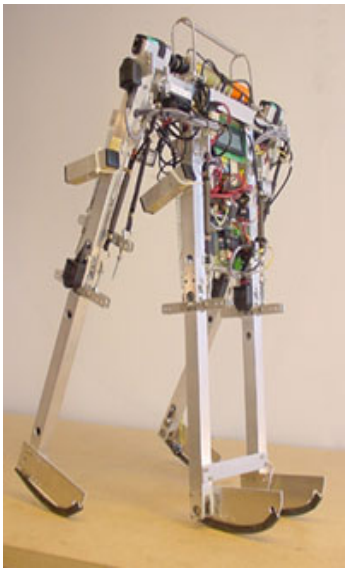

Example: Mike - Delft Biorobotics Laboratory [5.02]

Advantages:

- perfect symmetry
- portable robot
- robot can walk autonomously, because it is not connected to the surroundings

Disadvantages:

- unnatural looking *biped*
- difficult when knee and ankles are actuated: actuators have to be duplicated or limbs have to be linked
- Small asymmetry (outer leg length) can have large effect
- Extra weight

Slider mechanism

A combination of a horizontal, a vertical slider and a rotational joint can be placed in a plane, parallel to the sagittal plane of the robot. The robot can be connected to this slider mechanism in any point, but for reasons of symmetry, it is usually done in the hip joint or the upper body.

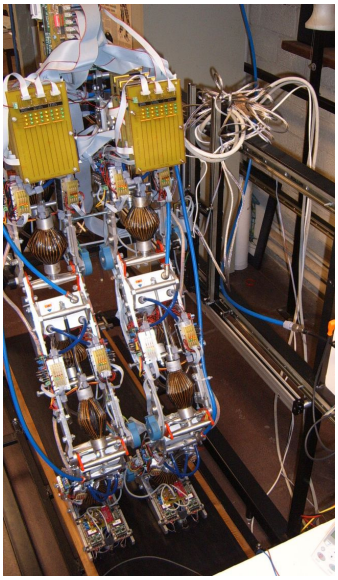

Example: Lucy - Vrije Universiteit Brussel [5.07]

Advantages:

- cables can be guided by sliders to an external control and power unit
- sliders can be lifted to reduce influence of gravity
- absolute position can be measured easily

Disadvantages:

- limited path length, can be resolved by using treadmill
- rather large, heavy and expensive construction

Round feet

The feet can be shaped in such a way that the robot will toddle to the side of the stance leg. In this way, the robot does not fall sideways. This concept was already patented in 1888 by G.T. Fallis [5.17].

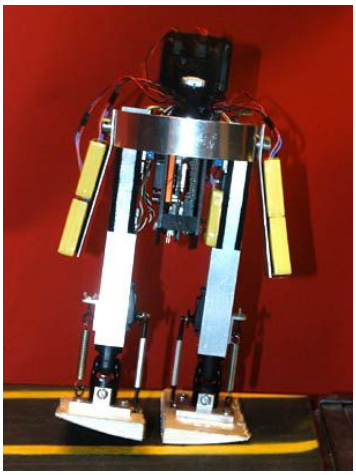

Example: Toddler

Massachusetts Institute of Technology [5.08]

Advantages:

- no special mechanism required
- robot can walk autonomously, since it is not connected to the surroundings

Disadvantages:

- toddle motion cannot be adapted for different walking speeds
- sideways balance is dynamic
- power and controller need to be onboard
- 3D motion

Inner foot support

Another way to ensure lateral stability is the placement of one or more protrusions on the side of both feet, so that the supporting polygons of the feet overlap. The main disadvantage is that both feet cannot be placed side-by-side, due to the overlapping of the inner supports (assuming symmetry).

Example: BaRt-UH - Universität Hannover [5.09]

Advantages:

- no special mechanism required
- robot can walk autonomously, since it is not connected to the surroundings

Disadvantages:

- the feet cannot be placed next to each other
- power and controller are preferably onboard
- Stability influenced by dynamics

Moving lateral mass

Some older static walking bipeds carried an extra mass that could be moved laterally to the side of the stance leg. In this way, the centre of gravity could be placed above the supporting foot.

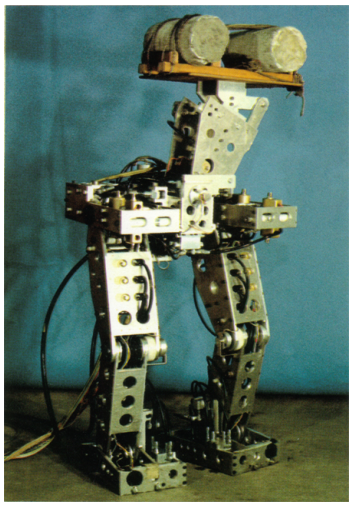

Example:WL-5 - Waseda University, Japan [5.10]

Advantages:

- robot can walk autonomously, since it is not connected to the environment

Disadvantages:

- requires actuation, which is not desired for a passive robot
- unnatural looking biped
- used in slow moving statically balanced bipeds
- extra weight
- 3D Motion

Conclusion

As was shown, various mechanisms exist to stabilise the lateral motion of a 2D walking robot. The option where the robot is connected to the environment with sliders is withdrawn, since the friction introduced obstructs the passive motions, and the path would not be very long. The moving lateral mass solution requires actuation, which is not an option for passive walking robots. The symmetric leg setup would require extra actuators since the ankles are actuated, and cannot easily be connected by a mechanism. The round feet are tuned for one fixed walking speed, which contradicts with the idea of Controlled Passive Walking. The option with the inner foot support was tested, but was found not to give enough lateral stability during the tuning experiments. Therefore the option with a rotating beam is chosen. A picture of the implementation is shown in figure 5.8.

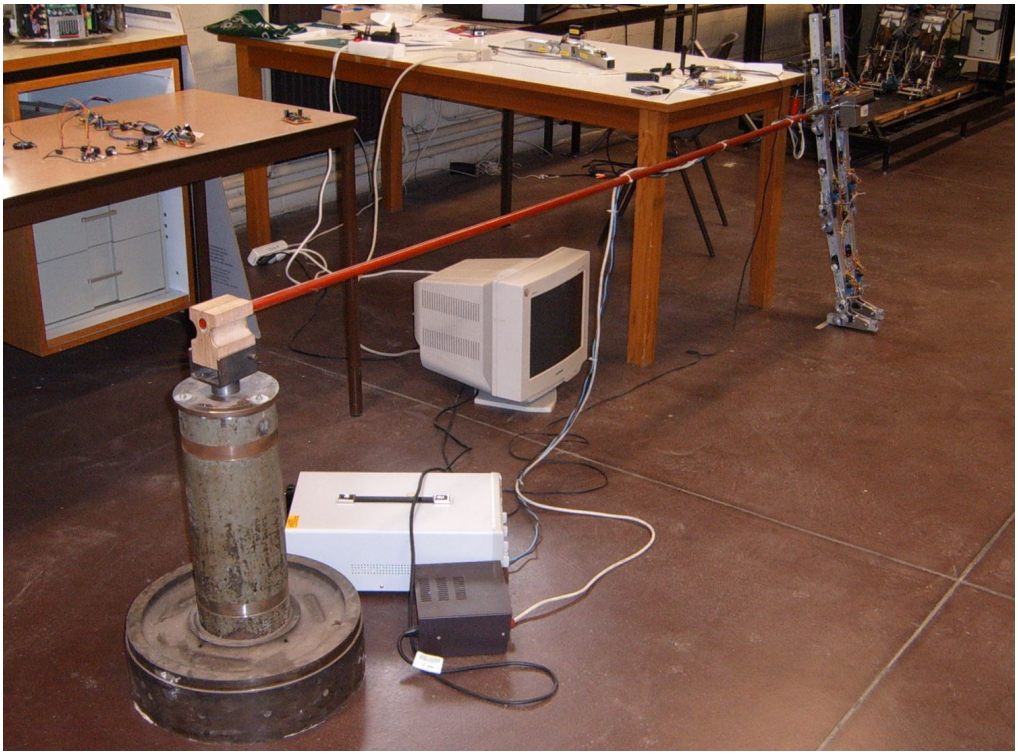

Fig.5.8 Rotating beam setup for lateral balance of Veronica

5.2 Electronic design

The robot uses 6 MACCEPA actuators. Since the mechanical parts are designed in a modular way, this is also done for the electronics. One microcontroller is used for each joint. This controller will command both the servo motor for the compliance and the one for the equilibrium position. The controller will also measure the angle and angular velocity

of the joint. The controllers for the ankle joints will also sense the ground contact. All controllers have to exchange data with a central processing unit. In the test phase this is done in a *Visual Basic* environment on a PC. When using the paradigm of precise angle control, a high data transfer rate between controller and actuators is required, typically in the order of 1000Hz. When working with passive motions, data has to be sent to the actuators only at the beginning of a step, similar to human walking [5.11]. For normal walking, the frequency of the data transfer is in the order of a few Hz. During a swing motion, no data communication is required, as will be shown in the next chapter. However, in order to acquire data for analysis later, data communication with a sample rate around 100 Hz is established. In a later stage, when the parameters are tuned, the program can be transferred into one of the microcontrollers. An overview of the data communication is given in figure 5.9. (μC means microcontroller)

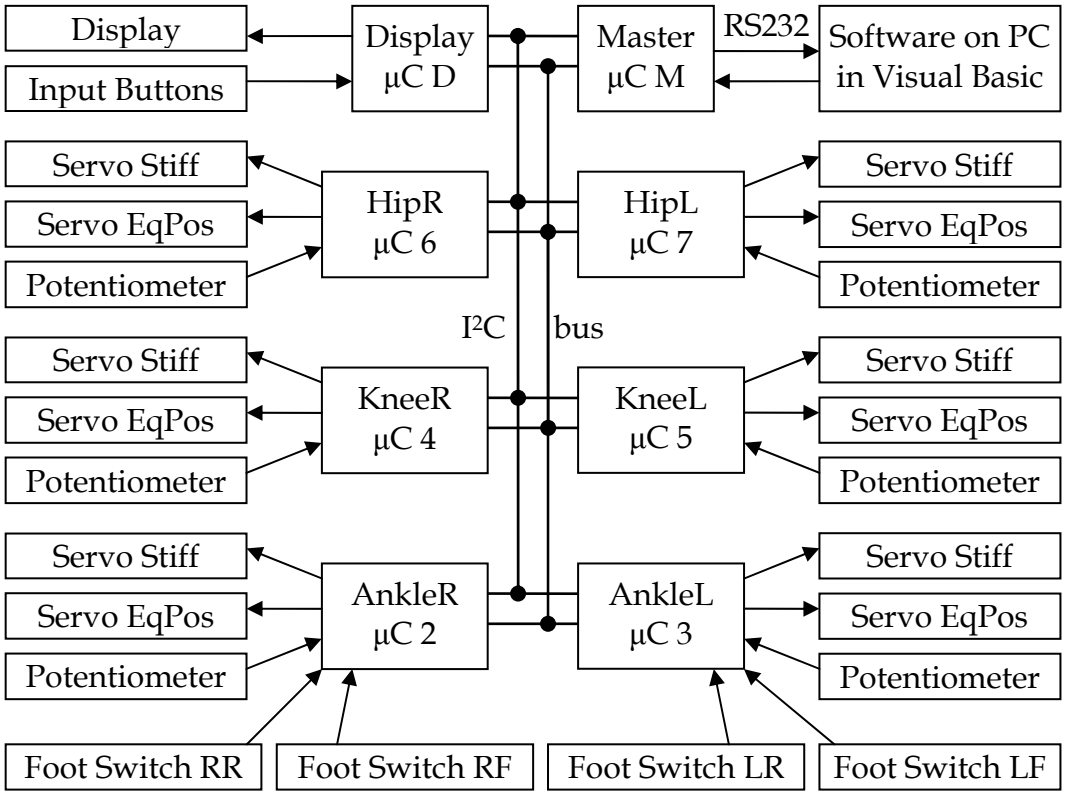

Fig.5.9 Data communication in Veronica

In the following sections, the different units and the communication between them is described in detail. In table 5.1, a typical overview of one data path between the lowest level actuators and sensors (on top of the table), and the PC (at the bottom of the table) is presented. One extra microcontroller is used for the display and the input interface, which can

be used to adapt the walking parameters when the robot is made autonomous. This controller will be discussed in section 5.6.8.

Description unit/communication	*Described in section*
Local Sensor and Actuators	*5.2.1*
Pulse/bit/analogue – Communication	*5.2.2*
Local Joint Microcontrollers	*5.2.3*
I2C bus – Communication	*5.2.4*
Master Microcontroller	*5.2.5*
Serial RS232 – Communication	*5.2.6*
Visual Basic program on PC	*5.2.7*

Table 5.1 One Data Communication path in Veronica

5.2.1 Local sensor and actuators

Each module consists of two servomotors and one potentiometer for the joint angle. The ankle module has two additional ground contact sensors. These are implemented by two on/off push buttons: one in the front of the sole and one in the back.

The servomotors used for Veronica are of the type HSR-5995TG [5.12], from Hitec/Multiplex. These are digital servos, with an integrated ATMEL microcontroller that allows modification of the internal parameters, such as direction, velocity and endpoints. The standard range is 180 degrees and the maximum speed is 0.12 sec/60 degrees. Their dimensions are 20x40x40mm^3 and they can deliver up to 30kgcm or 3Nm, which is very high for a hobby servo motor of this size. Due to the high torque, the reduction unit contains double ball bearings and titanium gears. The drawback of these servo motors for this application is the absence of a self locking gearing mechanism. In Controlled Passive Walking the position of the servomotor is not controlled continuously, but only adapted a few times during each step. The introduction of a worm gear would be ideal to overcome this shortcoming, since no power would be required anymore to keep the desired position, once it is reached. The servo motors in Veronica do not have this advantage, because of the unavailability of small sized servo motors with integrated worm gears.

To measure the joint angle, a high resolution potentiometer is used. The measurement could be done with an incremental encoder for higher

precision, but this would require a conversion to an absolute angle. When applied in the microcontroller without special submodule, it would generate a lot of interrupts. This could disturb the interrupt driven communication with the master controller. Another option is using absolute encoders, this solution is however more expensive. The increased precision is not necessary, since the measurement of the angle is not used for feedback control, but only to trigger the next phase or to collect data for analysis purposes of the walking motion. The microcontroller has an internal analogue-to-digital converter, with a 10 bit resolution. The potentiometer having an angle range of 300 degrees, this results in an angular resolution of about 0.3 degrees, which is sufficient for the purpose.

5.2.2 Pulse/bit/analogue - communication

The servos are controlled via the standard protocol of hobby servomotors [5.13]. The required position sent to the motor is encoded in the length of a pulse. On top of figure 5.10, the timing diagram of the pulse is shown. The pulse length can vary from 1 tot 2ms. The time between the pulses may vary, but should be at least 20ms. The length of the pulse defines the position of the servomotor, as shown in figure 5.9.

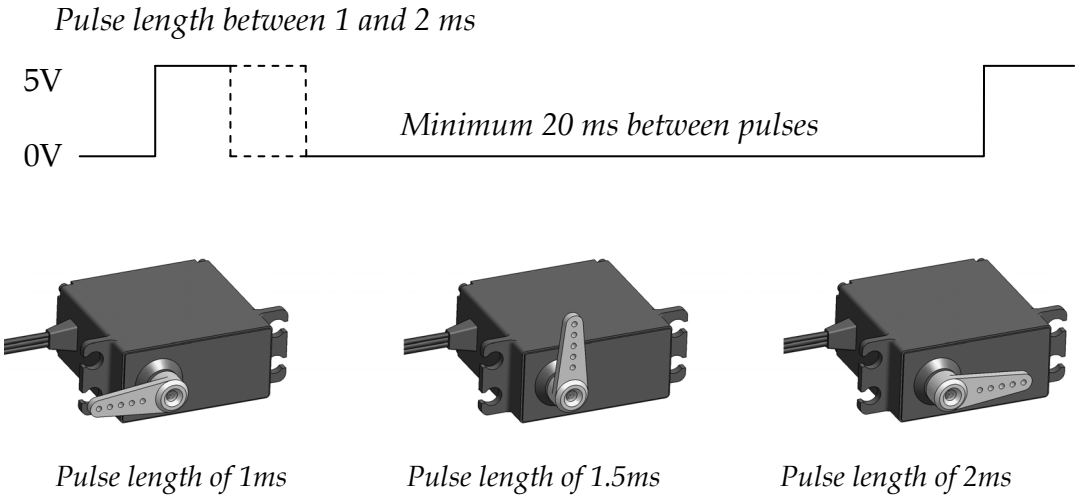

Fig.5.10 Servo Control Pulse

The signal - coming from the potentiometer - for the angular position is an analogue signal between 0 and 5V. To diminish the noise on the signal, the wires are twisted and kept as short as possible.

5.2.3 Local joint microcontrollers

Many different types of microcontrollers are available, all with their specific properties like internal program memory, data memory, AD

converters, number of inputs and outputs, processing speed, instruction set, PWM module, I2C [5.14] module, dimensions, … The joint microcontrollers do not have to perform many calculations, but should have an internal 10 bit AD converter and dedicated I2C module. The PIC16F876A [5.15] is a sensible choice. It has a high performance RISC processor, 8K Flash EEPROM for the program, 3 timers, an I2C module, a 28 pin PDIP footprint and it can be programmed without being unplugged from the application.

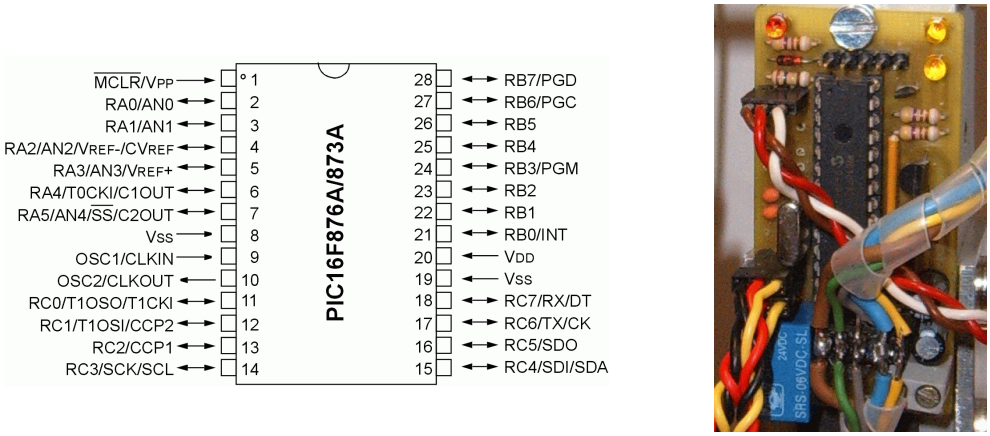

Fig.5.11 Pinout of PIC16F876A and picture of assembled joint controller

In table 5.2, an overview of the function of the pins of the joint controller is given. As can be seen, almost all pins are used.

Pins 1,27,28	*In Circuit Serial Programming (ICSP)*
Pin 2	*Analogue input for potentiometer signal*
Pins 3,4	*Digital inputs for the foot switches*
Pins 8,19,20	*Ground and power supply*
Pins 9,10	*8Mhz Crystal Oscillator*
Pins 12,13	*Pulse output for servo motors*
Pin 14,15	*I2C serial communication*
Pins 17,18	*RS232 Port, added for debugging*
Pins 21,22,23,24	*Identification code, specific for each joint*
Pins 25,26	*Status LEDs*

Table 5.2 Usage of the pins of the PIC16F876A as joint controller

Each joint microcontroller has 4 tasks:

1. Generating a servo signal for 2 servo motors. Since this is a very time critical task, it is done with a timer interrupt. If the pulse length varies, the motor vibrates. At the start of a pulse, the value of

the timer is captured. A time delay between 1 and 2ms is added to this value according to the desired position. When the timer equals this new value, the pulse has to stop. At this time the next timer interrupt occurs and the output will be set to zero.

2. 10bit AD conversion of the signal, originating from the potentiometer. Since this is the least time critical, it is done repetitively in the main program. The value is stored in an internal register and is sent to the PC in order to analyse the step.

3. Calculating the joint velocity. A real time interrupt will take samples of the position and calculate the velocity. A software filter is added to diminish the noise on the velocity signal.

4. I2C communication with the master microcontroller. This is interrupt driven, since the slave has to reply to the master within a specified time. The I2C communication can generate four types of triggers: address received for read, data required to send, address received for write, data received. Each of these triggers has to be answered with the correct response.

Since the timing of the I2C communication, the servo signals and the real time interrupt for the velocity are very critical, the different interrupts will be enabled one after another. When the I2C communication with one joint controller is terminated, the master communicates with the next one. While the master exchanges data with the other controllers, the interrupt for the first servo is enabled. When the pulse is sent to the first servo, the interrupt for the pulse of the second servo is enabled. When the interrupt for the second servo is processed, the interrupt for the calculation of the velocity is enabled. During all these interrupts, the main program makes the AD conversions. When the master starts the I2C communication again with the joint controller, the servos are controlled and the new values of the angular joint position and angular joint velocity are available and filtered.

5.2.4 I2C bus - communication

The data communication system between the master and the microcontrollers in each joint can be done with several protocols. Since the communication speed with the servomotors is limited to 50Hz (due to the required 20ms in between commands), no high speed communication protocol is required. The most common communication protocols between microcontrollers are the Serial Peripheral Interface (SPI) and the Inter IC bus (I^2C, also written as I2C) [5.14]. The SPI required 2 wires, clock and data, and one chip select signal for each slave. The I2C is a two-wire serial

bus, developed by Philips. One wire is the Serial Clock Line (SCL), and the other is the Serial Data Line (SDL). The bus is controlled by a bus master device that tells slave devices when they can access the bus. Each slave has a unique 7-bit or 10-bit address. When the master device accesses a slave, it sends the address and a read/write bit. Subsequently, the addressed slave acknowledges the connection and the master can send or receive data to or from the slave. This way, more than 1000 slaves can be connected to the same bus, requiring only 2 wires. The communication speed can be set to 100kbit/s (Standard mode), 400kbit/s (Fast mode) or 3.4Mbit/s (High Speed mode). The High Speed Mode is not feasible with the PIC microcontrollers, but even the lowest speed is fast enough due to the limited communication speed of the servos. An integrated subsystem in the microcontrollers will handle the communication, requiring a limited number of interruptions of the CPU.

5.2.5 Master microcontroller

For the master microcontroller, the same PIC16F876A version as for the local microcontrollers will be used. In the RAM memory, two buffers are defined: McToPc and PcToMc. The first is used to store the data read from the joint controllers through the I2C bus, the latter to store the data received from the PC to the joint controllers.

Controller	*PcToMc Data in Buffer*	*McToPc Data in Buffer*
Ankle Right	*01 Equilibrium position* *02 Compliance Setting*	*01 Measured Position, H Byte + switches* *02 Measured Position, Low Byte* *03 Measured Angular Velocity*
Ankle Left	*03 Equilibrium position* *04 Compliance Setting*	*04 Measured Position, H Byte + switches* *05 Measured Position, Low Byte* *06 Measured Angular Velocity*
Knee Right	*05 Equilibrium position* *06 Compliance Setting*	*07 Measured Position, High Byte* *08 Measured Position, Low Byte* *09 Measured Angular Velocity*
Knee Left	*07 Equilibrium position* *08 Compliance Setting*	*10 Measured Position, High Byte* *11 Measured Position, Low Byte* *12 Measured Angular Velocity*
Hip Right	*09 Equilibrium position* *10 Compliance Setting*	*13 Measured Position, High Byte* *14 Measured Position, Low Byte* *15 Measured Angular Velocity*
Hip Left	*11 Equilibrium position* *12 Compliance Setting*	*16 Measured Position, High Byte* *17 Measured Position, Low Byte* *18 Measured Angular Velocity*
Display	*13 Data For Display*	*19 Data From Display Contr. Buttons*
Master	*14 Data For Master*	*20 Data From Master*
Synch Data	*15 Synchronisation Byte: '0'*	*21 Synchronisation Byte: '0'*

Table 5.3 Overview data packages sent over RS232 serial communication

The main program will handle the I2C communication in a loop. The first joint controller is addressed for a write action and then the corresponding data, stored in the PcToMc buffer, is sent. Afterwards, the same controller is addressed for a read action and the data is received and stored into the McToPc buffer. Thereafter, the communication with the other controllers is done in a similar way. When all controllers have been addressed, the loop restarts. The RS232 communication is done with interrupts. The receive interrupt will store the data from the PC into the right place in the PcToMc buffer. The transmit interrupt sends the data stored in the McToPc buffer to the PC. An overview of the buffer structure is shown in table 5.3. More information on this communication is found in the next section.

5.2.6 RS232 - communication

During the development stage, it is convenient to be able to tune the parameters on the PC and visualize data on the screen of the PC. Therefore, a link with the PC is made via a standard EIA 232 serial port, also known as RS232, working on 19200 bits/s. This is not the maximum speed, but it is comparable with the rate of data-communication with the servos and the measurement of positions and velocities.

The position of the servos can be updated 50 times per second. To send 8 bit position data to all 12 servos 50 times per second, a speed of 600 bytes per second is required. The measured angular position and angular velocity of each of the joints require 3 bytes. The position has a 10 bit resolution, the velocity 8 bit, the communication protocol requires 3 bits and 2 bits are used for the foot switches. Thus 18 bytes are required, to send data of the 6 joints to the PC, plus 1 additional byte from the display controller and 1 byte from the master controller. A rate of 50 Hz results in 1000 bytes per second. A bit rate of 19200 corresponds with approximately 2000 bytes per second, which is sufficient for the application.

As synchronisation byte *zero* is used in both directions of the data communication to define the end of a data package. Therefore, none of the other data bytes can be zero. This is not a problem for the position control of the servos, since these are two 8bit values, with a value between 20 and 220. The measured position is a 10 bit value, which could give a byte with value zero. To overcome this problem, the 10bit value is split in the 7 LSB and the 3 MSB. In both bytes the 8^{th} bit is set to one by default. The second byte also includes the data from the footswitches, for the ankle controllers. The velocity is sent as signed byte, where the value *zero* is replaced by 128. In this way, no byte other than the synchronisation byte can be zero.

5.2.7 Visual Basic program on PC

On the PC, a program is running in *Microsoft Visual Basic* [5.16]. The programming environment, which is user friendly to develop a graphical user interface, is not the most adequate for real time applications, but is fast enough for Controlled Passive Walking. The program communicates through the RS232 port with the master controller. The software on the PC also works with 2 buffers: one stores the received data from the robot, the other is sent to the robot.

The controller in the *Visual Basic* program, which will be explained in detail in chapter 6, is based on 10 sets of the 12 control parameters of the robot: 6 equilibrium positions and 6 compliances. For each set a condition can be selected to go to the next set. These conditions can be the setting or clearing of one of the foot switches, the stretching of one of the knees, a certain angle for each of the joints or a timer. All the control parameters can be seen and adjusted on the main screen of the program. The program allows saving the control parameters to disk and loading them again. Another screen of the program is made to be shown on a separate monitor. This screen shows the active parameters in a very large font in order to capture the essential information with a camera, together with the walking motion. This way, the walking motion, defined by the shown set of control parameters, can be analysed in slow motion.

An option can be selected to save the settings of compliance and equilibrium positions, measured joint angles, angular velocities and status of the foot switches. The data is saved to a *.csv* file, which can easily be opened and visualised in e.g. Microsoft Excel.

5.2.8 Display and display controller

On the torso of the robot an extra controller is placed, which is also connected to the I2C bus, with a 2*16 digit LCD display and four buttons for user input, as shown in figure 5.12. During the development-stage, the control algorithms will be running on the PC, but these can be transferred to the master controller in a later stadium. The display and buttons will then be used to choose walking parameters.

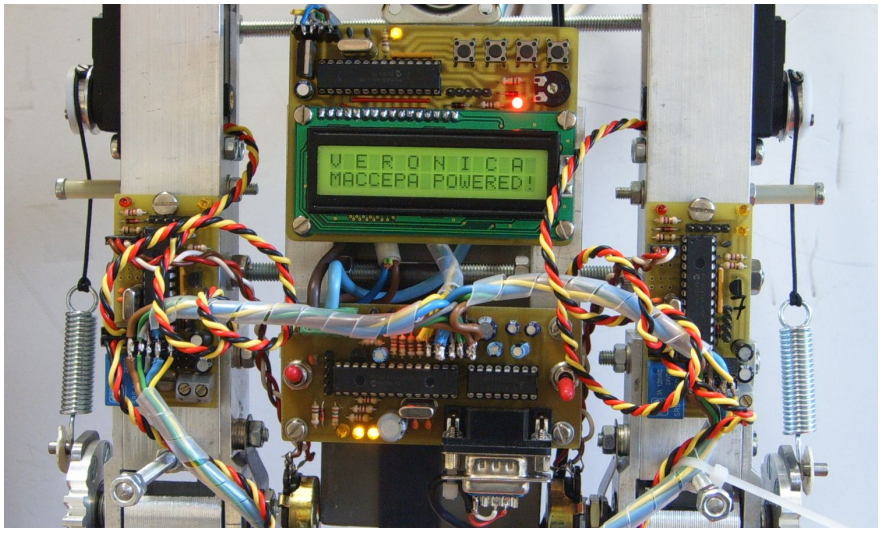

Fig.5.12 Close-up of master controller PCB and display

5.3 Calibration

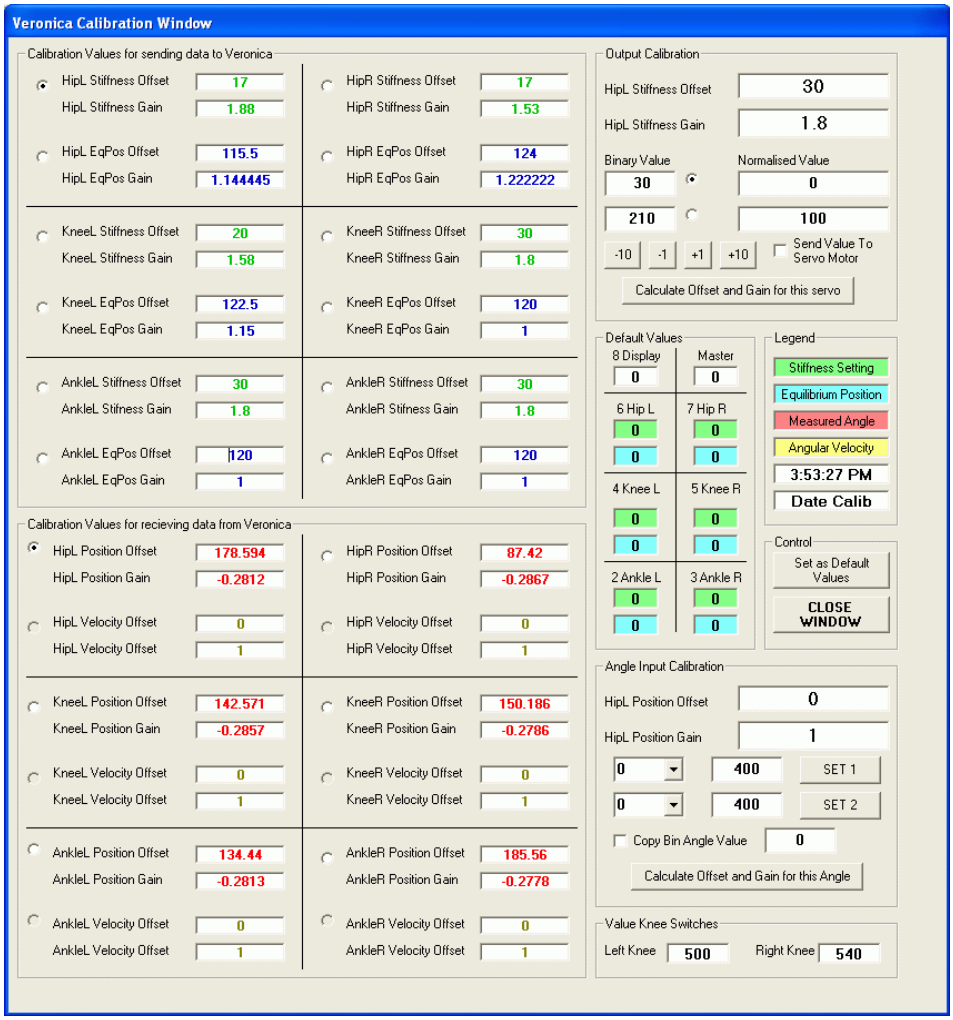

Fig.5.13 Calibration Window

For each joint, 4 signals need calibration: the position of both servomotors, the measured angle and the measured angular velocity. To simplify the calibration, the software has a dedicated window, shown in figure 5.13. In the next section, the calibration of the input and output parameters is discussed.

5.3.1 Calibration of the servo motors

The servo motors are internally calibrated, to convert a pulse length of 1 to 2 ms to an angle of +90 to -90 degrees, as described in section 5.7.2. However, with the external gearing mechanism, the position of the lever arm or the angular position of the spool is not calibrated anymore. Fortunately, the linearity is preserved with the gearing mechanism, which means that only two points are required for the calibration. The upper frame on the left in figure 5.12 performs the calibration of the servos. In this frame two positions, which can be measured easily on the robot, can be chosen. The specific servo can then be controlled to go to that position. When two positions are defined, the program will calculate gain and offset and place it in the frame on the top left. Subsequently, the next servo can be calibrated. All the calibration parameters can be saved to disk, and reloaded for future experiments.

5.3.2 Calibration of the angular position

The potentiometers used to measure the angle are linear and have a range of approximately 300 degrees. The AD converter has an input from 0 to 5V. Since the angular position between the axle of the potentiometer and the joint is not defined, the angular positions need calibration. This can be done with the left frame at the bottom. Within the calibration procedure, the angle of each joint of the robot is kept in a predefined position, e.g. -90, -45, 0, 45 or 90 degrees and the program captures the current reading. Once this is done for two positions, the offset and gain can be calculated and put in the frame at the bottom right. Normally this calibration should be done only once. The calibration values are saved to a file and will be loaded automatically at the next start of the program.

5.3.3 Calibration of the angular velocity

The angular velocity can be calculated from the position data in the software on the PC or be measured in the joint controllers by a timer interrupt. The first velocity signal is noisy, but has the correct scaling. The latter has less noise, but needs calibration for several reasons: the timer interrupt has an interval that is an exponent of 2 and not a rounded decimal value, the measured angle is converted to a signal between 0 and 5V and the measured range is approximate 300 degrees instead of 360

degrees. However, for this calibration, the offset is zero, and only the gain needs to be identified. This gain is the same for all joints, since the joint controllers have the same frequency and the potentiometers are the same; only the angular offset differs.

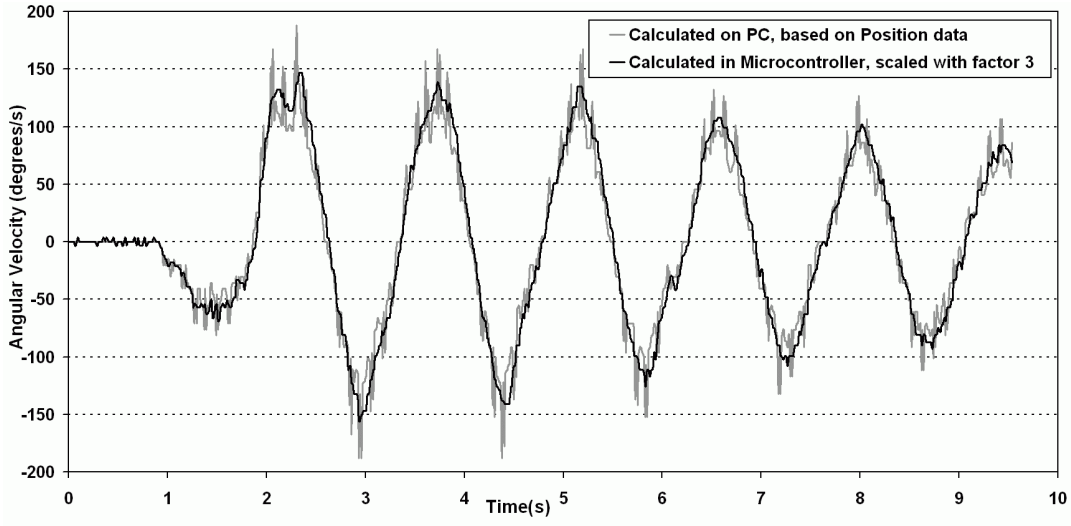

Fig.5.14 Calibration of velocity signal

The calibration is done by measuring a swing motion and comparing the velocity from the controller with the velocity derived from the position data. It can be seen in figure 5.14 that a gain of 3 is suitable. It is worth mentioning that the calculation of the derivative of the position is not obvious, since the position data sometimes remains the same for two samples, due to the bandwidth of the communication that is designed to analyse motions and not for control purposes.

5.4 Conclusions

In this chapter, the mechanical design of the biped Veronica was explained. Figure 5.15 shows a picture of the complete biped Veronica. Since the use of MACCEPA actuators allows the on-line modification of the natural frequencies, the mass distribution is not as important in the design stage as is often the case for other passive based walkers. The electronic design is explained bottom-up, from the sensors and actuators on each joint to the control program on the PC. Additionally, the implementation of the calibration of the sensors and the actuators in the program was discussed.

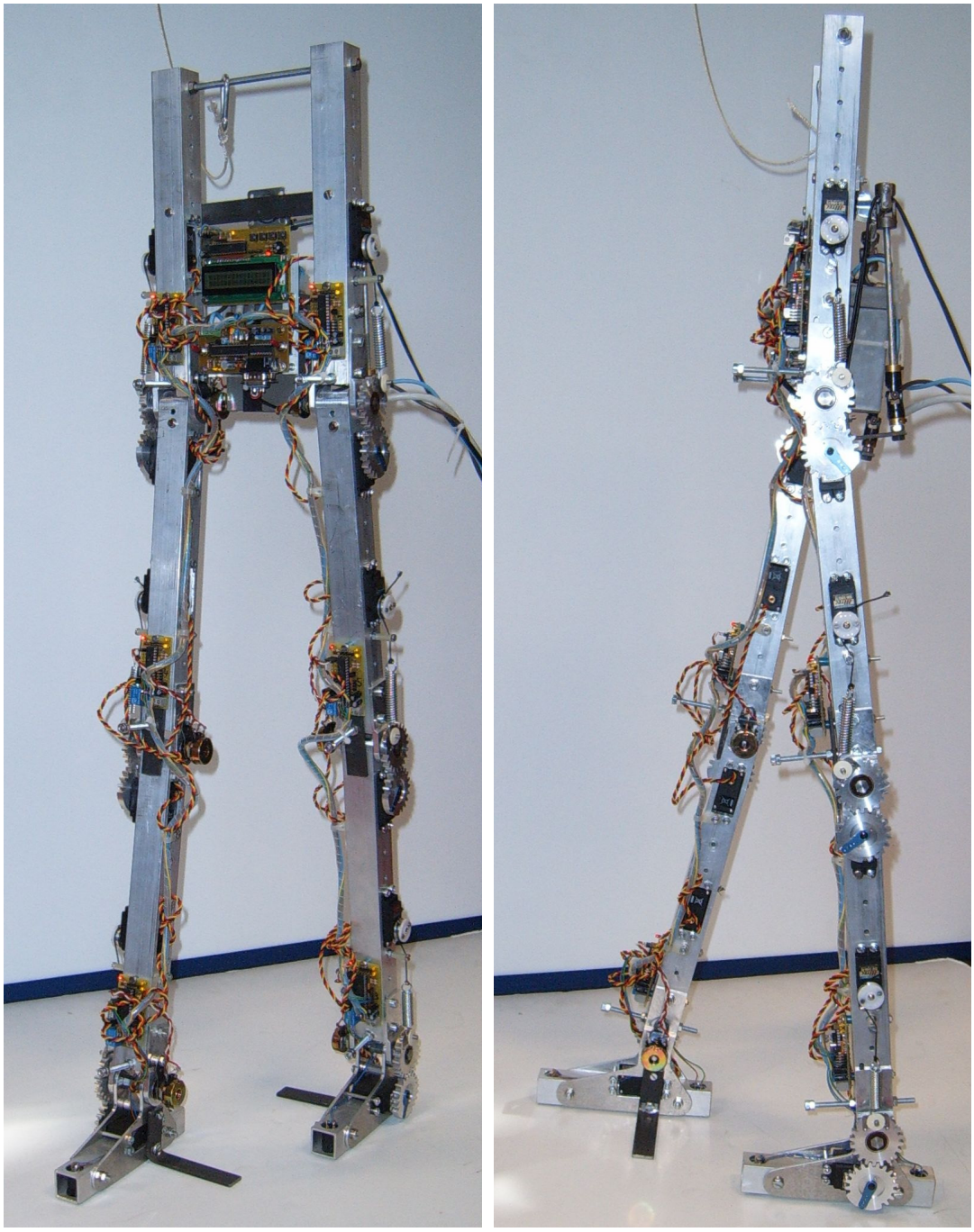

Fig.5.15 Pictures of the complete biped Veronica

References

[5.01] T. McGeer, Passive walking with knees, In: *Proc. 1990 IEEE Robotics & Automation Conference,* Cincinnati, OH, 1990, pp. 1640-1645.

[5.02] M. Wisse. Essentials of dynamic walking - Analysis and design of two-legged robots. PhD Thesis, Delft University of Technology, Delft, The Netherlands, September 2004

[5.03] T. McGeer. Passive dynamic biped catalogue. In R. Chatila and G. Hirzinger, editors, Proc., Experimental Robotics II: The 2nd International Symposium, pp. 465–490, Berlin, 1992. Springer–Verlag.

[5.04] R.Q. van der Linde. Bipedal walking with active springs, gait synthesis and prototype design. PhD Thesis, Delft University of Technology, Delft, The Netherlands, November 2001.

[5.05] M. J. Ijzerman, G. Baardman, H. J. Hermens, P. H. Veltink, H. B. K. Boom, and G. Zilvold. The influence of the reciprocal cable linkage in the advanced reciprocating gait orthosis on paraplegic gait performance. Prosthetics and orthotics international, 21: pp. 52–61, 1997.

[5.06] J. E. Pratt. Exploiting Inherent Robustness and Natural Dynamics in the Control of Bipedal Walking Robots. PhD Thesis, Massachusetts Institute of Technology, June 2000

[5.07] B. Verrelst, R. Van Ham, B. Vanderborght, F. Daerden, D. Lefeber. The Pneumatic Biped "LUCY" Actuated with Pleated Pneumatic Artificial Muscles. Autonomous Robots 18, pp. 201-213, 2005

[5.08] R. Tedrake, T. W. Zhang and H. S. Seung. Learning to Walk in 20 Minutes. In Proceedings of the Fourteenth Yale Workshop on Adaptive and Learning Systems, Yale University, New Haven, CT, 2005.

[5.09] M. Gerecke, A. Albert, J. Hofschulte, R. Strasser, W. Gerth. Towards an autonomous, bipedal service robot. Tagungsband 10 Jahre Fraunhofer IFF, 24.-28.06.2002, Magdeburg, S. pp. 163-168

[5.10] http://www.humanoid.waseda.ac.jp/booklet/katobook.html

[5.11] S.Mochon and T.A. Mc Mahon. Ballistic walking. J. Biomechanics, Vol. 13: pp. 49–57, 1980.

[5.12] http://www.robonova.de

[5.13] http://www.geocities.com/BourbonStreet/3220/servobasics.html

[5.14] http://www.semiconductors.philips.com/acrobat_download/

literature/9398/39340011.pdf

[5.15] http://www.microchip.com

[5.16] http://msdn.microsoft.com/vbasic/

[5.17] G. T. Fallis. Walking toy ('improvement in walking toys'). U. S. Patent, No. 376,588, January 17 1888.

Chapter 6

Controlled Passive Walking

Het eenvoudigste dat werkt, is het beste
Dirk Lefeber

Do not quench your inspiration and your imagination;
do not become the slave of your model.
Vincent van Gogh

As explained in chapter 2, the walking speed of level-ground passive walkers is determined by the mass distribution of the design. To make a passive walker that can walk with different speeds, the natural frequency of the legs has to be controllable. Actuators with adaptable compliance are interesting for that purpose, as explained in section 2.6. This type of actuators allows one to change both the equilibrium position and the compliance of the joint, and thus also the natural motion. Because of the independent control of the equilibrium position and the compliance, the MACCEPA actuator will be used to explain the concept, but the same concept can be applied to other actuators with adaptable compliance. In section 6.1, the concept of adapting the natural motion of a single pendulum by varying the compliance is explained. Okada et al. [6.01] describe an analogous method for a shoulder joint, named *Skill of Compliance*, in order to provide robots with higher mobility, dexterity and safety. In section 6.2, some natural dynamics mechanisms are described. These are required for passive bipeds and are also used in human walking [6.02], e.g. the natural bending of the knee of the swing leg. In section 6.3, the intuitive control of passive bipeds is discussed. This control is in general much more intuitive than is the case for active controlled robots. The different phases of a step are defined and control strategies of other passive based walkers are discussed. Section 6.4 presents the implementation of Controlled Passive Walking in Veronica. Section 6.5 reports on the experiments with Veronica and the tuning of the controller.

6.1 Single Swing Motions

To explain the concept of *Controlled Passive Walking* several thought experiments with a pendulum, actuated by a single MACCEPA will be described. The concept *Single Swing Motion* is used to describe the swing motion of a pendulum from a point where the velocity is zero till the point where the velocity becomes zero again for the first time. Some other concepts have to be defined. The position where the experiment starts is defined as the *start position*. Note that this is in general not the equilibrium position, which is defined as the position where no torque is generated by the MACCEPA. Before the experiment, the pendulum is blocked by a brake. The experiment starts when the pendulum is released. *Releasing the pendulum* is defined as starting with a zero angular velocity from the start position. The position where the angular velocity of the pendulum will become zero again for the first time, thus after a *single swing motion*, is defined as the *end position*. What happens after the pendulum has reached the *end position* will not be taken into consideration, although in general a new natural motion can be chosen. It is worth mentioning that for the described thought experiments the start and end velocity are assumed to be zero, but in a further stage, when used in a walking biped, the natural motions can be linked without the velocity being zero.

In figure 6.1, one single pendulum setup is shown in 3 positions: -30°, 0° and 30°. The pendulum is placed vertically, so that the gravitational force is symmetrical with respect to the vertical position. Note that in this case the equilibrium position of the gravity is 0°. This is the position where the gravity applies no torque on the pendulum. The equilibrium position of the MACCEPA is set by one of the servomotor, so that it does not has to be the same as the equilibrium position of the gravity. The resulting equilibrium position is a weighted average of both, depending on the compliance setting of the MACCEPA.

Now, a series of thought experiments will be described, in which initially damping caused by air friction and mechanical friction will be neglected. The experiments will start from a very basic setup and will gradually introduce actuation, asymmetry and friction.

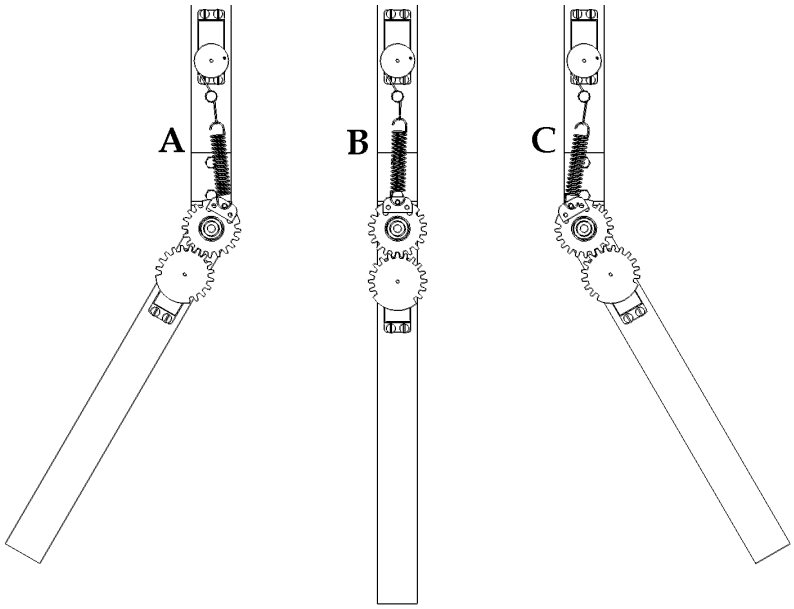

Fig.6.1: MACCEPA in 3 positions (A: -30°, B: 0°, C: +30°)

6.1.1 Single Swing Motion without actuation in gravitational field

A first, very basic, experiment that can be done is to consider the pendulum without friction nor actuation. This is thus actually a pendulum without a MACCEPA actuator. Note that in this case the equilibrium position is 0°, because in this position the gravitation does not apply any torque on the pendulum. When the pendulum is pulled manually to -30° and released without initial angular velocity, it will swing to +30°. This position is defined as the *end position*. The period of this motion will depends on the moment of inertia I. The motion of the pendulum is described for small angles by:

$$\theta = \theta_0 \cos\sqrt{\frac{g}{L}}.t \qquad 6.1$$

The time for a single swing motion is half the period of the pendulum. The period of a gravitational pendulum for small angles is given by:

$$T = 2\pi\sqrt{\frac{L}{g}} \qquad \text{(gravitational pendulum)} \qquad 6.2$$

It is worth mentioning that this equation is analogous to the equation for the period of a torsion pendulum, as described in section 2.6.

$$T = 2\pi\sqrt{\frac{I}{\kappa}} \qquad \text{(torsion pendulum)} \qquad 6.3$$

This analogy is the basis of Controlled Passive Walking, as will be explained with the following experiments.

6.1.2 Single Swing Motion with actuation, without gravitation

If the setup, depicted in figure 6.1 is used in a horizontal plane, the gravitation has no influence on the motion. This time however the MACCEPA actuation is added. The equilibrium position of the MACCEPA is set to 0° and no friction is considered. When the pendulum is pulled manually to -30° and released without initial angular velocity, it will swing to +30°, as was the case in the first experiment. The action of the MACCEPA actuator is thus comparable to the influence of gravitation, for small angles. Both will accelerate the pendulum between -30° and 0° and decelerate it between 0° and 30°, due to the exchange of potential energy and kinetic energy. The period of this single swing motion is given by equation 6.3 for a MACCEPA with torsion spring constant $\kappa = \mu.P$.

6.1.3 Single Swing Motion with actuation and gravitational field

In this experiment, the two previous experiments will be combined. If the setup depicted in figure 6.1 is used vertically, both gravity and the MACCEPA will exert a torque on the pendulum. If the equilibrium position of the MACCEPA is set to 0°, both gravitation and the MACCEPA will have a comparable influence on the motion. When no friction is considered and the pendulum is pulled manually to -30° and then released without initial angular velocity, it will still swing to +30°, as was the case in the previous experiments. The time of the motion between start point and end point however will be shorter than in the previous experiments, since the total torque applied to accelerate and decelerate the

pendulum is the sum of the torque due to gravitation and the torque generated by the MACCEPA. For small angles this results in:

$$\tau_{Total} = \tau_{MACCEPA} + \tau_{Gravitaion} \approx -\alpha.\mu.P - m.g.\alpha.L = -\alpha.(\mu.P + m.g.L) \quad 6.4$$

This leads to the period of the actuated pendulum for small amplitudes:

$$T = 2\pi\sqrt{\frac{I}{(\mu.P + m.g.L)}} \quad 6.5$$

6.1.4 Single Swing Motion with variable actuation

The parameter in equation 6.5 that is the easiest to change during operation in equation 6.5 is *P*, the pre-tension that defines the compliance of the MACCEPA. If the last experiment is repeated with another setting of the compliance, the pendulum will also move to +30°. If the compliance setting of the MACCEPA is made stiffer, the natural frequency will be higher and the time needed to move from -30° to +30° will be shorter. When the compliance is set higher, thus less stiff, this period will be longer. Thus, the swing time is controlled by the compliance setting of the MACCEPA. The MACCEPA has a comparable influence as gravity but, unlike the gravitational force, it is not fixed.

It is worth mentioning that the pre-tension cannot be made negative, and thus the minimal swing time that can be reached is the one with zero pre-tension, which approaches most the behaviour of the unactuated pendulum. Even with zero pre-tension, a torque will be applied when the pendulum is not in the equilibrium position. This means that the mass distribution of the unactuated pendulum and the design parameters of the MACCEPA define the maximum value of the swing time and as such the minimal natural frequency.

Although as described in section 4.1.7, the lever arm can be rotated 180° to obtain a negative spring constant. This cannot be done instantaneously, so a system with 2 lever arms could be used to increase and decrease the natural frequency, but makes the design more complex. It is easier to choose the mass distribution, to select the range of natural frequencies, in order to require only an increase or only a decrease of the natural frequency.

6.1.5 Non-symmetrical Single Swing Motion

In the next experiment the setting for the compliance is kept the same as in the previous one, but the equilibrium position of the MACCEPA is set to +5°. Friction is still neglected. If we pull the pendulum to -30° and release

it, it will swing to an end position—where the velocity is zero again—which lies further than 30°. If the equilibrium position would have been set to -5°, the end position would have been less then 30°. It can be concluded that the equilibrium position can be used to change the end position of a natural swing motion. When the pendulum is at -30°, the potential energy is higher when the equilibrium position is set to +5°, than when it is set to 0°. So when more energy is stored in the system at the beginning of the experiment, it results in a bigger swing angle. Note that the equilibrium position of the gravitation force remains 0°.

6.1.6 Single Swing Motion with friction

In all the previous experiments friction was neglected. Friction dissipates energy from the system, but the previous experiment showed a way to put more energy into the system. When the amount of dissipated energy can be estimated, this extra amount can be injected into the system, to compensate the influence of the friction. Thus, when a motion from -30° to 30° is required, and friction is present, the equilibrium position should be set slightly closer to the end position. This is the way that compliant actuators are used to put energy into level-ground passive walkers.

6.1.7 Experimental results

To show the relation between equilibrium position and end position, a series of experiments are performed on a single pendulum, powered by a MACCEPA actuator and under influence of gravity. All the results are plotted in figure 6.2. The grey curve is the setting of the equilibrium position, the black line is the measured angle. The black arrows on the top of the graph show the place where the different experiments start, the grey ones at the bottom show the end. Figure 6.2 is thus a series of 6 experiments where the joint is pulled to a start point of 45°, and released (black arrow) after a certain equilibrium position is set, the joint is released. The grey arrows show the end position, thus the position where the velocity becomes zero again for the first time. Note that the equilibrium position for the gravitational force is 0 degrees, while the equilibrium position of the MACCEPA actuator is variable.

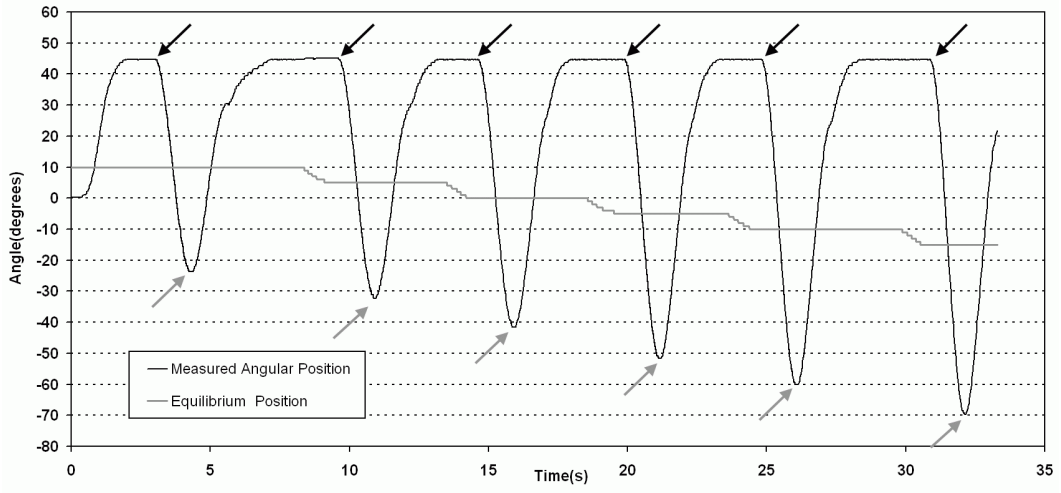

Fig.6.2: Variation of the end position by changing the equilibrium position

In table 6.1 the results of the experiments are summarised. The start position is always 45°. The equilibrium position of the gravitation is always 0°. The equilibrium position of the joint is a weighted average of the equilibrium position of gravity and of the equilibrium position of the MACCEPA actuator. The compliance setting of the MACCEPA, which is kept constant during the six experiments, defines the proportional relevance of the MACCEPA actuator.

To compensate for the influence of friction, as described in section 6.2.6, the equilibrium position of the joint should be set slightly closer to the end position than the middle between start and end position to compensate friction losses. Experimental results are shown in table 6.1.

$$CenterPos = \frac{StartPos + EndPos}{2} \qquad 6.6$$

and $$EqPos = CenterPos + FrictionComp \qquad 6.7$$

results in $$StartPos = 2.EqPos - EndPos + FrictionComp \qquad 6.8$$

This friction compensation is an angle, which is function of e.g. the swing angle, the velocity and the pretension.

Experiment number	*1*	*2*	*3*	*4*	*5*	*6*
Start Position	*45°*	*45°*	*45°*	*45°*	*45°*	*45°*
End Position	*-23.6°*	*-32.3°*	*-41.6°*	*-51.7°*	*-60.1°*	*-69.4°*
Eq.Pos. Gravitation	*0°*	*0°*	*0°*	*0°*	*0°*	*0°*
Eq.Pos. MACCEPA	*10°*	*5°*	*0°*	*-5°*	*-10*	*-15*

Table 6.1 Analysis of experiments showed in figure 6.2

These experiments were done by setting a specific equilibrium position and observing the obtained end position. Controlled Passive Walking requires the inverse relation: which equilibrium position should be set on the MACCEPA actuator of the joint to end up in a desired position? Since a non model-based controller will be used, it is important to investigate this relation, as it determines the number of data points used in the controller. In between these points the values will be interpolated. Therefore, the relation between desired end position and equilibrium position of the MACCEPA actuator, for a certain set of start position, gravitational equilibrium position and compliance setting, is plotted in figure 6.3. Since this relation is quasi linear, a limited number of data points can be used.

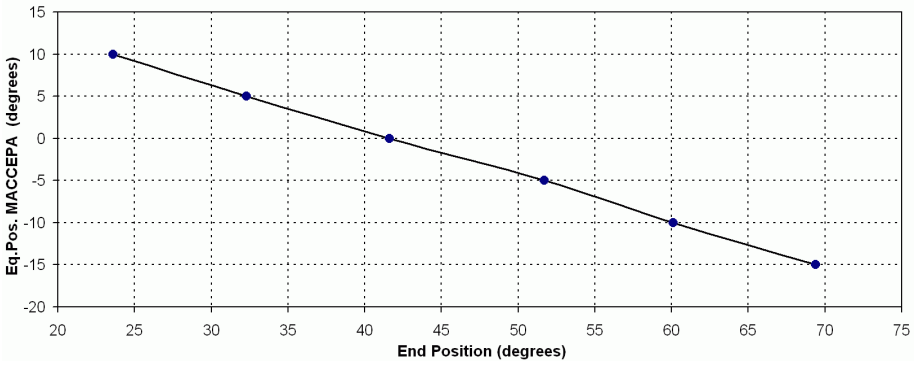

Fig.6.3: Relation between the end position and the equilibrium position MACCEPA, for a start position of 45°

6.1.8 Starting single swing motion without brake

Until now, the experiments were performed using a virtual brake system to keep the pendulum in position until the equilibrium position was set. When two single swing motions are linked, this is not the case and the time required by the servomotor to set the equilibrium position must be taken into account. When the servomotor starts setting the equilibrium position, in the beginning of the single swing motion, the torque applied by the MACCEPA is smaller than it should be. When the pendulum has passed the equilibrium position, which is then set, the deceleration torque is the same as before. Thus, the pendulum will not end up in the desired end position, since not enough energy was put into it from the beginning of the motion. This problem can be overcome in the same way as friction is dealt with. By setting the equilibrium position closer towards the end position, the pendulum will swing further.

6.1.9 Usage of other compliant actuators

In all the previous thought experiments, the MACCEPA actuator was used. When using other types of compliant actuators, some other

difficulties may be introduced. The MACCEPA actuator can be modelled as a torsion spring with a linear angle-torque characteristic. Most other compliant actuators do not have this linear relationship. But there are more important disadvantages. When an antagonistic setup of 2 pneumatic artificial muscles is used, both pressures have to be changed in order to change only one of the parameters: compliance or equilibrium position.

A second and more important consequence is that the pressures that should be set to obtain a certain equilibrium position, are function of the actual position of the joint. This can be shown by a simple though experiment: assume a horizontally placed joint actuated by two PPAMs in its equilibrium position. When the air inlet of the muscles is closed, and the joint is pulled out of the equilibrium position, the pressures will change. The new pressures are the pressures that should be set to obtain the original equilibrium position and they are different for each position. The use of pneumatic muscles for single swing motions would not pose a problem if the pressures could be set immediately, as is obviously not the case in a real setup. During the time that the pressures are set, the desired values of the pressures normally change, since the position also varies in case of walking. Thus, almost each sample time, the controller will send new desired pressures to the pressure regulating valves, which contradicts with the idea of Controlled Passive Walking: setting a certain equilibrium position and compliance and maintain these settings during a certain time, to save energy. With the MACCEPA actuator, the setting of the equilibrium position is independent of the actual position, and therefore this problem does not arise.

6.1.10 Conclusion

The previous experiments described a single pendulum actuated by a compliant actuator. Starting in a certain position, without initial velocity, it is possible to end up in a desired position. This is achieved in a passive way without continuous control. As compliant actuator a MACCEPA actuator was used. Other compliant actuators can however be used as well.

6.2 Natural mechanisms in bipeds

In the previous sections, the concept of controlling a single swing motion of a single pendulum was described. To develop a control strategy for Controlled Passive Walking, some remarks concerning actuated passive walkers with articulated legs have to be considered [6.02].

6.2.1 Natural bending of the knee joint of a swing leg

An articulated leg is a means to give a biped foot clearance, allowing the leg to swing forward. But other ways to achieve this also exist, e.g. with blocks placed at the footholds, see figure 2.4, or round feet that make the robot move out of the sagittal plane, see figure 2.5d in section 2.3. Humans use a combination of knee bending and hip rotation in frontal plane. Since the latter is of minor importance in a 2D biped, it is not implemented in the biped Veronica.

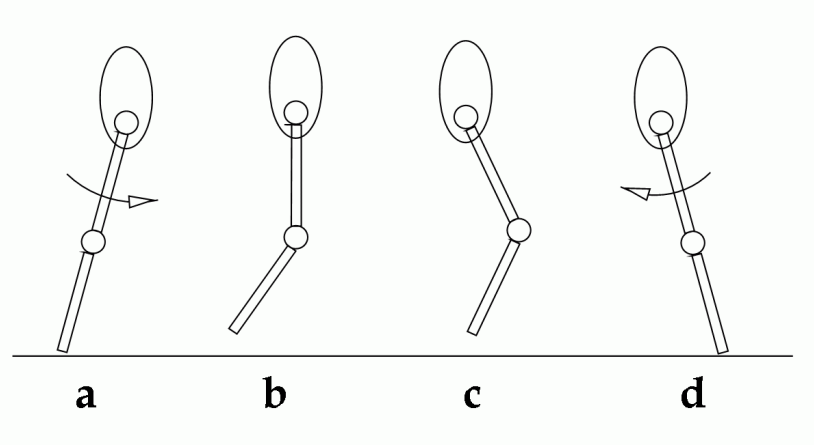

Fig.6.4: Passive swing of an articulated leg, figure taken from [6.02].

In figure 6.4 the passive swing motion of an articulated leg is shown. The motion is generated by a forward torque on the hip shown in figure 6.4.a, supplied either by hip actuators or gravity. The leg can swing passively (figure 6.4 b and c) until the swing is stopped (figure 6.4.d) by a backward torque on the hip, again supplied either by hip actuators or gravity. It is worth mentioning that this motion can be achieved without applying any torque at the knee joint. In fact it is a double pendulum, but only the upper joint is actuated. The mass distribution of the lower leg should be tuned so that the leg becomes stretched again when the upper leg is in the forward position. In the biped Veronica, the natural frequency of the lower leg can be chosen by the compliance setting of the MACCEPA actuator. Note that in human walking there is no muscle activity during the mid swing motion of the leg [6.03], which indicates that human walking is based on passive motions.

6.2.2 Stretched stance leg

In passive walking robots with articulated legs, the legs are stretched when they are supporting the weight of the robot. This is because the actuators are only designed to replace the energy lost due to friction and can generally not produce enough torque to support the weight of the robot when the legs are bent. To keep the legs stretched, a kneecap is useful to prevent buckling [6.02], as shown in figure 6.5.

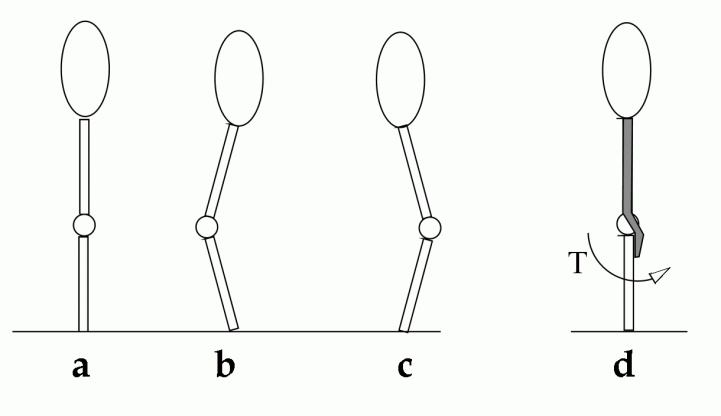

Fig.6.5: Usage of kneecap to prevent buckling of leg, figure taken from [6.02].

When a leg without kneecap (figure 6.4a), needs to be stabilized by a feedback controller, it results in chatter between knee inflections (figure 6.5.b and c) due to control delay, etc. With a kneecap, as shown in figure 6.5.d, a small constant torque is enough to stabilize the system against buckling; a controller is not required. Note that unactuated passive walkers with articulated legs also use kneecaps, without applying torque on the knee with an actuator. A slightly overstretched knee however, applies a torque in the correct direction when supporting the weight of the robot. In Veronica, the slightly overstretched knees are combined with an actuator applying a small constant torque, as described in section 5.3. This is because the actuation in the ankles can apply a torque on the knee joint.

6.2.3 Compliant actuation in the ankle

Most actuated passive walkers have unactuated ankles, and rounded. But the use of flat feet and compliant ankle joints has advantages. In normal walking, the centre of pressure on the foot travels forward as the centre of mass travels forward (figure 6.6a-d). A compliant ankle (figure 6.6) can achieve this effect naturally [6.02], as is the case for round feet. But when the compliant ankle is actuated, as is the case in the Spring Flamingo [6.02], Meta [6.04] and Veronica, extra energy can be inserted in the toe-off phase [6.05].

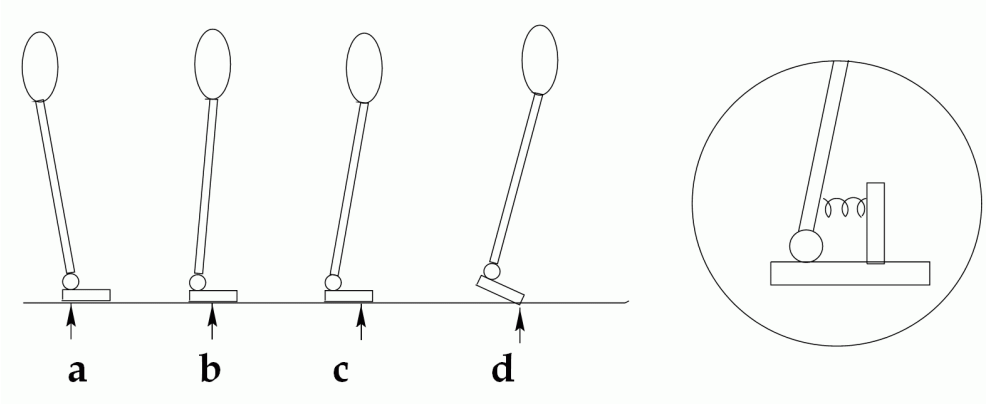

Fig.6.6: Position of centre of pressure with compliant ankle, figure taken from [6.02].

6.2.4 Natural mechanisms in human walking

In the latter three sections, three natural dynamics mechanisms in bipeds were discussed. All three of them are also used in human walking, as can be seen in figure 6.9. This series of pictures [6.6], taken in 1880, is obtained by firing still cameras in rapid succession to study the principles of human walking. The natural bending of the swing leg, as described in section 6.2.1, can be seen in figure 6.9b and 6.9c. The almost stretched stance leg, described in section 6.2.2 can be observed. The toe-off phase, discussed in section 6.2.3 can also be seen in figure 6.9. It is not a coincidence that all the described natural dynamics mechanisms for bipeds can all be found in human walking, since the mechanisms are essential for energy efficient walking.

6.3 Intuitive control of passive bipeds

In this section, the intuitive control of passive walking bipeds is explained. Note that it is based on the observations of human walking, and thus biologically inspired. Conversely, building robots mimicking human locomotion are useful to understand human walking [6.07].

In figure 6.6, the stretched stance leg is depicted as a single inverted pendulum. In figure 6.4, the swing leg is a double pendulum, of which the hinge point moves along a curve. It is clear that there are different phases in bipedal walking. The two main phases that can be found for each leg in walking robots is the stance phase and the swing phase. The transition from swing to stance phase is the touchdown of the foot; the transition from swing to stance phase is the toe-off. The transition in control mode from one phase to the next is triggered by timing delays or sensor info, e.g. the touchdown of the foot can be detected by a footswitch. In figure 6.7, the phases of a step used in the Que-Kaku robot [6.08] are depicted. The touchdown of the foot starts the double support phase. After a time T_0 the

swing phase is initiated by pressurizing the set of pneumatic muscles in front of the robot. A certain time S(k) later, the pressure in the muscles is decreased again. Note that there is a phase where the robot remains in the same internal configuration, and actually just falls forward. The increased pressure level is fixed, but the time it is applied can be varied in order change the amount of inserted energy, to adapt the walking cycle as a function of the surface. This control strategy is comparable with the pneumatic bipeds from Delft University [6.07].

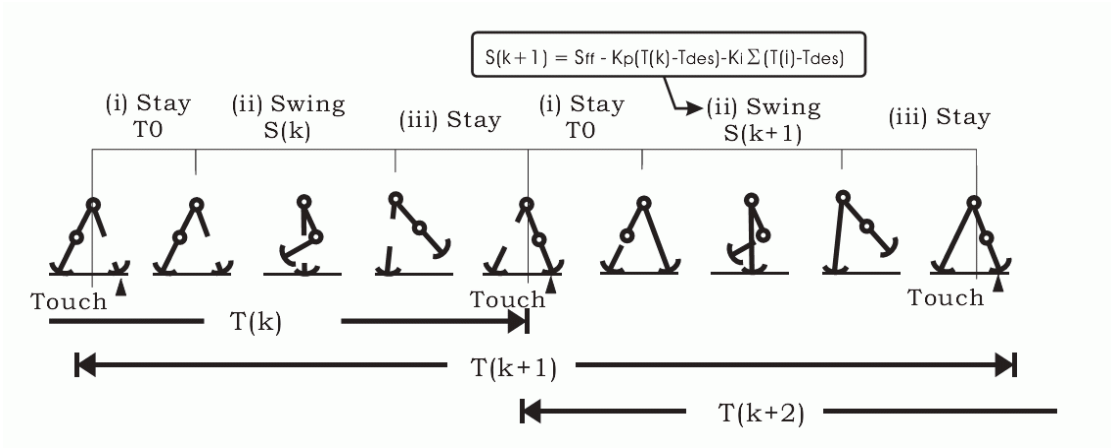

Fig.6.7: Step sequence of Que-Kaku robot [6.08]

In figure 6.8, the different phases used in Spring Flamingo [6.02] are depicted. Here the toe-off phase starts from the moment of heel strike of the other foot, until the moment the toe leaves the ground. In this phase, as explained in section 6.3.3, the toe is used to push the robot forward, and thus putting energy into the system. The swing phase makes the upper leg go forward and bends the knee, as explained in section 6.3.1. Once the leg is stretched, the knee is locked so the leg is kept stretched until the end of the toe-off phase. Note that the diagram depicted in figure 6.8 is only for one leg. In the support phase (0) of one leg, the other leg has three phases (1, 2 and 3). This results in 6 phases for a double step, which is the same as in figure 6.7. However, the phase in figure 6.7 in which the robot is supported by two stretched legs is much shorter—being almost instantaneous—than the toe-off phase in figure 6.8, since in the latter an ankle joint is present to rotate the foot. The advantage of the double support phase is that the robot can be fully controlled.

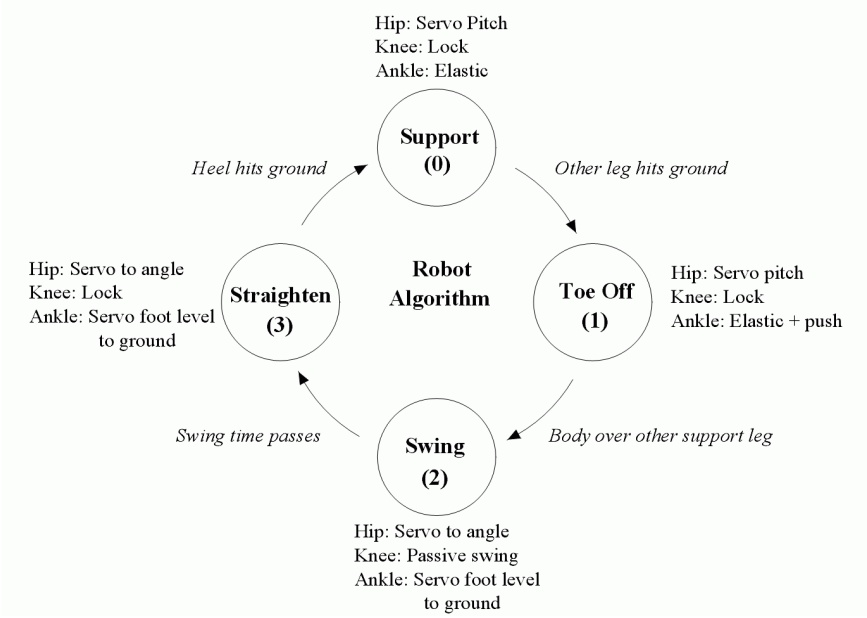

Fig.6.8: Control scheme Spring Flamingo [6.02]

Some researchers already have proposed the idea to use a range of the compliances instead of a discrete number of compliances, in order to be able to vary the walking speed. In [6.09] the concept of Active Variable Passive Stiffness (AVPS) is explained. This theory however was never implemented in a prototype, due to the lack of suitable actuators with adaptable compliance. It was reduced to what is called phasic activation of pneumatic muscles. Here two predefined pressures are alternatively applied to the muscles. This is implemented in the pneumatic powered bipeds at Delft University [6.07]. In [6.10], the idea to vary the compliance to adapt the walking speed is also put forward. Since Veronica is equipped with MACCEPA actuators, the concept of Controlled Passive Walking, which is similar to the ideas mentioned in [6.09] and [6.10], can be implemented.

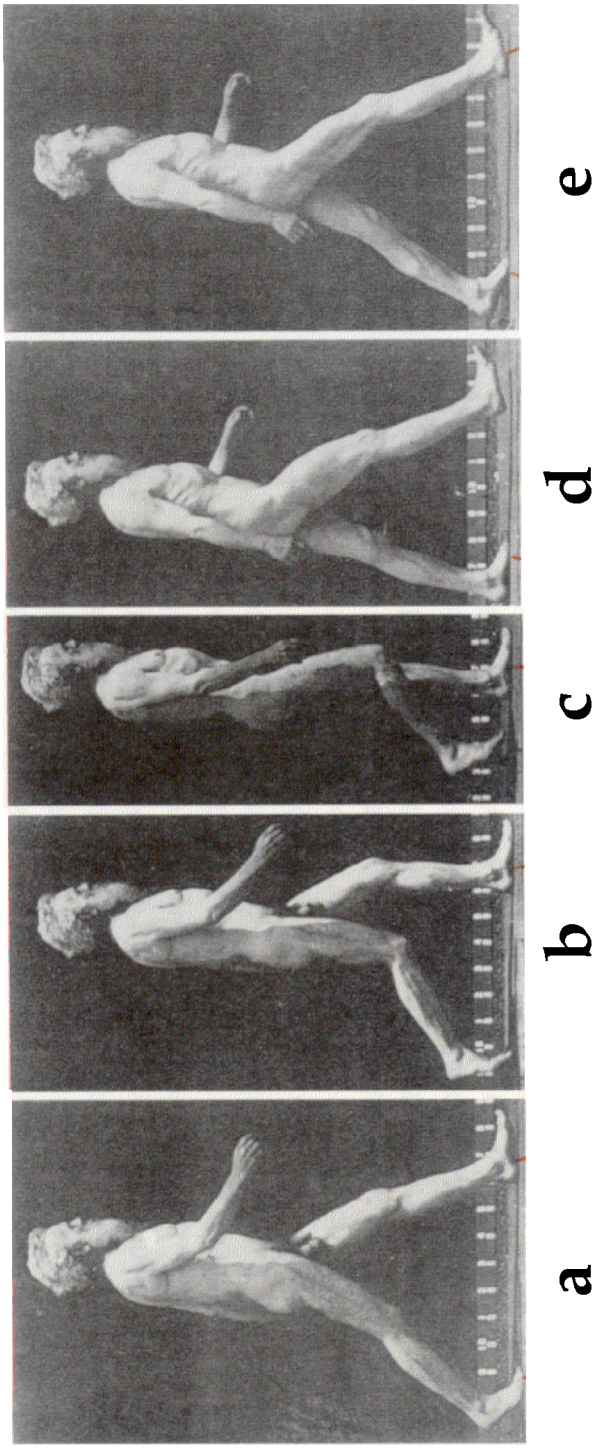

Fig.6.9: Stages of walking stride [6.06]

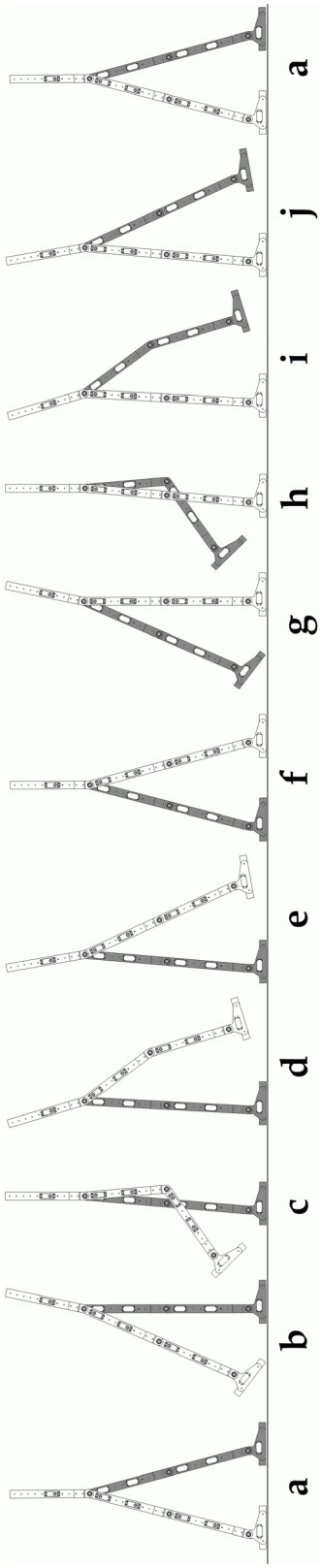

Fig.6.10: Walking sequence of Veronica

6.4 Implementation of Controlled Passive Walking in Veronica

As explained in section 5.6.7 the controller of Veronica will be implemented on a standard PC in a Visual Basic environment. The main idea of Controlled Passive Walking is to set equilibrium position and compliance for each joint in the beginning of a single swing motion and keep them constant until the next single swing motion, so the robot moves passively and thus energy efficiently according to the chosen natural motions. To be able to vary all the equilibrium settings and compliances independently, twelve parameters for each phase are shown on the screen and can be modified. Note that due to symmetry actually only half of the phases are unique, since the parameters of the right leg are the same as the parameters of the left leg in the opposite phases. This is because initially a cyclic gait is chosen. The bisecting mechanism, described in section 5.4, results in another reduction of the parameters, since the actual angle of the left and right upper leg are opposite. Thus both MACCEPA actuators in the hip are working in parallel. Therefore the compliance will be set equal for both MACCEPAs, and the equilibrium position will be set opposite.

In figure 6.10, the walking sequence of Veronica, which is comparable to other passive walkers, is depicted and ten snapshots of the walking gait are shown. Only the leg structures are shown, and the left leg is coloured grey for clarity.

In figure 6.10a and 6.10f, the robot is in double support, with two stretched legs. Figure 6.10b and 6.10g show the push-off: this is used to insert energy into the system and push the robot forward. Both legs are stretched in order to be able to support the weight of the robot. Once the toe leaves the ground, the upper leg is pulled forward, as shown in figure 6.10c and 6.10h. The knee of the swing leg is unlocked and made compliant, so due to the motion of the upper leg, the knee is bent and foot clearance is created. Figure 6.10d and 6.10i are snapshots of the upper leg being in the most forward position and ready to go back again. Due to this backward motion, the knee is stretched, as shown in figure 6.10e and 6.10j. Note that the leg should be stretched again before touchdown of the foot, which is shown 6.10a and 6.10f.

These ten positions are now used to define the phases of the controller, as shown in table 6.1. The first phase starts with the touchdown of the foot, as shown in figure 6.10a. This event is triggered by an electrical switch in the sole of the foot. Note that the configuration shown in figure 6.10a, the double support with both feet flat on the ground, is instantaneous. The next configuration, figure 6.10b, is the end of the push-off phase. Since the

settings should be changed here to bend the knee, this is the start of the next phase in the controller. The first phase is the motion between figure 6.10a and 6.10b. The second phase starts with the toe-off and ends with the leg stretched again. Note that in this phase the upper leg first swings forward and then backward to stretch the knee. This can be achieved with compliant actuators, without changing the settings of the MACCEPA. The end of the second phase—when the leg is stretched again as shown in figure 6.10e—can be detected by the potentiometer in the knee joint. The third phase starts at figure 6.10e and ends at figure 6.10f. In this phase the robot falls forward to end up in the double support with the other leg in front. The second phase is the most interesting phase, since here the rear leg is brought to the front, while the leg is passively bent and stretched again, without control of the actuators. The other phases, 4 to 6, are analogous to phases 1 to 3.

In table 6.1, an overview of the settings in each phase is given. Note that the locked knee can be achieved by setting the equilibrium position to the front and by choosing a high stiffness, as described in section 5.3.

Phase	*Left Leg*	*Right Leg*
1	*Hip: Eq.Pos. Back, Compliant*	*Hip: Eq.Pos. Front, Compliant*
(a- b)	*Knee: locked*	*Knee: locked*
	Ankle: Push off with toe	*Ankle: Make robot fall forward*
2	*Hip: Eq.Pos. Front, Stiff*	*Hip: Eq.Pos. Back, Stiff*
(b-e)	*Knee: Compliant*	*Knee: locked*
	Ankle: Compliant	*Ankle: Make robot fall forward*
3	*Hip: Eq.Pos. Front, Stiff*	*Hip: Eq.Pos. Back, Stiff*
(e-f)	*Knee: locked*	*Knee: locked*
	Ankle: Compliant	*Ankle: Make robot fall forward*
4	*Hip: Eq.Pos. Front, Compliant*	*Hip: Eq.Pos. Back, Compliant*
(f-g)	*Knee: locked*	*Knee: locked*
	Ankle: Make robot fall forward	*Ankle: Push off with toe*
5	*Hip: Eq.Pos. Back, Stiff*	*Hip: Eq.Pos. Front, Stiff*
(g-j)	*Knee: locked*	*Knee: Compliant*
	Ankle: Make robot fall forward	*Ankle: Compliant*
6	*Hip: Eq.Pos. Back, Stiff*	*Hip: Eq.Pos. Front, Stiff*
(j-a)	*Knee: locked*	*Knee: locked*
	Ankle: Make robot fall forward	*Ankle: Compliant*

Table 6.1: Control Scheme of Veronica

The controller software consists of the parameters of each phase and the triggers to go to the next phase. These triggers can be the setting or clearing of one of the foot switches, the stretching of a knee, a certain angle for each of the joints or a timer. Once a condition occurs that starts the next phase, the parameters of the new phase are sent to the joint microcontrollers, which control the servomotors in the MACCEPA actuators. In order to obtain a stable walking gait by tuning the parameters, all the parameters are shown on the screen and can be modified directly, as shown in figure 6.11.

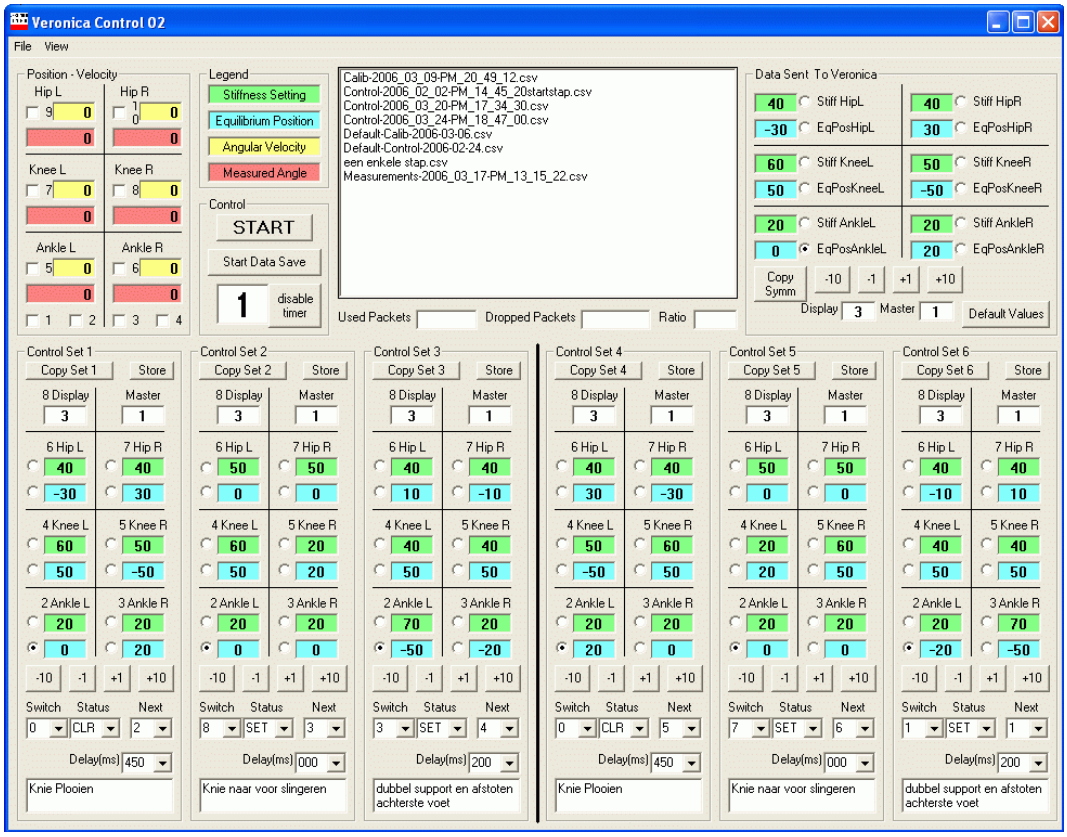

Fig.6.11: Screenshot of the controller software on the PC

6.5 Walking experiments with Veronica

At first the tuning of the parameters is done roughly to get a motion according to the natural dynamics mechanisms of bipedal walking, as explained in section 6.2. Thus, the leg is bent during the forward swing, stretched again when being in the forward position and the knee is locked when supporting the weight of the robot. It should be noticed that this walking motion is not stable, and requires human assistance.

In a second stage the robot is filmed, together with an overview on an extra PC screen of all the settings of equilibrium positions and compliances at that moment and the current phase, as shown in figure

6.12. When this is replayed in slow motion, the natural motions can be observed and the settings can be adjusted intuitively. For example, when the motion of the upper leg is not fast enough the stiffness can be increased, as explained in section 6.1.

Fig.6.12: Picture of test setup

Videos of the walking pattern can be found at:

http://mech.vub.ac.be/maccepa

In this video Veronica was not yet attached to the beam, as described in section 5.1.5. Since the lateral extensions where unable to balance the robot during the tuning of the parameters, it was decided to use the beam structure for lateral balance during the tuning experiments.

6.6 Remarks on Controlled Passive Walking

In Veronica Controlled Passive Walking is implemented in a non-model based controller. However, it can also be used for a model-based trajectory tracking controller. Instead of defining an artificial trajectory, it is possible to calculate the settings of equilibrium position and compliance, which are required to achieve natural trajectories according to the desired locomotion parameters.

The tuning of the control parameters of Veronica was done manually. A self learning algorithm could however also be used to find the parameters

for a desired walking motion, as is done in [6.11]. A controller which can react on changes in ground, slope or other environmental parameters can be implemented as well [6.12]. But Veronica was built in the framework of this PhD to be a test platform and a proof of concept for Controlled Passive Walking.

The servomotors used in Veronica are back-driveable, which means that in case of an external torque, they have to be powered continuously to remain in the same position. For Controlled Passive Walking implemented with MACCEPA actuators, the position of the servomotor has to be changed only in the beginning of each phase. In Veronica, built to demonstrate the concept of Controlled Passive Walking, the servomotors are thus continuously consuming power, which is of course not energy efficient. This type of servomotor was chosen, since the motor, gearbox, position sensor, controller and power circuit are all combined in a standard off-the-shelf unit. The use of non back-driveable servomotors should be taken into consideration in future biped designs.

6.7 Conclusions

In this chapter, the concept of Controlled Passive Walking is explained through a series of thought experiments, with increasing complexity. A number of natural dynamics mechanisms used both in human and passive walking robots are described. The control strategy of some other actuated passive walkers is given to introduce the controller implemented in the biped Veronica. The methodology of tuning the parameters of the controller in Veronica is given.

References:

[6.01] M. Okada, S. Ban and Y. Nakamura, Skill of Compliance with Controlled Charging/Discharging of Kinetic Energy. Proceedings of the 2002 IEEE International Conference on Robotics & Automation, Washington, DC, May 2002

[6.02] J. E. Pratt and G. A. Pratt. Exploiting Natural Dynamics in the Control of a Planar Bipedal Walking Robot. Proceedings of the Thirty-Sixth Annual Allerton Conference on Communication, Control and Computing, Monticello, Illinois, September 1998

[6.03] S. Mochon and T.A. McMahon. Ballistic walking. J. Biomechanics, Vol. 13: pp. 49–57, 1980.

[6.04] E. Schuitema, D. G. E. Hobbelen, P. P. Jonker, M. Wisse, J. G. D. Karssen. Using a controller based on reinforcement learning for a passive dynamic walking robot, Proceedings of 2005 5th IEEE-RAS International Conference of Humanoids Robots

[6.05] R. F. Ker , R. McN. Alexander and M. B. Bennett, 1988. Why are mammalian tendons so thick? Journal of Zoology, London, Vol. 216: pp. 309-324.

[6.06] R. McN. Alexander, Exploring Biomechanics – Animals in Motion, Scientific American Library

[6.07] M. Wisse. Essentials of dynamic walking-Analysis and design of two-legged robots. PhD Thesis, September 2004, Delft

[6.08] T. Takuma, K. Hosoda, M. Ogino, M. Asada. Stabilization of quasi-passive pneumatic muscle walker. 4th IEEE/RAS International Conference on Humanoid Robots, 2004

[6.09] R.Q. van der Linde, Actively controlled ballistic walking, Proceedings of the IASTED International Conference on Robotics and Applications 2000,August 14-16, 2000 – Honolulu, Hawaii, USA

[6.10] V. Duindam and S. Stramigioli. Optimization of Mass and Stiffness Distribution for Efficient Bipedal Walking. IROS 2005 Workshop on Morphology, Control, and Passive Dynamics, IEEE/RSJ International Conference on Intelligent Robots and Systems (IROS 2005), August 2, 2005, Edmonton, Alberta, Canada

[6.11] T, Geng, B. Porr and F. Wörgötter. Fast Biped Walking with a Sensor-driven Neuronal Controller and Real-time Online Learning. The International Journal of Robotics Research Vol. 25 Issue 3 - 1 March 2006

[6.12] S. Collins, A. Ruina, R. Tedrake, M. Wisse. Efficient Bipedal Robots Based on Passive-Dynamic Walkers. Science magazine, Vol. 307, 18 February 2005

Chapter 7

General conclusions

Imagination is more important than knowledge.
Albert Einstein

The beginning is the most important part of the work.
Plato

In this work two types of compliant actuators and their implementation in bipedal walking robots have been studied: the PPAM in the active controlled biped Lucy and the MACCEPA in the Controlled Passive Walking biped Veronica. In section 7.1 an overview of the research done during this PhD is given. Section 7.2 describes the outcomes and section 7.3 describes future work.

7.1 Overview

During the PhD the 2nd generation of PPAM was developed and tested, which resulted in an increased lifespan. A design of a 3rd generation PPAM is proposed in order to further increase the lifetime and to ease the production process. To control the pressure in the PPAM, a special valve island with 6 on/off valves was designed. By using a speed-up circuitry and a multilevel bang-bang controller a fast and lightweight pressure regulating valve can be built. A number of test setups are built to investigate the different applications of compliance of the PPAM. A 1 DOF hopping robot, actuated by 2 PPAMs, was studied. It was found that energy could be stored in the PPAM and by applying short pressure pulses the hopping motion could be sustained. Subsequently a single pendulum, actuated by 2 PPAMs, was studied. By adapting the compliance setting of the joint the number of control actions and power consumption could be drastically influenced. The planar bipedal walking robot Lucy is actuated by 12 PPAMs, resulting in 6 joints with adaptable compliance. The trajectories for each joint are computed on a PC from the set of given objective locomotion parameters. The joint trajectory tracking controller consists of a computed torque, delta P unit and multilevel bang-bang controller. In the current control strategy the compliance of all the joints is fixed, and thus the robot is controlled as an actively controlled robot.

Parallel to the improvements of the PPAM, the MACCEPA was developed. This electrical actuator with adaptable compliance allows independent control of equilibrium position and compliance. It has a quasi linear angle-torque characteristic and the required pressures for a certain equilibrium position are independent of the current position. Therefore, this actuator is used for Controlled Passive Walking. This concept is based on the control of passive motion, by setting the equilibrium position and the compliance of the actuator only at the beginning of a swing motion. This concept is comparable with actuated passive walkers. However, the natural frequency is not fixed by design, as is the case for passive walkers, but can be varied online during the walking motion. This control strategy is implemented in the planar biped Veronica.

7.2 Results

This text is mainly focussed on the development of the MACCEPA and the concept of Controlled Passive Walking that is implemented in the biped Veronica.

7.2.1 MACCEPA

The MACCEPA actuator developed during this PhD is patented. The advantages of this novel type of compliant actuator are:

- The torque is symmetrical around the equilibrium position (T is an odd function of α)
- The torque is a quasi linear function of the angle α (at least with proper dimensioning)
- The torque is a quasi linear function of the pre-tension P
- The linearised formula for the torque is straightforward and usable angles up to 60°

$$T = \alpha . \mu . P$$

- The torque is independent of the equilibrium position. This implies that compliance (determined by spring constant k and pre-tension P) and equilibrium position can be controlled independently.
- Since both settings—equilibrium position and compliance—are done by position controlled actuators, a non-backdrivable gearing mechanism can be used. In the proposed control strategy power is consumed only when the set points of the motors are changed, thus not during passive dynamic motions.
- Since each servo motor in the MACCEPA has its specific function, the dimensions can be optimised for the specific task.
- The MACCEPA is a simple and straightforward design, which can be built with a limited number of standard off-the-shelf components.
- Joints with 2 and 3 rotational degrees of freedom can be built, according to the same principle.
- The actuation in not limited to electrical power. Also hydraulic drives can be used.

7.2.2 Controlled Passive Walking

Opposite to the control of Lucy, where the compliance will be adapted during the tracking of an artificially generated trajectory in order to increase efficiency, the control strategy of Veronica is based on a combination of natural trajectories. The concept of Controlled Passive Walking is similar to actuated passive dynamic walkers, but the natural frequencies are not tuned by varying the mass distributions of the limbs, but by adaptation of the compliances of the joints. The advantage is that this can be done during the walking motion, resulting in the ability to vary the walking speed.

The control strategies of both Lucy (active) and Veronica (controlled passive) use compliance to lower energy consumption. The required computing power for Lucy (up to 2000Hz) is however some orders of magnitude higher than for Veronica (3 control actions for each step).

Control strategies based on passive walkers give deeper insight in human walking, e.g. natural bending of swing leg, passive swing motions and stretched stance leg.

7.3 Future work

In the future, the controller of Veronica will be extended to more than one cyclic motion—walking speed—and to transitions between different motion patterns. A self learning algorithm can be introduced into the controller, in order to optimize the efficiency of the walking pattern or to find other stable walking patterns.

In Veronica, the MACCEPA actuator was used to adapt the natural frequencies of the limbs. This variation of natural frequency can also be used in prostheses, in order to increase the comfort for the user on different types of terrain and different walking speeds. When used in active ankle-foot prosthesis, the MACCEPA actuator can insert energy in the walking cycle, as is done in Veronica.

The adaptable compliance of the MACCEPA can also be used for safe human-robot interaction. In industrial robots, compliance is generally avoided, since it complicates control. The co-operation of humans and robots gives interesting possibilities, but requires safe robots. This can be done by using compliant actuators, allowing the robot to be compliant when moving fast, and stiff in case of slow and precise position control.

This safe human-robot interaction is also required in rehabilitation robotics. Since the patient is linked with the robot, the actuation of the

robots should be able to absorb e.g. spasms without hurting the patient. This can be done with compliant actuators. The compliance can be adapted during the rehabilitation process, in order to improve the motion of the patient.

Controlled Passive Motions can also be used in pick and place robots. These robots generally perform repetitive motions, where the trajectory between start and end position is of minor importance. For the precise position control at the end position, a combination with a traditional position controller can be used.

The use of compliance is a new concept in control. In the past, compliance was generally avoided. However, for a growing number of applications, it proves to be an interesting extra parameter, it makes applications inherently safer and leads to lower energy consumption. In this work a number of aspects related to the compliant actuators and their control were introduced. Hopefully, these concepts will inspire other researchers.

Appendix A1

Pressure control with on-off valves of Pleated Pneumatic Artificial Muscles in a modular one-dimensional rotational joint

R. Van Ham, B. Verrelst, F. Daerden & D. Lefeber

International Conference on Humanoid Robots, Karlsruhe and Munich, October 2003, abstract p. 35 + CDROM

Pressure Control with On-Off Valves of Pleated Pneumatic Artificial Muscles in a Modular One-Dimensional Rotational Joint.

Ronald Van Ham, Björn Verrelst, Frank Daerden and Dirk Lefeber

Vrije Universiteit Brussel, Department of Mechanical Engineering
Pleinlaan 2, 1050 Brussel, Belgium {Ronald.Van.Ham@vub.ac.be}

Abstract. The power to weight ratio of the actuators is an important design factor for running robots. In this regard pleated pneumatic artificial muscles are excellent actuators. Another advantage is that they can actuate a joint directly, avoiding the additional weight of a gearbox. Obviously the weight of the pressure control valves has to be taken into consideration as well. For this application, standard pressure regulating valves are rather heavy and slow. An intelligently controlled array of fast switching on-off valves was tested as an alternative. Ways to decrease the opening and closing times of these valves are discussed in this paper. Simulations and experimental results will be compared. The design of a modular rotational joint with an antagonistic set-up of two pleated pneumatic artificial muscles will be presented.

1 Introduction

During the last decades research groups working on walking robots have increasingly focused on developing dynamically balanced robots in order to achieve higher speed and smoother motion. For these robots, all parts, including the actuators, need to be lightweight in order to limit inertia and motion power. Since electric motors are quite heavy, some research groups [1] and companies [2] started to work with other actuators.

In the research lab of the mechanical department of the Vrije Universiteit Brussel, a member of the European thematic network on Climbing and Walking Robots (CLAWAR) [3] the Pleated Pneumatic Artificial Muscle (PPAM) has been developed [4]. Currently a dynamically controlled biped robot, named Lucy, with PPAMs is being built. [5]. Lucy is designed to run dynamically, which requires a lightweight design. The frame of the robot is made of a high-grade aluminium alloy. PPAMs—the actuators of the robot—have a very high power to weight ratio and an inherent and adjustable compliance which is important for energy recuperation in faster gaits. To power a bi-directional joint, two muscles have to be antagonistically coupled, since PPAMs are one-way acting. By choosing the points where the PPAMs are attached in a specific way, the angle of the joint depends on a weighted difference of both muscle gauge pressures while its compliance is determined by a weighted sum of the pressures. This means both angle and compliance of a joint can be adjusted independently.

As is the case for all pneumatic muscle actuators, the pressure in the PPAMs needs to be controlled by pneumatic valves. This can be done by off-the-shelf pressure regulating servo-valves, either continuously or on-off controlled. The former type was found to be too heavy and too slow for our application. Therefore fast switching on-off valves have been used to make fast and lightweight proportional pressure servo-valves. By making them ourselves, full control over the servo-valve control system was gained, which is usually concealed in commercial valves. The control system can be tuned and adapted for a specific application—e.g. in order to use the springiness of the muscles to bend the knee after touchdown and jump back up again, thereby saving valuable energy, it must be able to close the muscles completely which cannot be done by all commercial valves.

The design of the biped is based on modularity and flexibility, in order to decrease design efforts and costs, and to be able to make minor modifications during the building process. Due to the flexible design of the biped, it can be configured easily for other experiments—e.g. using different points of attachment to achieve other force-angle characteristics and other joint angle limits.

As a first step in the design the pressure control was developed and tested on a constant volume. Since the volume of a pneumatic muscle is function of the contraction, further experiments were done with a preliminary joint actuated by two pneumatic muscles, of which the pressure control is done by a number of on-off valves in parallel.

From the experience with a preliminary setup, a final modular 2 dimensional joint was designed. Angle and pressure sensors were evaluated and where necessary replaced by more suitable devices. In the biped the concept of modularity will not only be implemented in mechanical design and on pneumatics, but also on the electronics and low-level control.

2 Pleated Pneumatic Artificial Muscles

A pneumatic artificial muscle is, in essence, a membrane that will expand radially and contract axially when inflated, while generating high pulling forces along the longitudinal axis. Different designs have been developed. The best known is the so called McKibben muscle [6]. This muscle contains a rubber tube which will expand when inflated, while a surrounding netting transfers tension. Hysteresis, due to dry friction between the netting and the rubber tube, makes control of such a device rather complicated. Typical of this type of muscles is a threshold level of pressure before any action can take place. The main goal of our new design [7] was to avoid both friction and hysteresis, thus making control easier while avoiding the threshold. This was achieved by arranging the membrane into radially laid out folds that can unfurl free of radial stress when inflated. Tension is transferred by stiff longitudinal fibres that are positioned at the bottom of each crease. A photograph of the inflated and deflated state of the Pleated Pneumatic Artificial Muscle is given in figures 1 and 2.

Fig. 1: Photograph of deflated PPAM

Fig. 2: Photograph of inflated PPAM

If we neglect the influence of elasticity of the high tensile strength material used for the membrane, the characteristic for the generated force is given by :

$$F_t = pl^2 f_t \left(\epsilon, \frac{l}{R}\right) \tag{1}$$

where p is the applied gauge pressure, l the muscle's maximum length, R it's unloaded radius and ϵ the contraction. The dimensionless function f_t, which depends only on contraction and geometry, is given for different values of broadness R/l on the graph in figure 3.

The higher R, the less it contracts and the higher the force it generates. Contraction can reach up to 54% in a theoretical case with $R/l = 0$, which is bounded in practice because of minimum space needed to fold the membrane.

Forces at low contraction are extremely high, causing excessive material loading, and generated forces drop very low for large contraction, thus restricting the useful contraction range to about 5 to 35%, depending on R/l. The graph in figure 4 gives the generated force for different pressures of a muscle with initial length $l = 100mm$ and unloaded diameter $R = 25mm$. Forces up to $3000N$ can be generated with gauge pressure of only $3bar$ while the device weighs about $100g$.

The graphs shown are derived from a mathematical model which match experimental results with deviations of less than a few percent. This mathematical model will be of great importance for the design process of the different joints. Low values of the broadness R/l result in the highest possible contractions, however space limitations impose a lower limit on R/l. Once the broadness is chosen and the pressure limits are set at 3 to $4bar$, to prevent rupture of the membrane, length becomes the major design factor. Expression (1) shows that the generated

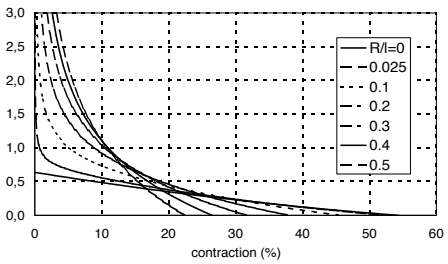

Fig. 3: Dimensionless function f_t

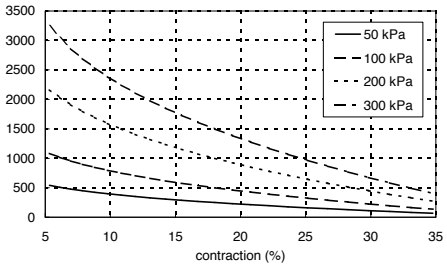

Fig. 4: Generated forces (N)

force is proportional to l^2. Once the PPAM is made with a certain length and radius, the pressure is the only way to control the PPAM.

3 The Valves

In order to realize a fast and accurate pressure control, fast on-off valves are used. Since the pressure control is designed for the dynamically balanced biped, the weight should be restricted. The pneumatic solenoid valve 821 2/2 NC made by Matrix [8] weights only $25g$. With their reported opening times of about $1ms$ and flow rate of $180Nl/min$, they are about the fastest switching valves currently available. In figure 5 a picture of the valve is shown.

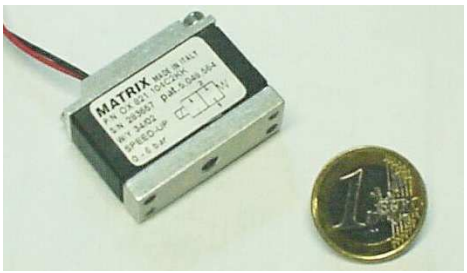

Fig. 5: Photograph of Matrix 821 2/2 NC Valve

Since experiments resulted in switching times of more than $1ms$ for most of the permitted values of pressure difference across the valve, ways to speed up the valve were studied. In the 821 valves the airflow is interrupted by a flapper forced by an internal spring to close the outlet. The electromagnetic force of the coil opens of the valve. To decrease the opening time the manufacturer proposes a speed up in tension circuitry using $24V$ during $2.5ms$ and $5V$ afterwards. The flapper is thus mainly subjected to 3 forces: the spring, the electromagnetic force and the resultant force caused by the difference in pressure. The influence

of each of these forces on opening and closing times will be studied. The magnetic force was varied by the level of the initial opening voltage. Running tests with and without spring revealed the influence of the spring. It was found that to ensure proper closing of the valve, the spring cannot be removed if the pressure difference across the valve is less than $2bar$.

Distinct and easy determinable opening and closing times have to be defined to compare test results. The moment the valve is fully opened can be determined from the electrical current pattern [9]. However the airflow through the valve starts before the valve is fully opened and closing times cannot be defined consistently by the current pattern, the outlet pressure pattern was studied. Opening the valve resulted in a step like increase of outlet pressure, closing in a step like decrease. The moments of opening and closing are defined as the time 10% of the full step size was measured.

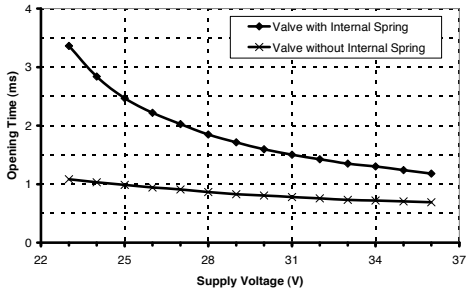

Fig. 6: Influence of supply voltage on the opening time of the valves, $\Delta p = 4.6bar$

The influence of the level of opening voltage is diagrammed in figure 6. Increasing this voltage reduces opening time, so it needs not to be applied for $2.5ms$.

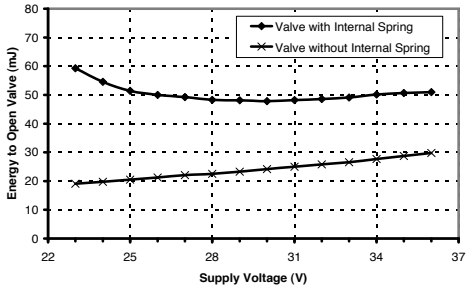

Fig. 7: Influence of supply voltage on energy to open valve, $\Delta p = 4.6bar$

Figure 7 shows the consumed electric power—a measure for the produced heat—if the voltage is dropped to $5V$ as soon as the valve is open. These results show that increasing the voltage to $35V$ followed by an immediate drop to $5V$ when the valve is open, will reduce opening times without increasing the produced heat, which is of major influence on the valves service life. Figure 8 shows enhanced opening times as function of the difference across the valve.

To improve the closing times, a resistor was added to the coils discharge circuit. This will dissipate the electromagnetic energy but, at the same time, impose a reverse voltage on the coil. Too high a resistance will thus destroy the coil. Too low a resistance will slow down the energy dissipation. Experiments showed a resistor of 200Ω to be a good compromise. The reverse voltage will be kept beneath $50V$ and the demagnetization time remains less than about $200ms$. This results in shorter closing times, as can be seen in figure 9.

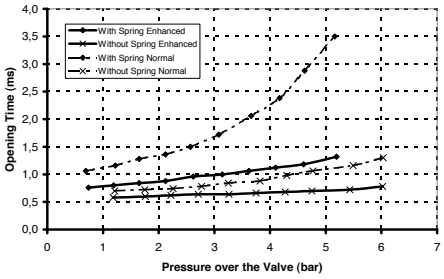

Fig. 8: Opening times of valves

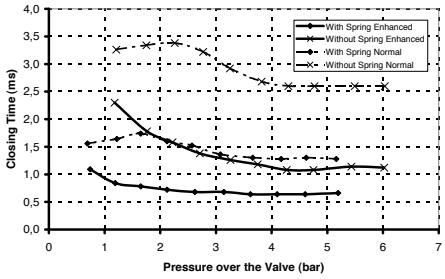

Fig. 9: Closing times of valves

Due to the enhancements to the speed up in tension circuit and the resistor to dissipate the energy of the coil, opening times and closing times are reduces significantly. In the targeted system—pressure control of a PPAM—the differential pressure across the inlet valves is at all times higher than 3 bar and the differential pressure across outlet valves is always lower than $3bar$. This justify the use of the valve with internal spring as outlet valve and a valve without spring as inlet valve.

Figure 10 points out that removing the spring from the inlet valves justifies the $35V$ to be applied only for $1ms$, since all opening times are within this time. Figure 11 shows that in these cases closing times are always less than $1.5ms$, in case of using the valves in combination with PPAMs, working between $0bar$ and $3bar$.

4 Pressure Control of a Constant Volume

When using on-off valves instead of a proportional valve, a controller is needed to generate the command signals for the valves. A Motorola 68HC916Y3 microcontroller [10] will be used because of the experience with this type of controller,

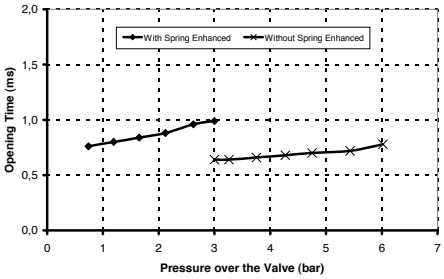

Fig. 10: Opening times of valves, in pressure range for PPAMs

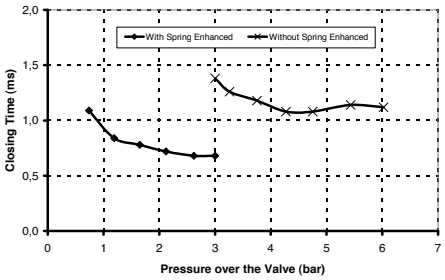

Fig. 11: Closing times of valves, in pressure range for PPAMs

the processing power, the internal memory and certain valuable features—e.g. analog to digital convertor, incremental encoder readout. In order to control the pressure with 2/2 valves a minimum of 1 inlet and 1 outlet valve is required. Obviously the more valves used in parallel, the faster a volume can be pressurized or depressurized, but power consumption, price and weight of the pressure control will increase.

A model of the valves and volume was made in Matlab - Simulink [11] and tuned with experimental results to ease the simulation of different control algorithms. In the simulations a volume of 300*cc* was used, since this is comparable to the volume of the PPAMs used in the biped robot.

To optimize the number of valves, the ability to pressurize and depressurize the volume in approximately the same amount of time is used as criterion. As is well known from fluid mechanics, the mass flow is proportional to the supply pressure. This results for the 821 valves and 300*cc* volume in a twice as fast increase compared to decrease of pressure. Therefore the number of outlet valves should be twice the number of the inlet valves. Secondly, the use of the pressure control for a PPAM in a dynamical biped requires the ability to change the pressure in the volume faster than in case of 1 inlet and 2 outlet valves. Therefore the number of valves was doubled, resulting in a set-up with 2 inlet valves and 4 outlet valves. From the satisfactory results of the simulations as shown in figure 12, the decision was taken not to increase the number of valves any further.

One should realize the pressure limit of the PPAM—being 4*bar*—introduces an even more unbalanced situation: since the pressure difference across the inlet valve is minimum 4 bar and across the outlet valves it is maximum 3 bar, the inlet mass flow—when not choked—will be larger than the outlet mass flow, even through the double number of valves.

Two control algorithms will we simulated and the better will used for experiments. The use of Pulse Width Modulation requires modification of the algorithm, since a standard PWM controller generates only one output signal of which the duty cycle is function of the error between the requested value and measured value. For the discussed pressure control a positive error—pressure too low—requests an action of the inlet valves. A negative error triggers the

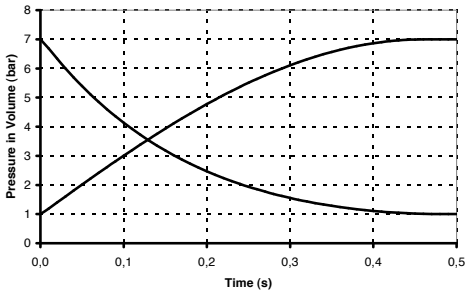

Fig. 12: Comparison 2 Inlet and 4 Outlet valves on 300cc volume

outlet valves. Therefore, the absolute value of the error is used to generate the PWM signal and its sign determines which valves are used. Simulations showed improvement in accuracy when different inlet and outlet valves were controlled separately. Therefore the duty cycle was calculated as if there was only one inlet and one outlet valve. In case of a duty cycle higher than 100% more valves are used and the duty cycle is divided by the number of valves.

Secondly a bang-bang controller, which normally takes only the sign of the error between the requested value and measured value in consideration, was studied. The output signal was split to control inlet and outlet valves and a dead zone was introduced to eliminate oscillations about the requested pressure. As was the case for the PWM, the separate control of the 2 inlet or 4 outlet valves showed improvement in accuracy. Therefore, in case of the outlet valves, the value of the error was compared to 4 levels, each controlling 1 outlet valve. Since no significant improvement was seen compared to 2 levels—1 valve or 4 valves—the outlet valves were controlled in 2 levels, as was done with the inlet valves. Figure 13 visualizes the actions of the modified bang-bang controller.

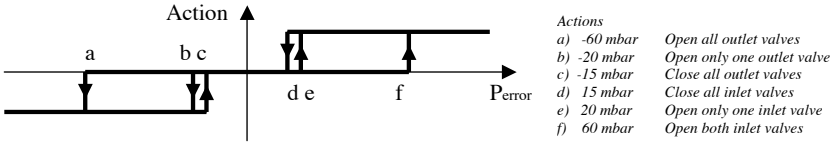

Fig. 13: Visualization of the actions of the bang-bang controller

The simulations of PWM and bang-bang control gave comparable results, but the bang-bang algorithm requires less processor time, which is important when incorporated in a higher-level controller. To structuralize the program, the bang-bang controller is programmed as a real time interrupt with a period of 723μs, because figure 10 shows this the shortest opening time. Figure 14 shows the experimental results of an increase of pressure from 1 bar to 1.5, 2, 3 and 4

bar, while figure 15 shows the results for a decrease from 4 bar to 3, 2, 1.5 and 1 bar in the volume.

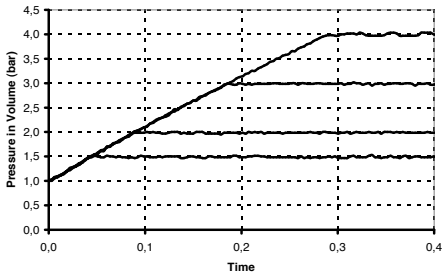

Fig. 14: Pressure Control (Increasing Pressure)

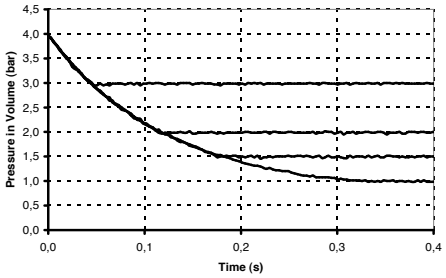

Fig. 15: Pressure Control (Decreasing Pressure)

As can be seen from previous figures, this pressure control is fast and accurate. Experiments showed the different levels of the bang-bang controller can be adapted to optimize the controller in case of higher or lower requested pressures.

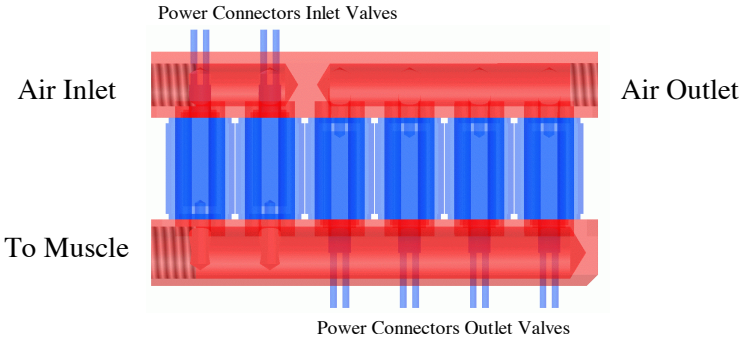

Fig. 16: Pressure control block with 2 inlet and 4 outlet valve

To connect the 6 valves into one compact pressure regulating valve two special collectors were designed. This collectors replace the original aluminium connector plates of the valves, resulting in a weight of the complete pressure valve not more than the weight of 6 single valves. In figure 16 a section this pressure valve is shown.

Worked until now on a constant volume, one should realize the volume of PPAM increases when contracting, resulting in a less accurate pressure control.

5 Preliminary Rotational Joint with PPAMs

Since the PPAM is a unidirectional actuator, two antagonistic coupled PPAMs are needed to actuate a rotative joint. The joint controller will consist of two pressure controllers, one for each muscle, and a higher-level position controller. In figure 17 the system under test, see also [4], is sketched. The points of attachment of the PPAMs together with muscle dimensions determine the torque characteristics and also the range in which the joint can rotate, since the muscles have limited contraction ratios. These points are chosen such that the highly non-linear force characteristics of the PPAMs transform to a linear angle-torque and the rotation of the lever arm is ranging from $-30°$ to $+30°$.

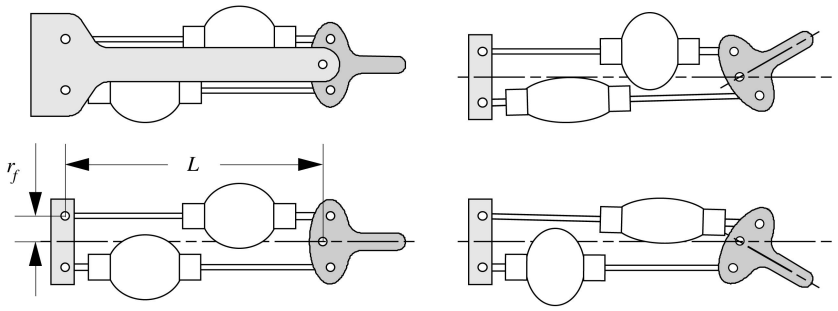

Fig. 17: Rotative joint actuated by 2 antagonistic PPAMs

Since the optimal number of valves was determined for a constant volume, a new criterion is needed for this set-up, involving the controllability of the angle. To reduce oscillations when moving the lever arm at constant compliance, the pressure in one muscle should decrease as fast as the pressure in the other muscle increases. The joint angle controller was simulated with different number of inlet and outlet valves for an average pressure of 2.5 bar. The response times for a variation of 0.8 bar, which results in a rotation from $0°$ to $21°$, are plotted figure in 18.

The curves start at the same level due to the fact that all three set-ups initially make use of 2 outlet valves, which determine the speed. The curve with 2 inlet valves rises when used in combination with 7 outlet valves because the difference between inlet and outlet speed creates strong oscillations, which decrease the average speed. Two inlet valves will be used, since response times are satisfactory on a comparable constant volume with 2 inlet valves. Although when two inlet valves are used speed still can be increased slightly, 4 outlet valves are a preferred compromise on price, electric power consumption and weight.

The complete system is highly non linear since it has two bang-bang controllers with a dead zone and two levels, twelve on-off valves and 2 PPAMs. Standard linear techniques are not able to create a robust angle controller for

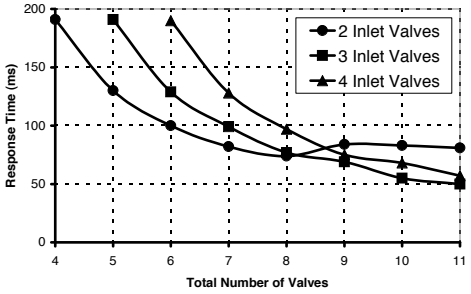

Fig. 18: The open loop step response time with different number of valves.

this system. A PID controller will be studied by simulating the different actions separately on a system without external load.

Since elimination of the final error requires an I–action, first a purely I–controller was tested. Too high an I–gain will create an overshoot. Too low an I–gain slows down the system response. Since the optimal gain depends strongly on the average pressure and on the angle variation, an adaptive controller is required. The oscillations appearing in the step response can be eliminated almost completely by introducing a D–action with a small gain, independent of the pressure. To complete the PID controller a P–action was added, but since no significant improvement was seen on the system without load, the P–action will be disabled temporarily.

In figure 19 the simulated response of steps of 0° to 10°, 20° and 30° with an average pressure of 2.5*bar* are plotted. Figure 20 shows the corresponding experimental results. Figure 20 shows the system without load and with an adaptive ID-controller is fast and accurate, except in the extreme limits. A small overshoot can be seen for angles around 30°, probably because the PPAMs cannot deliver enough force to stabilize the joint when fully contracted [4].

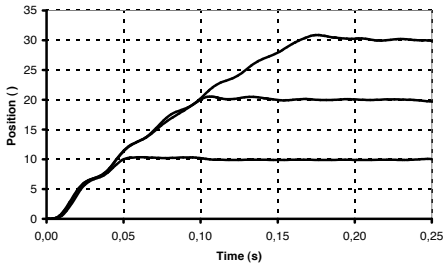

Fig. 19: Simulated step response without load

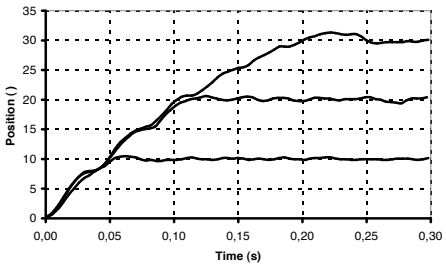

Fig. 20: Experimental step response without load

When an arm with a length of $195mm$ is charged with a load of $1kg$, the P-action of the controller becomes more useful to decrease the response time. The gains of the PID controller have to be tuned again as a function of angle variation and average pressure. Although the simulation (figure 21) shows the joint can be controlled without oscillations, this cannot be achieved in the experimental set-up (figure 22). Modification of the D-gain cannot eliminate the oscillations, since the noise on the pressure measurements is blown up in the differentiator.

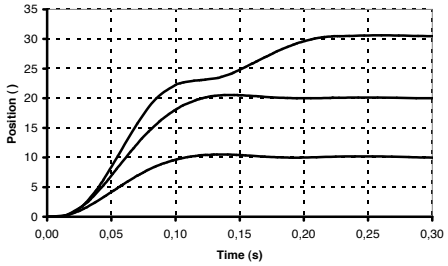

Fig. 21: Simulated step response with load

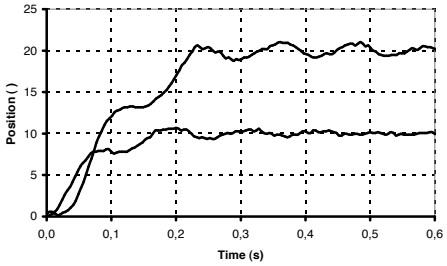

Fig. 22: Experimental step response with load

The analogue pressure sensor, placed outside the muscle, is linked to the internal AD converter of the microcontroller by relatively long wires, which are subject to noise from power circuits of the valves and the microcontroller clock. Preliminary tests with a digital pressure sensor increased the resolution of the pressure measurement by a factor 4, which will allow the D-action to lower the oscillations. The digital pressure sensor will be incorporated in the muscle, to improve the quality of the pressure signal.

6 Modular 2-Dimensional Rotative Joint with PPAMs

Modularity is gaining importance in robot design to reduce cost [12]. In order to be able to build our 2-dimensional robot Lucy with modular parts, the joints have all been chosen to be rotational. Since the lower-leg, upper-leg and torso have approximately the same length, one leg can be built with 3 quasi-identical modules. However, the modules should be configurable for a specific range of motion and specific force characteristics. Both are determined by the length, diameter and points of attachment of the PPAMs.

A photograph of such a modular element is given in figure 23. Figure 24 shows a more detailed view of the joint. The two darker plates—which determine the points where the PPAMs are attached—can easily be replaced to configure the range of motion and force characteristics of the joint in order to configure the module to be a hip, knee or ankle joint.

In the preliminary design a potentiometer was used to measure the angle. The analog signal was digitized in the microcontroller by an internal 10 bit AD

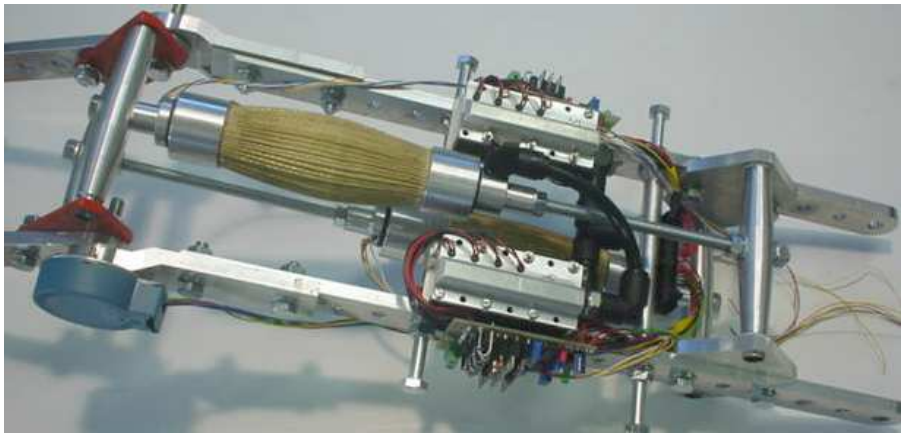

Fig. 23: Modular part, configured as knee joint

convertor. The noise on the analog signal, induced in the long wires by the electromagnetic field of the speed up circuitry of the valves, disturbed the angle measurement and therefore determination of the angular velocity. Therefore an optical incremental encoder was preferred. The microcontroller has a special submodule, which can be configured to read out an incremental encoder and convert it to a absolute position, without taking any resources from the main processor. In figure 24 the encoder, which has a resolution on 0.044°, is shown.

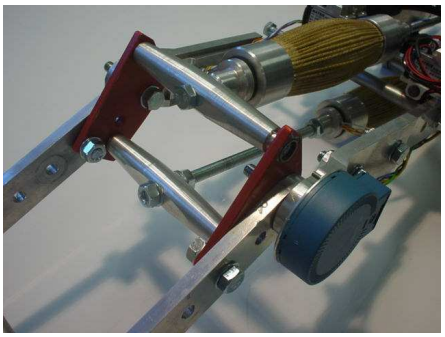

Fig. 24: Detailed view of the attachment points of the muscles

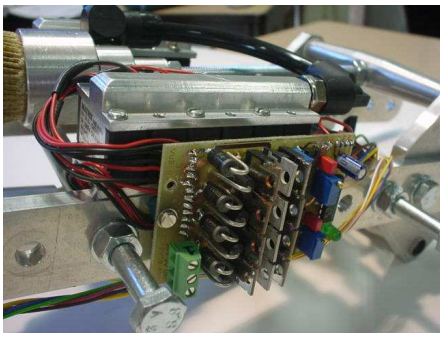

Fig. 25: Detailed view of the valves with speed up circuitry

Although the dimensions of the muscles have their influence, not only on maximum torque, but also on air consumption, all muscles will initially be identical for practical reasons. In later designs the muscle volume can be decreased in order to achieve a better match between provided torque and the torque needed

for powering a specific joint. This increases efficiency: the smaller the muscle the less air needed to inflate them.

Figure 25 shows a detailed view of the pressure valves, placed on the modular part. Since the bang-bang controller works with 2 levels for the outlet valves—resulting in 3 valves controlled simultaneously (see figure13)—the speed up circuits of these 3 outlet valves are combined into 1. On the side of the module the electronics of the 4 speed up circuits are combined on one printed circuit board.

One connector, containing all electrical signals to and from the joint, is linked with the 68HC916Y3 controller board. The controller measures the angle of the joint and pressure in both PPAMs, communicates with the high-level controller and generates the control signals for the 12 on-off valves.

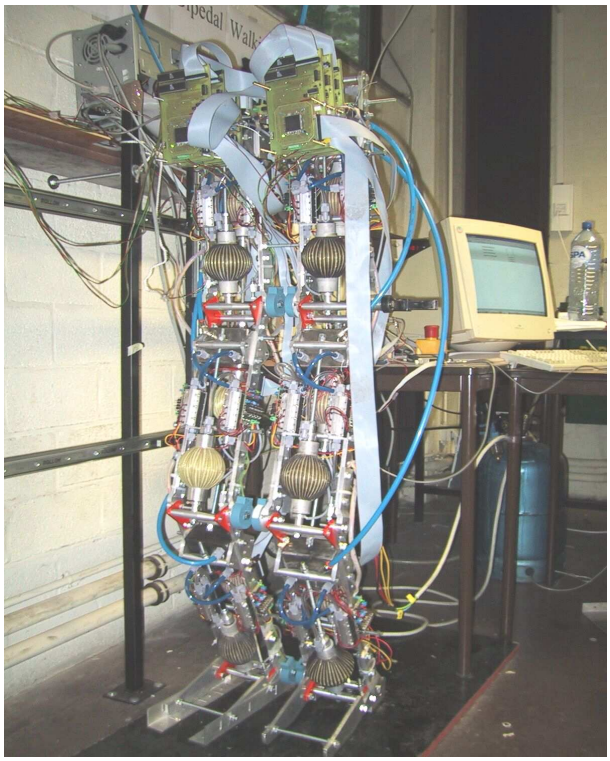

Fig. 26: The Biped Lucy

Figure 26 shows a photograph of the complete assembly of 6 modular parts, resulting in the biped Lucy. The horizontal and vertical sliders reduce the movements into a plane parallel with the sliders.

7 Conclusion

A lightweight on-off valve with enhanced speed up circuitry and in some cases removal of the internal spring, showed significantly reduced opening and closing times. These enhanced valves are used to build a fast and accurate pressure control, which is lighter and cheaper than existing proportional valves. The low-level bang-bang controller with dead zone is shown to be an excellent pressure controller, which is easy to program, needs little computing power and results in good performance.

A rotative joint actuated by two pneumatic muscles and controlled by an adaptive PID angle controller combined with two bang-bang pressure controllers was designed. Due to the concept of modularity and flexibility, coupling 6 of these modules—each configured as specific joint—results in the 2-dimensional biped Lucy.

References

1. S. T. Davis and D. G. Caldwell. The bio-mimetic design of a robot primate using pneumatic muscle actuators. In *CLAWAR 2001: Proceedings of the 4th International Conference on Climbing and Walking Robots*, pages 197–204, Karlsruhe,Germany, 2001. Professional Engineering Publishing.
2. http://www.shadow.org.uk/
3. http://www.clawar.com/
4. F. Daerden, D. Lefeber, B. Verrelst, and R. Van Ham: Pleated pneumatic artificial muscles: actuators for automatisation and robotics. In IEEE/ASME International Conference on Advanced Intelligent Mechatronics, pages 738-743, Como, Italy, 2001.
5. B. Verrelst, R. Van Ham, F. Daerden, and D. Lefeber: Design of a Biped Actuated by Pleated Pneumatic Artificial Muscles. In CLAWAR 2002: 5th International Conference on Climbing and Walking Robots, Paris, France
6. H.F. Schulte: The characteristics of the McKibben artificial muscle. In The Application of External Power in Prosthetics and Orthotics, number Publication 874 pages 94-115. National Academy of Sciences-National Research Council, Lake Arrowhead, 1961.
7. F. Daerden and D. Lefeber: The concept and design of pleated pneumatic artificial muscles, International Journal of Fluid Power 2(3), p41-50, 2001
8. Pneumatic division on http://www.matrix.to.it/
9. Robert Eschmann. Modellbildung und Simulation pneumatischer Zylinderantriebe. PhD thesis, RWTH Aachen, 1994, pp45-47
10. 68HC916Y3 Datasheet on http://e-www.motorola.com/
11. http://www.mathworks.com/
12. S. Murata, E. Yoshika, K. Tomita, H. Kurokawa, A. Kamimura, S. Kokaji: Hardware Design of Modular Robotic System, Proc. of IEEE/RSJ International Conference on Intelligent Robots and System, pp. 2210-2217, 2000

Appendix A2

Fast and Accurate Pressure Control Using On-Off Valves

R. Van Ham. B. Verrelst, F. Daerden, B. Vanderborght & D. Lefeber

International Journal of Fluid Power 6 (2005) No. 1 pp 53-58

FAST AND ACCURATE PRESSURE CONTROL USING ON-OFF VALVES

Ronald Van Ham, Bj rn Verrelst, Frank Daerden, Bram Vanderborght and Dirk Lefeber

Vrije Universiteit Brussel, Department of Mechanical Engineering, Pleinlaan 2, 1050 Brussel, Belgium
Ronald.Van.Ham@vub.ac.be

Abstract

Pneumatic cylinders and pneumatic muscles are lightweight, clean and multifunctional actuators, requiring pressure-regulating valves for positioning. To use them in mobile applications commercial pressure-regulating valves are quite heavy and rather slow. Therefore an intelligent controlled array of fast switching on-off valves is presented as an alternative. The speed of the on-off valves determines the performance of the pressure-regulating valve. To reduce the opening time of the valves, a higher voltage is applied on the coil for a short time. The influence of this method on the heating of the valve will be discussed. A diode, which drains away the electromagnetic power from the coil, reduces the closing time. When working with pneumatic muscles, it is in some cases justified to remove the internal spring to enhance the opening time. A modified bang-bang controller, with more than one level and a dead zone is presented. Experimental results on a fixed volume are discussed. A special designed collector combines 6 on-off valves into a lightweight pressure control valve island, which is perfectly suited for walking robots such as the pneumatic actuated biped Lucy.

Keywords: Pressure control, Pneumatic muscles, Bang-bang controller

1 Introduction

During the last decades several research groups working on walking robots have increasingly focused on developing dynamically balanced robots in order to achieve higher speed and smoother motion. For these robots, all parts, including the actuators, need to be lightweight in order to limit inertia and motion power. Since electric motors are quite heavy, some research groups [1] and companies [2] started to work with other actuators.

The multibody mechanics research group of the mechanical department of the 'Vrije Universiteit Brussel', a member of the European thematic network on Climbing and Walking Robots (CLAWAR) has developed the Pleated Pneumatic Artificial Muscle (PPAM) [3]. Currently, a dynamically controlled biped robot, named Lucy, with PPAMs is being built [4]. Lucy is designed to walk dynamically, which requires a lightweight design. Therefore the frame of the robot is made of a high-grade aluminium alloy and is actuated with PPAMs, which a very high power to weight ratio and an inherent and adjustable compliance. To power a bi-directional joint, two muscles have to be antagonistically coupled, since PPAMs are one-way acting. By only choosing the points where the PPAMs are attached in a specific way, the angle of the joint depends on a weighted difference of both muscle gauge pressures, while its compliance is determined by a weighted sum of the pressures. This means both angle and compliance of a joint can be adjusted independently, which can be very useful for walking robots and is not the case with most other actuators.

As for all pneumatic muscle actuators, the pressure in the PPAMs needs to be controlled by pneumatic valves. This can be done by off-the-shelf pressure regulating servo-valves, either continuously or on-off controlled. The former type was found to be too heavy and too slow for our application. Therefore fast switching on-off valves have been used to make fast and lightweight proportional pressure servo-valves. This solution is used more and more recently in pneumatics [4a] as in hydraulics [4b], since putting the valves together yourselves, gives full control over the servo-valve control system, which is usually concealed in commercial valves. The control system can be tuned and adapted for a specific application—e.g. in order to use the springiness of the muscles to bend the knee after touchdown and jump back up again, thereby saving valuable energy, it must be able to close the muscles completely which cannot be done by all commercial proportional valves.

Controlling the on-off valves can be done by using various algorithms, such as a PWM controller or a bang bang controller. Of importance for each algorithm is the response time of the valves, which is also a function of the pressure over the valve. As a first step the opening and closing times of the valves were measured in a comparable way. Then several approaches to decrease opening time and closing time were studied.

Since the flow rate of the on/off valves was too small to reach adequate speed for the dynamic biped, the pressure control is done by a number of on-off valves placed in parallel.

This pressure control, however designed for a walking robot application, can be used in the much broader field of pneumatics, since not only the weight is an advantage, but also the speed and the price of the designed valve system.

2 Pleated Pneumatic Artificial Muscles

A pneumatic artificial muscle is, in essence, a membrane that will expand radially and contract axially when inflated, while generating high pulling forces along the longitudinal axis. Different designs have been developed. The best known is the so-called McKibben muscle [5]. This muscle contains a rubber tube, which will expand when inflated, while a surrounding netting transfers tension. Hysteresis, due to dry friction between the netting and the rubber tube, makes control of such a device rather complicated. Typical for this type of muscles is the existence of a threshold level of pressure before any action can take place. The main goal of the new design was to avoid both friction and hysteresis, thus making control easier, while avoiding the threshold. This was achieved by arranging the membrane into radially laid out folds that can unfurl free of radial stress when inflated. Stiff longitudinal fibres, which are positioned at the bottom of each crease, transfer the tension. A photograph of the inflated and deflated state of the Pleated Pneumatic Artificial Muscle is given in Fig. 1.

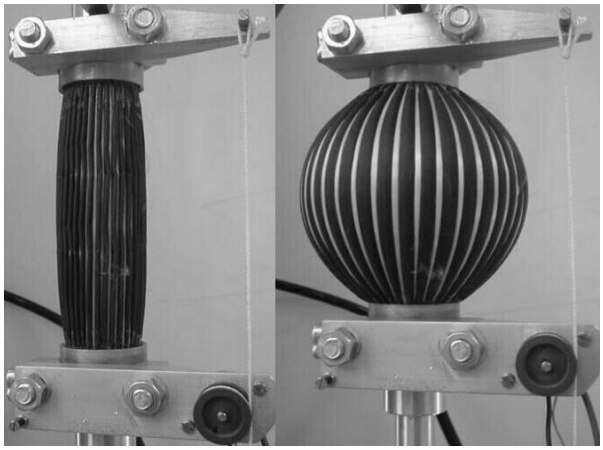

Fig. 1: *Deflated and inflated PPAM*

If we neglect the influence of the elasticity of the high tensile strength material used for the membrane, the characteristic for the generated force is given by:

$$F_t = pl^2 f_t\left(\varepsilon, \frac{l}{R}\right)$$

where p is the applied gauge pressure, l the muscle's maximum length, R it's unloaded radius and ε the contraction. The dimensionless function f_t depends only on contraction and geometry. The higher R, the less it contracts and the higher the force it generates. Contraction can reach up to 54% in a theoretical case with R/l = 0, which is bounded in practice because of minimum space needed to fold the membrane. Forces at low contraction are extremely high, causing excessive material loading, and generated forces drop very low for large contraction, thus restricting the useful contraction range to about 5 to 35%, depending on R/l. The graph in Fig. 2 gives the generated force for different pressures of a muscle with initial length l=100mm and unloaded diameter R=25mm. Forces up to 3000N can be generated with gauge pressure of only 3bar while the device weighs about 100g.

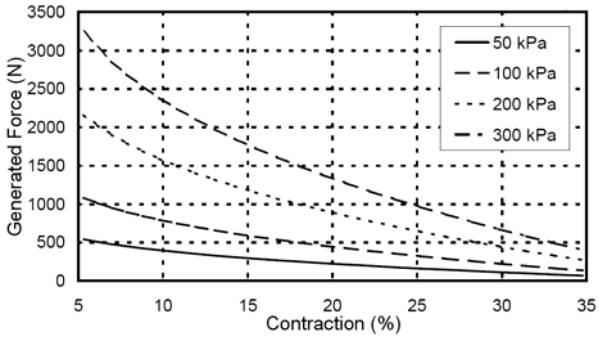

Fig 2: *Generated forces PPAM (N)*

The graphs shown are derived from a mathematical model, which match experimental results with deviations of less than a few percent [3]. This mathematical model will be of great importance for the design process of the different joints. Low values of the broadness R/l result in the highest possible contractions. However space limitations impose a lower limit on R/l. Once the broadness is chosen and the pressure limits are set at 3 to maximum 4bar, to prevent rupture of the membrane, length becomes the major design factor. Expression 1 shows that the generated force is proportional to l^2. Once the PPAM is made with a certain length and radius, the pressure is the only way to control the PPAM.

3 The Valves and Speedup Circuitry

In order to realize a fast and accurate pressure control, fast on-off valves are used. Since the pressure control is designed for the dynamically balanced biped, the

weight should be restricted. In [5a] a solution with small on-off valves is described to build a robotic arm with pneumatic muscles. Figure 3 shows the pneumatic solenoid valve 821 2/2 NC made by Matrix [6], which weights only 25g. With their reported opening times of about 1ms and flow rate of 180Nl/min, they are about the fastest switching valves currently available.

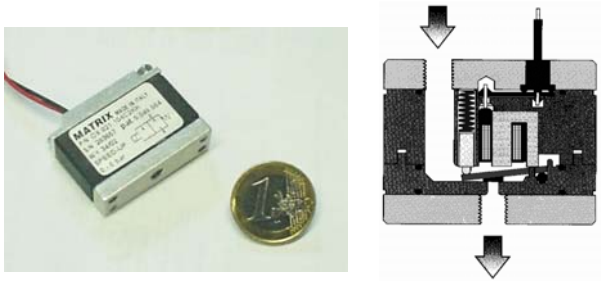

Fig. 3: *Picture of the Matric 821 2/2 NC Valve and sliced view [6]*

Since experiments resulted in switching times of more than 1ms for most of the permitted values of pressure difference across the valve, ways to speed up the valve were studied. The airflow through these valves is interrupted by a flapper, which is forced by the pressure difference over the valve and additionally by an internal spring to ensure proper closing of the valve. The electromagnetic force of the coil working on this flapper opens of the valve. To decrease the opening time the manufacturer proposes a speed up in tension circuitry using 24V during 2.5ms and 5V afterwards. The flapper is thus mainly subjected to 3 forces: the spring, the electromagnetic force and the resultant force caused by the pressure difference over the valve. The influence of each of these forces on opening and closing times was studied. The initial magnetic force was varied by the level of the initial voltage to open the valve. Since opening the valve requires more force than keeping the valve open, the voltage over the coil will be reduced to 5V once the valve is opened. Running tests with and without spring revealed the influence of the spring. The force of the spring acts in the same direction as the pressure over the valve. It was found that to ensure proper closing of the valve, one of these forces is required, so the spring cannot be removed if the pressure difference across the valve is less than 2bar.

Distinct and easy determinable opening and closing times have to be defined to compare test results. The moment the valve is fully opened can be determined from the electrical current pattern [7]. However the airflow through the valve starts before the valve is fully opened, also closing times cannot be defined consistently by the current pattern. Therefore the outlet pressure pattern was studied. Opening the valve resulted in a steplike increase of outlet pressure, while closing resulted in a step like decrease. The moments of opening and closing are defined as the time at which 10% of the full step size in outlet pressure was measured.

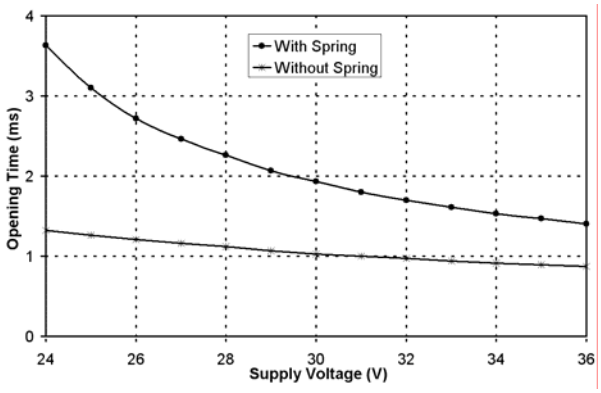

Fig. 4: *Influence of supply voltage on the opening time of the valves, Δp=4.6bar*

The influence of the opening voltage level, for a pressure over the valve of 4.6 bar, is diagrammed in Fig. 3. Increasing this voltage reduces opening time, so the higher voltage doesn't need to be applied for 2.5ms.

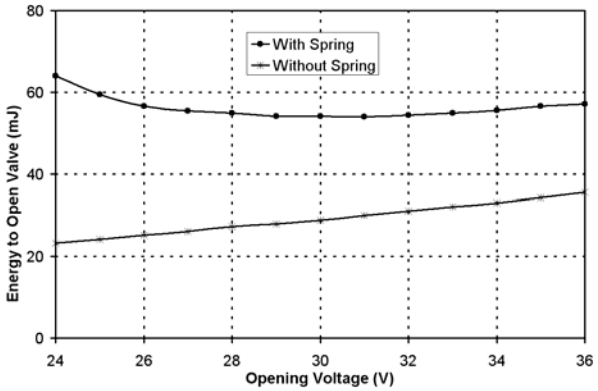

Fig. 5: *Influence of supply voltage on energy to open valve, Δp=4.6bar*

Figure 5 shows the consumed electric power to open the valve, which is a measure for the produced heat. These results show that increasing the voltage to 35V followed by an immediate drop to 5 V, when the valve has opened, will reduce opening times without increasing the produced heat, which is of major influence on the valve's service life. Figure 6a shows enhanced opening times as function of the pressure difference across the valve. A significant improvement can be seen in case of larger pressure differences over the valve.

To improve the closing times, a diode between the negative contact of the coil is connected to the 35V, so the demagnetization time drops to about 200ms. Obviously, this results in much shorter closing times, as can be seen in Fig. 6b.

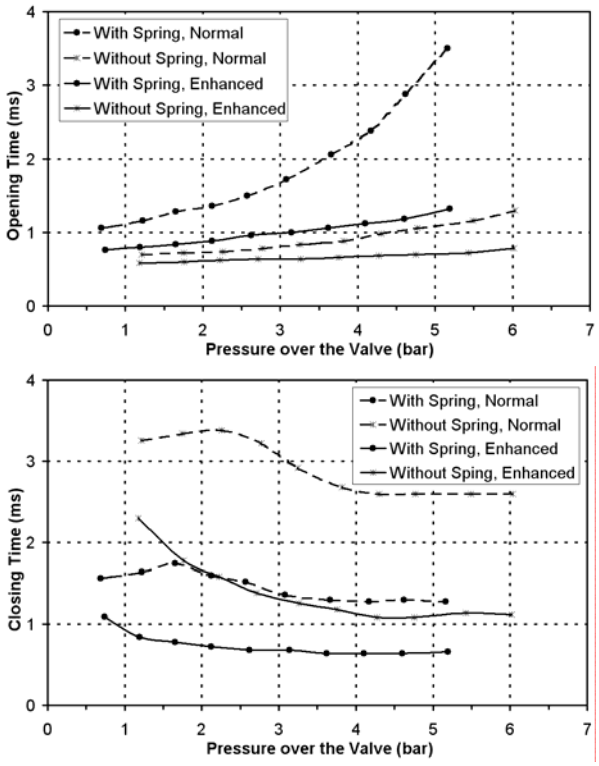

Fig. 6: *(a) Opening times and (b) closing times of valves*

Due to the enhancements to the speed up in tension circuit and the placement of the diode, opening times and closing times are reduced significantly, in some cases to less than 50%.

In the targeted system—the pressure control of a PPAM working between 0 and 3 bar, with a supply pressure of 6 bar—the differential pressure across the inlet valves is at all times higher than 3 bar and the differential pressure across outlet valves is always less than 3 bar. In Fig. 7, showing partly the same data as Fig. 6, the enhanced opening and closing times of the outlet valve with spring and the inlet valve without spring are plotted. Figure 7 shows that the use of the valve with internal spring as outlet valve and a valve without spring as inlet valve is justified.

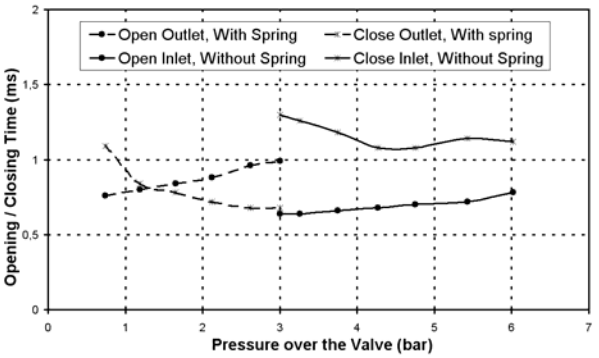

Fig. 7: *Opening times and closing times of valves – when using PPAM between 0 and 3 bar*

Figure 7 points out that removing the spring from the inlet valves justifies the 35V to be applied only for 1ms, since all opening times are within this time. In our setup we'll use a fixed time of 1ms, since detecting the actual opening of the valve would require an extra pressure sensor placed nearby the outlet of the valve. This was avoided to reduce costs. On the other hand when several valves will be placed in parallel, it's difficult to detect the exact opening moment of each valve by looking at the pressure.

Figure 7 also shows that closing times are always less than 1.5ms when using the valves in combination with PPAMs, working between 0 bar and 3bar and with a supply pressure of 6 bar.

4 Pressure Control of a Constant Volume

When building a pressure control with on-off valves, a controller is needed to generate the command signals for the valves. A Motorola 68HC916Y3 microcontroller [8] is used because of the experience with this type of controller, the processing power, the internal memory and certain valuable features: e.g. analogue to digital converter, incremental encoder counter. In order to control the pressure with 2/2 valves a minimum of 1 inlet and 1 outlet valve is required. Obviously, the more valves used in parallel, the faster a volume can be pressurized or depressurized, but power consumption, price and weight of the pressure control will increase.

A model of the valves and volume is made in Simulink™ and tuned with experimental results to ease the simulation of different control algorithms. In the simulations a volume of 300cc is used, since this is comparable to the volume of the PPAMs in the biped robot Lucy [4].

To optimize the number of valves, the ability to pressurize and depressurize the volume in approximately the same amount of time is used as a first criterion. As is well known from fluid mechanics, the mass flow is proportional to the supply pressure. This results for the 821 valves with a supply pressure of 6 bar and 300cc volume in a twice as fast increase compared to decrease of pressure. Therefore the number of outlet valves should be twice the number of the inlet valves. Secondly, the use of the pressure control for a PPAM in a dynamical biped requires the ability to change the pressure in the volume faster than is feasible with 1 inlet and 2 outlet valves. Therefore the number of valves was doubled, resulting in a set-up with 2 inlet valves and 4 outlet valves.

One should realize the pressure limit of the PPAM - being 3 bar—introduces an even more unbalanced situation: since the pressure difference across the inlet valve is minimum 3 bar and it is maximum 3 bar across the outlet valves, the inlet mass flow—when not choked —will be larger than the outlet mass flow, even when the number of valves is doubled.

Two control algorithms were simulated and the better was used for experiments. First a Pulse Width Modulation (PWM) was studied. The use of a PWM requires modification of the algorithm, since a standard PWM controller generates only one output signal of which the duty cycle is function of the error between the requested value and measured value. For the dis-

cussed pressure control, a positive error—meaning that the pressure is too low—requests an action of the inlet valves. A negative error triggers the outlet valves. Therefore, the absolute value of the error is used to generate the PWM signal and its sign determines which valves are used. Since controlling the inlet valves separately improves the accuracy, the PWM algorithm was modified. The calculated duty cycle was divided over the valves, e.g. when the duty cycle for the two inlet valves is 60%, one valve will be opened continuously (duty cycle equals 100 %) and the other with a duty cycle of 20%.

Secondly a bang-bang controller, which normally takes only the sign of the error between the requested value and measured value in consideration, was studied. The output signal was split to control inlet and outlet valves and a dead zone was introduced to eliminate oscillations around the requested pressure. As was the case for the PWM, the separate control of the 2 inlet or 4 outlet valves showed improvement in accuracy. Therefore, in case of the outlet valves, the value of the error was compared to 4 levels, each controlling 1 outlet valve. Since no significant improvement was seen compared to 2 levels—1 valve or 4 valves—the outlet valves were controlled in 2 levels, as was done with the inlet valves. Figure 8 visualizes the actions of the modified bang-bang controller.

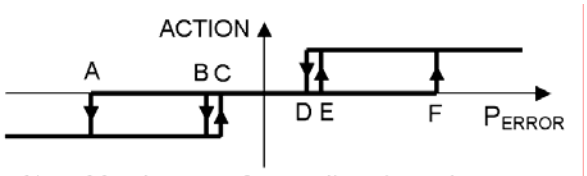

A)	-60 mbar	Open all outlet valves
B)	-20 mbar	Open only one outlet valve
C)	-15 mbar	Close all outlet valves
D)	15 mbar	Close all inlet valves
E)	20 mbar	Open only one inlet valve
F)	60 mbar	Open both inlet valves

Fig. 8: *Visualisation of the actions of the bang-bang controller*

The simulations of PWM and bang-bang control gave comparable results, but the bang-bang algorithm can be adjusted in a more intuitive way; e.g. when the final error is to big, the dead zone can easily be reduced or when small oscillations around the final value occur, they can be reduced by enlarging the dead zone. This is useful when this pressure controller will be incorporated in a higher-level controller.

To structuralize the program, the bang-bang controller is programmed as a real time interrupt with a period of 723 microsec, because Fig. 7 shows this the shortest opening time. Figure 9 shows the experimental results for an increase of pressure from 1 bar to 1.5, 2, 3 and 4 bar. Figure 8 shows also the results for a decrease from 4 bar to 3, 2, 1.5 and 1 bar in the volume.

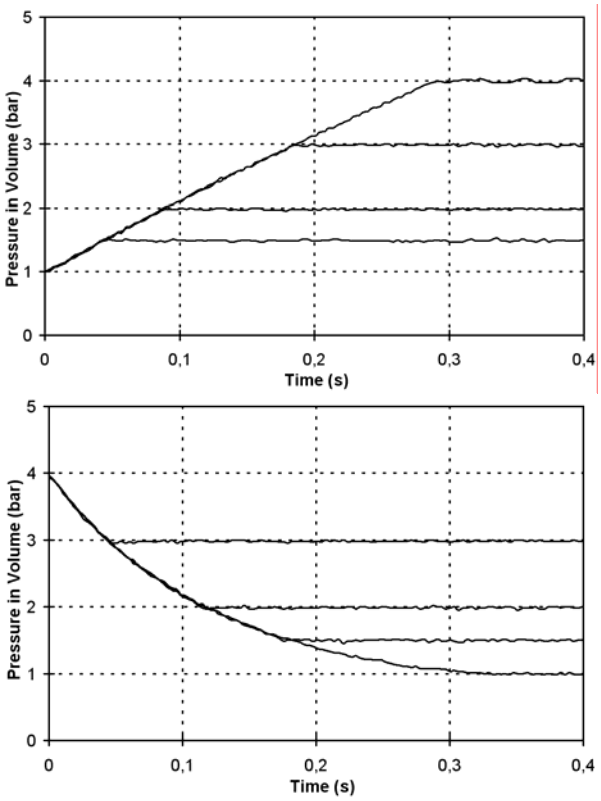

Fig. 9: *Pressure Control (Increasing and decreasing pressure)*

As can be seen from Fig.9, this pressure control is fast and accurate. Additionally, experiments showed that the different levels of the bang-bang controller could be adapted to optimize the controller in case of higher or lower requested pressures.

Since each valve has it's own collector to connect the in and outlet tubes, a lot of useless weight is present. To remove this extra weight and make the valve array as compact as possible, a special collector was designed. The complete pressure-regulating valve, built with 6 single on-off valves and the two special collectors are shown in Fig 10.

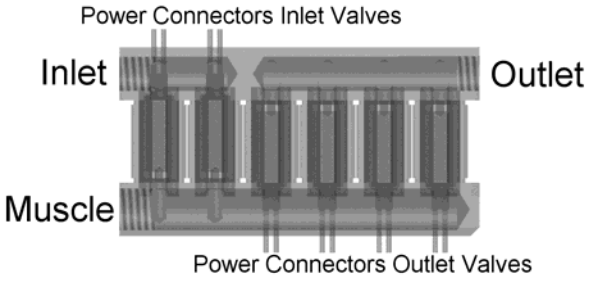

Fig. 10: *Sliced view of the complete pressure control valve island with 2 inlet and 4 outlet valves*

These collectors replace the original aluminium connector plates of the valves, resulting in a weight of the complete pressure valve not more than the weight of 6 single valves.

4 Conclusions

In this paper a fast and lightweight pressure-regulating valve was presented. It was constructed with 6 on-off valves and 2 special designed collectors. The opening times of the on-off valves were enhanced significantly by increasing the initial value of the supply voltage and, depending on the pressure difference over the valve, removing the internal spring. A diode to drain away the electromagnetic power from the coil reduced the closing time to less than 50% in some cases. Since these adaptations do not increase heat production, the life span of the valves is not reduced

A multilevel bang-bang controller was presented. This control strategy allows the user to modify easily the parameters of the controller. The presented pressure-regulating valve allows the volume of a muscle, used in the biped Lucy, to be fully pressurized and fully depressurized in less than 300 ms.

This pressure control, which was designed to be used in walking robots, can however be used in the much broader field of pneumatics, not only due the low weight, but also due to high operation speed and low cost.

References

[1] J. Albiez, T. Kerscher, F. Grimminger, U. Hochholdinger, and K. Berns, “PANTER-prototype for a fast running quadruped robot with pneumatic muscles," in *Proceedings of CLAWAR 2003, 6th International Conference on Climbing and Walking Robots and the Support Technologies for MobileMachines*, (Catania, Italy), pp. 617-624, 2003.

[2] http://www.shadow.org.uk/index.shtml

[3] The concept and design of pleated pneumatic artificial muscles Daerden, F. & Lefeber, D. *International Journal of Fluid Power*, 2(3):41–50, 2001.

[4] Experimental results on the first movements of the pneumatic biped "Lucy". Van Ham, R., Verrelst, B., Vanderborght, B., Daerden, F.& Lefeber, D. 6th International conference on Climbing and Walking Robots and the Support Technologies for Mobile Machines, Catania, September 2003, pp. 485-492.

[4a] Experimental Based Analysis of the Pressure Control Characteristics of an Oil Hydraulic Three-Way On/Off Solenoid Valve Controlled by PWM Signal, Heon-Sul Jeong & Hyoung-Eui Kim, Journal of Dynamic Systems Measurement and Control; vol 124;1(2002), Pages 196-205

[4b] Accurate Position Control of a Pneumatic Actuator Using On/Off Solenoid Valves, R. B. van Varseveld & G. M. Bone, IEEE ASME Transactions on Mechatronics; vol 2;3(1997) Pages 195-204

[5] H. F. Schulte, ``The characteristics of the McKibben artificial muscle," in {The Application of External Power in Prosthetics and Orthotics}, no. Publication 874, pp.94–115, Lake Arrowhead: National Academy of Sciences–National Research Council, 1961.

[5a] T.Raparelli, P.Zobel, F.Durante, “The design of a 2 dof robot for functional recovery therapy driven by pneumatic muscles”, paper RD-078, RAAD 2001, 10th Int. Workshop on ROBOTICS IN ALPE – ADRIA - DANUBE REGION, Vienna, May 16-18, 2001.

[6] Pneumatic division on http://www.matrix.to.it/

[7] Robert Eschmann. Modellbildung und Simulation pneumatischer Zylinderantriebe. PhD thesis, RWTH Aachen, 1994, pp45-47

[8] 68HC916Y3 Datasheet on http://e-www.motorola.com/

Ronald Van Ham (1976)

Study of Electro-Mechanical Engineering at the Vrije Universiteit Brussel, graduated in 1999. Since 1999 researcher and teaching assistant at the Vrije Universiteit Brussel. The focus of his research is the use of adaptable compliance of pneumatic artificial muscles in the walking biped Lucy.

Björn Verrelst (1972)

Study of Mechanical Engineering at the Vrije Universiteit Brussel, graduated in 1996. Since 1998 researcher and teaching assistant at the Vrije Universiteit Brussel. The focus of his research is the use of pneumatic artificial muscles in the walking biped Lucy for dynamically balanced walking.

Frank Daerden (1966)

Study of Mechanical Engineering at the Vrije Universiteit Brussel. PhD in Applied Sciences, Vrije Universiteit Brussel, 1999. Research and teaching assistant at the Vrije Universiteit Brussel, 1991–1999. Doctor-Assistant at the dept. of Mechanical Engineering, Vrije Universiteit Brussel since 1999, visiting Professor since 2003.

Bram Vanderborght (1980)

Study of Mechanical Engineering at the Vrije Universiteit Brussel, graduated in 2003. Since 2003 researcher at the Vrije Universiteit Brussel, supported by the Fund for Scientific Research Flanders (Belgium). The focus of his research is the use of adaptable compliance of pneumatic artificial muscles in the dynamically balanced biped Lucy.

Dirk Lefeber (1956)

Study of Civil Engineering at the Vrije Universiteit Brussel. PhD in Applied Sciences, Vrije Universiteit Brussel, 1986. Professor at the dept. of Mechanical Engineering, head of the Multibody Mechanics Research Group, Vrije Universiteit Brussel.

Appendix A3

Experimental results on the first movements of the pneumatic biped "Lucy"

R. Van Ham, B. Verrelst, B. Vanderborght, F. Daerden & D. Lefeber

6th International conference on Climbing and Walking Robots and the Support Technologies for Mobile Machines, Catania, September 2003, pp. 485-492

Experimental Results on the First Movements of the Pneumatic Biped "Lucy"

R. Van Ham, B. Verrelst, B. Vanderborght, F. Daerden and D. Lefeber
Ronald Van Ham: Vrije Universiteit Brussel, Departement of Mechanical Engineering, Pleinlaan 2, 1050 Brussels, Belgium tel: +32-2-629.28.62, fax: +32-2-629.28.65,
e-mail: Ronald.Van.Ham@vub.ac.be ; website: http://www.vub.ac.be/lucy

Abstract

This paper presents the biped Lucy and the first experimental results of this robot. Lucy is actuated by Pleated Pneumatic Artificial Muscles, which have a very high power to weight ratio and an inherent adaptable compliance. These characteristics will be used to make Lucy walk in a dynamic stable way while exploiting the adaptable passive behaviour of these muscles.
The paper will describe briefly the concept of the pleated pneumatic artificial muscle and the creation of the revolute joint used for the biped. The design and implementation of the pressure control unit will be discussed followed by an overview of the complete robot.
During the assembly and debugging phase of the robot a quasi-static global control has been implemented while using adapted PID techniques for the local feedback joint control. These initial control techniques resulted in the first movements of Lucy, which will be shown and discussed.

1 INTRODUCTION

During the last decades the field of robotics encounters new directions in which novel applications are gaining more and more commercial interests. The mobility of robots, however, has not been an issue for long since research focused on the development of robots to be used in factory plants in order to enhance and automate the production process. Mobile robots and especially legged robots were exclusive research topics for the academic and military world. But as domotics and certain areas in the leisure industry are becoming more and more important in our society, as such the idea of mobile robots is also inspiring

commercial companies. One example is the Honda Motor Corporation, that developed the Honda Human Robot followed by its successors P1, P2 and recently ASIMO focusing on the field of domotics [5]. In the leisure industry the Sony Company already made one commercially available four-legged robot, AIBO [7], and a humanoid robot SDR-4X [6] will become available soon. But also legged robots for industrial use are increasingly gaining interest. For instance the maritime industry with climbing robots developed in Spain [1].
These examples show that legged robots are no longer only futuristic elements for science fiction movies but that they will become fully-fledged part of technological evolution. In spite of the magnificent models already created this evolution has however just began. A dextrous, intelligent, fast and fully autonomous humanoid robot is still far-off.
A lot of research in many different fields ranging from artificial intelligence to mechanical design is needed. One of the topics is the implementation of novel actuators replacing the widely spread electrical drives in order to make lightweight structures and compliant joints. Compliance characteristics can be used to reduce shocks and decrease energy consumption exploiting the natural dynamics of the system.
Extreme models are the so called Passive Walkers (Garcia, Ruina et al. [4]) which have no active control at all, since only gravity leads them down a sloped surface. In order to walk on a horizontal plane, minimum actuation should be provided to compensate energy loss due to collision and friction. This concept gets more and more attention. A recent example is the two- legged Spring Flamingo [8] developed in the Leg Laboratory at MIT. This model uses standard passive elements for which the eigenfrequency of the system is determined by the mechanical construction. Flexibility, with the ability to change this frequency, is increased by implementing passive elements with variable compliance. In this context the group of Takanishi developed the two-legged walker WL-14 [9], where a complex non-linear spring mechanism makes changes in stiffness possible. A more elegant way to implement variable compliance is to use pneumatic artificial muscles, where the applied pressures determine stiffness. Research on this topic is done by Van der Linde and Wisse [10] and Caldwell [3] by implementation of Mc Kibben muscles.
Our research group Multi-body Mechanics of the Vrije Universiteit Brussel is focusing on developing a biped actuated by pleated pneumatic artificial muscles. The goal is to achieve a lightweight bipedal robot able to walk in a dynamically stable way exploiting the passive behaviour of the pleated pneumatic artificial muscles.

2 PLEATED PNEUMATIC ARTIFICIAL MUSCLE

2.1 Concept and Characteristics

A pneumatic artificial muscle is, in essence, a membrane that will expand radially and contract axially when inflated, while generating high pulling forces along the longitudinal axis. Different designs have been developed. The best known is the so-called McKibben muscle. This muscle contains a rubber tube, which will expand when inflated, while a surrounding netting transfers tension. Hysteresis, due to dry friction between the netting and the rubber tube, makes control of such a device rather complicated. Typical of this type of muscle is a threshold level of pressure before any action can take place. The main goal of the new design [2] was to avoid both friction and hysteresis, thus making control easier while avoiding the threshold. This was achieved by arranging the membrane into radially laid out folds that can unfurl free of radial stress when inflated. Tension is transferred by stiff

longitudinal fibres that are positioned at the bottom of each crease. A photograph of the deflated and inflated state of the Pleated Pneumatic Artificial Muscle is given in figure (1).

Fig 1 Photograph of the deflated and inflated state of the PPAM

The generated force is non-linear and proportional to the applied gauge pressure in the muscle and square of the initial length while slenderness of the muscle determines the force characteristic. At a pressure of 3 bar the force can be as high as 4000N for a device with initial length of 10cm, weighing only 100g.

2.2 Revolute joint

Pneumatic artificial muscles only generate force when they bulge. To have a bi-directional working revolute joint one has to couple two muscles antagonistically while generating revolute motion. A rod transmission was chosen because of its inherent asymmetrical operation about its central position, which can compensate the high non-linear muscle characteristic. Large differences for the forces between low and high contractions can be flattened at torque level by choosing appropriate muscle connection points in the leverage mechanism. Figure (2) shows the straightforward connecting principle.

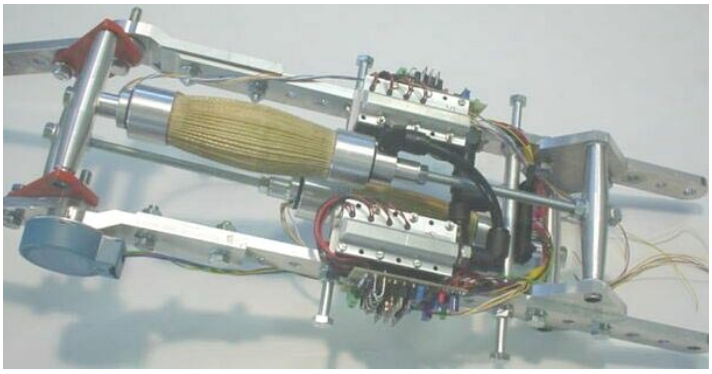

Fig. 2 Photograph of antagonistic set-up

Thus the dimensions of both muscles, being slenderness and its initial length, together with the positions of the points of attachment determine torque characteristics for each joint. Depending whether the joint is a knee, ankle or hip these dimensions can be chosen in order to meet the needs of the specified joint function, not only in torque levels but also in range of motion which is completely different for an ankle and a knee.

In such an antagonistic set-up position will be determined by pressure differences in both muscles while stiffness is set by the sum of pressures. Position of the joint can be maintained while for example increasing the stiffness can be realised by increasing the sum of pressures.

3 PRESSURE CONTOL OF A CONSTANT VOLUME

The previous paragraph showed that pressure control is a key element and lowest level in the control hierarchy. In order to realize a fast, accurate and lightweight pressure control, fast on-off valves are used. The pneumatic solenoid valve 821 2/2 NC made by Matrix weights only 25g. With their reported opening times of about 1 ms and flow rate of 180 Nl/min, they are about the fastest switching valves currently available.
In the 821 valves a flapper forced by an internal spring to close the outlet interrupts the airflow. The electromagnetic force of the coil opens the valve. The flapper is thus mainly subjected to 3 forces: the spring, the electromagnetic force and the resultant force caused by the difference in pressure. The influence of each of these forces on opening and closing times were studied. The magnetic force was varied by the level of the initial opening voltage. Running tests with and without spring revealed the influence of the spring. To ensure proper closing of the valve, the spring cannot be removed if the pressure difference across the valve is less than 2 bar.
Ways to enhance opening and closing times of the valve were studied. Opening and closing times were defined as the time between the moment the corresponding signal is given and the moment the outlet pressure reach 10% of it's final level, in case of opening, or a 10% drop in the outlet pressure, in case of closing. To decrease the opening time the manufacturer proposes a speed up in tension circuitry using 24V during 2.5ms and 5V afterwards. Raising the level of the opening voltage up to 36V resulted in a shorter opening time of the valve. If the voltage is dropped to 5V when the valve is open, the energy when using 36V is lower than when using 24V during the proposed 2.5ms. This opening energy is a measure for the produced heat, which is of major influence on the valve's service life.
To improve the closing times, a resistor was added to the coil's discharge circuit. This will dissipate the electromagnetic energy faster but, at the same time, impose a reverse voltage on the coil. Too high a resistance will thus destroy the coil. Too low a resistance will slow down the energy dissipation. Experiments showed a resistor of 200Ω to be a good compromise. The reverse voltage will be kept beneath 50V and the demagnetisation time remains less than about 200ms. This results in shorter closing times, as can be seen in figure (4).

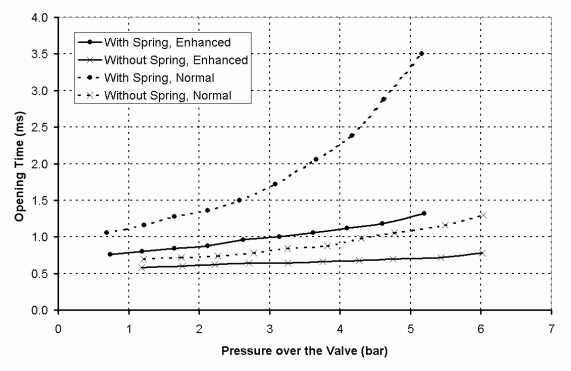

Fig. 3 Opening times of valve

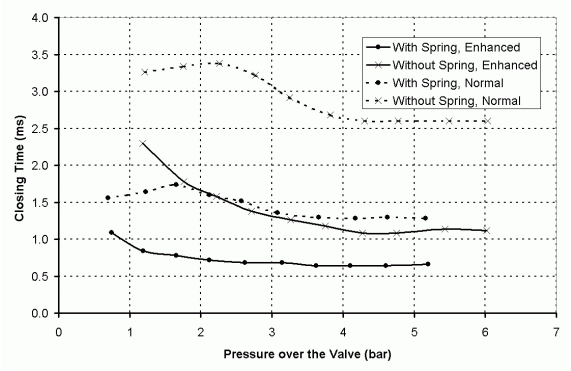

Fig. 4 Closing times of valve

Due to these enhancements opening times and closing times are reduces significantly. In the targeted system – pressure control of a PPAM - the differential pressure across the inlet valves is at all times higher than 4 bar and the differential pressure across outlet valves is always lower than 3 bar. Figure (3) points out that removing the spring from the inlet valves justifies the 35V to be applied only for 1ms, since all opening times are within this time.

In order to control the pressure with 2/2 valves a minimum of 1 inlet and 1 outlet valve is required. Obviously the more valves used in parallel, the faster a volume can be pressurised or depressurised, but power consumption, price and weight of the pressure control will increase. In simulation the valves and a volume of 300cc, since this is comparable to the volume of the PPAMs used in the biped robot, were studied. Out of the simulations we could conclude that the use of 2 input valves and 4 output valves was a good compromise between weight, price and speed.
A bang-bang controller, which normally takes only the sign of the error between the requested value and measured value in consideration, was studied. The output signal was split to control inlet and outlet valves and a dead zone was introduced to eliminate oscillations about the requested pressure. To make the pressure control more accurate the inlet valves and outlet valves were divided in two levels: for the inlet 1 or 2 valves, for the outlet 1 or 4 valves. Figure (5) visualizes the actions of the modified bang-bang controller.

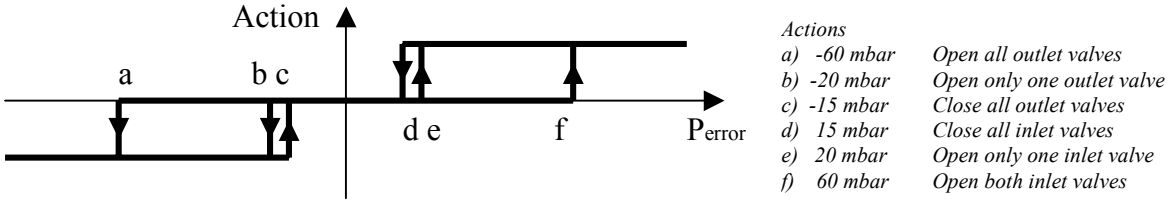

Fig. 5 Visualisation of the actions of the bang-bang controller

Figure (6) shows the experimental results of an increase of pressure from 1 bar to 1.5, 2, 3 and 4 bar, while figure (7) shows the results for a decrease from 4 bar to 3, 2, 1.5 and 1 bar in the volume.

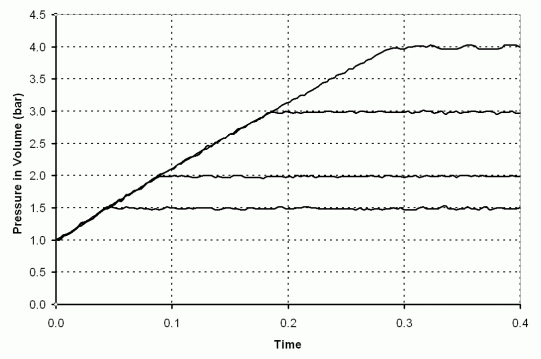

Fig. 6 Pressure Control (increasing pressure)

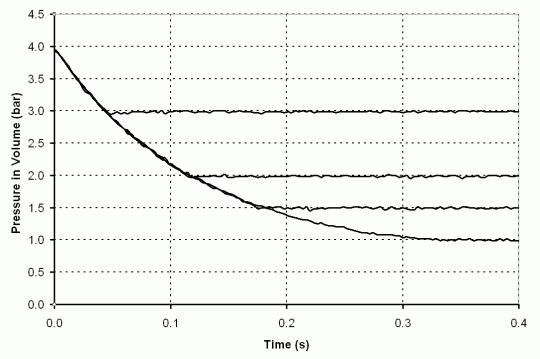

Fig. 7 Pressure Control (decreasing pressure)

As can be seen from previous figures, this pressure control is fast and accurate. Experiments showed the different levels of the bang-bang controller could be adapted to optimise the controller in case of higher or lower requested pressures.

4 GENERAL DESCRIPTION OF LUCY

Presently Lucy has been assembled and tested. A picture of the complete set-up is given in figure (8). The movement of Lucy is restricted to the sagittal plane by a sliding mechanism. The structure is made of a high-grade aluminium alloy, AlSiMg1, and is composed of two legs and an upper body. The legs are identical, each having a foot, a lower leg and an upper

leg. All parts are connected by one-dimensional pin joints creating the ankle, knee and hip. The hip is connected to a horizontal and vertical sliding mechanism by means of a seventh pin joint to avoid turning over in the frontal plane. The robot, all included, weighs about 30kg and is 150cm tall. Key elements in the design phase are modularity and flexibility regarding the ability to make changes to the robot configuration during the experimental process. This resulted in nearly the same configuration for each structural element such as lower-leg, upper-leg and body. A photograph of such an element is given in figure (2).

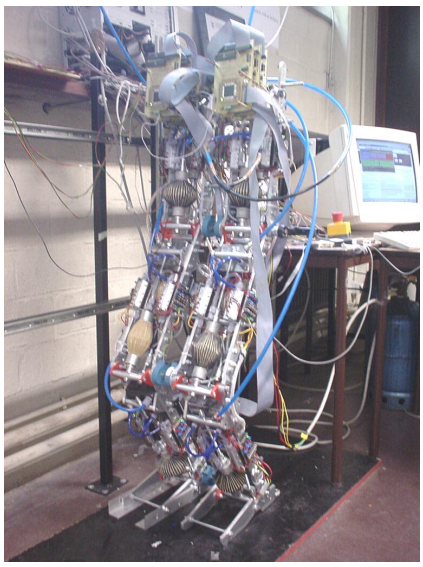

Fig. 8 Photograph of Lucy

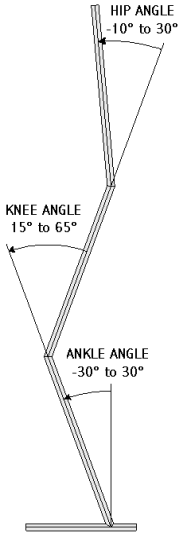

Fig. 9 Range of motion for the joints

The only difference between the elements used for the various functions such as hip, knee and ankle are muscle dimensions and the connection plates of the leverage mechanism. The latter can be seen at the left side of figure (2). These connection plates and muscles can be replaced easily ensuring the required flexibility of the set-up. Figure (2) shows the two pressure control units with its electronic circuitry aside. The low-level control of these two units is for each joint implemented on separate 16-bit MC68HC916Y3 micro-controller unit. These controllers are responsible for reading the joint position from HEDM6540 encoders with 2000 pulses per revolution and the serial data originating from the pressure sensors inside the muscles. Both these encoder and pressure signals are captured by a separate processor, TPU, on the micro-controller in order not to load the CPU whilst reading their values. The high-level control will be implemented on a PC, which is connected to the different low-level micro-controllers by a 16-bit parallel data bus with in between dual ported RAM units. For each joint, six in total, one such unit is used for transfer and buffer agent between PC and micro-controller. Additional information such as contact with the ground and absolute position of the body are observed by a seventh micro-controller. The absolute position includes absolute rotation and vertical and horizontal displacement of the body. The latter two, being redundant information to evaluate the movement of the robot, are measured along the sliding mechanism. All three position signals are captured by the same type of incremental encoders via the TPU of the seventh micro-controller which also masters the 16-bit communication bus by handling bus control bits.

The modularity for the different structural elements in the mechanical design is also present in the electronic design, which makes it possible to change the configuration of the set-up. This aspect can be used to perform experiments on different mechanical set-ups such as for instance a one-legged hopping robot.

5 FIRST STEPS OF LUCY

The last months Lucy has been assembled and debugged, therefore basic control strategies were implemented. On high level a quasi-static trajectory generation was used to balance the robot and to make it's first steps. On joint level an adapted feedback PI controller was implemented to settle position. The output of this controller is a delta-p signal, which will be added by and subtracted from a chosen mean pressure resulting in two new pressure values for both muscles of a joint. These new values are the set points for the bang-bang pressure controllers.

In order to avoid overshoots the integral term was made adaptive. When pressure differences are too high, the pressure controller won't be able to settle the pressure and thus the integral term will be lowered. In addition different sets for P and I values were used depending whether a leg is support leg or swing leg.

The graphs below show results of the first movements of Lucy. Here Lucy stands up from its rest position with both feet on the ground, lifts up and positions the left leg 0.1m further than the ankle of the stance leg. The same action is than performed by the right leg and next the left leg lifts again and places the feet back together after which the robot finally goes to its rest position.

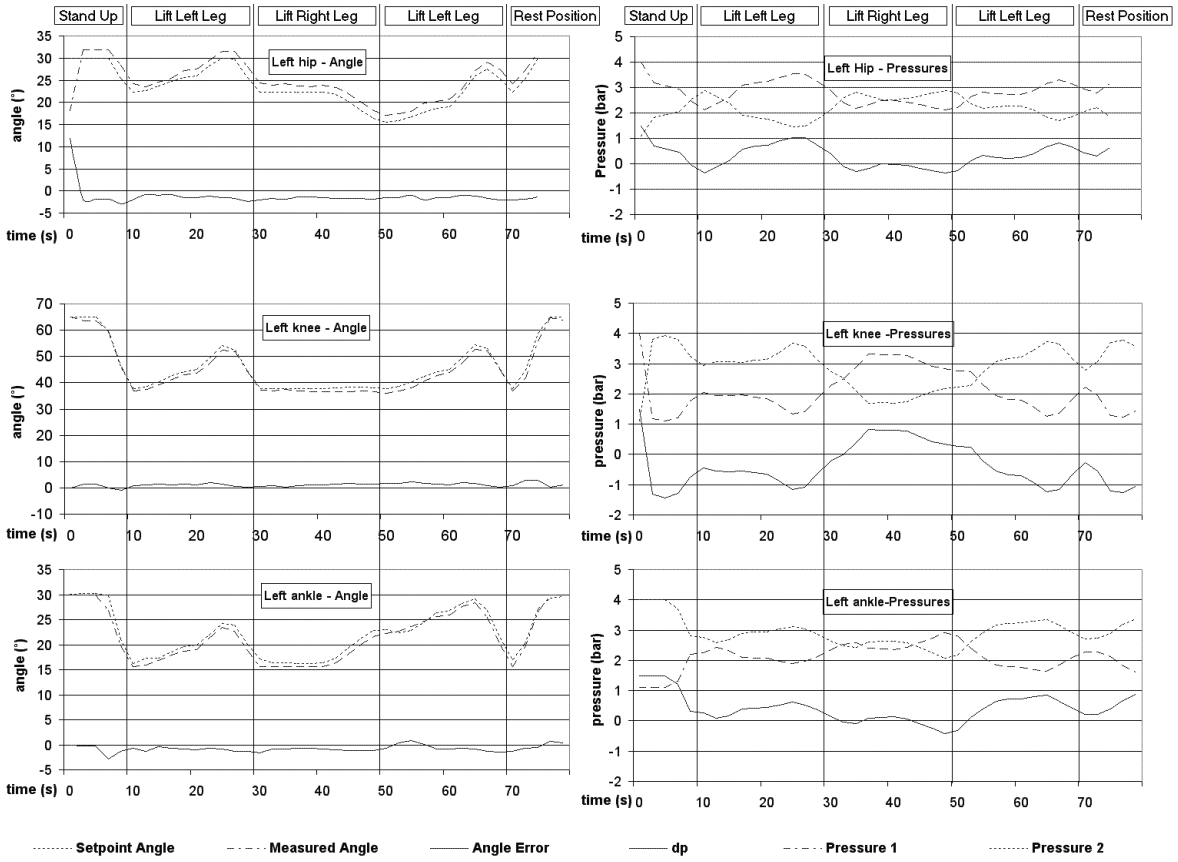

Fig. 10 First experimental steps: angle and pressure values for the left leg

At the left side of figure (10) angle, desired angle and the difference between them is given for the hip, knee and ankle of the left leg. At the right the pressures in both muscles of each corresponding joint and the control value delta-p is depicted. The definition of the angles can be found in figure (9).

The graphs show clearly the control strategy of keeping the mean pressure constant, which in this case is set at a value of 2.5 bar. One can have an understanding of the antagonistic working principle of the muscles when looking at the pressures for the knee between 10 and 50 seconds. During this time period the left leg switches function from swing leg to stance leg. From 10 to 30 seconds pressure 2, in the flexor muscle, must be higher than pressure 1, in the extensor muscle, to lift the weight of the lower left leg while from 30 to 50 seconds the pressure in the extensor muscle must be higher to hold the weight of the robot.
The results of this first control implementation with basic PID techniques show already satisfactory behaviour. Following step will be the implementation of a dynamic control scheme to induce faster and smoother motion for which the local feedback controller has to be redesigned with non-linear control techniques.

6 CONCLUSIONS

The Pleated Pneumatic Artificial Muscle has interesting characteristics, which make it very suitable to power a smooth walking bipedal robot. This actuator has a high power to weight ratio and an inherent adaptable passive behaviour. Two antagonistically coupled muscles can be implemented in a straightforward manner to power a rotative joint. The angular position of such a rotative joint depends on the difference in gauge pressures of both muscles and the stiffness of the joint is determined by the sum of pressures. Thus stiffness can be controlled while changing angular position. The biped Lucy is a robot actuated with these muscles. Both mechanical and electronic design of the robot was discussed showing the machine's modularity and elaborate hardware leading to a flexible experimental platform. For debugging reasons, basic control techniques were implemented which allowed Lucy to make her first steps. These first experiments showed already promising results.

7 REFERENCES

1. M. Armada. Climbing and walking-from research to applications. In *CLAWAR 2000: 3th International Conference on Climbing and Walking Robots*, pages 39-47, Madrid, 2000
2. F. Daerden and D. Lefeber. The concept and design of pleated pneumatic artificial muscles. *International Journal of Fluid Power*, 2(3):41-50, 2001.
3. S.T. Davis and D.G. Caldwell. The bio-mimetic design of a robot primate using pneumatic artificial muscle actuators. In *CLAWAR 2001: 4th International Conference on Climbing and Walking Robots*, pages 197-204*, Karlsruhe*, Germany, 2001.
4. G. Garcia, A. Chatterjee, A. Ruina, and M. Coleman. The simplest walking model: Stability, complexity, and scaling. *ASME Journal of Biomechanical Engineering, 1998.*
5. http://world.honda.com/ASIMO/
6. http://www.sony.co.jp/en/SonyInfo/News/Press/200203/02 0319E/
7. http://www.us.aibo.com
8. J.E. Pratt and G.A. Pratt. Exploiting natural dynamics in the control of a planar bipedal walking robot. In *36th annual Allerton Conference on Communication, Control, and Computing, Monticello, Illinois, 1998.*
9. D. Nishino, J. Yamguschi, and A. Takanishi. Realization of dynamic biped walking varying joint stiffnes using antagonistic driven joints. In *IEEE International Conference on Robotics and Automatisation*, pages2022-2029, Leuven, Belguim, 1998.
10. R.Q. van der Linde. Active leg compliance for passive walking. *IEEE International Conference on Robotics and Automatisation*, pages2339-2344, Leuven, Belguim, 1998.